REMOVAL OF PHARMACEUTICALS FROM SECONDARY EFFLUENT BY GRANULAR ACTIVATED CARBON ADSORPTION

by

Başak Kılıç

B.Sc. in Environmental Engineering, Istanbul Technical University, 2012

M.Sc. in Environmental Technology, Boğaziçi University, 2014

Submitted to the Institute of Environmental Sciences

in partial fulfillment of the requirements for the degree of

Doctor of Philosophy

in

Environmental Technology

Boğaziçi University

2025

REMOVAL OF PHARMACEUTICALS FROM SECONDARY EFFLUENT BY GRANULAR ACTIVATED CARBON ADSORPTION

APPROVED BY:

Prof. Dr. Ferhan Çeçen Dissertation Advisor	. . . . .
Prof. Dr. Özgür Aktaş	. . . . .
Prof. Dr. Kozet Bakırcı	. . . . .
Prof. Dr. Nadim Copty	. . . . .
Assoc. Prof. Dr. Başak Güven	. . . . .

DATE OF APPROVAL: 18/03/2025

dedicated to my family…

ACKNOWLEDGEMENTS

First of all, I would like to express my sincere gratitude to my supervisor Prof. Dr. Ferhan Çeçen for her guidance, support and valuable comments throughout my PhD and for her generous time in proof readings. It was an honor for me to meet her and I am grateful that she shared her extensive knowledge and experience during my study in all these years.

Also, I would like to express my sincere thanks to the committee members Prof. Dr. Özgür Aktaş, Prof. Dr. Nadim Copty, Prof. Dr. Kozet Bakırcı and Assoc. Prof. Dr. Başak Güven for their valuable comments and spending their time for this study.

Special thanks to Assoc. Prof. Dr. Ulaş Tezel for his help, guidance and support with the use of LC-MS/MS and his valuable contributions. I highly appreciate Duygu Özçelik and Tuna Sürmeli for their patience and help throughout LC-MS/MS analyses.

I would like to express my sincere thanks to Assoc. Prof. Dr. Duygu Ağaoğulları for providing access to her laboratory at Istanbul Technical University Chemical and Metallurgical Engineering Faculty Metallurgical and Materials Engineering Laboratories. Also, thanks to Sıddıka Mertdinç Ülküseven, Seyfullah Ceylan and İlayda Süzer from the same department for their help during the use of laboratory equipment for granular activated carbon grinding.

I would like to thank Filiz Ayılmaz for her technical support in laboratory and her kindness.

I want to thank my colleague Gökçin Gül whom I worked with from the beginning to the end of my study. I am grateful that we shared our knowledge and experience with each other. I highly appreciate her for her help and friendship during this long journey.

I thank my dear friend Berivan Ülger Vatansever for always being by my side. She is not only a colleague, but also a close friend. I am grateful for all the memories we shared in all these years. I am also thankful to my dear friends Zeynep Akdoğan, Elif Bal, Suat Vardar, Binnur Aylin Alagöz and Buse Yetişti for their valuable friendship and support during my study.

The financial support of this study by Bogazici University Research Fund Grant Number 19Y00D6 is gratefully acknowledged.

Lastly, my special thanks go to my family whom I dedicate this work to. I owe more than thanks to my mother, father and brother, for their patience, believing, understanding and never-ending love throughout my life. Without their encouragement and support, I could not attain what I have achieved.

ABSTRACT

REMOVAL OF PHARMACEUTICALS FROM SECONDARY EFFLUENT BY GRANULAR ACTIVATED CARBON ADSORPTION

This study investigates the removal of four pharmaceuticals: acetaminophen (ACT), carbamazepine (CBZ), erythromycin (ERY) and sulfamethoxazole (SMX) by granular activated carbon (GAC). Firstly, sorption and biodegradation potential of these pharmaceuticals was studied and removal mechanisms (primary, secondary, cometabolic substrate, etc.) were investigated. After that, adsorption experiments were carried out in batch reactors to obtain isotherm constants. Then, the removal of pharmaceuticals was examined in rapid small-scale continuous-flow GAC columns. The results were compared with outputs of a model called AdDesign. Results showed that sorption of these pharmaceuticals was very low and they were biodegraded by activated sludge to some extent. ACT was highly biodegradable, whereas CBZ was the least biodegraded pharmaceutical. Adsorption experiments showed that the affinity of pharmaceuticals to adsorb onto GAC was higher when they were the only pharmaceutical, but when they were in the mixture the affinities were lower. This indicated that there was a competition between them. On the other hand, adsorption of the bulk organics present in secondary effluent on GAC was very low. Small-scale column tests showed that there was no full breakthrough of either of the pharmaceuticals in the experimental period because of the low initial concentrations. In the presence of background organic matter, higher concentrations of pharmaceuticals were observed in the effluent which indicated a competition between the pharmaceuticals and the background organic matter. Through the use of AdDesign model the column performance could be studied in a longer term and the full breakthrough of pharmaceuticals could be demonstrated under various conditions.

ÖZET

İKİNCİL ARITMA ATIKSUYUNDA KALAN FARMASÖTİKLERİN GRANÜLER AKTİF KARBON ADSORPSİYONUYLA GİDERİMİ

Bu çalışma, dört farmasötiğin: asetaminofen (ACT), karbamazepin (CBZ), eritromisin (ERY) ve sülfametoksazol (SMX), granüler aktif karbon (GAK) kullanılarak giderimini araştırmaktadır. İlk olarak, bu farmasötiklerin sorpsiyon ve biyobozunma potansiyeli incelenmiş ve giderim mekanizmaları (birincil, ikincil, kometabolik substrat, vb.) araştırılmıştır. Daha sonra, izoterm sabitlerini elde etmek için kesikli reaktörlerde adsorpsiyon deneyleri yapılmıştır. Ardından, farmasötiklerin giderimi hızlı, küçük ölçekli sürekli akışlı GAK kolonlarında incelenmiştir. Bu deneylerden elde edilen sonuçlar AdDesign adı verilen bir modelin çıktılarıyla karşılaştırılmıştır. Sonuçlara göre bu farmasötiklerin aktif çamura adsorpsiyonu oldukça düşüktür ve hepsi aktif çamur tarafından bir dereceye kadar biyolojik olarak parçalanmaktadır. ACT biyolojik olarak yüksek oranda parçalanabilirken, CBZ biyolojik olarak en az bozunan farmasötik olmuştur. Adsorpsiyon deneyleri, farmasötiklerin GAK'a adsorbe olma eğiliminin, tek farmasötik olarak bulunduklarında daha yüksek olduğunu, ancak karışım içindeyken bu eğilimin daha düşük olduğunu göstermiştir. Bu durum, aralarında bir rekabet olduğunu belirtmiştir. Öte yandan, ikincil arıtma atıksuyundaki organiklerin GAK'a adsorpsiyonu çok düşük çıkmıştır. Küçük kolon testleri, başlangıç konsantrasyonlarının düşük olması nedeniyle çalışılan deney sürelerinde hiçbir farmasötiğin tam kırılma noktasına ulaşmadığını göstermiştir. Arka planda organik madde olduğunda, çıkışta farmasötik konsantrasyonlarının daha yüksek olduğu gözlemlenmiştir; bu durum, farmasötikler ile organik maddeler arasında bir rekabet olduğunu göstermiştir. AdDesign modelinin kullanılmasıyla kolon performansı daha uzun sürede incelenerek, çeşitli koşullar altında farmasötiklerin tam kırılma noktaları gösterilebilmiştir.

TABLE OF CONTENTS

LIST OF FIGURES

LIST OF TABLES

LIST OF ABBREVIATIONS

Abbreviation	Explanation
ACT	Acetaminophen
AMO	Ammonia Monooxygenase
AS	Activated Sludge
ATU	N-Allylthiourea
BAC	Biological Activated Carbon
BOD	Biochemical Oxygen Demand
BTC	Breakthrough Curve
BV	Bed Volume
CAS	Conventional Activated Sludge
CBZ	Carbamazepine
COD	Chemical Oxygen Demand
CPHSDM	Constant Pattern Homogeneous Surface Diffusion Model
CUR	Carbon Usage Rate
DF	Design Factor
DOC	Dissolved Organic Carbon
EBCT	Empty Bed Contact Time
ECM	Equilibrium Column Model
ERY	Erythromycin
GAC	Granular Activated Carbon
IS	Internal Standard
LC-MS/MS	Liquid Chromatography Tandem Mass Spectrometry
MBR	Membrane Bioreactor
MF	Microfiltration
MLSS	Mixed Liquor Suspended Solids
MLVSS	Mixed Liquor Volatile Suspended Solids
MTZ	Mass Transfer Zone
NF	Nanofiltration
NH_4-N	Ammonium nitrogen
PAC	Powdered Activated Carbon
PSDM	Pore Surface Diffusion Model
R1	Reactor 1

R2	Reactor 2
RO	Reverse Osmosis
RSSCT	Rapid Small Scale Column Test
SCFB	Semi-Continuously Fed Batch (Reactor)
SCOD	Soluble Chemical Oxygen Demand
SF	Scaling Factor
SMX	Sulfamethoxazole
TOC	Total Organic Carbon
UF	Ultrafiltration
UV	Ultraviolet
VSS	Volatile Suspended Solids
WW	Wastewater
WWTP	Wastewater Treatment Plant

1. INTRODUCTION

Micropollutants are contaminants present at low concentrations such as ng/L or μg/L. Since micropollutants are persistent, they are not biodegradable completely and cannot be removed with conventional wastewater treatment technologies. Especially in recent years, a great amount of micropollutants is released into water bodies and they are of great concern all around the world. It is believed that they have many adverse effects on both human and environment health. These micropollutants include pharmaceuticals, personal care products, industrial chemicals, steroid hormones and pesticides. Toxic properties and adverse effects of these micropollutants on living organisms are still not well known. So, their removal becomes increasingly important (Nas et al., 2017; Tüzün, 2017).

Municipal wastewater treatment plants (WWTPs) are not designed for removing micropollutants, as their primary aim is to remove biodegradable carbon, nitrogen and phosphorous compounds that arrive at the WWTPs in concentrations at the order of mg/L. However, micropollutants are generally in the range of μg/L or ng/L. Their removal in conventional treatment systems are insufficient. As a consequence, these contaminants present in water bodies pose a risk for the environment and human health. Since in WWTPs it is not possible to remove the micropollutants completely, appropriate treatment techniques should be used to reduce the ecotoxicological effects of micropollutants on living organisms (Nas et al., 2017; Verlicchi et al., 2012).

There is not a specific treatment for complete removal of micropollutants. Conventional treatment processes cannot eliminate the micropollutants and bulk substances together. Some options used for micropollutant removal are coagulation-flocculation, ozonation and advanced oxidation, membrane processes and membrane bioreactor (MBR) and activated carbon adsorption (Nas et al., 2017).

Activated carbon adsorption is a very effective method for the removal of these contaminants in advanced treatment. Activated carbons are porous carbonaceous adsorbents. A high number of organic and inorganic solutes can be removed from water and wastewater by adsorption onto activated carbon. Since activated carbon has a high adsorptive surface area (500–1500 m^2/g), the amount of material adsorbed by it may be potentially very large. It is mainly used in the form of powdered activated carbon (PAC) or granular activated carbon (GAC). PAC is generally produced

from wood and the average particle size is in the range of 15–25 μm. It is widely used in the treatment of both wastewater and drinking water. In addition, the particles size of GAC is ranging from 0.2 to 5 mm. GAC filters are also widely used in purification of groundwater, drinking water and wastewater as an advanced treatment step (Çeçen and Aktaş, 2011).

To study the effectiveness of GAC filtration in micropollutant removal, laboratory-scale studies (often called pilot-scale studies) can be conducted. Even though a full-scale GAC system is an effective technique for some toxic organics removal from drinking water and wastewater, it may be an expensive process if it is designed improperly. For the proper design, expensive and time-consuming pilot-scale studies are necessary (Crittenden et al., 1986). Pilot-scale studies simulate full-scale systems in terms of GAC particle size, hydraulic loading rate, bed depth and empty bed contact time (EBCT). Since these parameters are kept constant, contaminant breakthrough in pilot-scale studies occurs at the same time as at the full-scale systems. As a result, pilot-scale studies require large volumes of water and are expensive and time consuming (Reinert, 2013).

Studies have been carried out for finding alternative ways to determine GAC adsorber performance in a more cost and time effective manner. In response to this situation, a rapid method for large-scale design from small column studies, Rapid Small Scale Column Test (RSSCT) was developed and evaluated. There are some advantages of this test: A smaller volume of water is needed, less time is required and extensive isotherm and kinetic studies are not needed to obtain a full-scale performance prediction. These advantages make it a very effective alternative instead of pilot-scale studies. By using the similarity principle, dimensionless parameters are kept constant in RSSCT and full-scale adsorbers. GAC particle size is reduced in RSSCT. So, identical breakthrough profiles can be obtained and adsorber performance evaluations can be conducted over a short period of time (Crittenden et al., 1986; Reinert, 2013).

2. AIM OF THE STUDY

The main aim of this study is to investigate the removal of organic micropollutants from secondary effluent of wastewater treatment plants (WWTPs) by using Granular Activated Carbon (GAC) adsorption. Micropollutants that are named hazardous, priority or emerging contaminants according to international criteria have been chosen for this study. These are the pharmaceutical compounds acetaminophen (paracetamol) (ACT), carbamazepine (CBZ), erythromycin (ERY) and sulfamethoxazole (SMX). Removal of these selected micropollutants was studied by using GAC filters in Rapid Small-Scale Columns (RSSC). Since secondary effluents from WWTPs contain biomass, GAC filters are expected to convert to Biological Activated Carbon (BAC) filters as time passes. As a result, BAC combines carbon adsorption and biological activity. This process was also investigated within the scope of this study. Table 2.1 shows the main parts of this study.

Table 2.1. The main parts of the study.

<table>
<tr><th>1st PART</th><th>2nd PART</th></tr>
<tr><td>

Estimation of biodegradation potential of pharmaceuticals by BIOWIN (US EPA, 2012)
Comparison of results with experimental data from literature

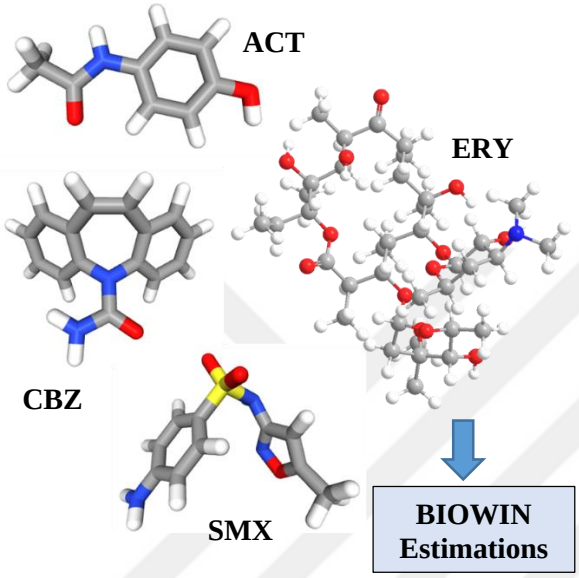

</td><td>

Biodegradation of selected pharmaceuticals in batch reactors
Batch experiments with two types of activated sludge (R1 and R2 reactors)
Investigation of removal mechanisms (primary, secondary, cometabolic substrate, etc.)

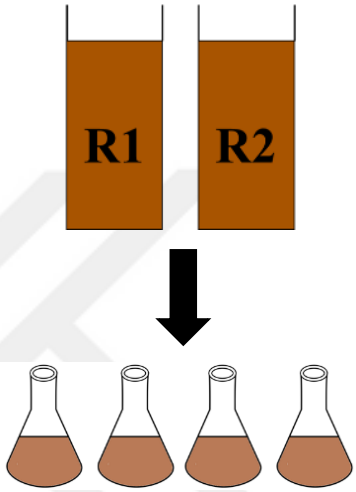

</td></tr>
<tr><th>3rd PART</th><th>4th PART</th></tr>
<tr><td>

Kinetic and isotherm experiments with Granular Activated Carbon (GAC)
Determination of equilibrium time and isotherm constants

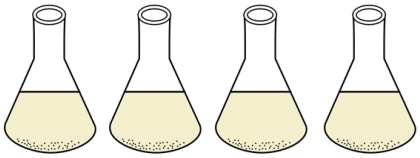
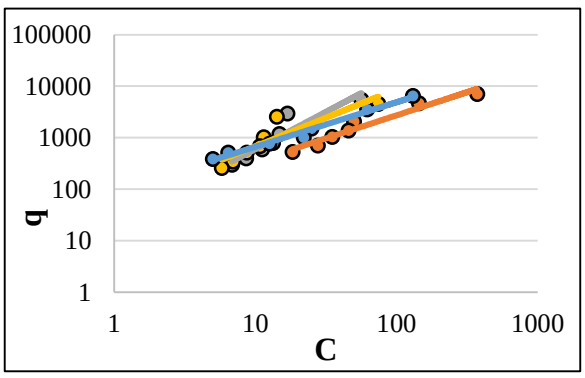

</td><td>

Removal of selected pharmaceuticals by GAC adsorption in Rapid Small Scale Column Tests (RSSCTs)
Removal of selected pharmaceuticals by Biological Activated Carbon (BAC) in Rapid Small Scale Column Tests (RSSCTs)
Simulation of RSSCTs by a simulation program called AdDesignS™ and comparison of experimental results with model data

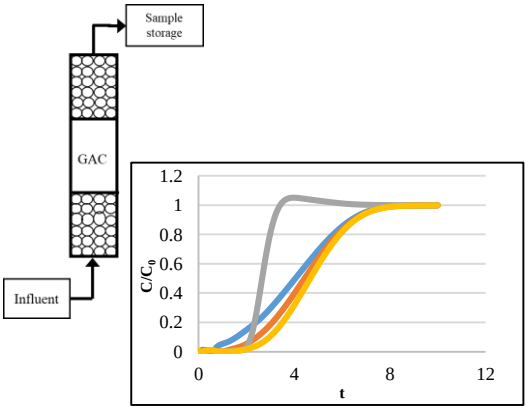

</td></tr>
</table>

In the first step, biodegradation potential of 27 pharmaceuticals from different groups was searched with BIOWIN models. Then the results were compared with the experimental data from the literature. After that, biodegradation properties of micropollutants selected for this study (ACT, CBZ, ERY and SMX) were examined in batch reactors. Experiments were carried out with two types of activated sludge from two reactors R1 and R2. R1 reactor was fed with a synthetic domestic wastewater which contained both organic and inorganic compounds in order to enrich both heterotrophic and nitrifying bacteria. R2 reactor was fed with inorganic substrates only. The feed was rich in terms of ammonium sulfate for enhancement of nitrifying bacteria. The purpose of these experiments was to investigate the removal mechanisms (primary, secondary, cometabolic removal, etc.) of pharmaceuticals.

In the next step, adsorption properties of selected micropollutants were examined in batch reactors. For this purpose, kinetic and isotherm experiments were carried out with Granular Activated Carbon (GAC). After this step, micropollutant removal was investigated in continuous-flow activated carbon filters. Experiments were carried out in Rapid Small-Scale GAC columns. Also, the removal of selected micropollutants was investigated with BAC in RSSCs which is an originality of this study. Additionally, the adsorption of background organic matter in synthetic secondary effluent was studied with respect to its effect on the adsorption of micropollutants. In the last step, a simulation model called AdDesignS^{TM} was used to simulate the RSSCTs and the outputs from the model compared with the experimental data. This model provides three models that can be used for simulating gas and liquid phase adsorption in fix bed adsorbers. These models can be used separately or combined with each other to provide desired simulation (Mertz et al., 1999). The details of the model are presented in the following sections.

3. THEORETICAL BACKGROUND

3.1. Micropollutants

Until the 1990s, heavy metals and persistent organic pollutants were the main concern as primary pollutants. However, with the help of appropriate measures and regulations, a reduction in the emissions of these contaminants has been achieved over the years. In the last decades, the emission of “emerging pollutants” has become an environmental problem. These pollutants are generated in everyday life due to the use of pharmaceuticals, hormones, personal care products, surfactants and surfactant residues, pesticides and industrial products. They are present in industrial wastewaters, domestic wastewaters, landfill leachates and other sources. Pollutants which are present in the concentration range of µg/L to ng/L in the environment are named as micropollutants and currently receive special attention. Conventional wastewater treatment systems are not able to remove these micropollutants completely. As a result, from influent to effluent, most micropollutants are removed to a degree, but they still remain in the effluent at low concentrations. So, reuse of treated wastewater or their discharge into water bodies may have direct or indirect risk to both people and aquatic environment. Consequently, the occurrence of micropollutants in wastewaters and their behavior during wastewater treatment require further study. Advanced wastewater treatment methods should be applied for the elimination of these contaminants (Çeçen and Aktaş, 2011; Petrovic et al., 2003; Thanh, 2018).

Pharmaceuticals are a group of micropollutants that are used in large quantities in human and veterinary medicine all over the world. These pharmaceuticals are introduced into environment over anthropogenic or industrial activities. Figure 3.1 shows the possible sources and pathways of pharmaceuticals in the aquatic environment. The first source is wastewater that contains high concentrations of pharmaceuticals from human excrement and also disposal of expired or unused drugs. Another source is agricultural and livestock waste. In addition, effluents from pharmaceutical industry are another source (Ortuzar et al., 2022). WWTPs are considered as the biggest pathway of pharmaceuticals into water bodies (Bofill, 2023). High concentrations of pharmaceuticals are observed in the influent of WWTPs. Since they cannot be removed totally, the potential risk in relation with the presence of pharmaceuticals in aquatic environment is currently under consideration, even though they are at low concentrations (Rattier et al., 2012b; Xu and Duran, 2017).

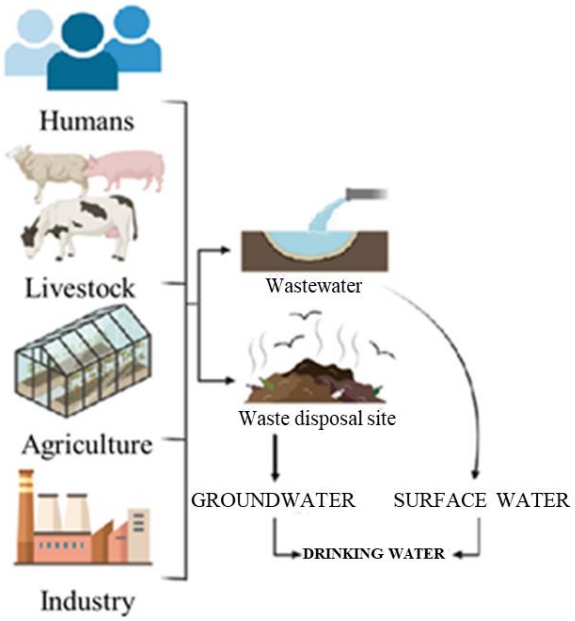

Figure 3.1. Sources of pharmaceuticals in the environment (Adapted from Ortuzar et al., 2022).

Within the scope of this study, acetaminophen (ACT), carbamazepine (CBZ), erythromycin (ERY) and sulfamethoxazole (SMX) have been selected as model substances. Acetaminophen is an anti-inflammatory pharmaceutical. Erythromycin and sulfamethoxazole are antibiotics from the highly risky compounds group and they cause antibiotic resistance in pathogens (Göktaş and Macleod, 2017; Verlicchi et al., 2012). Carbamazepine, which is an antiepileptic pharmaceutical, is known to have very low removal in treatment systems. It is stated that these selected pharmaceuticals are at high concentrations at the end of treatment processes (Petrie et al., 2015).

According to a study, average influent concentrations of acetaminophen, carbamazepine, erythromycin and sulfamethoxazole from different WWTPs are 38 µg/L, 1.20 µg/L, 1.80 µg/L and 0.92 µg/L, respectively. Additionally, average effluent concentrations of these pharmaceuticals from WWTPs are 0.89 µg/L for acetaminophen, 1.04 µg/L for carbamazepine, 0.73 µg/L for erythromycin and 0.28 µg/L for sulfamethoxazole (Verlicchi et al., 2012). According to other studies, the ranges of these pharmaceuticals in some secondary effluents are given in Table 3.1.

Table 3.1. Range of selected pharmaceuticals in secondary effluents.

Micropollutant	Range in Secondary Effluents (ng/L)	Reference
Acetaminophen	1.9 – 19 (Korea)	Kim and Zoh, 2016
	32 – 4300 (Spain)	
	25 – 4319 (Norway)	Al-Kaf et al., 2017
	129 – 11733 (UK)	
Carbamazepine	73 – 729 (Korea)	Kim and Zoh, 2016
	1680 (Sweden)	
	10.8 – 163 (Japan)	
Erythromycin	182.7 (Sweden)	Baresel et al., 2015
	1000 – 6000 (Germany)	Schafhauser et al., 2018
	1 – 838 (Canada)	
	9 – 353 (Italy)	
Sulfamethoxazole	310 (USA)	Kim and Zoh, 2016
	3.8 – 407 (Korea)	

Removal efficiencies for pharmaceuticals in WWTPs varied widely from less than 20% to more than 90%. In some cases, even up to 99% removal was observed. While acetaminophen showed 90% and higher removal, the removal efficiency of carbamazepine was about 20% or less (Thanh, 2018). In another study, the removal of carbamazepine was studied with some other micropollutants (diclofenac, gemfibrozil, ibuprofen, naproxen, atenolol, metoprolol, trimethoprim and triclosan) in operating WWTPs in five EU countries. Results showed that carbamazepine was removed less than 10% (Paxéus, 2004).

In another research, the efficiency of a conventional wastewater treatment plant, including physical removal, biological oxidation and disinfection, on removing pharmaceuticals and some other micropollutants was investigated. The removal of 95 different micropollutants was studied. The results showed that while the majority of targeted pharmaceuticals was removed at least 80%, there were some persistent micropollutants such as desmethyl citalopram, phenytoin and carbamazepine. It was stated that their physicochemical properties make these micropollutants resistant to degradation in WWTPs. However, three micropollutants, paracetamol (acetaminophen), caffeine and salicylic acid found initially at concentrations of 289.40 μg/L, 78.09 μg/L and 32.74 μg/L respectively in the influent were not detected in the effluent which showed their total removal (Cardenas et al., 2016).

3.1.1. Regulations

A study published by The European Commission states that current European Union legislation does not have specific provisions on micropollutants and further work is needed to address emerging contaminants in the current revision of policy legislation packages. In 2022, a proposal for Urban

Wastewater Treatment Directive was published by the European Commission to provide micropollutant removal. This proposal requires large WWTPs to add a fourth stage treatment process by 2030 at the latest to remove at least 80% of certain micropollutants, especially pharmaceuticals.

In addition, The Water Framework Directive addresses micropollutants, but partially. It covers a Watch List which is a system to monitor and control selected chemicals that pose an environmental risk across river basins in the European Union. The first Watch List included 17 substances (mostly hormones, insecticides, and antibiotics) that must be monitored at least once per year and in the last update, two types of antibiotics (ciprofloxacin and amoxicillin) were added to the Watch List.

The full removal of micropollutants in water is currently not legally regulated in the European Union, but some countries are developing regulations relating to this issue. For example, Switzerland passed a law to reduce micropollutant loads from wastewater treatment plants serving at least 2000 people. The increased reuse of wastewater for irrigation strengthens the need to remove micropollutants from treated wastewater, particularly in water-scarce countries. Furthermore, countries like Germany, France and the Netherlands are regarding the reduction of micropollutants in treated wastewater through additional treatments to the traditional treatment processes. Common methods of these advanced treatments are ozonation, granular and powdered activated carbon (Bofill, 2023).

In Türkiye, there is no legislation or regulation limiting the discharge of micropollutants (Akkurt & Oğuz, 2019). The discharge standards are included in the Water Pollution Control Regulation (Su Kirliliği Kontrol Yönetmeliği, 2020) and Urban Wastewater Treatment Regulation (Kentsel Atıksu Arıtımı Yönetmeliği 2006). These regulations are mainly used to control conventional and collective parameters such as Biochemical Oxygen Demand (BOD) and Chemical Oxygen Demand (COD) rather than micropollutants.

Within the current legislation, wastewater discharges do not control any micropollutants, such as hormones, pharmaceuticals and nanomaterials. Additionally, in Surface Water Quality Regulation (Yerüstü Su Kalitesi Yönetmeliği, 2021) there is a list of specific pollutants that includes major pesticides, but there are also pharmaceuticals. In this list, there is a quality standard for sulfamethoxazole. Annual average environmental quality standard is specified as 5 µg/L and maximum allowable environmental quality standard is specified as 50 µg/L for both rivers/lakes and coastal and transitional waters. Otherwise, in the current situation there is no discharge standard for organic micropollutants and it is clear that collective parameters BOD and COD cannot meet the need

for control of micropollutants. For this reason, if treated wastewater is recycled and reused, exposure to micropollutants may occur (Doğruel et al., 2022).

Pharmaceuticals and personal care products that cannot be fully removed in treatment plants accumulate in soil and water. They threaten clean water resources. They are constantly transferred from soil to plants, from plants to animals and humans. So the use of treated wastewater for irrigation causes the accumulation of these micropollutants in soil. In Türkiye, there are some standards for the use of treated wastewater as irrigation water in Circular on Technical Procedures for WWTPs (Atıksu Arıtma Tesisleri Teknik Usuller Tebliği, 2010). But, these limits were determined for parameters such as salinity, heavy metals and conductivity. There is no legal limit for micropollutants on the use of treated wastewater as irrigation water (Akkurt & Oğuz, 2019).

3.2. Micropollutant Removal Methods

There are different methods used for removing micropollutants from water and wastewater. Some of them are biological removal, ozonation, membrane filtration and activated carbon adsorption.

3.2.1. Biological Removal

In a biological system removal of micropollutants generally take place by biodegradation and biosorption (sorption onto sludge). The details of these mechanisms are given in the next sections.

3.2.1.1. Biodegradation. The biodegradation potential of a micropollutant depends on its physicochemical properties and solubility in the aqueous phase. A high solubility increases the bioavailability to microorganisms. In addition, environmental conditions, such as lack of oxygen and nutrients; the presence, type and activity of microorganisms also affect the biodegradation of micropollutants. Biological removal of micropollutants may occur by three mechanisms: removal as a primary substrate, removal as a secondary substrate or cometabolic removal.

In the removal as a primary substrate, the micropollutant often is removed by normal metabolism where it is utilized as an energy and growth substrate. Biodegradation of the compound can take place under aerobic, anoxic and anaerobic conditions. In the case of removal as a secondary substrate, if the concentration of the micropollutant is very low, no net growth of biomass can take place using this substrate. However, bacteria can still consume this substrate if there is another substrate at a high concentration to support the growth of the existing population. In these cases, the substrate at the high

concentration is defined as the primary substrate and the micropollutant at the low concentration becomes the secondary substrate which also serves as a source of energy and carbon.

If a micropollutant is totally resistant to biodegradation under the specific condition, it can be still removed by a mechanism called cometabolism. Cometabolism is the biological transformation of a non-growth substrate by bacteria through enzymes which can only be induced in the presence of a primary substrate providing energy for cell maintenance and growth. In cometabolic transformation, bacteria cannot get energy and use the carbon benefit, so a growth substrate, such as easily biodegradable compounds like glucose, must be supplied to the microorganism for the growth of new cells. Cometabolic removal is often observed in the treatment of domestic, municipal and industrial wastewaters (Çeçen and Aktaş, 2011).

The biodegradation of a pharmaceutical in a domestic wastewater usually follows first-order kinetics due to the low concentration (Çeçen, 2017). Accordingly, the first-order biodegradation rate constant k_{biol} is used in the expression of biodegradation rate. It is assumed that no substantial biological degradation would take place if k_{biol}<0.1 L.g_{SS}^{-1}.d^{-1}. For 0.1 L.g_{SS}^{-1}.d^{-1}<k_{biol}<10 L.g_{SS}^{-1}.d^{-1} partial removal takes place by biological transformation. For k_{biol}>10 L.g_{SS}^{-1}.d^{-1}, more than 95% removal can be expected for a compound, but the removal strongly depends on reactor configuration as well as sludge recycle flow (Ternes and Joss, 2006). Also, another classification on the basis of VSS indicates compounds as recalcitrant (k_{biol} <0.1 L.g_{VSS}^{-1}.d^{-1}) slowly biodegradable (0.1 L.g_{VSS}^{-1}.d^{-1} <k_{biol}<0.5 L.g_{VSS}^{-1}.d^{-1}), moderately biodegradable (0.5 L.g_{VSS}^{-1}.d^{-1}<k_{biol}<1 L.g_{VSS}^{-1}.d^{-1}) and highly biodegradable (k_{biol}>1 L.g_{VSS}^{-1}.d^{-1}) (Fernandez-Fontaina et al., 2016). The first-order biodegradation rate constant (k_{biol}) is calculated according to the following equation:

$$\frac{C_i}{C_0} = e^{-k_{biol}.VSS.t} \tag{3.1}$$

$$\ln \frac{C_i}{C_0} = -k_{biol}.VSS.t \tag{3.2}$$

where C_0 is initial concentration (µg/L), C_i is final concentration (µg/L), k_{biol} is the first-order biodegradation rate constant, VSS is the mixed liquor volatile suspended solid (MLVSS) concentration (mg/L) and t is the elapsed time in the batch reactor (day), respectively.

Gauthier et al. (2010) investigated the fate of pharmaceuticals known to be resistant to biodegradation. For this purpose, glucose was added as a readily degradable carbon source for studying the cometabolism of selected pharmaceuticals. It was observed that the difficult to degrade

micropollutants can be biodegraded if there is an easily used carbon source in the medium. Microorganisms were not able to grow if there were only pharmaceuticals available as the carbon source. However, with the addition of glucose, the selected pharmaceuticals could be degraded if they were contacted with the biomass for an enough period of time. It is reported that around 20% removal of carbamazepine, sulfamethoxazole and sulfamethizole was observed with the cometabolism of these micropollutants.

Similarly, the cometabolic removal of sulfamethoxazole was studied in activated sludge at bench scale (Müller et al., 2013). This study focused on both sulfamethoxazole cometabolism with acetate and ammonium nitrate and when sulfamethoxazole utilization was present as the only carbon and nitrogen source. Activated sludge was able to degrade sulfamethoxazole both as a carbon and/or nitrogen source, but biodegradation was improved with the addition of acetate and ammonium nitrate as readily degradable compounds, since they provided energy for heterotrophic biomass growth and metabolic activity.

In another study, the biodegradation of 10 selected micropollutants, including diclofenac, carbamazepine, ibuprofen, propyphenazone, etc. was studied by enriched nitrifier cultures in the presence of different growth substrates and inhibitors. The enriched nitrifier culture showed higher degradation of the selected pharmaceuticals than the conventional activated sludge (CAS). Also, when ammonium and organic substrates were added, higher removal efficiencies of some pharmaceuticals were observed. In addition, experiments with the addition of allylthiourea (ATU) were carried out in order to inhibit nitrification. Results showed that there was only a partial degradation of selected pharmaceuticals due to the activity of heterotrophic bacteria. It was concluded that the removal of targeted pharmaceuticals was enhanced by nitrification (Tran et al., 2009).

3.2.1.2. Biosorption. Sorption onto sludge is another mechanism for biological removal of micropollutants. The sorption potential of a pollutant onto sludge can be predicted based on its octanol–water partition coefficient (K_{ow}). High K_{ow} values indicate less solubility of micropollutants in water, resulting in high affinity to sludge. Generally, low sorption potential is indicated by log $K_{ow}<2.5$, whereas medium and high potentials are indicated by $2.5<\log K_{ow}<4$ and $\log K_{ow}>4$, respectively (Çeçen and Aktaş, 2011; Rogers, 1996).

In addition, in experimental studies with activated sludge, the solid-water partition coefficient K_d can be used to express sorption. This value is dependent on the characteristic of the sludge and the sorbing compound, so it may be a better indicator of sorption. For a compound under equilibrium

conditions, the concentration sorbed onto sludge (C_{sorbed}) is assumed to be proportional to the concentration in solution ($C_{dissolved}$):

$$C_{sorbed} = K_d \,.\, SS \,.\, C_{dissolved} \quad (3.3)$$

where C_{sorbed} is the sorbed concentration of compound (µg/L), K_d is the solid-water partition coefficient (L/g SS), SS is the suspended solids concentration (g/L) and $C_{dissolved}$ is the dissolved concentration of compound (µg/L). Although there is no strict limit, the removal by sorption onto sludge in a WWTP is considered negligible if $K_d < 0.500$ L/g SS (Çeçen and Gül, 2021; Ternes et al., 2004). In that case, biodegradation may be considered as the main removal mechanism.

Although biological treatment methods have many advantages, they also have some limitations. Even though high removal efficiencies can be obtained for a wide range of micropollutants, they are not very effective in the total elimination of some compounds which are resistant, like carbamazepine and benzothiazole (Matamoros et al., 2015). The studies showed that even if WWTPs remove more than 90% of pharmaceuticals, very low concentrations of these are still being released into the environment daily. These pharmaceuticals can accumulate with time resulting in a risk for both environment and human health. As a conclusion, some other methods should be investigated to remove the majority of pharmaceuticals from wastewater. Micropollutants can be potentially removed from water and wastewater by different processes, such as ozonation, membrane processes and sorption on activated carbon. These processes are reviewed in the next sections.

3.2.2. Ozonation

Ozonation is a method that is widely used in water treatment for disinfection, to eliminate odor and taste and to remove inorganic materials. Nowadays, ozone has been tested for removing pharmaceutical residues in water with the increased awareness of these harmful substances. It is reported that ozonation is a promising method for reducing pharmaceutical concentrations in full-scale WWTPs with high efficiencies (Hollender et al., 2009; Thanh, 2018).

Sui et al. (2010) investigated the application of ozone after ultrafiltration as tertiary treatment of secondary effluent in a WWTP. Results showed that ozonation is an effective method to remove most of the pharmaceuticals including carbamazepine, diclofenac, trimethoprim, etc. When the ozone dosage was 5 mg/L at 15-minute contact time; carbamazepine, diclofenac, sulpiride, indomethacin and trimethoprim were significantly eliminated by more than 95%. Gerrity et al. (2011) stated that

the application of ozone with H_2O_2 can eliminate some targeted micropollutants with high removal rates including carbamazepine, ibuprofen, diclofenac, fluoxetine. According to this study, average secondary effluent concentrations of carbamazepine and sulfamethoxazole were 180 (±10) ng/L and 443 (±172) ng/L, respectively. Results showed that the average removal of these pharmaceuticals after O_3/H_2O_2 were >99% for carbamazepine and 98% for sulfamethoxazole.

Besides the high effectiveness of ozonation on pharmaceutical removal, this method has some disadvantages. The production of ozone is an energy intensive process and its application is costly. An ozone treatment system may increase the energy consumption of a conventional WWTP by 40-50% (Ahmed et al., 2017). In addition, there is a formation of some by-products during ozonation. It is reported that potentially carcinogenic compounds such as N-nitro-sodimethylamine (NDMA) and bromate may be formed during the application of ozone. These by-products are generally at low concentrations, but they may reduce the water quality (Ahmed et al., 2017; Hollender et al., 2009; Luo, et al, 2014; Thanh, 2018).

3.2.3. Membrane Processes

Membrane processes are also used for removing micropollutants from drinking water and wastewater. Generally, removal of micropollutants takes place by adsorption onto membrane. Microfiltration (MF) and ultrafiltration (UF) are effective for removing turbidity in treatment systems, but they are not as effective in eliminating micropollutants because of their sizes. So, these processes are not used alone because of the poor performance. They should be used in combination with some other methods like nanofiltration (NF) and reverse osmosis (RO) (Nas et al., 2017). In a study, the combination of MF/RO as tertiary treatment was used to remove micropollutants from secondary effluent of a WWTP. Results showed that this method is very effective and all the targeted micropollutants except caffeine were totally removed. In addition, more than 90% removal of carbamazepine was achieved with this system (Sui et al., 2010).

In another study, removal of pharmaceuticals and endocrine disrupting compounds from secondary municipal WWTP by an UF pressure-vessel skid was evaluated. It was seen that this UF system was not very effective in eliminating selected compounds. For example, while influent concentrations of acetaminophen, carbamazepine, erythromycin and sulfamethoxazole were 18, 191, 289 and 66 ng/L, respectively; the effluent concentrations from UF pilot testing were 17, 161, 245 and 63 ng/L for these pharmaceuticals, respectively. These results showed that there was almost no removal of these micropollutants. In the same study, removal of some micropollutants in a membrane

bioreactor (MBR) system using primary WWTP effluent as feed water was also investigated. Results of the research showed that some compounds were effectively removed, for example carbamazepine was reduced from 281 ng/L to less than 10 ng/L and erythromycin was reduced from 800 ng/L to 34 ng/L (Snyder et al., 2007).

Removal of some micropollutants, including diclofenac, ibuprofen, carbamazepine, diazepam, sulfamethoxazole in a pilot-scale membrane bioreactor was compared to conventional activated sludge plants. It is reported that carbamazepine was not removed during the wastewater treatment and the effluent concentrations were in the range of influent concentrations. This compound was also not removed in the MBR. Moreover, compounds including ibuprofen and sulfamethoxazole showed a removal potential both in conventional activated sludge and MBR. The results showed that these compounds could be degraded during wastewater treatment and there is a slight difference in the effluent concentrations between conventional WWTPs and MBRs. However, it was concluded that MBRs are more advantageous than conventional activated sludge systems, because lower effluent concentrations of micropollutants could be obtained from these systems (Clara et al, 2005). On the other hand, MBRs have a disadvantage which is the high energy and operational costs.

3.2.4. Adsorption on Activated Carbon

Adsorption on activated carbon is another micropollutant removal method. Adsorption is considered to be an important phenomenon in most natural physical, chemical and biological processes. Adsorption is the accumulation or concentration of substances at a surface or interface. The adsorbent is the adsorbing phase and the adsorbate is the material being adsorbed. Adsorption can occur between two phases: gas–liquid, gas–solid, liquid–solid or liquid– liquid interfaces. In the case of activated carbon adsorption, the adsorbing phase is a solid.

In most types of wastewater and water treatment practice, there are two driving forces that result in the adsorption of a solute from a solution onto a solid phase. The first one is the solvent disliking (lyophobic) character of a solute. The solubility of a dissolved substance is the most important factor for the intensity of adsorption. A hydrophilic substance tends to stay in the water, so it is less adsorbable on a solid phase. Contrary to this, a hydrophobic substance tends to be adsorbed and does not stay in water. Complex contaminants like humic acids have both hydrophilic and hydrophobic groups, so while the hydrophilic part of the molecule tends to stay in the solution, the hydrophobic part is adsorbed. The second driving force is the affinity of the solute for the solid. It is due to electrical

attraction of the solute to the solid and this adsorption type may occur as a result of van der Waals attraction or chemical interaction with the adsorbent (Çeçen and Aktaş, 2011).

Adsorption can be classified as chemical adsorption and physical adsorption. In chemical adsorption, a chemical reaction occurs between the adsorbed solute and the solid. There is an exchange of electrons between specific surface sites and solute molecules which result in a chemical bond. Chemical adsorption is generally predominant at high temperatures. This type of reaction rarely occurs in wastewater and water treatment. However, physical adsorption generally occurs in the treatment of water and wastewater. It is due to van der Waals' forces and is a reversible process. When the molecular forces of attraction between the adsorbent and the solute are greater than the forces of attraction between the solvent and the solute, the solute will be adsorbed onto the surface of adsorbent materials. Exchange of electrons does not occur in physical adsorption. The physically adsorbed molecule is free to move within the interface due to less strong attachment to a specific site compared to chemical adsorption (Çeçen and Aktaş, 2011; Hung et al, 2005).

The chemical and physical adsorption interact together in adsorption. Adsorption of organic molecules exhibit a large range of binding energies. Higher energies are associated with chemical adsorption, whereas lower energies are associated with physical adsorption. As a result, it is usually difficult to differentiate between chemical and physical adsorption in wastewater treatment aiming the removal of organic pollutants (Çeçen and Aktaş, 2011).

3.2.4.1. Factors affecting adsorption. There are many factors that affect the adsorption process. Some of them are surface area of the adsorbent, physical and chemical characteristics of the adsorbate, pH and temperature. Generally, liquid-phase adsorption of organic pollutants by activated carbon is increased with decreasing pH. The degree of this effect may change due to the characteristic of wastewater and activation technique of the activated carbon. In addition, the extent of adsorption usually increases with decreasing temperature, because the adsorption reactions are exothermic (Çeçen and Aktaş, 2011).

3.2.4.2. Adsorption equilibrium and adsorption isotherms. The adsorption isotherm represents the distribution of the adsorbed material between the solution phase and the adsorbed phase at equilibrium. The adsorption isotherm gives the information on the adsorption process and it is a functional expression for the variation of adsorption with concentration of adsorbate in bulk liquid at constant temperature (Equation 3.4). Here, C_e is the concentration in the liquid phase, q is the amount adsorbed, and T is the temperature.

$$q = q(C_e) \text{ at } T \quad (3.4)$$

Figure 3.2 shows the adsorption isotherm curves. Generally, if its shape is convex upward an isotherm is favorable. If it is concave upward, the isotherm is unfavorable. Any point on an isotherm curve gives the adsorption capacity at a particular equilibrium concentration.

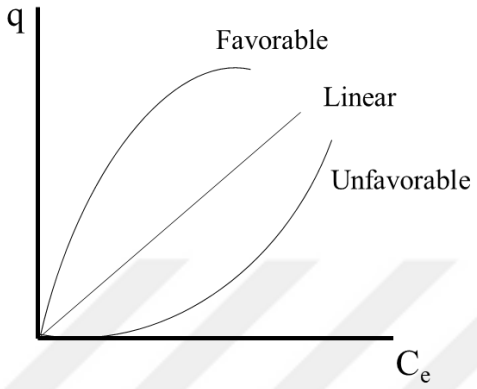

Figure 3.2. Adsorption isotherm curves (Adapted from Çeçen and Aktaş, 2011).

Adsorption isotherms are described in many mathematical forms. Some of them are based on a simplified physical picture of adsorption, and others are purely empirical and intended to correlate the experimental data in simple equations. The most widely used mathematical expressions of adsorption equilibrium are the Freundlich and Langmuir isotherms (Crittenden et al. 2012; Çeçen and Aktaş, 2011).

The Freundlich isotherm is commonly employed to describe the adsorption of molecules onto activated carbon. It offers insights into the correlation between the concentration of the adsorbate (molecules being adsorbed) in the liquid phase and the amount of adsorbate adsorbed onto the surface. The Freundlich isotherm is an empirical equation that describes heterogeneous adsorption onto surfaces with non-uniform energies. The equation and the linearized form are expressed as in Equation 3.5 and Equation 3.6, respectively:

$$q_e = X/M = K.C_e^n \quad (3.5)$$

$$\log q_e = \log K + n.\log C_e \quad (3.6)$$

where q_e is the adsorption capacity of activated carbon (mg of substance adsorbed/g activated carbon), X is the adsorbed amount (mg), M is weight of activated carbon (mg), C_e is the equilibrium concentration of the adsorbate (mg/L), K is Freundlich exponent and n is Freundlich slope.

The K value is an indicator of adsorption capacity and it shows the strength of adsorption. Higher K value indicates higher adsorbent loading that can be achieved. The adsorption intensity (n) is shown by the slope of the adsorption isotherm curve. When n value is lower, the isotherm shape becomes more concave. An increase in activated carbon dose is more effective at low n values than in the case of steeper isotherm curves with high n values (Çeçen and Aktaş, 2011; Worch, 2012).

In addition, the theoretical Langmuir equation is also used as an adsorption isotherm. Although this equation generally does not describe adsorption data as accurately as the Freundlich equation, it introduced a clear concept of the monomolecular adsorption on energetically homogeneous surfaces. In Langmuir isotherm, adsorbents are supposed to contain fixed individual sites and each site adsorbs only one molecule, forming a monolayer. In contrast to Freundlich equation, the constants in the Langmuir equation have a strictly defined physical meaning. The equation and the linearized form are expressed as in Equation 3.7 and Equation 3.8, respectively. By using Equation 3.8, b and q_{max} can be calculated from the slope and intercept (Çeçen and Aktaş, 2011):

$$q_e = \frac{q_{max}\ b\ C_e}{(1+b\ C_e)} \tag{3.7}$$

$$\frac{1}{q_e} = \frac{1}{q_{max}} + \left(\frac{1}{b\ .q_{max}}\right)\left(\frac{1}{C_e}\right) \tag{3.8}$$

where q_{max} is the maximum solute adsorbed per unit weight of adsorbent in forming a complete monolayer on the surface (mg/g) and b is Langmuir adsorption constant (L/mg).

Upon these two isotherms, the Freundlich isotherm is widely used for defining the adsorption from aqueous solutions, especially adsorption on activated carbon. It is a kind of standard equation for describing adsorption processes in water treatment (Worch, 2012).

3.2.4.3. Transport mechanisms. In an adsorption system, equilibrium is built between the adsorbate and the adsorbent. The adsorption kinetics is defined by the rate of approach to equilibrium. The rate of adsorption is generally limited by different transport mechanisms shown in Figure 3.3.

The first transport mechanism is advection. In this process, adsorbates must be first transported from the bulk solution to the liquid film (the boundary layer of water) surrounding the activated carbon particle. This transport may occur through diffusion (Çeçen and Aktaş, 2011).

There is a liquid film or external film that surrounds the adsorbent particles. Mass transport through this layer occurs by molecular diffusion. The film or external diffusion consists of the transport of the adsorbate from the bulk liquid to the external surface of the adsorbent particle. The rate of this diffusion depends on the hydrodynamic properties of the system (Çeçen and Aktaş, 2011; Worch, 2012).

The other transport mechanism is internal (intraparticle) diffusion. It involves the transfer of adsorbate from the surface of a particle like the activated carbon to sites in the particle. It depends on the size and pore structure of the particle, but is independent of the hydrodynamic properties of the system. There are two types of internal diffusion, namely pore diffusion and surface diffusion. The surface diffusion is usually assumed to be the dominant internal transport mechanism (Çeçen and Aktaş, 2011).

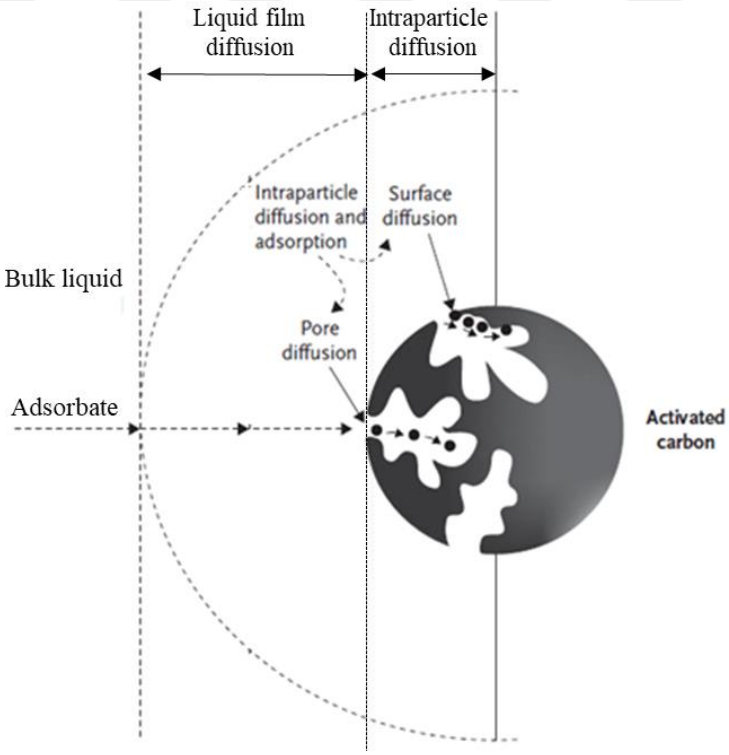

Figure 3.3. Internal and external transport of an adsorbate in an activated carbon particle (Adapted from Çeçen and Aktaş, 2011).

In surface diffusion, the mass transfer occurs in the internal surface of the adsorbent particle. In this model, the adsorbent is considered a homogenous medium and the adsorption equilibrium is assumed to exist only at the outer surface of the adsorbent particle. If the film diffusion is very fast, surface diffusion limits the adsorption rate. The surface diffusion coefficient decreases with increasing adsorption strength according to the transport mechanism. For activated carbon, the typical

range of surface diffusion coefficients is found between 10^{-11} m^2/s for small molecules and 10^{-15} m^2/s for larger molecules such as humic substances.

In addition to surface diffusion, the adsorbate transport within the adsorbent particles can also take place in the pore liquid. This diffusion is called pore diffusion. In contrast to surface diffusion, the adsorption equilibrium has to be considered at each point of the pore system. In general, it is assumed that there is a local equilibrium between the pore fluid concentration and the solid-phase concentration. The typical range of pore diffusion coefficients are expected to be in the range of 10^{-10} m^2/s to 10^{-8} m^2/s for small- and medium-size molecules. The mass transfer within the adsorbent particle occurs generally by pore diffusion and surface diffusion in parallel (Worch, 2012).

3.3. Activated Carbon

Activated carbon is the most widely used adsorbent in water, municipal wastewater and industrial wastewater treatment. The ability to adsorb a wide variety of organic compounds and its economic feasibility make activated carbon the most preferable. In water treatment, it is used to remove organic compounds that cause odor, taste and color. In advanced wastewater and industrial treatment, it is used to remove toxic organic compounds. It is generally used in the granular form in the carbon adsorption column application in water and wastewater purification (Hung et al, 2005).

Activated carbon is a porous carbon material with high adsorption capacity because of its high surface area (between 500 and 1500 m^2/g). Due to this, the amount of material adsorbed is potentially very large. The total surface available for adsorption of solute includes the external surface of the particles and the surfaces of pores. The pore surface area is much larger than the external surface area of the particles. So adsorption occurs on the pores' surfaces mostly. The ratio of the total surface area to the mass of activated carbon is very large. As a result, activated carbon adsorption can be used in a tertiary treatment process for the removal of organic pollutants from the secondary effluent of biological wastewater treatment systems (Çeçen and Aktaş, 2011; Hung et al, 2005; Junpirom, 2006).

Activated carbon can be prepared by a one-step chemical activation with inorganic chemicals such as potassium hydroxide, zinc chloride and phosphoric acid or by a two-step physical activation with oxidizing gases such as steam or carbon dioxide. It can be produced from many different carbonaceous materials, such as coal, lignite, wood, coconut shell and some polymers (Junpirom, 2006; Çeçen, 2024).

3.3.1. Types of Activated Carbon

Activated carbon is mainly in the form of powdered activated carbon (PAC) and granular activated carbon (GAC). PAC is generally produced from wood in the form of sawdust and its average particle size is in the range of 15-25 μm. It is applied for the treatment of both wastewater and drinking water. In wastewater treatment, it may be added to activated sludge or contacted with wastewater in separate unit.

GAC is generally in the form of crushed granules of shell or coal and has sizes ranging from 0.2 to 5 mm. It is designated by mesh sizes like 8/20, 20/40 or 8/30 for liquid phase applications and 4/6, 4/8 or 4/10 for vapor phase applications. For liquid phase applications 12/42 mesh are advantageous. GAC filters are widely used for drinking water, groundwater and wastewater purification and removal of toxic organic compounds. In some GAC applications, a microbiological film may form on the particles. As a result, biological removal of contaminants is combined with GAC adsorption. The new material is called as biological activated carbon (BAC) (Çeçen and Aktaş, 2011).

3.3.2. Granular Activated Carbon Adsorbers

GAC adsorbers can be used for tertiary treatment of municipal and industrial wastewaters to adsorb organic molecules that are not removed in biological treatment. Figure 3.4 shows use of GAC in tertiary treatment of wastewaters.

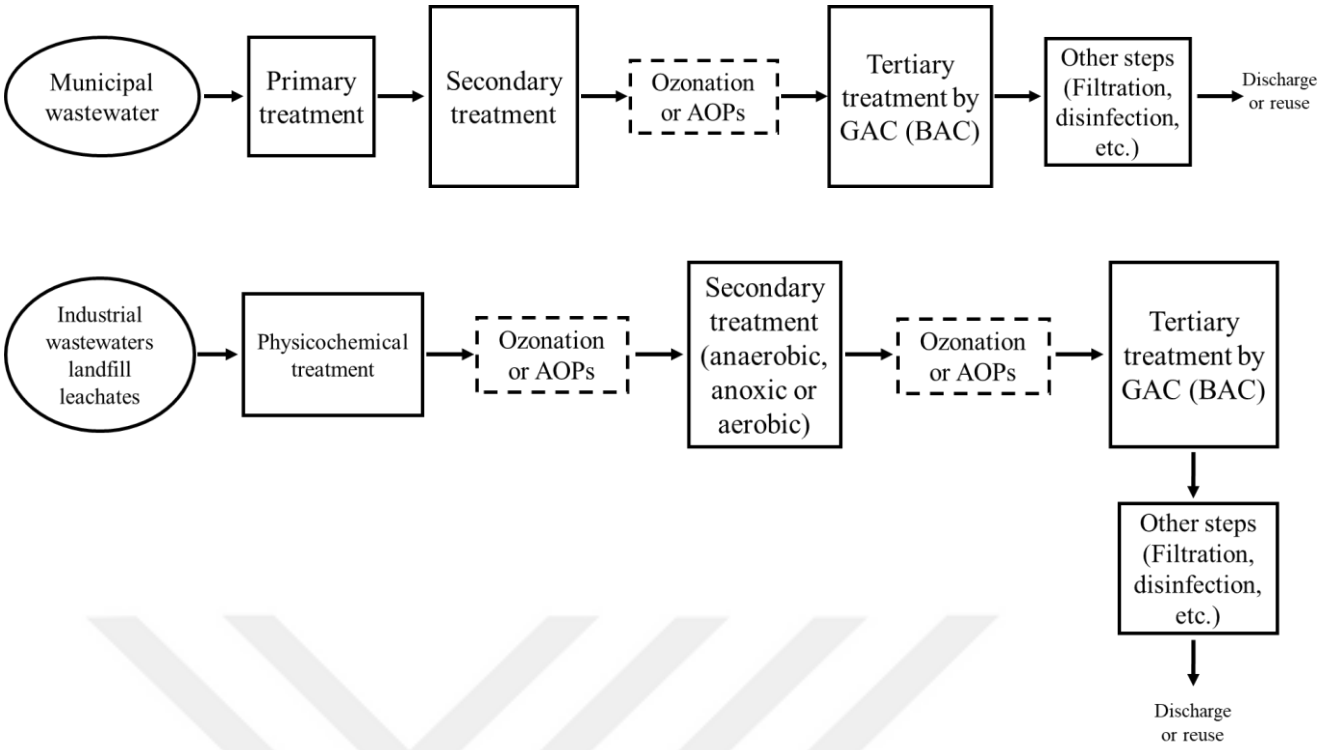

Figure 3.4. Use of GAC in tertiary treatment of wastewaters (Adapted from Çeçen and Aktaş, 2011).

In a carbon adsorption system, the operation conditions such as flow rate and contact time, the properties of activated carbon and mode of operation must be taken into consideration. Additionally, in sizing of GAC columns, the following factors are mainly important: the empty-bed contact time (EBCT), the hydraulic loading rate and the carbon depth. The explanations and equations of the important parameters are given in Table 3.2.

Table 3.2. Important parameters for GAC column operation.

Parameter	Definition	Equation
Empty-Bed Contact Time (EBCT)	The theoretical residence time in the filter in the absence of packing media.	$EBCT = V_B / Q$ V_B: volume of the GAC bed Q: flow rate
Filter Velocities	The velocity of liquid in an empty bed with a cross sectional area corresponding to the hydraulic loading rate (HLR).	$v_F = Q / A$ A: cross-sectional area of bed
Throughput Volume	The water volume which passes through the reactor during the filter operation time.	$V_L = Q \cdot t_F$ t_F: filter operation time
Bed Volume (BV)	The normalization of throughput volume to the carbon bed volume.	$BV = t_F / EBCT$
Carbon Usage Rate (CUR)	The mass of activated carbon required per unit volume of water treated until breakthrough.	$CUR = M_{GAC} / Q \cdot t_{bk}$ M_{GAC}: mass of GAC in the column t_{bk}: time to breakthrough

3.3.2.1. Mass Transfer Zone (MTZ) and Breakthrough Curves. As the water or wastewater flows down in a GAC adsorber, pollutants are removed by adsorption and this process takes place in a zone called the mass transfer zone (MTZ). As the operation of a GAC adsorber continues, MTZ moves to the end of the adsorber. The adsorbate appears in the adsorber outflow for the first time when the MTZ reaches the end of the adsorber and that time is called as breakthrough time. After the breakthrough time, the concentration in the outflow increases due to the adsorption progress in the MTZ. During that time there is a decrease in the remaining adsorbent capacity. If the whole MTZ has left the adsorber, the outflow concentration equals the inlet concentration. At that point, all particles on the adsorbent are saturated and there is no more adsorption. The concentration versus time curve is called as the breakthrough curve (BTC) (Worch, 2012). The definition of breakthrough is arbitrary. In practice, breakthrough is defined as the effluent concentration reaching either 5% of influent concentration or the required effluent quality. Saturation is generally defined as $C_e = 0.95xC_0$ (Hung et al, 2005). The MTZ and the breakthrough curve are shown schematically in Figure 3.5 (Worch, 2012).

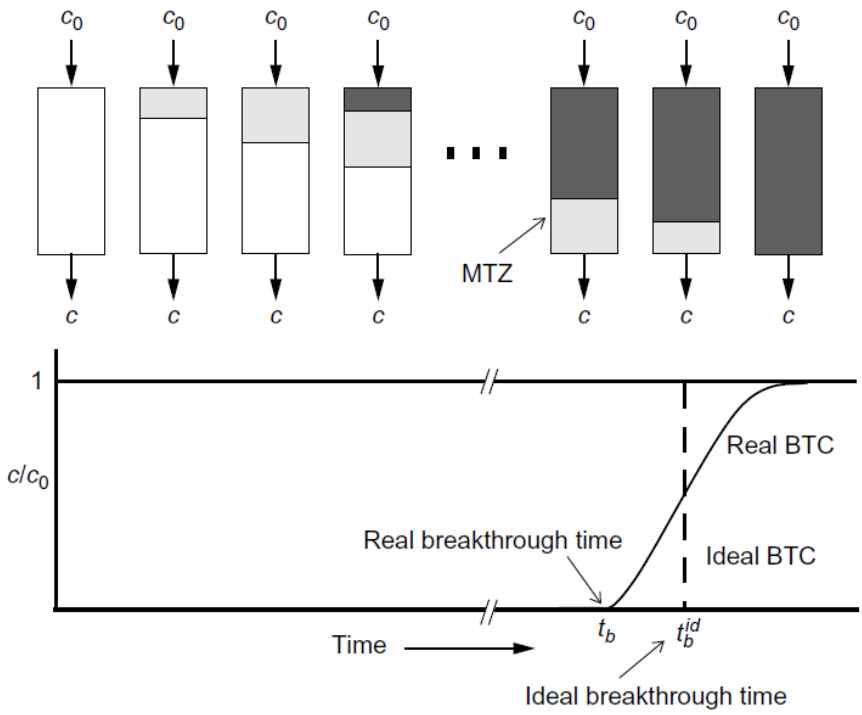

Figure 3.5. The MTZ through the adsorber bed and the BTC (Worch, 2012).

If single solutes are of interest, the prediction of breakthrough profiles is relatively easy in a GAC adsorber. However, it is not the case in real situations when multiple substances are removed from water or wastewater. In that condition, competition takes place for adsorption sites on activated carbon. If the adsorption is the only mechanism for removal, the breakthrough curve shape is affected

by the presence of compounds of different adsorbability. In the presence of multiple substances, individual MTZs for all components occur, which travel with different velocities through the adsorbent bed. As a result, displacement processes take place leading to quite different breakthrough behavior in comparison to single-solute adsorption (Çeçen and Aktaş, 2011; Worch, 2012).

3.3.3. Biological Activated Carbon Adsorbers

GAC applications can remove many adsorbable organic and inorganic compounds, but non-adsorbable contaminants cannot be eliminated. On the other hand, these pollutants can be removed by biological processes. So, the combination of both processes is seen as a solution for pollution prevention (Hung et al, 2005).

When activated carbon was initially introduced for tertiary treatment of industrial or municipal wastewaters, the main focus was the adsorption of pollutants on this material. However, it has been realized that in some applications when GAC adsorbers were receiving secondary effluents, a microbiological film formed on the particles. As a consequence of biological activity, GAC adsorbers were converted into biofilm (attached-growth) reactors as time passes. The new material is called as biological activated carbon (BAC) (Çeçen and Aktaş, 2011).

Organic material in the wastewater is degraded by microorganisms attached to GAC media and partially adsorbed by GAC. As the microorganisms grow during the process, the thickness of the layer increases. The pores of GAC are also progressively saturated by the target organic contaminants during adsorption process (Hung et al, 2005). Figure 3.6 shows the processes occurring in BAC systems.

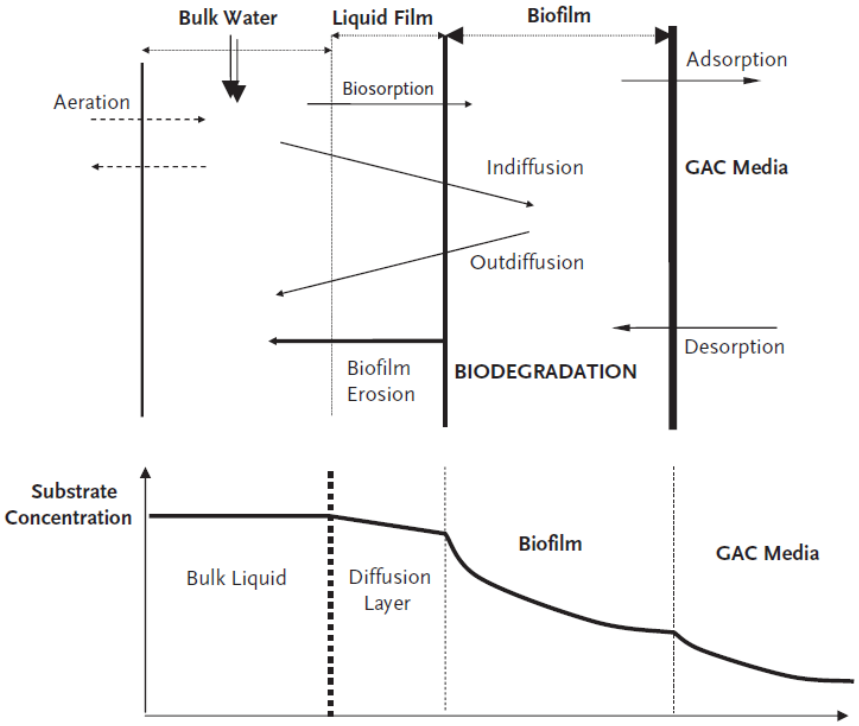

Figure 3.6. Processes on GAC media and change in substrate concentration from the bulk liquid to the GAC surface (Çeçen and Aktaş, 2011).

In BAC adsorbers the breakthrough curves are different from GAC adsorbers. In a GAC adsorber the breakthrough profile is determined by adsorption mechanisms only. The effluent concentration increases sharply with respect to time during the operation as the capacity of adsorption is decreased. Similarly, in BAC systems, adsorption is the dominant mechanism in the initial phases. As time passes, biological activity leads to the formation of a biofilm. Accordingly, lower concentrations can be achieved in the effluent compared to a GAC system. Finally, the adsorption capacity is completely exhausted and the BAC adsorber functions as a biofilm reactor only (Çeçen and Aktaş, 2011). The breakthrough curve profiles in GAC and BAC are shown in Figure 3.7.

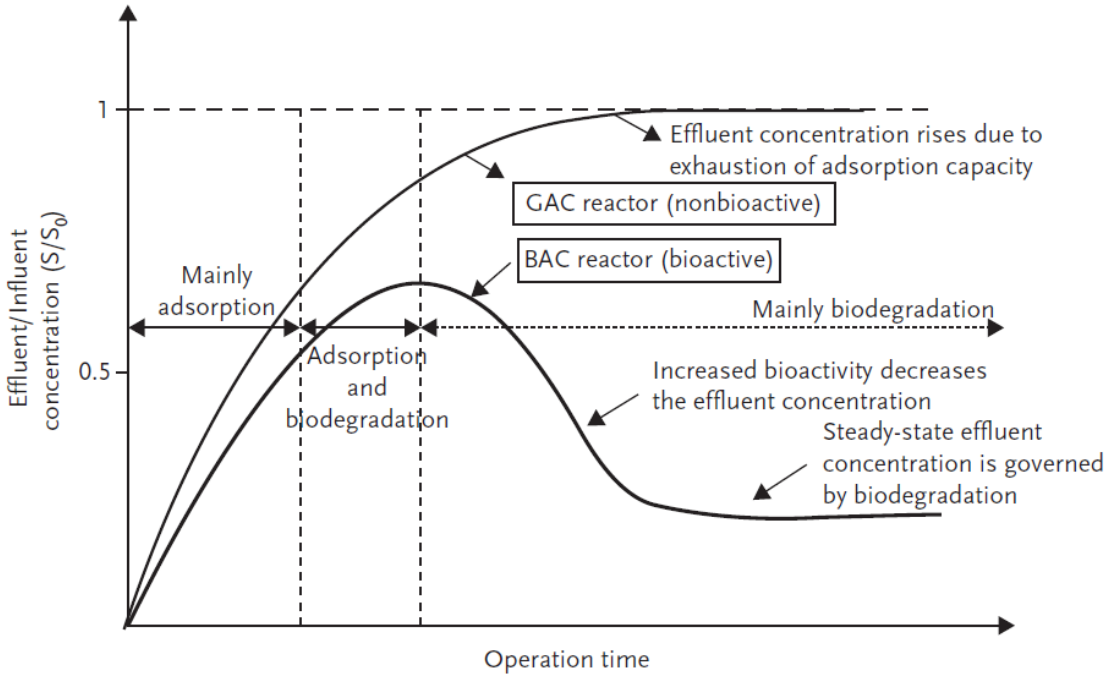

Figure 3.7. Breakthrough curves in the case of GAC and BAC adsorbers (Çeçen and Aktaş, 2011).

3.3.4. Removal of Micropollutants by Activated Carbon

Removal of micropollutants from wastewater by activated carbon was investigated in many studies. In a study, pharmaceutical removal in effluents from three WWTP was investigated. The aim was to achieve 95% removal of selected micropollutants in a Swedish WWTP through adsorption onto activated carbon and to compare the performance of PAC and GAC. Results showed that activated carbon is an efficient method to remove pharmaceuticals from WWTP effluents. 95% removal was achieved for almost all the targeted micropollutants including carbamazepine. It is stated that there is 95% removal in the use of PAC with applying the dose of 15-20 mg/L, and more than 90% removal in the use of GAC for all tested micropollutants (Karelid et al., 2017).

In another study, effluents from four different WWTPs were treated with PAC and ozone to compare removal efficiencies of targeted micropollutants including carbamazepine, diclofenac, sulfamethoxazole, etc. It is reported that diclofenac and carbamazepine were removed more than 90% at 20 mg/L PAC and 5-7 mg/L ozone dosage, while higher PAC dosages (up to 40-50 mg/L) were necessary to remove sulfamethoxazole, primidone, iomeprol and benzotriazole by 90%. Both treatment techniques were suitable to eliminate the targeted micropollutants with suitable dosages. For instance, higher dosages and longer contact times were required for removing sulfamethoxazole with PAC treatment, while it was easily removed with ozonation (Altmann et al., 2017).

In another study, a full-scale GAC system was used to remove steroidal estrogens and pharmaceuticals from the WWTP effluent. Results of the research showed that there was more than 43% to 64% reduction in the removal of steroidal estrogens. Additionally, many of the targeted pharmaceuticals, such as mebeverine, were removed between 84-99%. However, it is stated that some of the pharmaceuticals including carbamazepine and propranolol had removal efficiencies of 17-23%. It is said that removal of some organic micropollutants with GAC-based technology is less efficient, because adsorption sites become saturated as time passes (Grover et al., 2011).

As mentioned before, a microbiological film may form on GAC filters and they are converted to BAC as time passes. These BAC systems are also used to remove the micropollutants from water and wastewater. For example, in a study the objective was to investigate the BAC performance in removing pharmaceuticals from drinking water. The results showed that the concentration of almost all pharmaceuticals including carbamazepine, paracetamol (acetaminophen) and sulfamethoxazole were decreased below 0.01 µg/L by BAC, except for erythromycin and gabapentin. The biodegradability and hydrophobicity of pharmaceuticals were the main properties which affected their removal in BAC systems. The biodegradability is determined according to the biological rate of constant (k_{biol}). The water-octanol partition coefficient (log K_{ow}) is widely used as an indicator of hydrophobicity. Hence, the low k_{biol} and low K_{ow} of erythromycin might be the reason for the low removal in BAC. Likewise, the high k_{biol} of acetaminophen (58-80 $L.g_{SS}^{-1}d^{-1}$) indicates its high removal in a BAC process (Nugroho et al., 2010).

Moreover, the removal of some micropollutants by BAC media was investigated in another study. The role of biodegradation, adsorption and physicochemical properties of selected micropollutants, including acetaminophen, carbamazepine, erythromycin, sulfamethoxazole and other compounds, was evaluated in order to understand their removal during the BAC process. For this purpose, GAC, BAC and inhibited BAC (BAC + sodium azide) reactors were used. Sodium azide was used to inhibit the biomass activity and discriminate between adsorption and biodegradation in BAC. It is reported that GAC was very effective in the removal of selected micropollutants. However, the GAC performance decreased due to accumulation of effluent organic matter and microbial colonization as expected. Additionally, results showed that there was a reduction (more than 60%) in the concentrations of selected micropollutants after BAC process. Although compounds such as carbamazepine, diclofenac and sulfamethoxazole are known as resistant to biological transformation, this study showed that they were removed to a great extent by the BAC. Moreover, it is stated that removal of some compounds including sulfamethoxazole, hydrochlorothiazide, ibuprofen, diclofenac and erythromycin was negatively affected when the biomass in BAC was inhibited which indicated

that their removal was enhanced by the action of the microbial biomass in BAC systems. It was concluded that the combination of biodegradation and adsorption is advantageous in removing micropollutants from wastewater (Rattier et al., 2012a).

Overall, adsorption on activated carbon has many advantages in removing micropollutants:

- There is no production of toxic or pharmaceutically active products along the adsorption process.

  The operation of activated carbon system is less complicated.
- Activated carbon is environmentally friendly. It can be produced from recycling materials (biomass residues, coconut husk, etc.).
- High removal rates of different micropollutants from wastewater were seen in several studies (Thanh, 2018).

Use of activated carbon in the removal of micropollutants from water and wastewater is a common method all over the world. But it may be difficult to study in full-scale experiments, because of time and resource concerns. So, a rapid test method was developed in order to overcome the problems in experiments. Further information about this method is given in the next sections.

3.4. Rapid Small Scale Column Tests (RSSCTs)

Rapid Small Scale Column Test (RSSCT) was developed as an alternative test technique to time-consuming and costly pilot-plant studies (Crittenden et al., 1986). It is a very quick method for designing a large-scale adsorbent column from small-scale column experiments. It can be used to replicate a pilot-scale test column study for Empty Bed Contact Time (EBCT). In pilot-scale columns it takes a long time to reach a breakthrough curve, but in RSSCTs the breakthrough can be achieved in a very short time, like in hours or days (Poddar et al., 2013).

The RSSCTs rely on a dynamically-scaled physical model of full-scale GAC adsorbers. Some scaling equations are used to proportion the column length and diameter, flow rate and GAC particle size. In a RSSCT, it is possible to obtain data in a much shorter time than pilot-scale test due to smaller EBCT. The EBCT is proportional to the amount of GAC that is available for the adsorption. With the less available GAC amount in RSSC than in pilot-scale, the adsorption capacity of GAC is reduced proportionally. As a result, the breakthrough curve is “compressed” in time, for example it may be observed in about one week, while it may last 10 weeks in a pilot plant (DiGiano et al., 1999).

The main idea to use the specifically designed small columns for studying the breakthrough behavior is that the operational conditions in the small-scale column give the same situation in the large-scale fixed-bed adsorber. The downscaling equations were derived from mass transfer models to make certain that the effect of different mass transfer processes is equal in both scales. The breakthrough curves identified in small-scale columns can then be used as the source for adsorber design.

The major advantages of RSSCT are as follows:

(i) the RSSCT may be carried out in a shorter time (days) compared to a pilot-scale study (months) and it requires a smaller volume of water because the breakthrough can be obtained faster, (ii) extensive isotherm or kinetic studies are not required to predict the full-scale performance (Worch, 2012).

Mass transfer accelerates as the boundary layer around the GAC particles is increased by increasing the hydraulic load in the rapid small-scale columns. In rapid small-scale column tests, diameters of GAC, which is used in pilot-scale, are greatly reduced by grinding. In the design of RSSCT, a pilot-scale activated carbon column is reduced to a small scale by using some mathematical correlations given in Table 3.3. According to the equations, for example when the GAC particle size is reduced to one-tenth of the pilot-scale and x is generally taken as zero, EBCT is reduced to one-hundredth. Therefore, these filters work at very low EBCTs. As a result, very small columns are used in RSSCTs (Reinert, 2013).

Table 3.3. Basic mathematical equations used for RSSCT design (Reinert, 2013).

Parameter	Equation	Relationship
Scaling factor (SF)	$SF = \left[\frac{d_{p.LC}}{d_{p.SC}}\right]$	Provides initial basis for bench scale design dependence on GAC particle diameters (d_p)
Diffusion Coefficients (D)	$D_{SC} = \left[\frac{d_{p.SC}}{d_{p.LC}}\right]^{x} D_{LC} = [SF]^{-x} D_{LC}$	Dependence of intraparticle diffusivity on particle size
Empty Bed Contact Time (EBCT)	$\frac{EBCT_{SC}}{EBCT_{LC}} = \left[\frac{d_{p.SC}}{d_{p.LC}}\right]^{2} x \left[\frac{D_{LC}}{D_{SC}}\right]$	Empty bed contact time is related to the size of GAC in each adsorber and the dependence of intraparticle diffusivity on particle size
Design Factor (DF)	$\frac{EBCT_{SC}}{EBCT_{LC}} = \left[\frac{d_{p.SC}}{d_{p.LC}}\right]^{2-x} = \left[\frac{t_{SC}}{t_{LC}}\right] = [SF]^{x-2} = DF$	Provides relationship between scaling factor, empty bed contact time, intraparticle diffusivity, and times (t) to run the large column and small column

The most important point here is to provide a similitude between pilot-scale and small-scale columns by performing dimension analysis. If similarity is ideal, the RSSCT that uses a smaller adsorbent particle size compared to the pilot-scale adsorber, will have identical breakthrough as the pilot-scale process. Thus, it is possible to simulate pilot-scale performance by using different rapid small-scale columns. It is important that hydraulic loading and EBCT are selected appropriately in RSSCTs (Crittenden et al, 1986; Crittenden et al., 1991).

For example, when in pilot-scale experiments the column height is 74 cm, column diameter is 7.62 cm, GAC particle size is 1 mm, and in RSSCTs these parameters are 7.8 cm, 0.7 cm and 0.106 mm, respectively. Thus, while experiments continue for 7 months in order to reach breakthrough, it takes 22 days in RSSCTs (Reinert, 2013). By making the particle diameter of GAC smaller in small-scale columns than full-scale adsorber, in the small-scale column, the EBCT can be reduced. So, a smaller time is needed to reach breakthrough (DiGiano et al., 1999).

In a research, the feasibility of the RSSCT method for testing GAC in removing micropollutants from WWTP was investigated. For this purpose, effluent from a WWTP in Berlin/Germany was used in rapid small-scale columns. Results showed that the RSSCT system was applicable for testing GAC performance in removing micropollutants from WWTP effluent. RSSCTs' reproducibility and

robustness were satisfying for the experimental set-up used within this study. It is stated that RSSCTs can be used for comparing the performances of different GACs on removing micropollutants from WWTP effluents. Also, the performances of larger filters can be predicted using this rapid small-scale column method (Zietzschmann et al., 2014).

Overall, it is stated that the use of small-scale columns is very useful for the prediction of full-scale GAC columns. There are many advantages of using this method: it assesses the adsorption capacity and kinetics, has low capital and operational costs, etc. The small-scale columns can also be used to test different GACs before pilot testing. This will decrease the costs of pilot-scale systems (Crittenden et al., 1991).

According to the literature and the given information, RSSCTs have many advantages compared to the pilot-scale tests. So, this method was used for the experiments within the scope of this study.

3.5. Software Models for Simulating the RSSCTs

Several mathematical models can be used to simulate the adsorption behavior. Adsorption Design Software (AdDesignS^{TM}) developed by the National Center for Clean Industrial and Treatment Technologies at Michigan Technological University is a software model that provides evaluation and design systems which use granular activated carbon for the removal of contaminants from drinking water and wastewater. It consists of both equilibrium and mass transfer models, which can be used to simulate gas- and liquid-phase multicomponent adsorption in fixed bed adsorbers. There are three models in this software, namely the equilibrium column model (ECM), the constant pattern homogeneous surface diffusion model (CPHSDM), and the pore surface diffusion model (PSDM). These models can be used separately or in combination to provide the desired simulation depending upon the selected application.

The ECM is an adsorption model that ignores mass transfer resistance, uses Ideal Adsorbed Solution Theory (IAST) to predict the competitive adsorption effects in multi-component mixtures. The ECM can be used to determine the elution order of the adsorbing compounds, the highest carbon usage rate in multicomponent mixtures, and the highest effluent concentrations due to competitive adsorption.

The CPHSDM is an adsorption model for a single compound which is a favorably adsorbed compound ($n<1$). In situations where more than one component is present, ECM calculations can first

be performed to reduce the multicomponent system to a single target compound. Then, CPHSDM calculations can be performed with the target compound to obtain an estimate of the adsorbent usage rate. These types of calculations can be used for the early design stages to assess the cost effectiveness of using adsorption processes.

The PSDM is a dynamic fixed-bed model that includes the following assumptions:

- Flow rate is constant,
- Plug-flow conditions exist in the bed,
- Intraparticle mass flux is described by surface and pore diffusion,
- The Freundlich isotherm equation represents the adsorption equilibrium of individual compounds,
- There are no interactions between adsorbing compounds during the diffusion process.

Adsorption calculations using this model require equilibrium and kinetic parameters combined with several physical properties of the adsorbent and the adsorbing compound(s). PSDM requires much more calculation time than the two previous models but it results in breakthrough curves for each compound (Mertz et al., 1999).

The PSDM was used within the scope of this study for simulating the results of the experiments. This model was defined as an effective and useful method to simulate adsorption systems in different situations (Hand et al., 1997; Magnuson and Speth, 2005; Hristovski et al., 2008). By considering both surface and pore diffusion, the PSDM is referred as the most inclusive mass transfer model (Hand et al., 1997). This model in AdDesignS was also used for the simulation of adsorption in different studies. It was used to predict individual and competitive GAC column runs (Bausk, 2015; Patterson et al., 2019; Putz, 2004; Reinert, 2013; Stewart, 2011). Figure 3.8 shows the AdDesign software window where different parameters such as component properties (adsorption kinetics and equilibrium isotherm values), adsorber data (bed length, bed diameter, bed mass, flowrate, EBCT, etc) and adsorbent data (apparent density, particle radius, etc.) can be entered as inputs.

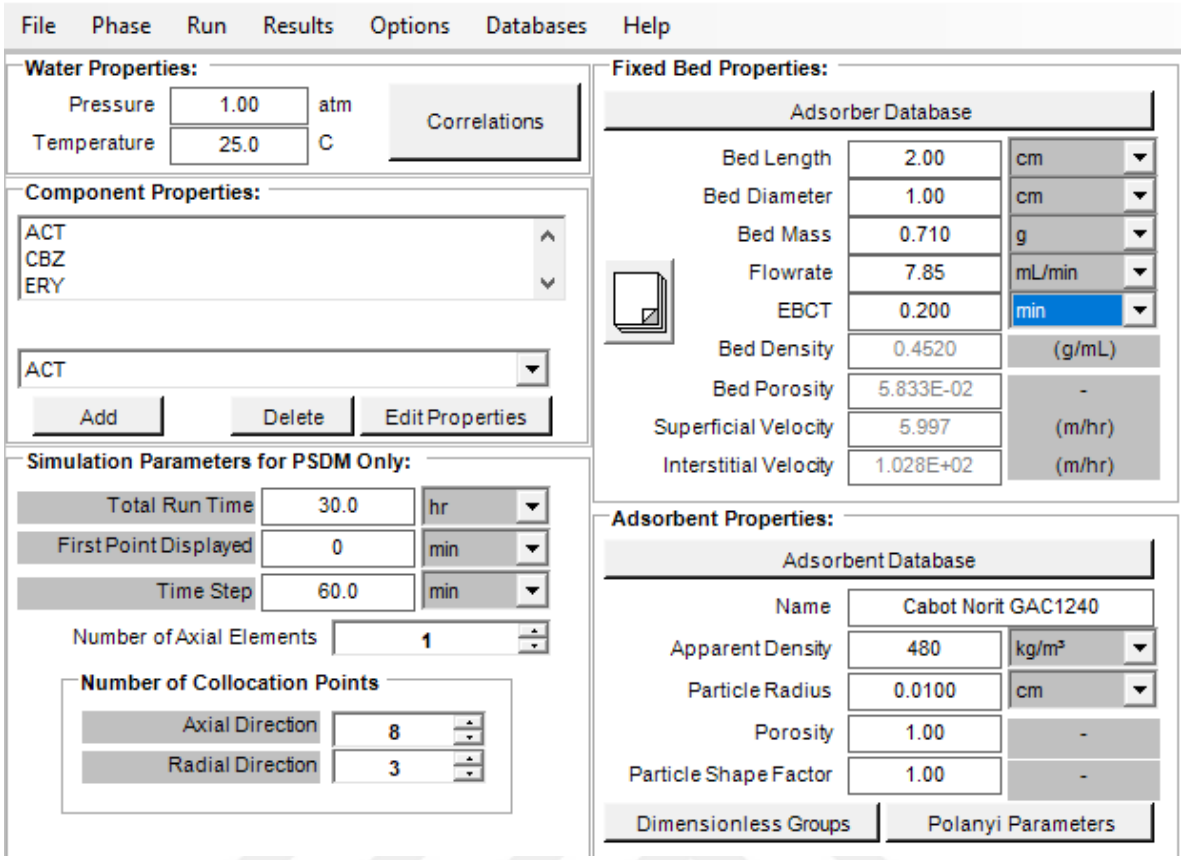

Figure 3.8. AdDesignS software window.

This model also calculates the film diffusion coefficient according to the Gnielinski correlation, the surface diffusion coefficient according to the Sontheimer correlation and the pore diffusion coefficient according to Hayduk and Laudie correlation for diffusion coefficient (Mertz et al., 1999). Equations are presented in Table 3.4.

Table 3.4. Equations of correlations for mass transfer coefficients (Mertz et al., 1999).

Correlations	**Equation**	
Gnielinski correlation for film diffusion coefficient (k_f)	$k_f = \frac{[1+15(1-\varepsilon)]\, D_L}{d_p}\left[2 + 0.644 Re^{1/2} Sc^{1/3}\right]$	d_p: adsorbent particle diameter D_L: adsorbate liquid phase diffusivity ε: bed void fraction Re: Reynolds number Sc: Schmidt number ε_p: porosity of the carbon C_0: initial inlet concentration τp: adsorbent tortuosity ρ_a: apparent adsorbent density q_0: solid phase concentration in equilibrium with C_o SPDFR: Surface to Pore Diffusion Flux Ratio V_b: molar volume of the chemical at the normal boiling point μ_L: water viscosity
Sontheimer correlation for surface diffusion coefficient (D_s)	$D_s = \frac{D_L\, \varepsilon_p\, C_0}{\tau_p \rho_a q_0}$ x SPDFR	
Hayduk and Laudie correlation for diffusion coefficient for pore diffusion coefficient (D_p)	$D_L = \frac{13.26 \times 10^{-5}}{\mu_L^{1.14}\, V_b^{0.589}}$ $D_p = \frac{D_L}{\tau_p}$	

Besides, dimensionless parameters are also calculated by the model. Some of these dimensionless parameters are Stanton number, Surface Biot number, Pore Biot number, Surface Diffusivity Modulus (Ed_s) and Pore Diffusivity Modulus (Ed_p). These values can be used to identify which mass transfer mechanism is controlling the adsorption process (Mertz et al., 1999). The equations of these parameters are presented in Table 3.5.

Table 3.5. Equations of dimensionless parameters (Crittenden et al. 2012; Worch, 2012).

Parameter	**Equation**	
Stanton number (St)	$\mathrm{St} = \frac{k_f t_r (1-\varepsilon_b)}{\varepsilon_b r_p}$	k_f: film mass transfer coeff. t_r: residence time ε_b: bed porosity r_p: particle radius C_0: initial concentration q_0: equilibrium loading related to the initial concentration, C_0 ρ_p: particle density D_s: surface diff. coeff. D_p: pore diff. coeff. ρ_b: Bed density ε_p: Particle porosity
Surface Biot number	$\mathrm{Bi} = \frac{k_f r_p C_0}{D_s \rho_p q_0}$	
Pore Biot number	$\mathrm{Bi} = \frac{k_f r_p}{D_p}$	
Solute distribution parameter (D_g)	$D_g = \frac{q_0 \rho_b}{C_0 \varepsilon_b}$	
Surface diffusivity Modulus (Ed_s)	$\mathrm{Ed_s} = \frac{D_s D_g t_r}{r_p^2}$	
Pore diffusivity Modulus (Ed_p).	$\mathrm{Ed_p} = \frac{D_p t_r (1-\varepsilon_b)\,\varepsilon_p}{r_p^2\,\varepsilon_b}$	

The Stanton number (St), and the diffusion modulus (Ed) describe the rate of the respective mass transfer process (film or surface/pore diffusion) compared to the rate of advection. The dimensionless Biot number (Bi) characterizes the relative influence of the external and internal mass transfer on the overall mass transfer rate and equals to St/Ed. Since film diffusion and surface diffusion are sequent processes, the slower process determines the overall kinetics. When Biot number is high, the film mass transfer becomes faster compared to the intraparticle mass transfer. In general, intraparticle mass transfer controls the adsorption rate at Bi>50, and film diffusion controls the adsorption rate at Bi<0.5. Both mechanisms are significant for the overall adsorption rate in the intermediate range (Worch, 2012). The value of these dimensionless groups can also be shown by the following equation:

$$\mathrm{St} = \mathrm{Bi}_s \times \mathrm{Ed_s} = \mathrm{Bi}_p \times \mathrm{Ed_p} \tag{3.9}$$

For example, if St is equal to 30, Ed_s is to 1 and Ed_p is to 0.1, it can be said that Bi_s (Surface Biot number) is 30 and the intraparticle diffusion mechanism is the controlling mechanism. Also, it can be concluded that the surface diffusion is 10 times faster than the pore diffusion and is the controlling diffusion mechanism inside the particle since these transport mechanisms act in parallel (Mertz et al., 1999).

For fitting the model data to experimental results, different methods were used in studies. Some of them were changing the isotherm parameter K, setting the n value the same for all components or varying the diffusion coefficient parameters. The purpose is to obtain the best fit of breakthrough curve from the model to the experimental results (Patterson et al., 2019; Putz, 2004; Reinert, 2013).

This method was used within the scope of this study to simulate the column experiments with GAC and the details were given in **Materials and Methods** section and results were presented in **Results and Discussion** section.

3.6. Grinding of Granular Activated Carbon for Application in RSSCTs

As mentioned before, GAC generally has a particle size of 0.2 – 5 mm. In order to use it in RSSCTs, the particle size should be smaller. Therefore, granular activated carbon is generally ground to desired sizes before use by different methods.

One of the methods used for grinding is using a mortar and pestle. In a study, the activated carbon samples that had different particle sizes were crushed using a mortar and pestle and then dry sieved by 63 μm sieve in order to obtain approximately 60 μm particle size. The schematic view of the method is given in Figure 3.9 (Shkal et al., 2018).

Figure 3.9. Schematic view of GAC grinding with a mortar and pestle.

In another study, three types of granular activated carbon samples with particle sizes ranging from 0.595 mm to 1.68 mm were first crushed by using a coffee grinder for few seconds and then crushed by using a mortar and pestle. After that it was wet sieved with deionized water through the mesh 140x170 which means the particle size ranges from 0.105 mm to 0.088 mm. Finally, the sample that had desired particle size was collected and stored (Ashani, 2017). The apparatus used for grinding procedure is given in Figure 3.10.

Mortar and pestle

Original and crushed GAC media

Figure 3.10. Apparutus used for grinding of GAC samples.

A Hamilton Beach blender is also used for grinding GAC particles. In a study, the GAC sample was ground for 20 seconds and it was sized using a sieve shaker. It is reported that the remaining part that was bigger than the desired range was ground for an additional 20 seconds and sieved again. Then, the particles were collected and stored in polypropylene bottles for use in future analyses (Patni et al., 2008).

The continuation of grinding until the desired particle size is also mentioned in another study. Two different kinds of GAC were used in analyses. For RSSCTs, GAC samples were crushed into smaller particle sizes and sieving was carried out with an electric sieve shaker. In the procedure a small volume of carbon was crushed using a ceramic mortar and pestle and the carbon was transferred to the top-most sieve periodically and the sieve cover was installed. Then, the sieve shaker was allowed to shake for 5-7 minutes. GAC remaining on the top sieve was returned to the mortar, ground again and the process was repeated. GAC retained in the desired size range was collected and stored in a desiccator for further experiments (Mastropole, 2011).

Although the mortar and pestle method and grinding with a blender are widely used for granular activated carbon grinding, there is a possibility of not having spherical shapes of activated carbon with these procedures. So, using a ball mill is another method that can be used.

SPEX Shaker Mill is one of the milling equipments. In this type of mill, about 10-20 gram of powder can be ground at a time. This device has a vial that contains the sample and the grinding

media, which is secured in the clamp and swung energetically back and forth several thousand times a minute. The back-and-forth shaking motion is combined with lateral movements of the ends of the vial. The milling media contains hard, spherical objects called “milling balls” and with each swing of the vial they impact against each other, both milling and mixing at the same time. Since the speed of the clamp motion is about 1200 rpm and ball velocities are high, on the order of 5 m/s, the force of the ball’s impact is generally great. The most common design of this type of mill has two vials milling the powders simultaneously in order to increase the throughput. There are various types of vial materials, such as hardened steel, zirconia, stainless steel, alumina, plastic, etc. There are researches of grinding different kinds of materials with these SPEX type mills (De Castro and Mitchell, 2002). The SPEX 8000D Mixer/Mill and stainless steel vial set are shown in Figure 3.11 and Figure 3.12, respectively. SPEX 8000D Mixer/Mill was used for grinding GAC particles in this study.

Figure 3.11. SPEX 8000D Mixer/Mill.

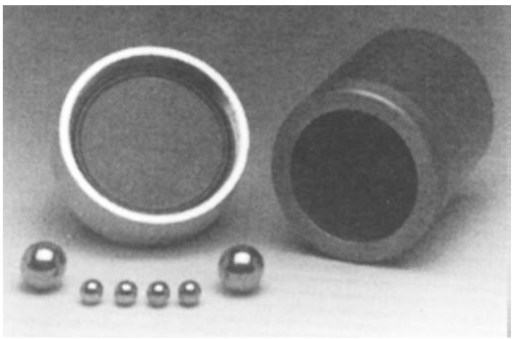

Figure 3.12. SPEX stainless steel vial set for SPEX 8000D Mill.

3.7. Analysis of Micropollutants

Analysis of emerging contaminants is difficult because of the diversity of chemical properties of compounds, their low concentrations (generally at μg/L or ng/L levels) and the complexity of matrices. There are different methods for analysis of different types of emerging contaminants, but LC-MS and GC-MS methods mainly in combination with solid-phase extraction (SPE) are being developed for the analysis of pharmaceuticals. Generally, GC and LC are used for separation and MS is used for detection widely. GC-MS analysis usually requires an additional derivatization because of the low volatility of pharmaceuticals, so sample preparation becomes time consuming and the possibility of contamination and errors increase.

In addition, some compounds, such as carbamazepine, decompose during GC analysis. Consequently, LC-MS and LC-MS/MS methods are used widely. The studies showed that LC-MS/MS can be used for assaying polar pharmaceuticals and their metabolites. Moreover, it is stated that the limits of detection achieved with LC-MS/MS methods were slightly higher than those obtained with GC-MS methods. But, LC-MS methodology showed advantages in terms of versatility and sample preparation is less complicated (Petrovic et al., 2003).

LC-MS/MS is claimed as a powerful analytical tool which is capable of screening samples for numerous compounds. It is able to analyze polar, non-polar and thermally labile compounds without extensive and time consuming sample preparation. Multiple Reaction Monitoring (MRM) is used because of its excellent selectivity, sensitivity and speed. Advanced software tools such as Scheduled MRM™ algorithm uses information of retention times to optimize automatically the MRM dwell time of each transition and total cycle time of the experiment resulting in highest data quality. To increase the confidence level in analytical results, QTRAP technology is used to acquire automatically fast and sensitive MS/MS spectra in Enhanced Product Ion (EPI) mode and to make search against mass spectral libraries for compound identification. As a result, the information of the complete molecular fingerprint saved into EPI spectra reduces the risk of false positive results (Latawiec and Schreiber, 2014; Schreiber, 2012).

In a study, a number of pharmaceuticals and personal care products (PPCP) were determined in surface waters by using LC-MS/MS. Water samples were injected into the LC-MS/MS directly to quantify the compounds at ng/L levels. MRM was used on an AB SCIEX QTRAP® 4500 system. Reproducibility and accuracy were increased by employing Scheduled MRM™ algorithm to maximize dwell times for each analyte. The method that was used provided very low detection limits

of common pharmaceuticals and personal care products. Limit of detection (LOD) in ng/L range was achieved even in the absence of any extensive sample preparation. It is stated that the large sample injection procedure provides an effective mechanism to monitor surface waters and drinking water for PPCP (Latawiec and Schreiber, 2014).

In this thesis study, for the analysis of selected micropollutants, LC-MS/MS method was used. The details of the method are given in the Materials and Methods Section.

4. MATERIALS AND METHODS

4.1. Estimation of Biodegradation Potential of Pharmaceuticals by BIOWIN Models

4.1.1. BIOWIN Models

Biodegradation is the major removal mechanism for most organics found in WWTPs. It depends on many factors such as molecular structure and environmental conditions. In a biological treatment unit, the main point is to estimate the biodegradation potential and biodegradation rate of a substance. Due to the complexity of this problem, some models have been developed to predict biodegradation. For example, BIOWIN models have been suggested as a screening tool to obtain information about the biodegradability of a vast number of substances found in water or wastewater. BIOWIN models belong to the EPI (Estimation Programs Interface) Suite (US EPA, 2012). EPI Suite™ is a Windows®-based program which provides users the estimates of physical/chemical and environmental fate properties. BIOWIN estimation tools consist of seven models. Six of them predict the rate of aerobic biodegradation of a chemical in the presence of mixed microbial populations (Dimitrov et al., 2007; Balakrishnan et al., 2020).

The values obtained from these models stand either for biodegradability or indicate the time required for biodegradation. In BIOWIN1 and BIOWIN2, the biodegradation rates are expressed as "fast biodegradation/does not biodegrade fast". On the other hand, BIOWIN3 and BIOWIN4 indicate the time required for ultimate and primary biodegradation, respectively. Primary biodegradation refers to the transformation of a parent compound to an initial metabolite. Ultimate biodegradation refers to the transformation of a parent compound to water, carbon dioxide, mineral oxides of any other elements present in the test compound, and new cell material. Also, BIOWIN5 and BIOWIN6 yield values standing for biodegradation rate. They classify compounds as "rapidly/not rapidly" biodegradable. These two models base on the Japanese MITI (Ministry of International Trade and Industry) ready biodegradation test. These models also use an approach similar to BIOWIN1 and BIOWIN2 (Dimitrov et al., 2007; Rücker and Kümmerer, 2012). More detailed information about the BIOWIN models can be found in a previous study (Çeçen and Gül, 2021).

4.1.2. BIOWIN Estimations in This Study

The biodegradation potential of 27 pharmaceuticals, which includes the pharmaceuticals chosen for this thesis study (**ACT**, **CBZ**, **ERY** and **SMX**), from four different drug classes under aerobic conditions was investigated. The first criterion in the selection of a pharmaceutical was its occurrence in a WWTP. A pharmaceutical with a high consumption rate is very likely to be found at a relatively high concentration in domestic wastewater. Another selection criterion was the octanol-water distribution coefficient (log K_{ow}). The log K_{ow} can be regarded as an indirect indication of the sorption capacity to biological sludge. As mentioned earlier, according to a classification, low, medium and high sorption potential is indicated by log K_{ow}<2.5, 2.5< log K_{ow}<4 and log K_{ow}>4, respectively (Rogers, 1996). In the present study pharmaceuticals with log K_{ow}<4 were selected. Due to the relatively lower sorption to sludge, a higher fraction of them would stay in liquid phase and be found at a relatively high concentration in secondary effluents unless sufficiently removed by biodegradation. In addition to these pharmaceuticals, three pharmaceuticals, namely diclofenac, azithromycin and glibenclamide, were selected from the group having log K_{ow}>4 in order to study the behavior of highly sorbing pharmaceuticals.

First, theoretical biodegradability of pharmaceuticals was searched using the BIOWIN models of the Estimation Programs Interface Suite. Then, the results were compared with experimental data from the literature. In evaluation of experimental results, biodegradation rates (k_{biol}) and biosorption of pharmaceuticals (log K_d) were considered.

Moreover, the BIOWIN results of **acetaminophen, carbamazepine, erythromycin** and **sulfamethoxazole** were compared with the biodegradation experiments carried out in this study. The outputs of the BIOWIN models 1-6 for the selected pharmaceuticals are given in the “Results and Discussion” section.

4.2. Selection of Micropollutants

In the scope of this study, 4 micropollutants: acetaminophen (ACT), carbamazepine (CBZ), erythromycin (ERY) and sulfamethoxazole (SMX) have been chosen for experimental studies. These micropollutants were chosen according to their octanol-water distribution coefficients (log K_{ow}). Micropollutants which have lower log K_{ow} adsorb to biological sludge less compared to more hydrophobic pollutants (log K_{ow} > 4). As a result, they are present at high concentrations in the effluent of secondary settling tanks. Moreover, pK_a ($-\log_{10}K_a$) is another property. K_a is the acid

dissociation constant of a solution. The pK_a value indicates the strength of an acid and the lower pK_a values show that the acid dissociates more in water. The properties of these micropollutants are given in Table 4.1.

Table 4.1. Properties of selected micropollutants.

Micropollutant	Subgroup	Chemical formula	Molecular weight (g/mol)	log K_{ow}	pK_a
Acetaminophen	Analgesic; anti-inflammatory	$C_8H_9NO_2$	151.165	0.46	9.38
Carbamazepine	Antiepileptic	$C_{15}H_{12}N_2O$	236.274	2.45	13.60
Erythromycin	Antibiotic	$C_{37}H_{67}NO_{13}$	733.937	3.06	8.86
Sulfamethoxazole	Antibiotic	$C_{10}H_{11}N_3O_3S$	253.276	0.89	pK_{a1} = 1.6; pK_{a2} = 5.7

4.3. Operation of Activated Sludge Reactors

One of the aims of this study was to investigate the biodegradation of selected pharmaceuticals. A pharmaceutical may be removed as a primary substrate by normal metabolism. In that case it serves as an energy- and growth substrate. On the other hand, if its concentration is very low, no net growth of biomass can take place. However, bacteria can still consume it in the presence of another substrate at a high concentration supporting the growth of the existing population. In this case, the substrate at the high concentration is defined as the primary substrate whereas the pharmaceutical becomes the secondary substrate. If a pharmaceutical is totally resistant to biodegradation under the specific redox condition, it can still be removed by another mechanism called cometabolism which is the biological transformation of a non-growth substrate by bacteria through enzymes which can only be induced in the presence of a primary substrate (Çeçen and Aktaş, 2011; Kılıç and Çeçen, 2023). This is most likely to happen in the presence of high nitrification activity at high sludge retention times during biological treatment. Furthermore, micropollutants can also be removed through heterotrophic cometabolism in an environment where organic matter is present.

For the purpose of investigating the biodegradation of pharmaceuticals, 5 L of concentrated activated sludge was taken from the recycle line of the Paşaköy Advanced Biological Wastewater Treatment Plant. Then, an activated sludge reactor (R1) having a volume of 4 L was started up in December 2022 and since then operated as a semi-continuously fed batch (SCFB) reactor. It was an operation that simulates the continuous-flow operation in batch type reactors. This reactor was fed with **Feed 1** which represents a domestic wastewater which has a C/N ratio of 10. The daily loading

rate is around 500 mg COD/L.day and 50 mg TKN/L.day. Daily 1/20 of the sludge was wasted from the reactor to have a sludge age of 20 days.

Additionally, in March 2023 another reactor (R2) was started up with the sludge taken from R1. It was also operated as a SCFB reactor. The feed of this reactor **(Feed 2)** consisted only of inorganic compounds and did not contain any organic carbon. It was rich in terms of ammonium sulfate for enhancement of nitrifying bacteria in R2. The aim was to investigate the biodegradation of pharmaceuticals in the presence of nitrification. The compositions of Feed 1 and Feed 2 are presented in Table 4.2.

Table 4.2. Composition of stock Feed 1 and stock Feed 2.

	Compounds	**Feed 1**	**Feed 2**
		Concentration (mg/L)	**Concentration (mg/L)**
Organics	D(+)-anhydrous glucose	5600	-
	Sodium acetate trihydrate	8000	-
	Peptone water	2000	-
Inorganics	Ammonium sulphate	4000	4714
	Sodium bicarbonate	2250	12000
	Di-potassium hydrogen phosphate	1000	1000
	Potassium dihydrogen phosphate	1000	1000
	Magnesium sulphate	1000	1000
	Manganese (II) sulfate monohydrate	25	25
	Calcium sulphate dihydrate	500	500
	Iron sulfate heptahydrate	343	343

In these two activated sludge rectors shown in Figure 4.1., Chemical Oxygen Demand (COD) (in R1) and NH_4-N (in R2), removal efficiencies and physical conditions, such as pH and temperature were monitored. For this purpose, regularly COD, NH_4-N, Mixed-Liquor Suspended Solids (MLSS), Mixed-Liquor Volatile Suspended Solids (MLVSS) and pH measurements were done. The information about the operation of the reactors is presented in detail in **Appendix A.** The sludges taken from these reactors were used to investigate the biodegradation potential of the selected pharmaceuticals shown in Table 4.1.

Figure 4.1. Activated sludge reactors (R1 and R2).

4.4. Biosorption of Pharmaceuticals by Activated Sludge

Biological removal may occur by biosorption of a pollutant or biodegradation by activated sludge. Within the scope of this study, biosorption of pharmaceuticals by activated sludge was investigated. Experiments were carried out in a total volume of 500 mL with R1 and R2 sludge (500 mg/L VSS) and selected pharmaceuticals (initial concentration of each one was 200 µg/L). 300 mg/L sodium azide (NaN_3) was also added in order to inhibit biodegradation. This way it would be possible to differentiate biosorption and biodegradation. Duration of the experiments was 15 days. Samples were taken at the beginning and at the end of the experiments. Figure 4.2 shows the experimental set.

Figure 4.2. The experimental set of biosorption experiment.

4.5. Biodegradation of Pharmaceuticals

4.5.1. Short-term Biodegradation Experiments

In this part, biodegradation kinetics of pharmaceuticals was studied. Experiments were carried out with R1 sludge and a mixture of the 4 selected pharmaceuticals (initial concentration of each one was 200 µg/L) in order to understand the biodegradation mechanisms. Erlenmeyer flasks were placed in an orbital shaker at 120 rpm and were kept a temperature of 25°C. The experiments were carried out with a total volume of 200 mL, at different activated sludge concentrations (20-500 mg/L). Figure 4.3 shows an example of a set of an experiment. Kinetic experiments were performed at the original pH of samples without the addition of a buffer. In order to monitor the pharmaceutical concentrations, samples were taken periodically during the experiments. The first experiment was carried out for 30 hours with only the mixture of pharmaceuticals and R1 sludge. The second experiment was carried out for 10 days with the addition of the synthetic secondary effluent for the purpose of investigating the biodegradation potential of pharmaceuticals in the presence of organic substances.

Figure 4.3. A set of a biodegradation experiment.

4.5.2. Long-term Biodegradation Experiments

In this part, biodegradation potential of the 4 selected pharmaceuticals in two types of activated sludge was investigated in a long term. Experiments were carried out in a total volume of 500 mL with R1 and R2 sludge (500 mg/L VSS) and with a mixture of pharmaceuticals (initial concentration of each one was 200 µg/L) for 49 days. These sludge samples from R1 and R2 were also continuously fed with Feed 1 and Feed 2 (Table 4.2), respectively. The purpose was to investigate the removal mechanisms (primary, secondary, cometabolic substrate, etc.) of micropollutants. It is known that generally in the presence of nitrification, cometabolic removal may occur. So, R2 sludge which was

enriched in terms of nitrifiers was used in order to observe the effect of nitrification on biodegradation of pharmaceuticals.

An experiment was also carried out with R1 sludge and a mixture of pharmaceuticals (200 µg/L of each) in the presence of 11.6 mg/L N-Allylthiourea (ATU) in order to inhibit the nitrification activity. During the experiment, R1 sludge was continuously fed with Feed 1. The purpose was to observe the removal of pharmaceuticals under heterotrophic activity only.

Additionally, experiments were carried out in a long term with individual pharmaceuticals (initial concentration of each one was 200 µg/L) and activated sludge samples (500 mg/L VSS) taken from R1 and R2 reactors.

4.6. Adsorption Experiments

4.6.1. Selection of Granular Activated Carbon

According to the properties of selected micropollutants, different kinds of granular activated carbons were searched and it was decided to use a coal-based activated carbon. Norit GAC 1240AF was suggested by Cabot considering the purpose of this study and it was selected for experiments. 500 g Norit GAC 1240AF sample was sent free of charge by the company. The properties of Norit GAC 1240AF activated carbon are given in Table 4.3.

Table 4.3. Properties of the granular activated carbon.

Activation Type	Steam activation
Iodine Number (mg/g)	min. 1000
Particle size > 12 mesh (1.70 mm) **Particle size < 40 mesh (0.425 mm)**	max. 5 mass-% max. 5 mass-%
Total Surface Area (B.E.T.)	1100 m^2/g
Mesopore Surface Area (S_{meso})	170 m^2/g (Sampaio et al., 2022)
Micropore Volume (V_{micro})	0.36 cm^3/g (Sampaio et al., 2022)
Specific Pore Volume (V_p)	0.54 cm^3/g (Sampaio et al., 2022)
Methylene Blue Adsorption	22
Apparent Density	470 kg/m^3
Density, backwashed and drained	415 kg/m^3
Moisture	max. 5%
pH	Alkaline
pH_{PZC}	7.6

4.6.2. Granular Activated Carbon Grinding

The particle size of selected GAC is around 1 mm. In order to use it in the rapid small scale column tests (RSSCTs), it should be ground into smaller sizes. Grinding process was carried out at the Istanbul Technical University Chemical and Metallurgical Engineering Faculty Metallurgical and Materials Engineering Laboratories. Since the scale factor was selected as 1/10, the desired particle size should be around 0.1 mm which is 100 μm.

Since there were Norit C Gran and Norit PKDA granular activated carbon samples from previous studies, these samples were used for optimization of the experiments. The grinding procedure was carried out in two steps. Firstly, the granular activated carbon was ground using SPEX type ball mill (Mixer/Mill 8000D) and then it was sieved by using Retch sieve shaker with different mesh sizes. Ball mill and sieve shaker are shown in Figure 4.4 and Figure 4.5, respectively. The ball mill was run with two vessels which contained alcohol for 15 minutes in order to clean the vessels before each run.

Figure 4.4. 8000D Mixer/Mill used for grinding GAC particles.

Figure 4.5. Retsch sieve shaker used for sieving GAC particles.

Different amounts of GAC and grinding balls were used in order to reach the desired particle size. For example, 4 g GAC and 24 g grinding balls were weighed and put in a vessel. The GAC and grinding balls that were weighed are shown in Figure 4.6. Two vessels were prepared for one run. Then, the vessels were put into the Ball Mill and run for 15 minutes at 1200 rpm. After that, GAC was separated from grinding balls and put in the sieve shaker which had different mesh size sieves for 10 minutes. The parts remaining on the different mesh size sieves were observed. As a result of several experiments, 10 g GAC grinding with 15 g grinding ball in Ball Mill for 4 minutes and 15 minutes in sieve shaker was decided as the grinding method.

Figure 4.6. GAC and grinding balls.

After the method was optimized, Norit GAC 1240 AF was ground. The original particle size of this GAC is around 1 mm and the desired particle size is 0.1 mm (100 µm). Firstly, the vessels were filled with alcohol and put into the Spex type Ball Mill. The ball mill was run for 15 minutes in order to clean the vessels. After that 10 g GAC and 15 g grinding ball were weighed and put in a vessel. Two vessels were prepared for one run and put in the ball mill for 4 minutes. Then, the GAC was separated from grinding balls and put in the sieve shaker which had four sieves with 71 µm, 100 µm, 125 µm and 150 µm mesh size. After 15 minutes, remaining GAC between 100 µm and 125 µm sieves was collected for further use in the experiments. The remaining parts of GAC on 125 µm and 150 µm sieves were separately collected and ground again in order to reach the desired particle size. Finally, all samples which have the particle size range between 100 µm and 125 µm were put in a bottle and stored for the next experiments. The GAC samples after sieving and final sample are shown in Figure 4.7 and Figure 4.8, respectively.

Figure 4.7. GAC after grinding and sieving.

Figure 4.8. Final GAC sample (particle size between 100 µm and 125 µm).

4.6.3. Preparation of Synthetic Secondary Effluent

In this study, a synthetic secondary wastewater which represents the secondary effluent of a WWTP was prepared in order to carry out the experiments in a controlled environment. Also, since a high volume of water was needed for the experiments, it was not possible to take real effluent samples from a WWTP continuously. The synthetic secondary effluent contains low amounts of organic substrates and different types of inorganic substrates. The composition and the characterization of this wastewater are presented in Table 4.4 and Table 4.5, respectively.

Table 4.4. Composition of synthetic secondary effluent.

Compounds	Concentration (mg/L)
Beef extract	1.8
Peptone	2.7
Humic acid	4.2
Tannic acid	4.2
(Sodium) lignin sulfonate	2.4
Sodium lauryle sulphate	0.94
Acacia gum powder	4.7
Ammonium sulfate ($(NH_4)_2SO_4$)	7.1
Monopotassium phosphate (KH_2PO_4)	7
Ammonium bicarbonate (NH_4HCO_3)	19.8
Magnesium Sulfate Trihydrate ($MgSO_4.3H_2O$)	0.71

Table 4.5. Characterization of synthetic secondary effluent.

Parameter	Value
DOC (mg/L)	6.01±1.9
NH_4-N (mg/L)	4.6±0.21
UV_{254} (1/cm)	0.171±0.008
Soluble UV_{254} (1/cm)	0.144±0.002
UV_{280} (1/cm)	0.155±0.008
Soluble UV_{280} (1/cm)	0.130±0.002
$Color_{436}$ (1/cm)	0.030±0.002
Soluble $Color_{436}$ (1/cm)	0.021±0.001
pH	6.94

4.6.4. Real Secondary Wastewater

In one case, 5 L of effluent from the Paşaköy Advanced Biological Wastewater Treatment Plant was taken in order to characterize and compare it with the synthetic secondary effluent prepared in this study. Table 4.6 shows the characterization of the real secondary effluent.

The concentrations of pharmaceuticals in the real effluent showed that ACT, ERY and SMX were lower than the average concentrations given in Table 3.1, whereas CBZ concentration was similar. On the other hand, all pharmaceuticals were found at lower concentrations in this real effluent compared to another study (Verlicchi et al., 2012).

Table 4.6. Real secondary effluent characterization.

Parameter	Value
DOC (mg/L)	7.9±1
COD (mg/L)	28.9±7
NH_4-N (mg/L)	0.27±0.05
pH	6.74
UV_{254} (1/cm)	0.206±0.04
Soluble UV_{254} (1/cm)	0.164±0.006
UV_{280} (1/cm)	0.165±0.035
Soluble UV_{280} (1/cm)	0.126±0.006
$Color_{436}$ (1/cm)	0.034±0.019
Soluble $Color_{436}$ (1/cm)	0.014
Temperature (°C)	19.2
Acetaminophen (µg/L)	0.009
Carbamazepine (µg/L)	0.524
Erythromycin (µg/L)	0.118
Sulfamethoxazole (µg/L)	0.056

4.6.5. Kinetic Experiments

4.6.5.1. Kinetic Experiments with the Synthetic Wastewater and GAC. Kinetic experiments were carried out in completely mixed batch reactors with synthetic secondary effluent and at different ground and original (non-ground) GAC doses in order to determine the time for adsorption to reach equilibrium (the balance between the GAC and liquid phase). In secondary effluent, there is background organic matter and this causes a competition between micropollutants and background organic matter. So, the experiments were carried out first with only background organic matter (synthetic secondary effluent) at 120 rpm and 25°C. The volume was 200 mL. pH was not adjusted at the beginning of experiments. pH of the synthetic wastewater was between 6.9 and 7.7. Figure 4.9 shows an example of a set of a kinetic experiment. During the experiments, bulk organic matter concentrations were monitored by measuring dissolved organic carbon (DOC) in all flasks hourly. Additionally, UV_{254}, UV_{280} and $Color_{436}$ of samples were also measured hourly for comparison. These parameters were chosen because of their ease of measurement and they represent aromatic and unsaturated organic compounds, lignin-derived compounds and color, respectively.

Figure 4.9. A set of a kinetic experiment.

4.6.5.2. Kinetic Experiments with Micropollutants and GAC. Kinetic experiments with a mixture of micropollutants in deionized water and different GAC doses were also carried out. Initial concentrations of 4 pharmaceuticals (ACT, CBZ, ERY and SMX) in the mixture were 1000 µg/L. The experiments were carried out at 120 rpm and 25ºC. The volume was 200 mL. Samples were taken hourly and filtered through 0.22 µm hydrophilic PTFE filters. Then, 0.8 mL MS-grade MeOH and 0.1 mL Internal Standard (100 µg/L methyl-d3-triphenylphosphonium iodide) were added to the vials.

4.6.6. Isotherm Experiments

After the equilibrium times were determined, isotherm experiments were carried out under the same conditions with synthetic secondary effluent at different ground and original (non-ground) GAC doses. The samples were taken at the beginning and at the equilibrium times (for example at 24^{th} or 120^{th} hour). DOC, COD, UV_{254}, UV_{280}, and $Color_{436}$ of samples were measured.

Additionally, isotherm experiments were carried out with pharmaceuticals in deionized water at different ground GAC doses. Isotherms were constructed a) with single pharmaceuticals in the presence of ground GAC, b) with a mixture of pharmaceuticals in the presence of ground GAC and c) with a mixture of pharmaceuticals in the presence of synthetic secondary effluent and ground GAC. Initial concentrations of pharmaceuticals were 1000 µg/L and GAC concentrations were 100, 200, 500, 750, 1000, 1500 and 2000 mg/L. The experiments were carried out for 24 hours with ground GAC at 120 rpm and 25ºC. The liquid volume was 200 mL. Samples were taken at the beginning and at the end of the experiments for the analyses.

Moreover, another isotherm experiment (t=24 hours) was also carried out with the mixture of pharmaceuticals and the real secondary effluent from the Paşaköy WWTP in order to observe the competition between micropollutants and background organic matter. Also, the results were

compared to the experiment with synthetic secondary effluent and the mixture of pharmaceuticals. GAC doses were 100, 200, 500, 750, 1000, 1500 and 2000 mg/L and the volume was 200 mL in all chambers. Samples were taken at the beginning and at the end of the experiment for the analyses.

4.7. Rapid Small-Scale Column Tests (RSSCTs)

A primary objective of this study was to investigate the removal of selected pharmaceuticals by adsorption onto granular activated carbon (GAC) in rapid small-scale columns. For this purpose, columns have been prepared with an inner diameter of 1 cm. The total length of columns was 10 cm, whereas 2 cm of them were filled with GAC. The rest of the column was filled with cotton and glass beads. A schematic diagram of a rapid small-scale column is shown in Figure 4.10.

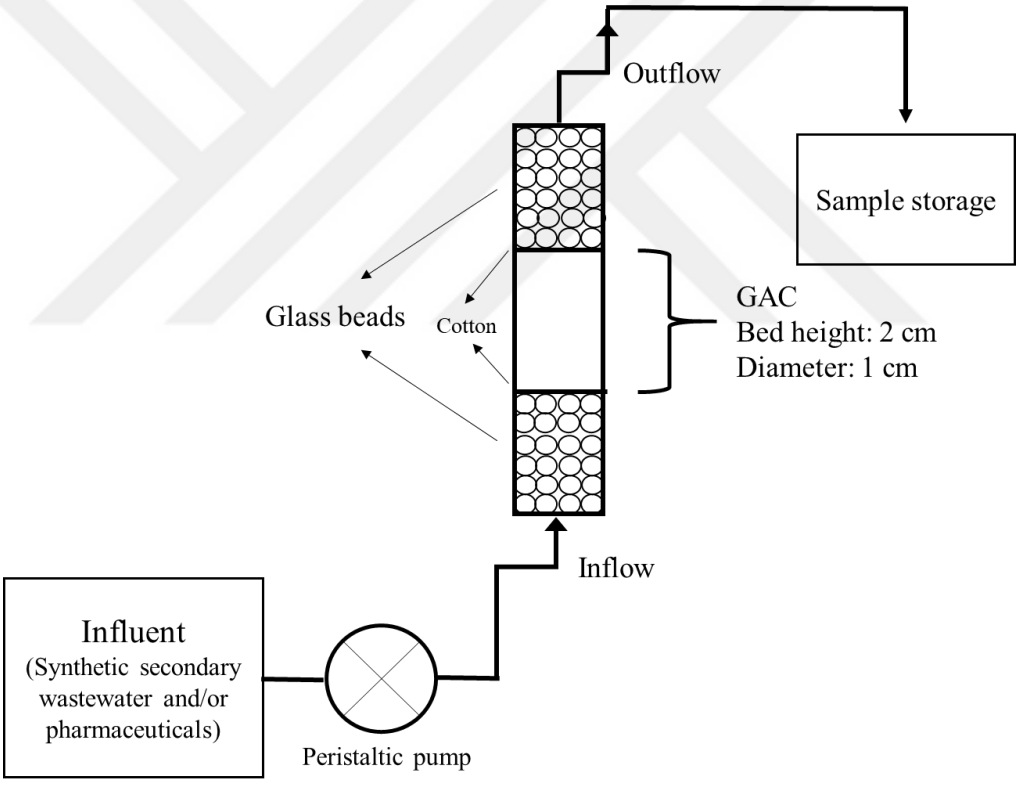

Figure 4.10. A schematic diagram of a small-scale column.

Figure 4.11 shows on the left the set-up for the Rapid/Small-Scale Column Tests (RSSCT) and on the right the column itself.

Figure 4.11. RSSCT set-up (left) and the small-scale GAC column (right).

The experiments were carried out with both original and ground GAC in order to make a comparison. Calculations were made according to the equations in Table 3.3 as mentioned before. Table 4.7 shows the operation conditions for RSSCTs with original and ground GAC.

Table 4.7. Operation conditions for RSSCTs.

GAC used in RSSCTs	Particle size (mm)	EBCT (min)	Flow rate (mL/min)
Original GAC	1	20	0.078
Ground GAC	0.1	0.20	7.85

The columns were fed with synthetic secondary effluent and/or a mixture of pharmaceuticals according to the purpose of different experiments. Samples were taken from the outflow for either the measurement of UV parameters and DOC or the analyses of pharmaceuticals.

4.7.1. RSSCTs with Biofilm

One of the aims of this study was to investigate whether Biological Activated Carbon (BAC) columns could be operated to observe both adsorption and biodegradation of selected micropollutants. As mentioned before, a microbiological film may form on GAC filters and they turn into BAC as time passes. This process combines the carbon adsorption and biological activity. Since empty-bed contact time (EBCT) is very small in GAC columns (0.20 minutes) there was no time for conversion of GAC to BAC filter. So, a known amount of ground GAC was contacted with an activated sludge sample (200 mg/L VSS) taken from the R1 reactor in an Erlenmeyer flask for 15 days. Synthetic domestic wastewater was added as a feed. After that, the column was filled with this GAC sample. Then a mixture of micropollutants (initial concentrations were all 200 μg/L) and

synthetic secondary effluent was fed to the column for 4 hours and 8 hours in two experimental sets. Samples were taken regularly for measuring pharmaceutical concentrations, UV_{254}, UV_{280}, $Color_{436}$ and DOC parameters during the experiment.

4.7.2. RSSCTs with Individual Pharmaceuticals

Two RSSCTs were carried out with CBZ and SMX in order to investigate the removal of individual pharmaceuticals by adsorption onto GAC. The columns were prepared as described in the previous section (Section 4.7). The initial concentrations of CBZ and SMX were 1000 μg/L and the duration of the experiments were 76 hours. Samples were taken regularly from the outflow of the column for the analyses of pharmaceuticals.

4.7.3. Tracer Test

A tracer test at 25°C was carried out to estimate the dispersivity parameters of the small-scale column used in the experiments. NaCl was used as the tracer. A GAC column was prepared as described before (Section 4.7). At the beginning the column was fed with deionized water for saturation, then 1 g/L NaCl was fed to the column. Samples were taken every two minutes and conductivity was measured by using WTW LF 320 Conductiviy Meter. When the NaCl concentration was equal to the initial concentration, the column was fed again with deionized water until the conductivity was approximately zero. The duration of the experiment was 120 minutes. The experimental data were compared with the following equation of 1-D advection-dispersion:

$$C\,(x,t) = \frac{C_0}{2}\left[\operatorname{erfc}\left(\frac{x-vt}{2\sqrt{D_x t}}\right) + \exp\left(\frac{vx}{D_x}\right)\operatorname{erfc}\left(\frac{x+vt}{2\sqrt{D_x t}}\right)\right] \quad (4.1)$$

where C_0 is influent concentration [M/L^3], V is velocity [L/T], D_x is longitudinal dispersion coefficient [L^2/T], x is length in the direction of flow [L], t is time [T]. The dispersion coefficient was determined such that the root mean square error of the sum of the squares difference between the predicted and measured effluent concentrations is minimum. Also, for calculations time that tracer spent in the inlet and outlet tubing was taken into consideration.

4.8. Use of a Mathematical Model for Simulating RSSCTs

The simulation model AdDesignS^{TM} was used to obtain breakthrough curves fitting the experimental results from RSSCTs and simulate the tests for longer time periods. The PSDM model was used within the scope of this study as mentioned before. Firstly, properties of pharmaceuticals, isotherm parameters from batch experiments, properties of activated carbon and column parameters were used as inputs to obtain breakthrough curves. Then, for calibrating the model, isotherm parameters (n values) and film diffusion coefficients were modified. For film diffusion coefficients values from 0.002 cm/s to 0.2 cm/s were tried in different runs. The change in n values of pharmaceuticals was 10%. The purpose was to obtain the best fit of breakthrough curves. After that, additional column tests were run for longer time periods to obtain the full breakthrough ($C/C_0=1$) and observe the adsorption behavior of pharmaceuticals.

4.9. Adsorption and Biodegradation Experiments in Batch Reactors with Individual Pharmaceuticals

The purpose of this step was to investigate the synergistic effect of granular activated carbon (GAC) and activated sludge on the removal of pharmaceuticals. For this purpose, two pharmaceuticals, namely carbamazepine (CBZ) and sulfamethoxazole (SMX) were chosen according to their biodegradation and adsorption potential in previous experiments. The experiments showed that these pharmaceuticals were slowly biodegraded by activated sludge and moderately adsorbed by GAC. In the experiments 500 mg/L GAC and activated sludge sample from R1 reactor (500 mg/L VSS) were used. Initial concentration of CBZ and SMX was 1000 µg/L. The details of the experiments were given in Table 4.8. Duration of the experiments was 4 days. Samples were taken hourly in the first day and daily in the rest of the experiments. Figure 4.12 shows the set of an experiment with CBZ.

Table 4.8. The details of the experiments.

Number of batch reactor	Feed
1	Control (1000 µg/L CBZ or SMX)
2	1000 µg/L CBZ or SMX + 500 mg/L GAC
3	1000 µg/L CBZ or SMX + 500 mg/L R1 sludge
4	1000 µg/L CBZ or SMX + 500 mg/L R1 sludge + 500 mg/L GAC

Figure 4.12. The set of an experiment with CBZ.

4.10. Analysis of Micropollutants

Presence and concentrations of selected micropollutants were determined by LC-MS/MS.

4.10.1. Method Development

Before the start of experiments, a significant part of the present study was devoted to method development for pharmaceutical measurements. LC-MS/MS (API Q-Trap 4500 triple quadrupole linear ion trap mass spectrometry) was used for both qualitative and quantitative analysis of pharmaceuticals. The properties of AB Sciex QTrap 4500 LC-MS/MS are given in Table 4.9 and the device is shown in Figure 4.13.

Table 4.9. Properties of AB Sciex QTrap 4500 LC-MS/MS.

Mass Range	Triple quadrupole: 5 – 2000 Da Linear ion trap: 50 - 2000 Da
Polarity Switching	50 msec in MRM Scheduled MRM modes
Detector Type	AcQuRate Pulse Counting CEM
Scan Types	Q1 MS, Q3 MS, Product Ion, Precursor Ion, MRM, MS^3, MRM^3, TripleTrap Scanning

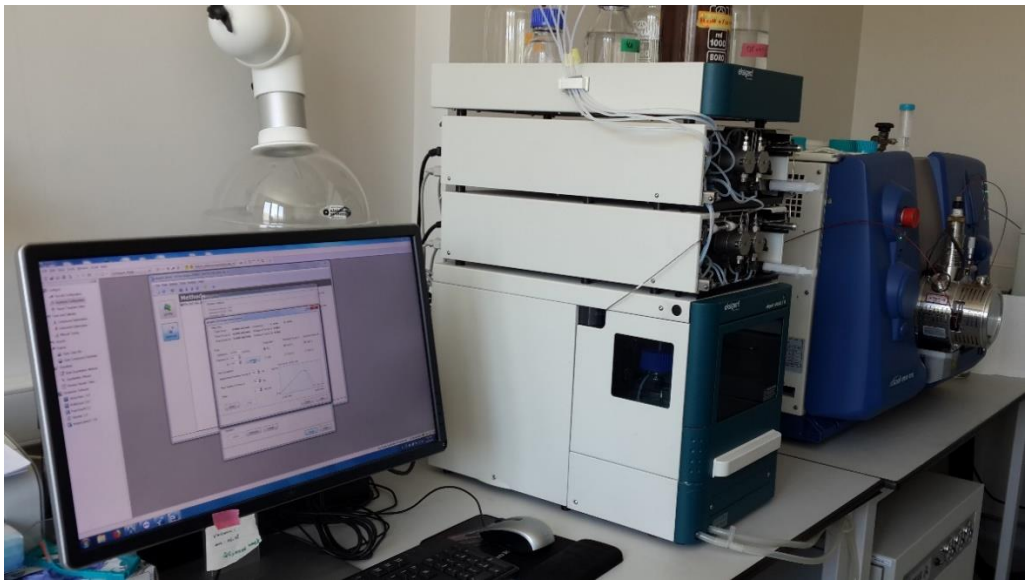

Figure 4.13. AB Sciex QTrap 4500 LC-MS/MS.

The Accucore aQ C18 column from Thermo Fisher Scientific was employed, and methyl-d3-triphenylphosphonium iodide was used as the internal standard. A binary solvent system was used as mobile phases, consisting of MS-grade methanol buffered with 0.1% formic acid (Pump A) and MS-grade water buffered with 0.1% formic acid (Pump B).

The analysis methodology is as follows: First, 1 mL of the sample was mixed with 0.8 mL of LC-grade methanol and filtered through a 0.22 μm porous syringe filter. Then, 0.9 mL of the filtered sample was placed in an HPLC vial, along with 0.1 mL of internal standard (IS) solution prepared at a concentration of 100 μg/L. Determination of pharmaceuticals in filtered samples was performed at the μg/L level, using non-scheduled multiple reaction monitoring (MRM) parameters for each pharmaceutical. The detection of pharmaceuticals based on scheduled MRM (sMRM) was performed using the ESI probe operating in a positive ionization mode. The source parameters for ESI positive mode were as follows: curtain gas (CUR): 30; ion spray voltage (IS): 5500 V/ 4500 V; temperature (TEM): 550°C; ion source gas 1 (GS1): 50 and ion source gas 2 (GS2): 60. For instrument control and data acquisition the Analyst Software 1.6.2 (AB Sciex) and MultiQuant 3.0.1 (AB Sciex) programs were used. A representative LC-MS/MS chromatogram of 4 selected pharmaceuticals and internal standard (methyl-d3-triphenylphosphonium iodide) is shown in Figure 4.14.

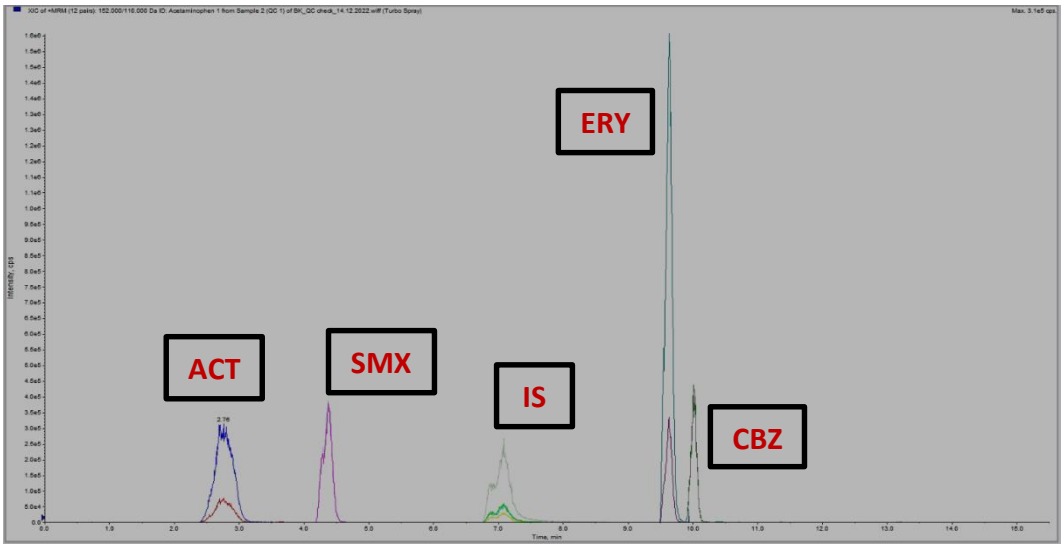

Figure 4.14. LC-MS/MS chromatogram of a sample containing ACT, CBZ, ERY, SMX and methyl-d3-triphenylphosphonium iodide (IS).

4.11. Analytical Methods

4.11.1. Total/Dissolved Organic Carbon Measurements

Total Organic Carbon (TOC) and Dissolved Organic Carbon (DOC) measurements were carried out during the experiments in order to observe the changes in the organic matter of samples. For this purpose, Shimadzu TOC-V WP Analyzer was used. For DOC measurements samples were filtered through 0.45 µm Hydrophilic PTFE filter in order to remove granular activated carbon particles.

4.11.2. Chemical Oxygen Demand (COD) Analysis

COD analyses were done to determine the change in organic matter during the experiments. Moreover, these analyses were carried out as an alternative method for DOC analyses and also for comparison. The dichromate closed reflux and colorimetric method was used. The soluble COD (SCOD) of samples were determined after filtering through 0.45 µm Hydrophilic PTFE filters. Samples were refluxed with diluted potassium dichromate ($K_2Cr_2O_7$) and concentrated sulfuric acid (H_2SO_4) for two hours at 150°C in the ECO 25 Thermoreactor COD digester, in the presence of Ag_2SO_4 as catalyst and $HgSO_4$ to prevent chloride interference. The digested samples were measured colorimetrically at 600 nm with the Hach DR3900 Spectrophotometer. Deionized water treated with the dichromate solution and sulfuric acid was used as reference and the difference between the absorbance of reference and sample was used to calculate COD of samples.

4.11.3. Spectrophotometric Measurements

Spectrophotometric measurements of samples were mainly carried out at wavelengths of 254 nm for aromatic and unsaturated organic compounds, 280 nm for lignin-derived compounds and 436 nm for color. All samples were filtered through 0.45 μm Hydrophilic PTFE filters to remove GAC particles and 1 cm quartz cells were used. For the absorbance measurements, Shimadzu UV-160A UV-Visible Recording Spectrophotometer was used. The absorbances were measured three times and the averages were reported.

4.11.4. pH Analysis

WTW Inolab-1 pH meter was used for pH measurements. The calibration of the pH probe was done every 2 or 3 weeks by using standard buffer solutions having pH values of 4 and 7.

4.11.5. Mixed Liquor Suspended Solid (MLSS) and Mixed Liquor Volatile Suspended Solid (MLVSS) Analysis

For the MLSS analysis, 10 mL sample was filtered through filter paper (Sartorius Stedim Biotech Glassfiber Prefilter 0.45 μm) and the residue on the filter paper was dried for one hour at 103^{o}C in the FN500 oven. For MLVSS analysis, the residue was ignited after MLSS analysis for 30 minutes at 550^{o}C in the Protherm muffle furnace. All MLSS and MLVSS analysis were done in duplicates and the averages were reported.

4.11.6. NH_4-N Analysis

The Nessler Method was used in NH_4-N analyses. For this purpose, the Method 8038 in the Hach Water Analysis Handbook, 5th edition was followed and Hach DR3900 Spectrophotometer was used. After necessary dilutions, 3 drops of Hach Mineral stabilizer, 3 drops of Hach Polyvinyl alcohol dispersing agent and 1 mL Merck Nessler reagent were added to 25 mL sample and 25 mL deionized water as the blank. After one minute, NH_4-N concentration of the sample was read in mg/L by using the spectrophotometer.

5. RESULTS AND DISCUSSION

5.1. Biodegradation of Selected Pharmaceuticals: Comparison of BIOWIN Estimations and Experimental Findings

5.1.1. BIOWIN Outputs

The selected compounds and the BIOWIN models outputs are given in Table 5.1 and Table 5.2, respectively. Pharmaceuticals that were used in biodegradation/adsorption experiments in this study are highlighted.

Table 5.1. Properties of pharmaceuticals.

Name	Group	CAS number	Formula	log K_{ow}
Acetaminophen	Anti-inflammatory	**103-90-2**	**$C_8H_9NO_2$**	**0.46**
Ibuprofen		15687-27-1	$C_{13}H_{18}O_2$	3.97
Diclofenac		15307-86-5	$C_{14}H_{11}Cl_2NO_2$	4.51
Tramadol		27203-92-5	$C_{16}H_{25}NO_2$	3.01
Naproxen		22204-53-1	$C_{14}H_{14}O_3$	3.18
Ketoprofen		22071-15-4	$C_{16}H_{14}O_3$	3.12
Codeine		76-57-3	$C_{18}H_{21}NO_3$	1.19
Fenoprofen		71720-56-4	$C_{15}H_{14}O_3$	3.90
Nimesulide		51803-78-2	$C_{13}H_{12}N_2O_5S$	2.60
Phenazone		60-80-0	$C_{11}H_{12}N_2O$	0.38
Erythromycin	Antibiotic	**114-07-8**	**$C_{37}H_{67}NO_{13}$**	**3.06**
Sulfamethoxazole		**723-46-6**	**$C_{10}H_{11}N_3O_3S$**	**0.89**
Trimethoprim		738-70-5	$C_{14}H_{18}N_4O_3$	0.91
Clarithromycin		81103-11-9	$C_{38}H_{69}NO_{13}$	3.16
Ciprofloxacin		85721-33-1	$C_{17}H_{18}FN_3O_3$	0.28
Azithromycin		83905-01-5	$C_{38}H_{72}N_2O_{12}$	4.02
Sulfamethazine		57-68-1	$C_{12}H_{14}N_4O_2S$	0.14
Norfloxacin		70458-96-7	$C_{16}H_{18}FN_3O_3$	0.46
Ofloxacin		82419-36-1	$C_{18}H_{20}FN_3O_4$	-0.39
Amoxicillin		26787-78-0	$C_{16}H_{19}N_3O_5S$	0.87
Carbamazepine	Antiepileptic	**298-46-4**	**$C_{15}H_{12}N_2O$**	**2.45**
Lamotrigine		84057-84-1	$C_9H_7Cl_2N_5$	2.57
Pregabalin		148553-50-8	$C_8H_{17}NO_2$	-1.78
Diazepam		439-14-5	$C_{16}H_{13}ClN_2O$	2.82
Phenobarbital		50-06-6	$C_{12}H_{12}N_2O_3$	1.47
Metformin	Anti-diabetic	657-24-9	$C_4H_{11}N_5$	-2.64
Glibenclamide		10238-21-8	$C_{23}H_{28}ClN_3O_5S$	4.79

According to BIOWIN1 and 2 values, all pharmaceuticals in the anti-inflammatory group are biodegraded fast, except for diclofenac and tramadol, while in the antibiotics group, only trimethoprim and amoxicillin are classified as fast biodegraded pharmaceuticals. Moreover, in the antiepileptics, lamotrigine is not biodegraded fast and glibenclamide in the anti-diabetic group is not biodegraded fast according to BIOWIN2 value. BIOWIN5 and 6 values also indicate that among all these pharmaceuticals, only acetaminophen (BIOWIN6 is 0.5090) and pregabalin (BIOWIN5 is 0.5006) are rapidly biodegradable, but since these values are very close to 0.5, these pharmaceuticals can also be classified as not rapidly biodegradable.

When BIOWIN3 and 4 values are taken into consideration, the time required for primary biodegradation of pharmaceuticals in the anti-imflammatory group varies between days and weeks, whereas the time required for ultimate biodegradation is from weeks to months. In the antibiotic group, erythromycin, clarithromycin, azithromycin and ofloxacin can be classified as refractory according to their BIOWIN3 values. Ultimate biodegradation of sulfamethoxazole, sulfamethazine and amoxicillin would take place in weeks or months while trimethoprim, ciprofloxacin and norfloxacin would require months. Among these pharmaceuticals in this group amoxicillin may be converted into smaller compounds within days with regard to BIOWIN4 value.

In the group antiepileptic, BIOWIN3 values show that the ultimate biodegradation of pregabalin would take place in weeks, while carbamazepine, diazepam and phenobarbital would require weeks or months. Ultimate biodegradation of lamotrigine requires longer time, at the order of months. BIOWIN4 values show that the primary biodegradation of pregabalin would take place within days. On the other hand, days or weeks are required for primary biodegradation of carbamazepine, diazepam and phenobarbital. Additionally, the time for lamotrigine to be converted into smaller compounds would be weeks. Among the pharmaceuticals in this group, lamotrigine seems to be resistant to biodegradation. In the anti-diabetic group, ultimate biodegradation of metformin would require weeks according to BIOWIN3 value. On the other hand, glibenclamide can be classified as refractory. BIOWIN4 values indicate that primary biodegradation of glibenclamide would be subject to primary degradation in weeks, but it may not reach ultimate degradation (BIOWIN3). In the case of metformin, primary degradation takes place earlier, in days or weeks. Thus, in any case metformin seems to be more biodegradable than glibenclamide (Kılıç and Çeçen, 2023).

Table 5.2. BIOWIN outputs of pharmaceuticals.

Name	BIOWIN 1	BIOWIN 2	BIOWIN 3	BIOWIN 4	BIOWIN 5	BIOWIN 6
	> 0.5: fast biodegradation < 0.5: not to degrade fast		5–4.75: hours 4.75–4.25: hours to days 4.25–3.75: days 3.75–3.25: days to weeks 3.25–2.75: weeks 2.75–2.25: weeks to months 2.25–1.75: months < 1.75: refractory		≥ 0.5: rapidly biodegradable < 0.5: not rapidly biodegradable	
Acetaminophen	**1.0015**	**0.9886**	**2.8673**	**3.8748**	**0.4866**	**0.5090**
Ibuprofen	0.8314	0.8672	2.9582	3.7986	0.1976	0.1521
Diclofenac	0.1353	0.0027	2.2863	3.2984	-0.1313	0.0029
Tramadol	0.3649	0.0810	2.0921	3.1034	0.2815	0.0823
Naproxen	0.8972	0.9611	2.9219	3.9097	0.4439	0.3447
Ketoprofen	0.8888	0.8770	2.9265	3.7806	0.3192	0.1848
Codeine	0.6931	0.7316	2.0396	3.1895	0.4191	0.0606
Fenoprofen	1.0196	0.9921	2.9174	3.8972	0.4324	0.3434
Nimesulide	0.5557	0.5423	2.3121	3.3765	-0.1313	0.0015
Phenazone	0.7860	0.8943	2.8052	3.5811	0.2003	0.0962
Erythromycin	**-1.4385**	**0.0000**	**1.2404**	**2.5869**	**-0.1005**	**0.0000**
Sulfamethoxazole	**0.4479**	**0.1281**	**2.4297**	**3.3054**	**-0.1165**	**0.0060**
Trimethoprim	0.5922	0.9164	2.0385	3.3749	0.0889	0.0172
Clarithromycin	-1.7926	0.0000	1.2007	2.5569	-0.1403	0.0000
Ciprofloxacin	-0.3974	0.0000	1.9170	3.2138	0.0597	0.0001
Azithromycin	-1.6578	0.0000	0.9748	2.2994	-0.3277	0.0000
Sulfamethazine	0.4906	0.1549	2.2994	3.2007	-0.1496	0.0040
Norfloxacin	-0.3916	0.0000	1.9435	3.2311	0.0934	0.0001
Ofloxacin	-0.6388	0.0000	1.5132	2.9163	0.0204	0.0001
Amoxicillin	1.1523	0.9843	2.5166	4.0465	0.2859	0.0160
Carbamazepine	**0.6351**	**0.4143**	**2.6770**	**3.5068**	**0.0873**	**0.0364**
Lamotrigine	-0.2067	0.0002	1.9501	2.9308	-0.3281	0.0006
Pregabalin	0.8983	0.9242	3.2363	4.0469	0.5006	0.4767
Diazepam	0.7678	0.8085	2.3311	3.4819	0.0837	0.0217
Phenobarbital	0.5811	0.4469	2.4958	3.3641	0.1798	0.0612
Metformin	0.6861	0.7640	2.9137	3.6614	0.3287	0.2379
Glibenclamide	0.7267	0.3764	1.7137	3.1837	-0.2668	0.0005

5.1.2. Comparison of BIOWIN Outputs with the Experimental Data in Literature

The BIOWIN outputs are compared with the experimental results obtained in a high number of studies reported in literature. These studies were carried out on biodegradation and sorption of various pharmaceuticals. Most of them originate from laboratory-scale aerobic biological treatment units, primarily activated sludge. The details of the comparison for ACT, CBZ, ERY and SMX are presented in a previous study (Çeçen and Gül, 2021). For other pharmaceuticals, results are discussed in another study (Kılıç and Çeçen, 2023).

It was seen that in general BIOWIN estimations were in accordance with experimental data in literature. However, in some cases experimental results indicated slightly higher biodegradation than predicted from BIOWIN models. It can be said that BIOWIN models tend to slightly underestimate the biodegradation of pharmaceuticals. This is mainly due to the fact that these models take only the single substance into consideration. However, in real systems the wastewater is composed of several substances and a complex microbial ecology is encountered.

Moreover, BIOWIN models use the molecular structure alone in order to estimate the biodegradability. However, it was shown in the literature studies that biodegradation of pharmaceuticals may be enhanced at different operation conditions, such as longer SRT, higher nitrification activity and the presence of easily biodegradable bulk organic matter. These conditions may lead to the removal of pharmaceuticals removal by co-degradation or cometabolism. In particular, the role of nitrification is very evident. SRTs longer than 20 days enhance nitrification rate and thus also the cometabolic removal of pharmaceuticals. Moreover, sorption of pharmaceuticals onto sludge may also be a factor.

Thus predictive tools such as BIOWIN models are be very helpful for having an initial idea about biodegradability of pharmaceuticals under aerobic conditions. These models can also be used for experimental design. However, there is probably a need for their improvement considering the experiences gained from experimental studies (Çeçen and Gül, 2021; Kılıç and Çeçen, 2023).

5.2. Biological Removal of Pharmaceuticals

5.2.1. Biosorption of Pharmaceuticals by Activated Sludge

Biosorption experiments were carried out with both R1 and R2 sludge, in order to observe the sorption of pharmaceuticals to activated sludge. Results showed that biosorption of the selected pharmaceuticals (ACT, CBZ, ERY and SMX) by both activated sludges (R1 and R2) was low. Table 5.3 shows that around 16% of ACT was sorbed by R1 and R2 sludges, followed by ERY and SMX with around 12% and 5%, respectively. Additionally, CBZ was sorbed only 4%, while it was not sorbed by R2 sludge.

As mentioned earlier, solid-water partition coefficient K_d is generally used to express sorption. For a compound under equilibrium conditions, the concentration sorbed onto sludge (C_{sorbed}) is assumed to be proportional to the concentration in solution ($C_{dissolved}$):

$$C_{sorbed} = K_d \,.\, SS \,.\, C_{dissolved} \qquad (5.1)$$

where C_{sorbed} is the sorbed concentration of compound (µg/L), K_d is the solid-water partition coefficient (L/g SS), SS is the suspended solids concentration (g/L) and $C_{dissolved}$ is the dissolved concentration of compound (µg/L). By using Equation 5.1, the K_d values of pharmaceuticals were calculated and presented in Table 5.3. Sorption onto R2 sludge (rich in nitrifiers) was less for all pharmaceuticals compared to R1 sludge. According to K_d values, sorption of ACT onto sludge was the highest followed by ERY, SMX and CBZ.

Table 5.3. Biosorption of pharmaceuticals by activated sludge.

Pharmaceutical	R1 Sludge (500 mg/L)				R2 sludge (500 mg/L)			
	Initial conc. (µg/L)	Final conc. (µg/L)	Sorption (%)	K_d (L/g SS)	Initial conc. (µg/L)	Final conc. (µg/L)	Sorption (%)	K_d (L/g SS)
ACT	173.1	143.8	17	0.409	168.9	144.1	15	0.343
CBZ	120.2	115.6	4	0.080	114.6	114.5	0	0.002
ERY	132.4	115.2	13	0.300	140.3	125.1	11	0.243
SMX	167.9	158.5	6	0.118	261.5	252.3	4	0.073

All K_d values were lower than 0.5 L/g SS which indicates that the sorption of these pharmaceuticals onto activated sludge was negligible. So, it can be said that biosorption is negligibly small and biodegradation is the main mechanism of their removal. These results are also in

accordance with other studies in the literature. The log K_{ow} values of these pharmaceuticals was low indicating low/medium sorption capacity to sludge. As reported in a study, experimental studies also showed that sorption of ACT, CBZ, ERY and SMX was very low (Çeçen and Gül, 2021).

5.2.2. Biodegradation Experiments

As mentioned in Section 4.1, the results of biodegradation experiments carried out in the present doctoral study were compared with the predictive BIOWIN results of acetaminophen (ACT), carbamazepine (CBZ), erythromycin (ERY) and sulfamethoxazole (SMX).

5.2.2.1 Short-term experiment without background organic matter. A short-term experiment was carried out for 30 hours with sludge taken from the R1 reactor for trial purposes in order to observe the decrease in the concentrations of pharmaceuticals in the presence of biological activity. In this experiment there were only a mixture of pharmaceuticals (200 µg/L of each) and different concentrations of activated sludge (AS) taken from the R1 reactor (20, 50, 100, 200 and 500 mg/L VSS) which contained both heterotrophic and nitrification activity. A steady concentration was reached in pharmaceuticals after 30 hours. Results showed that ACT was the most biodegraded pharmaceutical at the end of 30 hours compared to others. At all AS concentrations, the degradation efficiencies of CBZ, ERY and SMX were less than 20%, while it was higher than 50% for ACT. These results are in accordance with the BIOWIN estimations. BIOWIN 1 and 2 results indicate fast biodegradation for ACT, while not fast biodegradation for CBZ, ERY and SMX. According to BIOWIN calculations, primary biodegradation of ACT takes place in days, whereas days/weeks are necessary for CBZ and SMX and weeks/months are necessary for ERY. The decrease in concentrations of pharmaceuticals are presented in Figure 5.1, Figure 5.2, Figure 5.3 and Figure 5.4, respectively.

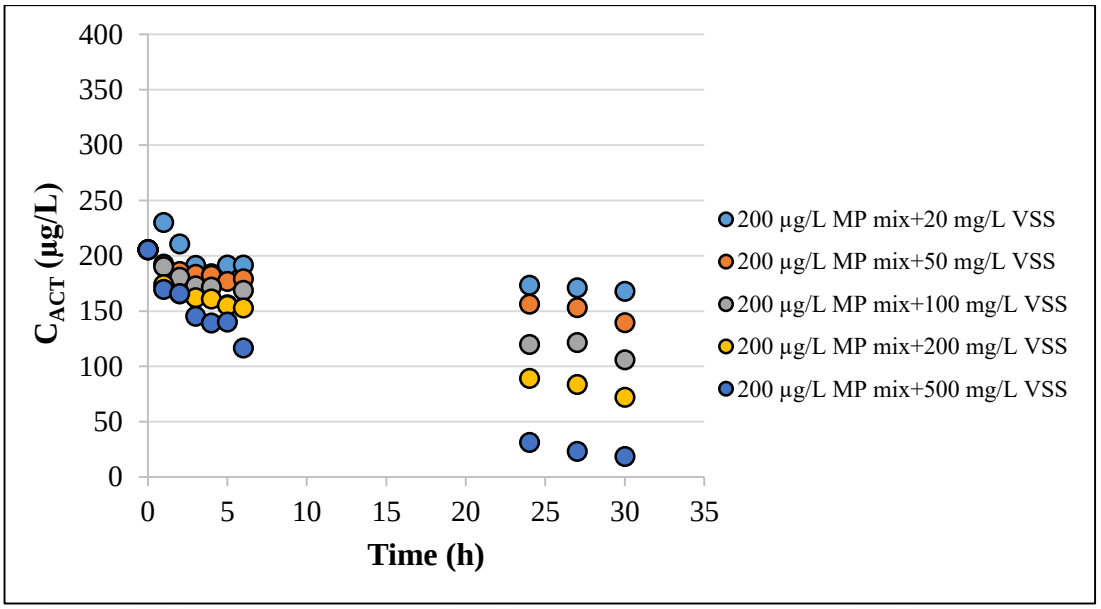

Figure 5.1. Decrease in the ACT concentration in the short-term experiment in a mixture of pharmaceuticals.

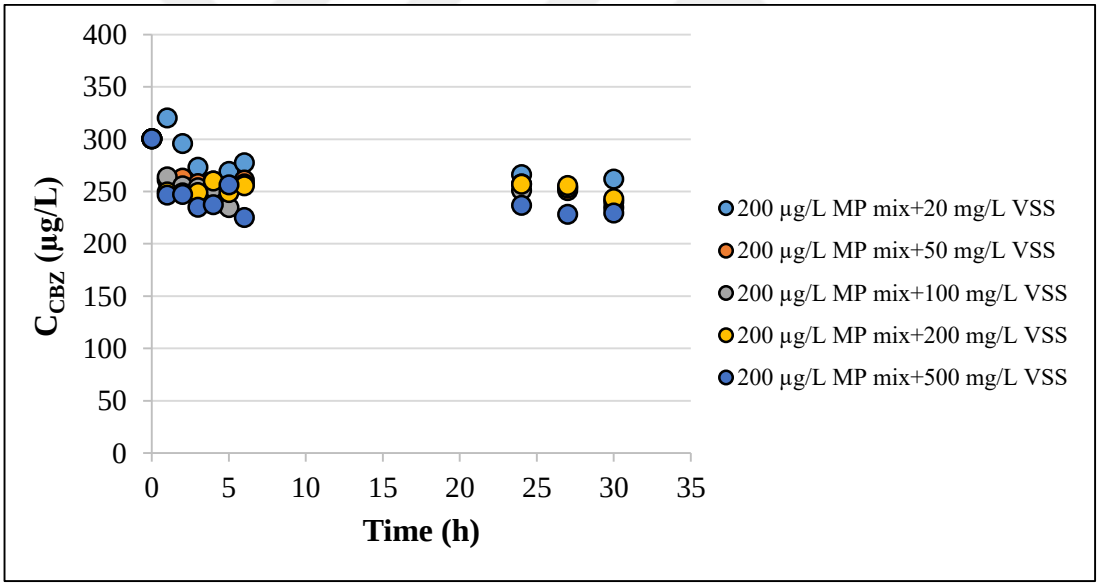

Figure 5.2. Decrease in the CBZ concentration in the short-term experiment in a mixture of pharmaceuticals.

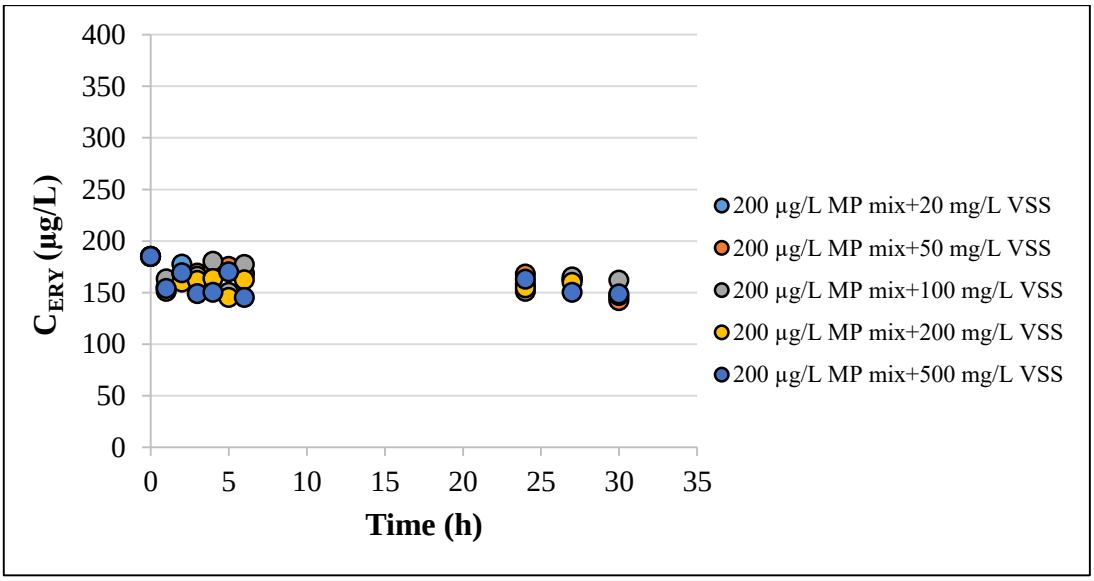

Figure 5.3. Decrease in the ERY concentration in the short-term experiment in a mixture of pharmaceuticals.

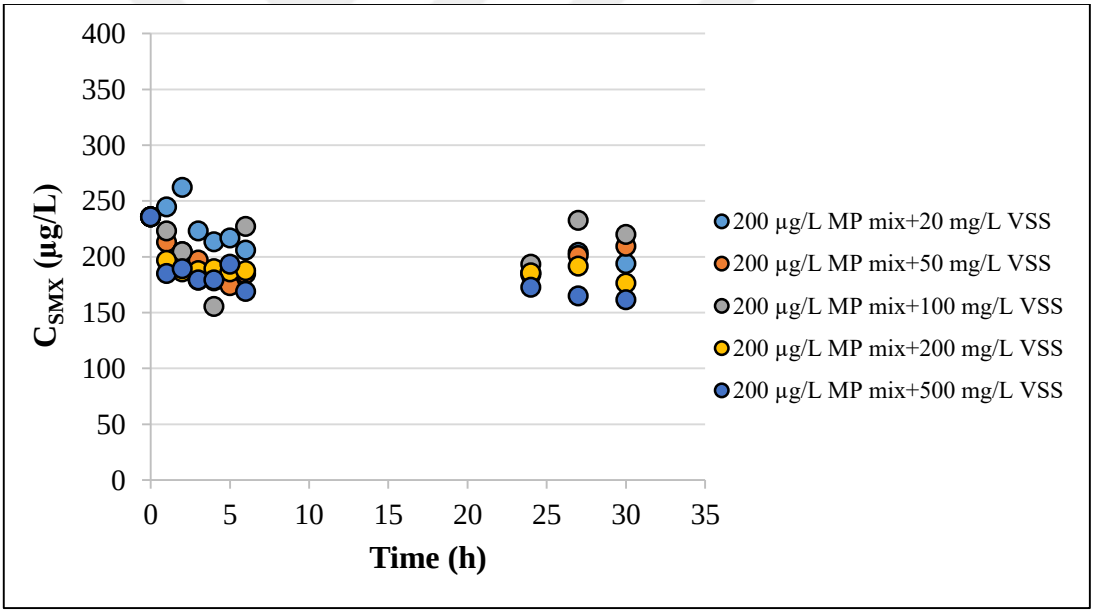

Figure 5.4. Decrease in the SMX concentration in the short-term experiment in a mixture of pharmaceuticals.

It was also observed that the change in activated sludge concentration did not significantly affect biodegradation of CBZ, ERY and SMX. On the other hand, ACT degradation increased at higher activated sludge concentrations. The removal efficiency of ACT at 500 mg/L AS was more than 90%.

As mentioned in previous sections, the first-order biodegradation rate constant k_{biol} is used in expression of biodegradation rate. A classification on the basis of VSS indicates compounds as recalcitrant (k_{biol} <0.1 $L.g_{VSS}^{-1}.d^{-1}$) slowly biodegradable (0.1 $L.g_{VSS}^{-1}.d^{-1}$ <k_{biol}<0.5 $L.g_{VSS}^{-1}.d^{-1}$),

moderately biodegradable (0.5 $L.g_{VSS}^{-1}.d^{-1}<k_{biol}<1$ $L.g_{VSS}^{-1}.d^{-1}$) and highly biodegradable ($k_{biol}>1$ $L.g_{VSS}^{-1}.d^{-1}$) (Fernandez-Fontaina et al., 2016). The first-order biodegradation rate constants (k_{biol}) of pharmaceuticals were calculated according to the following equation using the results of experiments:

$$\ln \frac{C_i}{C_0} = -k_{biol}.VSS.t \quad (5.2)$$

where C_0 is initial concentration (μg/L), C_i is final concentration (μg/L), k_{biol} is the first-order biodegradation rate constant, VSS is the mixed liquor volatile suspended solid (MLVSS) concentration (mg/L) and t is the elapsed time in the batch reactor (day), respectively. The k_{biol} values of ACT, CBZ, ERY and SMX were calculated as 5.5 $L.g_{VSS}^{-1}.d^{-1}$, 1.7 $L.g_{VSS}^{-1}.d^{-1}$, 3.2 $L.g_{VSS}^{-1}.d^{-1}$ and 2.4 $L.g_{VSS}^{-1}.d^{-1}$, respectively. These values indicate high potential of biodegradation of these pharmaceuticals by R1 sludge in the absence of background organic matter in short-term. It can be said that in this case these pharmaceuticals were used as primary substrate by microorganisms since no background organic matter was present.

5.2.2.2 Short-term experiment with background organic matter. In this experiment there were a mixture of pharmaceuticals (initially 200 μg/L of each) and different concentrations of activated sludge (AS) taken from the R1 reactor in which there were both heterotrophic and nitrification activity. At the beginning of the experiment the activated sludge was also fed with the synthetic secondary effluent in order to observe biodegradation potential of selected pharmaceuticals in the presence of bulk organic matter. This synthetic effluent contained a low amount of organic substrates and different types of inorganic substrates (Table 4.4). As mentioned previously, a pharmaceutical may be biodegraded as a secondary substrate when there are organic substances. Daily samples were taken for 10 days. The decrease in acetaminophen (ACT), carbamazepine (CBZ), erythromycin (ERY) and sulfamethoxazole (SMX) concentrations are presented in Figure 5.5, Figure 5.6, Figure 5.7 and Figure 5.8 respectively.

ACT: Results showed that around 99% of ACT was biodegraded after 10 days. This result was expected since BIOWIN 3 and 4 values, which indicate ultimate and primary biodegradation, respectively, showed that the time necessary for biodegradation of ACT is at the order of days. Moreover, it was observed that the presence of organic substances enhanced the biodegradation of this pharmaceutical. From Equation 5.2, the k_{biol} value of ACT was also calculated as 9.67 $L.g_{VSS}^{-1}.d^{-1}$ which indicates that ACT is a highly biodegradable pharmaceutical. This result is also in accordance with formerly reported studies as reviewed in a previous study (Çeçen and Gül, 2021).

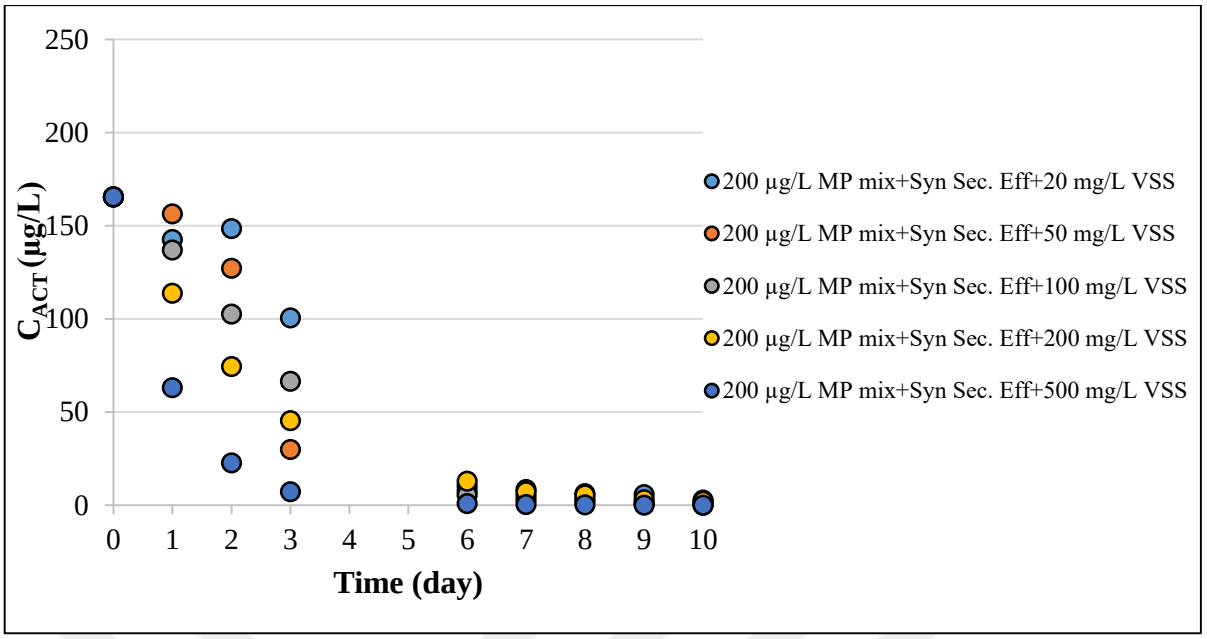

Figure 5.5. Decrease in the ACT concentration in short-term experiment in the presence of background organic matter.

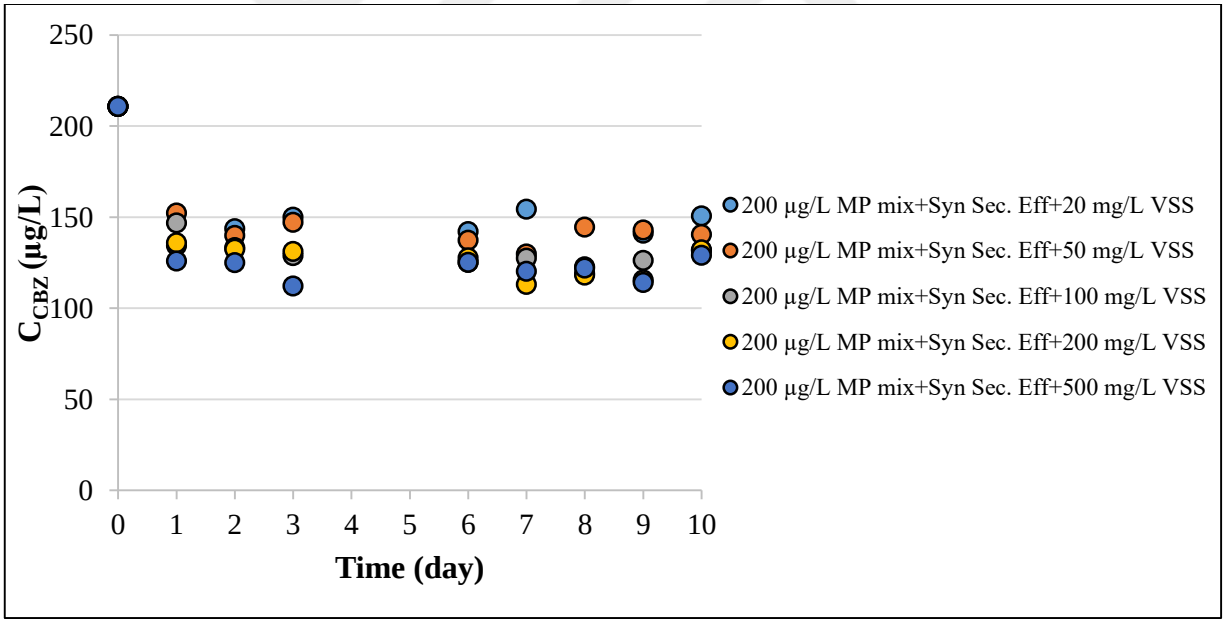

Figure 5.6. Decrease in the CBZ concentration in short-term experiment in the presence of background organic matter.

CBZ: The presence of organic matter in the synthetic secondary effluent slightly affected the biodegradation of CBZ. Also other studies report the same effect (Gauthier et al., 2010; Plosz et al., 2012). BIOWIN 4 value indicated the time needed for primary biodegradation of CBZ as weeks/months. Therefore, experimental results and previous theoretical calculations are in accordance with each other. The k_{biol} value of CBZ was calculated as 0.66 $L.g_{VSS}^{-1}.d^{-1}$ indicating that partial removal can be expected as seen in the experiment. This pharmaceutical can be classified as

moderately biodegradable. It is possible that this pharmaceutical was removed as a secondary substrate when enough biodegradable organic matter was available.

ERY: Biodegradation efficiency of ERY increased in the presence of organic matter up to 90% (in 500 mg/L VSS concentration). The BIOWIN values indicate that this compound is almost refractory as seen in Table 5.2. However, the calculated k_{biol} value, which is 1.30 $L.g_{VSS}^{-1}.d^{-1}$, indicates that partial removal may take place for this pharmaceutical. It was possibly removed as a secondary substrate in the presence of background organic matter.

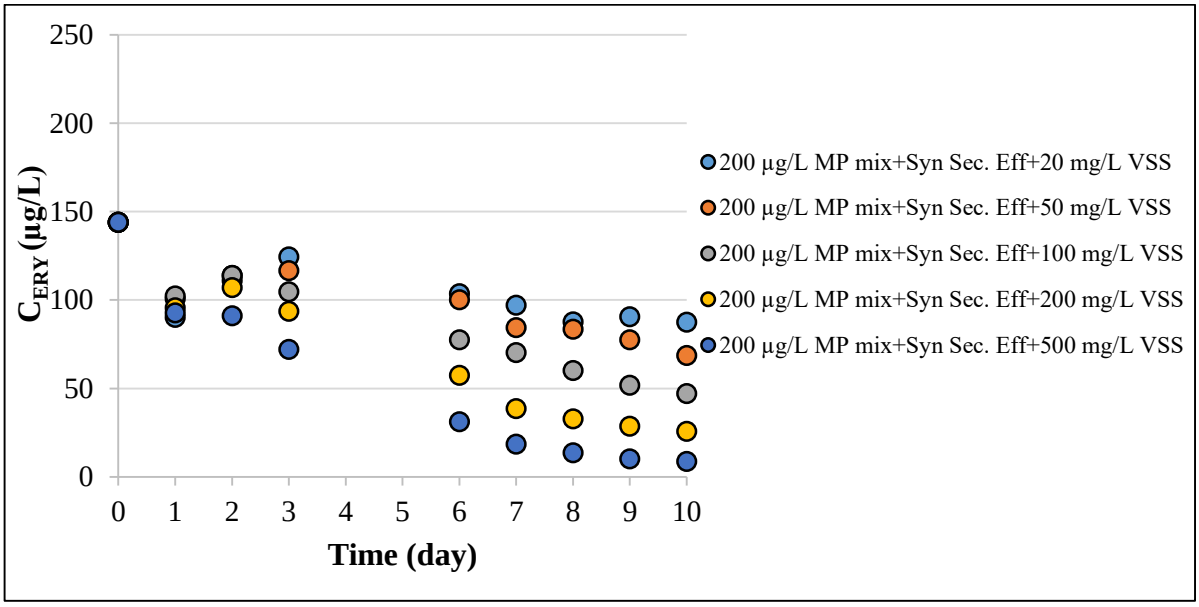

Figure 5.7. Decrease in the ERY concentration in short-term experiment in the presence of background organic matter.

SMX: On the other hand, SMX was the least biodegraded pharmaceutical in the presence of the synthetic secondary effluent (around 16% efficiency). The k_{biol} value, which is 0.20 $L.g_{VSS}^{-1}.d^{-1}$, is the lowest among all pharmaceuticals. This value indicates that SMX can be classified as a slowly biodegradable compound. According to the BIOWIN 3 value in Table 5.2 ultimate biodegradation would occur in weeks/months. Therefore, a longer experimental period might be needed for a higher biodegradation of this pharmaceutical.

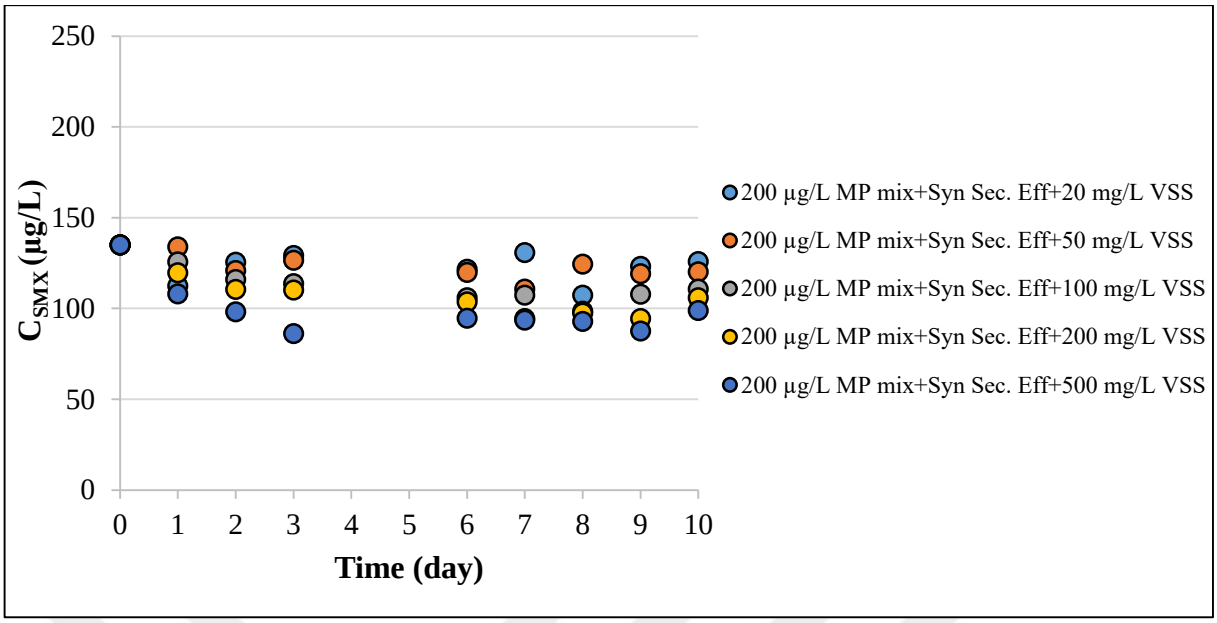

Figure 5.8. Decrease in the SMX concentration in short-term experiment in the presence of background organic matter.

Additionally, UV_{254} and UV_{280} parameters were measured in order to determine the biodegradation of specific groups in background organic matter in the synthetic secondary effluent. Figure 5.9 and Figure 5.10 shows the decrease in UV_{254} and UV_{280}, respectively. Notably, results showed that there was a successful removal of the specific organic groups in background organic matter. This organic matter was possibly used as primary substrate to serve energy and growth requirements of microorganisms and enhance the removal of pharmaceuticals.

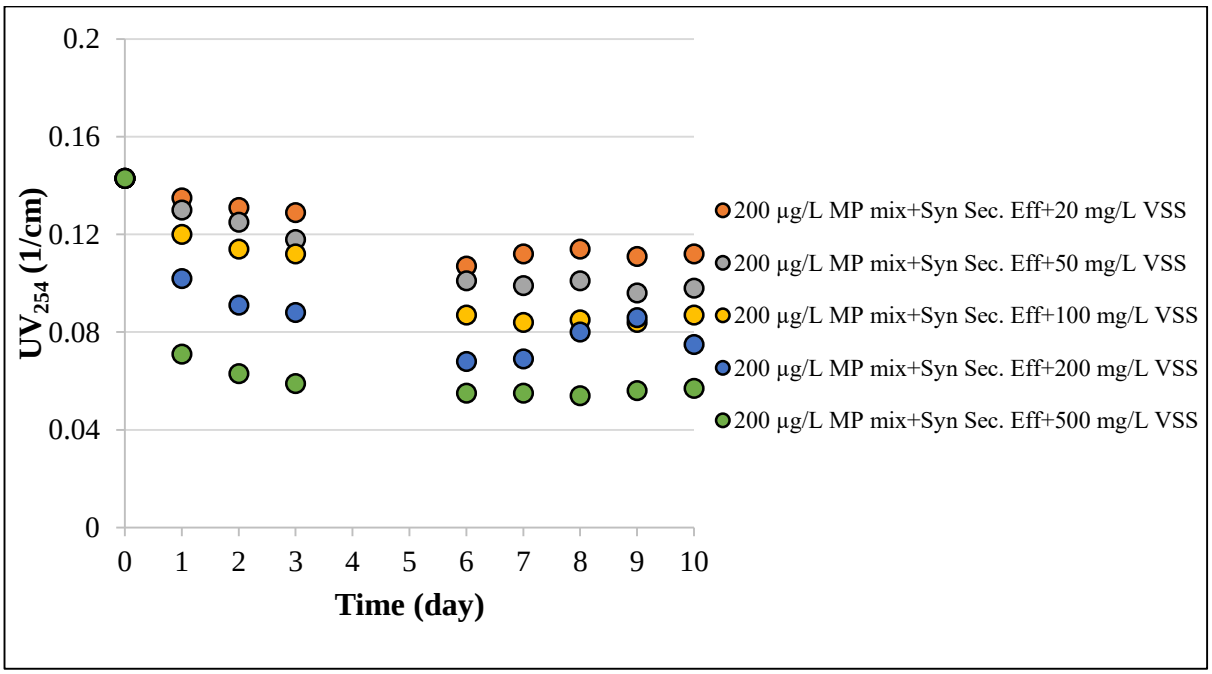

Figure 5.9. Decrease in UV_{254} values in the synthetic secondary effluent.

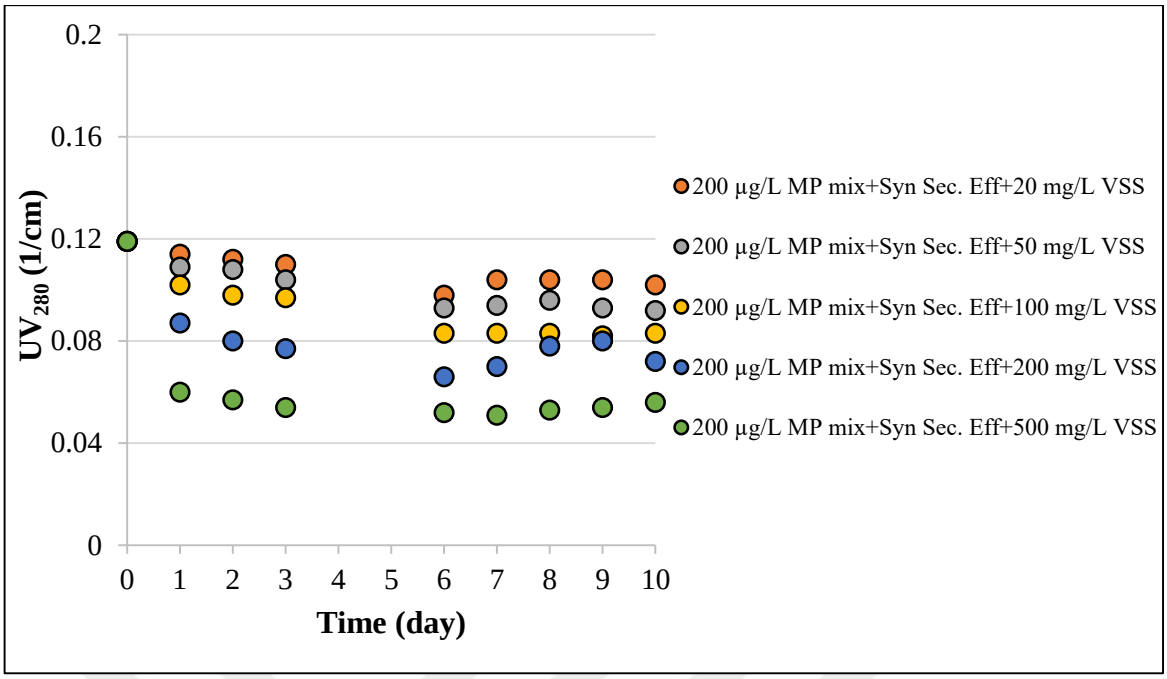

Figure 5.10. Decrease in UV_{280} values in the synthetic secondary effluent.

5.2.2.3. Long-term experiments with synthetic domestic wastewater. In the light of the results of short-term experiments, long-term experiments were carried out for the purpose of investigating the biodegradation potential of pharmaceuticals in the presence of organic substances in order to understand the removal mechanism in long-term. In these experiments activated sludge samples taken from R1 and R2 reactors were used. Firstly, a mixture of pharmaceuticals (200 µg/L of each) was added to the Erlenmeyer flasks containing activated sludge taken from R1 and R2 reactors (500 mg/L VSS). Then, the experiments were repeated with individual pharmaceuticals (200 µg/L) with R1 and R2 sludges in order to compare their biodegradation potential both in a mixture and alone. During the experiments, R1 and R2 sludges were continuously fed with Feed 1 and Feed 2 (Table 4.2), respectively. Feed 1 contained easily biodegradable organics such as glucose, and Feed 2 was rich in terms of ammonium sulfate. R1 sludge was fed with 149±17 mg COD/L.day and average removal efficiency was 75%. R2 sludge was fed with 15±4 mg NH_4-N/L.day and average removal efficiency was 40%.

In addition, one experiment was carried out with a mixture of pharmaceuticals (200 µg/L of each) and R1 sludge in the presence of N-Allylthiourea (ATU) (11.6 mg/L) in order to inhibit the nitrification activity. During the experiment, R1 sludge was continuously fed with Feed 1 (Table 4.2). The details and the results of the experiments are given in Table 5.4. The k_{biol} values of ACT, CBZ, ERY and SMX belonging to these long-term experiments were also calculated using Equation 5.2.

Table 5.4. Long-term biodegradation experiments with R1 and R2 sludge.

Experiment	Duration	k_{biol} ($L.g_{VSS}^{-1}.d^{-1}$)	
A mixture of pharmaceuticals with R1 sludge[(1)] and F1[(3)]	49 days	ACT	0.20
		CBZ	0.02
		ERY	0.46
		SMX	0.15
A mixture of pharmaceuticals with R1 sludge [(1)] and F1[(3)] and ATU[(5)] (Nitrification inhibited)	28 days	ACT	0.31
		CBZ	0.01
		ERY	0.44
		SMX	0.29
A mixture of pharmaceuticals with R2 sludge [(2)] and F2[(4)]	49 days	ACT	0.27
		CBZ	0.03
		ERY	0.45
		SMX	0.05
Single ACT with R1 sludge [(1)] and F1[(3)]	17 days	0.55	
Single ACT with R2 sludge [(2)] and F2[(4)]	17 days	0.60	
Single CBZ with R1 sludge [(1)] and F1[(3)]	56 days	0.04	
Single CBZ with R2 sludge [(2)] and F2[(4)]	56 days	0.03	
Single ERY with R1 sludge [(1)] and F1[(3)]	21 days	0.20	
Single ERY with R2 sludge [(2)] and F2[(4)]	21 days	0.18	
Single SMX with R1 sludge [(1)] and F1[(3)]	45 days	0.15	
Single SMX with R2 sludge [(2)] and F2[(4)]	45 days	0.24	

[(1)]R1 sludge: both heterotrophic and nitrification activity
[(2)]R2 sludge: enriched in nitrifiers
[(3)]Feed 1: containing readily biodegradable background organic matter
[(4)]Feed 2: rich in terms of ammonium sulfate, no organic compounds
[(5)]ATU: used for inhibition of nitrification

ACT: It was observed that ACT was biodegraded almost completely (99% removal efficiency) by both activated sludges when it was alone or in a mixture. Moreover, its biodegradation in the presence of ATU was also high (99% removal efficiency), indicating that it can also be biodegraded by heterotrophic activity alone. These results are in accordance with the BIOWIN estimations (Table 5.2) and the other experiments in the literature as reviewed in a study (Çeçen and Gül, 2021). As mentioned before, BIOWIN 1 and 2 values of ACT shows fast biodegradation. Also, BIOWIN 3 and 4 values showed that the time necessary for biodegradation of ACT is at the order of days/weeks. It was seen that biodegradation of ACT took place at the beginning of the experiments (around at 2^{nd} – 3^{rd} days). The results of the experiments belonging to ACT are given in Figure 5.11.

On the other hand, k_{biol} values of ACT presented in Table 5.4 varied between 0.20 and 0.60 $L.g_{VSS}^{-1}.d^{-1}$ indicating partial removal by biological transformation. Its degradation rate was higher in both sludges when it was the only pharmaceutical in the feed as expected.

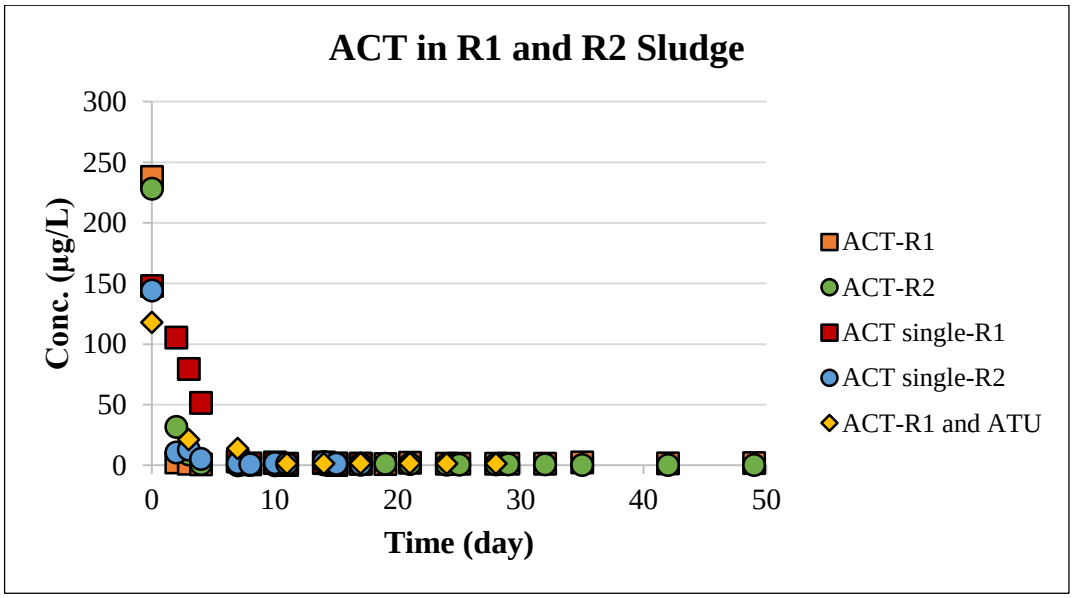

Figure 5.11. Change in the ACT concentration with respect to time in long-term biodegradation experiments.

Additionally, to determine the statistical significance of differences between the biodegradation of ACT by R1 and R2 sludges, t-test was applied. Significant differences were determined at $p<0.05$. Results showed that biodegradation of this pharmaceutical by R1 and R2 sludges was not statistically different from each other ($p>0.05$) when it was in the mixture or it was the single pharmaceutical as indicated by the t-test at 95% confidence level.

CBZ: The biodegradation of CBZ by both types of activated sludge was lower than in the case of other pharmaceuticals. The k_{biol} values were close to each other as presented in Table 5.4. This showed that no substantial degradation could be expected for CBZ. This effect was reported also in other studies. It is possible that this pharmaceutical was removed to some extent as a secondary substrate when enough biodegradable organic matter was available (Gauthier et al., 2010). The k_{biol} values also showed that the nitrification activity did not significantly enhance the biodegradation of this pharmaceutical.

BIOWIN models also indicate that CBZ is hardly biodegradable. According to BIOWIN 3 value, the time needed for ultimate biodegradation of CBZ is weeks/months as seen in Table 5.2. Accordingly, previous theoretical calculations and experimental results are in accordance with each other. Furthermore, in other studies it was reported that the removal of CBZ was extremely slow in nitrifying sludge (Suarez et al. 2010), and it was neither removed by heterotrophic nor nitrifying activity (Fernandez-Fontaina et al., 2016).

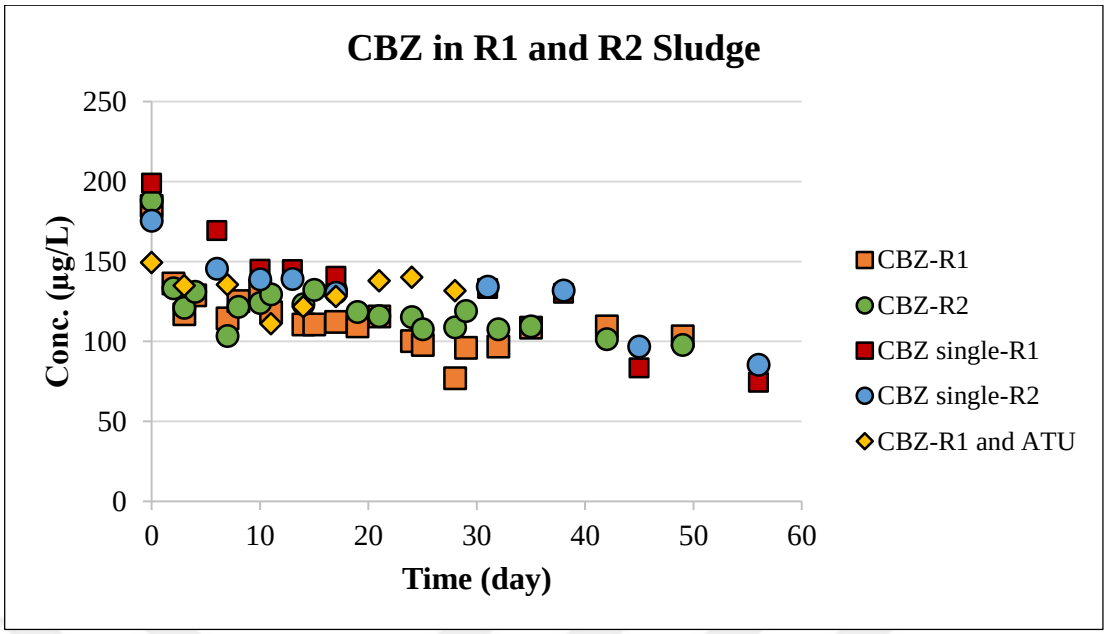

Figure 5.12. Change in the CBZ concentration with respect to time in long-term biodegradation experiments.

Additionally, t-test was applied for the biodegradation of CBZ by R1 and R2 sludges. According to the results, biodegradation of this pharmaceutical by R1 and R2 sludge was significantly different from each other ($p<0.05$) when it was in the mixture. On the other hand, when it was the single pharmaceutical, its biodegradation by both sludges was not statistically different from each other ($p>0.05$). It was thought that the presence of other pharmaceuticals might have affected the biodegradation potential of CBZ.

ERY: According to the BIOWIN 3 value in Table 5.2, ERY is classified as refractory meaning that it is not biodegradable. However, experimental results showed that it was biodegraded by both activated sludges when it was in a mixture or alone. Also, k_{biol} values of ERY presented in Table 5.4 were close to each other at all experimental conditions and indicated partial removal by biological transformation. It was possibly removed as a secondary substrate in the presence of organic matter and as a cometabolite in the case of nitrification activity alone (R2 sludge). The results of the experiments belonging to ERY are given in Figure 5.13. These results are also in accordance with the other studies in the literature as reviewed in a study (Çeçen and Gül, 2021). High biodegradation rates were reported for ERY under nitrification conditions (Fernandez-Fontaina et al., 2012; Suarez et al., 2010).

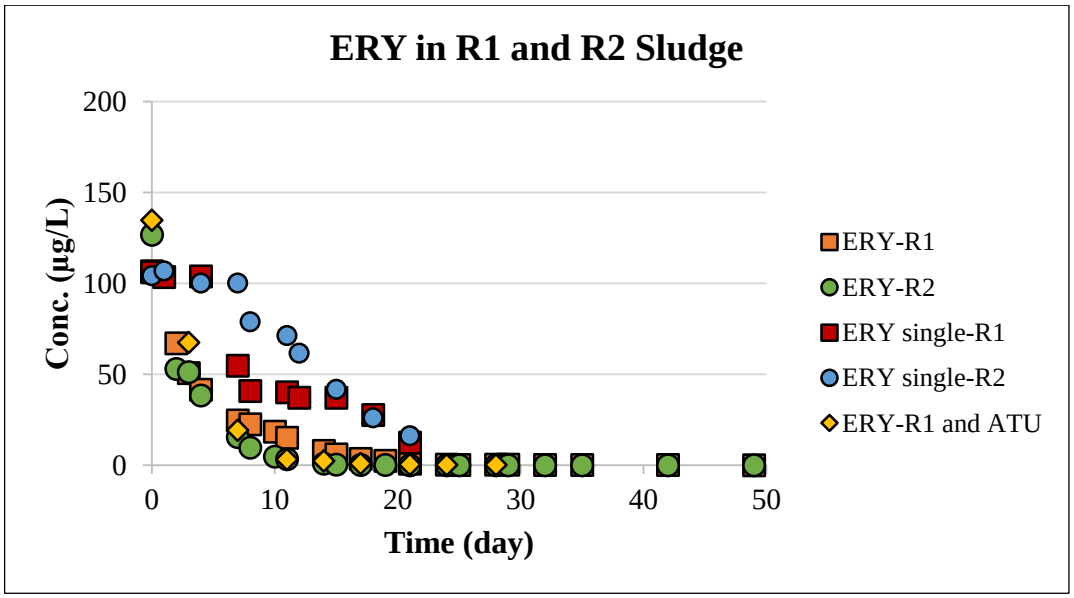

Figure 5.13. Change in the ERY concentration with respect to time in long-term biodegradation experiments.

Also, t-test was applied to determine the significant differences between biodegradation of ERY by R1 and R2 sludges. Results showed that biodegradation of ERY by R1 and R2 sludge was not statistically different from each other ($p>0.05$) when it was in the mixture. On the other hand, when it was the single pharmaceutical, its biodegradation by both sludges was significantly different from each other ($p<0.05$). The nitrification activity in R2 sludge may have caused this difference between the biodegradation potential of ERY by two sludges.

SMX: SMX is also slowly biodegradable according to the BIOWIN values (Table 5.2). According to BIOWIN 4 value, the time needed for primary biodegradation of SMX is days/weeks. However, it was observed that SMX was biodegraded almost completely by R1 sludge when it was in the mixture, whereas its biodegradation was lower in R2 sludge which was enriched in nitrifiers. It was concluded that the presence of readily biodegradable organics enhanced its removal whereas nitrification activity had a slight effect on biodegradation of SMX in the presence of a mixture of pharmaceuticals. In addition, k_{biol} values indicated that biodegradation rate of SMX was the same (0.15 $L.g_{VSS}^{-1}.d^{-1}$) in the R1 sludge both when it was in a mixture or alone.

On the other hand, when SMX was the single pharmaceutical, its biodegradation rate by R2 sludge (k_{biol} = 0.24 $L.g_{VSS}^{-1}.d^{-1}$) was higher than when it was in the mixture (k_{biol} = 0.05 $L.g_{VSS}^{-1}.d^{-1}$). At the end of 45 days, it was almost completely biodegraded. This might be explained with the effect of nitrification activity since R2 sludge was enriched in nitrifiers and there was no organic compound in the solution. In this case, SMX may be removed as a cometabolite when nitrifying bacteria oxidize

ammonia and produce the enzyme ammonia monooxygenase (AMO) which causes cometabolism of compounds. The results belonging to SMX are given in Figure 5.14.

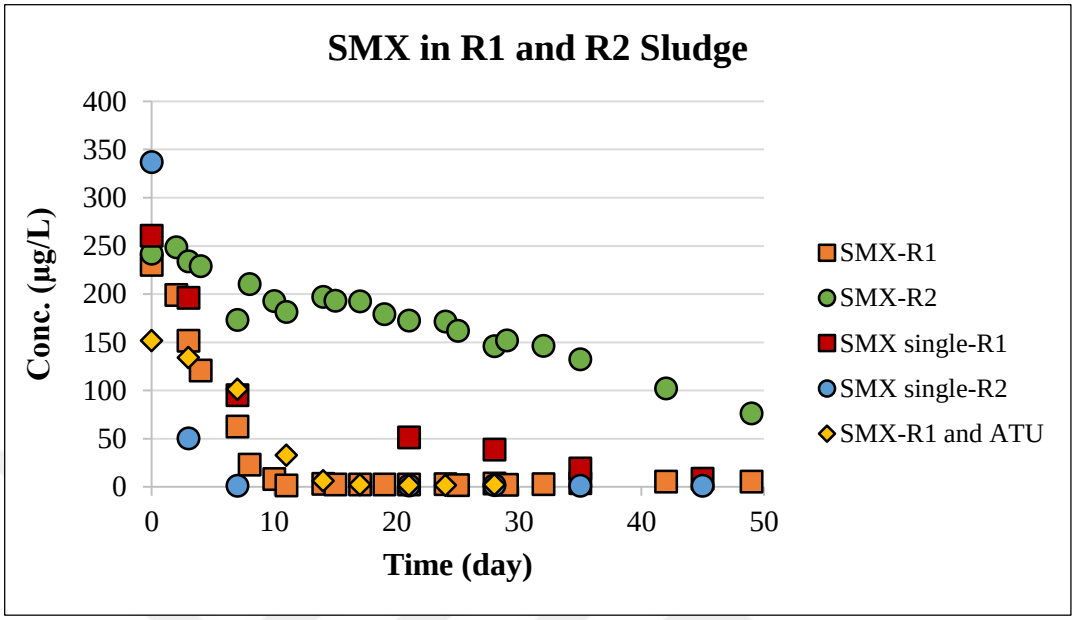

Figure 5.14. Change in the SMX concentration with respect to time in long-term biodegradation experiments.

Other studies also showed different results on biodegradation of SMX. It was reported in a study that heterotrophic activity was mainly responsible for SMX degradation and nitrification had a minimal effect. When the sludge was fed with organic carbon, this pharmaceutical could be biodegraded. It was suggested that SMX was used as a secondary substrate (Fernandez-Fontaina et al., 2016). However, in some other studies, SMX was removed by cometabolism too by nitrifying bacteria (Müller et al. 2013; Kassotaki et al. 2016).

Additionally, t-test was applied for the biodegradation of SMX by R1 and R2 sludges. Biodegradation of this pharmaceutical by R1 and R2 sludge was significantly different from each other ($p<0.05$) when it was in the mixture, in fact the p value was very low ($1.05xe^{-10}$). This was also stated by the low $k_{bio}l$ value (0.05 $L.g_{VSS}^{-1}.d^{-1}$**)** in Table 5.4 which showed SMX was slightly biodegraded by R2 sludge (enriched in nitrifiers) in the presence of other pharmaceuticals. On the other hand, when it was the single pharmaceutical, its biodegradation by both sludges was not statistically different from each other ($p>0.05$). The presence of other pharmaceuticals might have affected the biodegradation potential of SMX.

Overall, in the presence of enough organic matter, some pharmaceuticals, even at low concentrations, can be used as secondary substrates or they can be removed by cometabolism due to

heterotrophic or nitrification activity. This is particularly true in the case of slowly biodegradable compounds CBZ, SMX and ERY (Çeçen, 2017; Çeçen and Gül, 2021).

5.3. Experiments for Adsorption Kinetics

5.3.1. Kinetic Experiments with Ground GAC and Synthetic Secondary Effluent

Kinetic experiments were performed with ground GAC having a particle size of around 100 μm using the synthetic secondary effluent. One of the experiments carried out for 50 hours showed that equilibrium was reached after around 24 hours which means that the concentrations in the liquid phase reached a constant value at that time. During the experiment, UV_{254}, UV_{280} and $Color_{436}$ of samples from all chambers were measured hourly. As mentioned before, these parameters stand for some of the organic fractions in the synthetic effluent. The results are shown in Figure 5.15, Figure 5.16 and Figure 5.17, respectively.

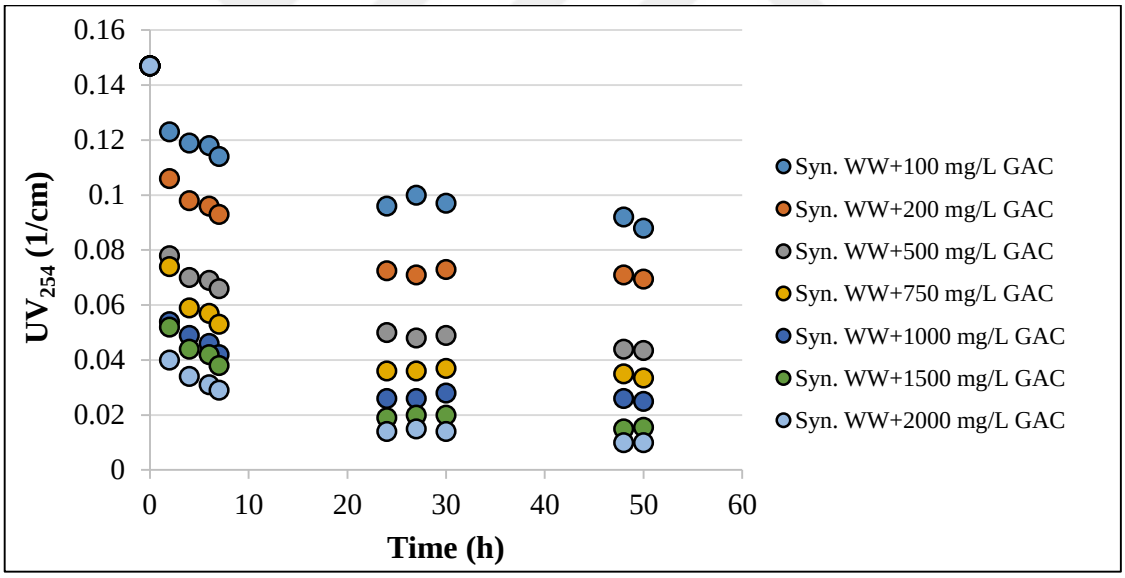

Figure 5.15. Change in UV_{254} of the samples with respect to time.

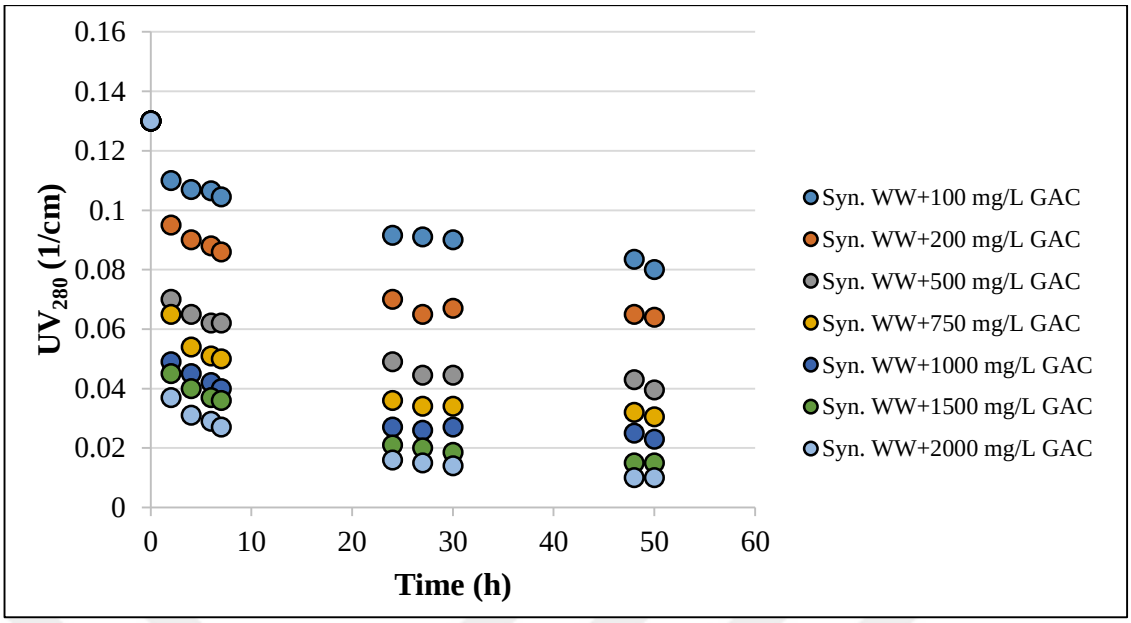

Figure 5.16. Change in UV_{280} of the samples with respect to time.

According to UV_{254} and UV_{280} results, it can be said that higher amount of aromatic and unsaturated organic compounds and lignin-derived compounds in the synthetic secondary effluent were adsorbed at higher GAC concentrations.

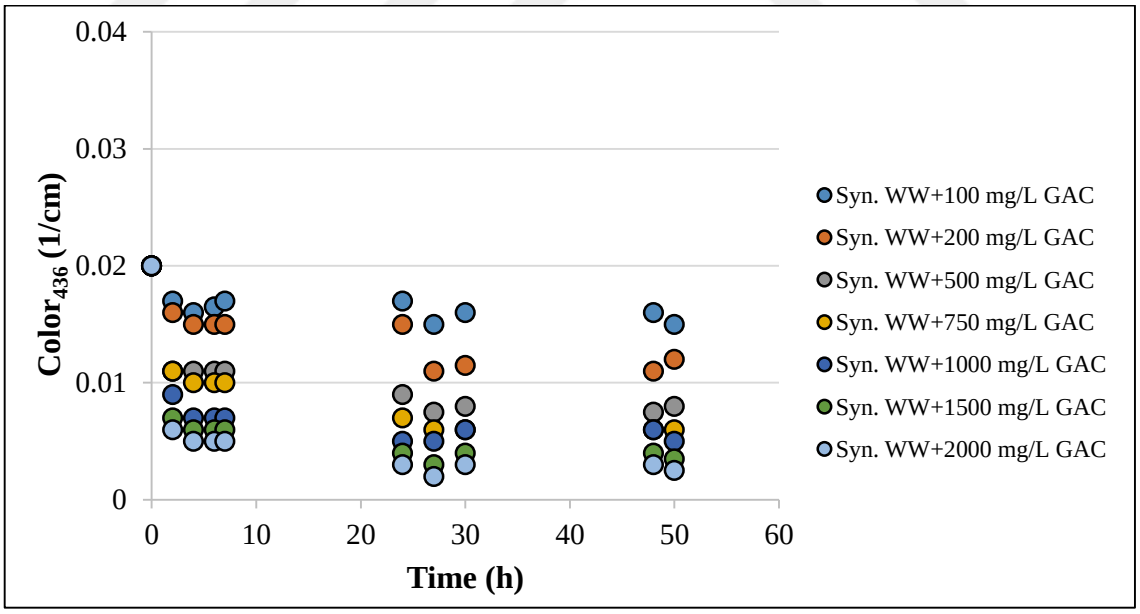

Figure 5.17. Change in the $Color_{436}$ of the samples with respect to time.

In addition, it was observed that at low GAC concentrations there was low adsorption in terms of color, while at concentrations higher than 1000 mg/L, adsorbances decreased to very low levels which indicates high adsorption onto granular activated carbon.

5.3.2. Kinetic Experiments with Original (Non-ground) GAC and Synthetic Secondary Effluent

Another kinetic experiment was carried out with original GAC (particle size = around 1 mm) in order to compare the results with ground GAC. When the GAC has a bigger particle size, the adsorption takes place at a slower rate. As a result, equilibrium takes place in a longer period of time. Since the particle size of the original GAC was 10 times bigger than ground GAC, it was expected to reach the equilibrium in a longer time. So the experiment was carried out during 120 hours. UV_{254}, UV_{280} and $Color_{436}$ parameters were observed during the experiment and results showed that the time for equilibrium was around 100 hours. The results are shown in Figure 5.18, Figure 5.19 and Figure 5.20, respectively.

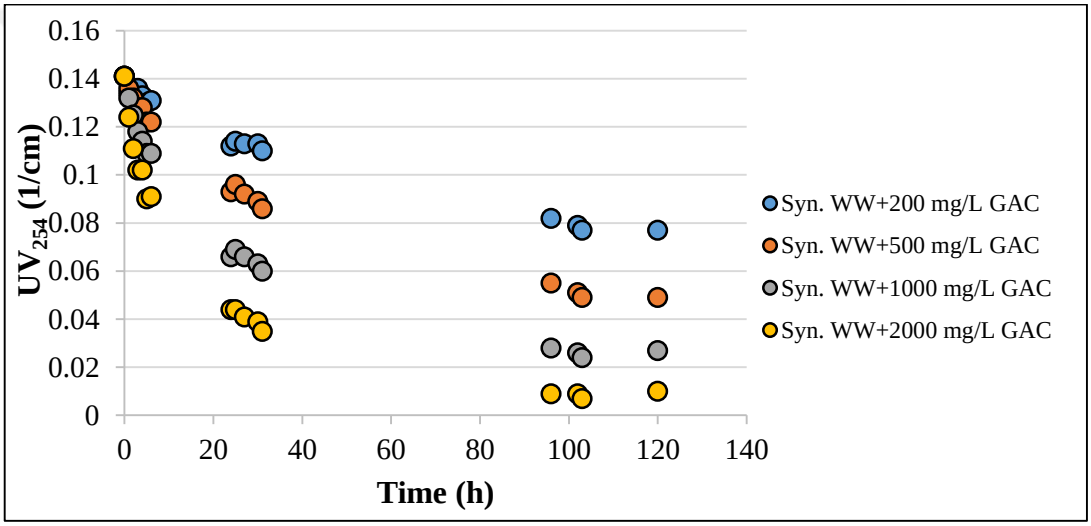

Figure 5.18. Change in the UV_{254} of the samples with respect to time.

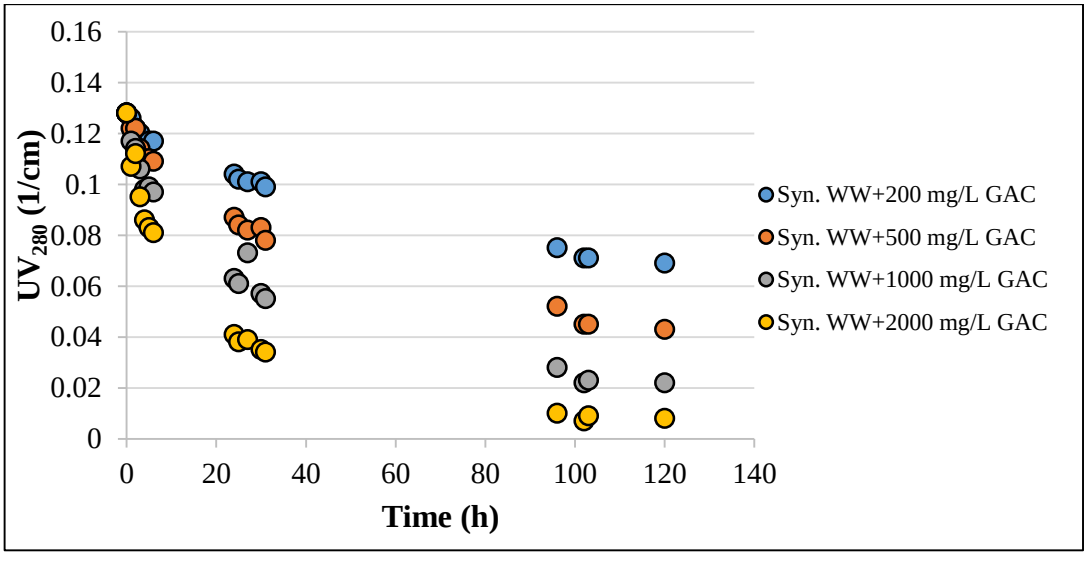

Figure 5.19. Change in the UV_{280} of the samples with respect to time.

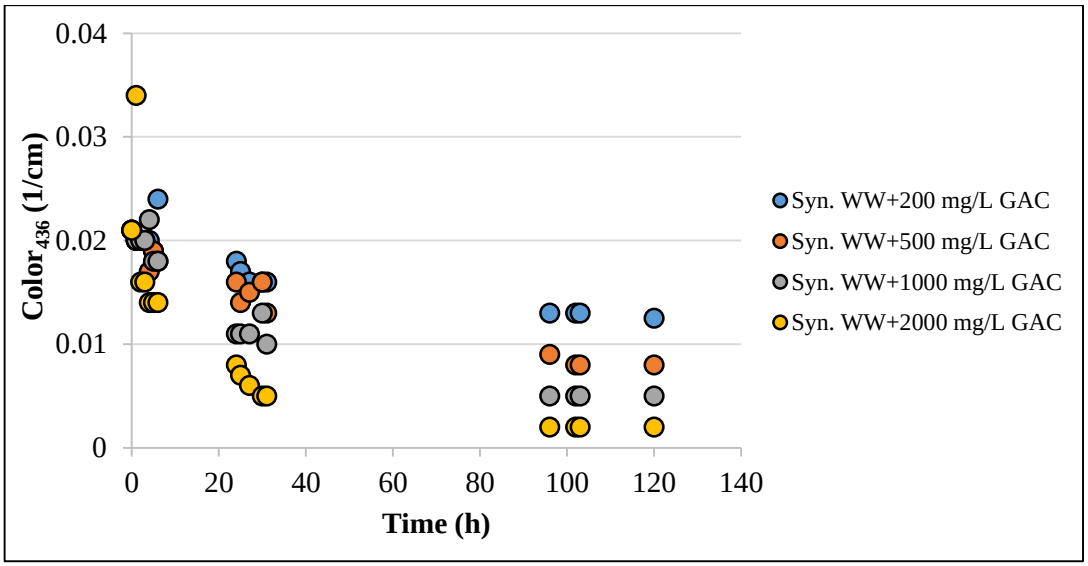

Figure 5.20. Change in the $Color_{436}$ of the samples with respect to time.

These results emphasize the importance of using ground GAC, which effectively reduces the equilibration time. In the case of ground GAC, the diffusion of substances into GAC is enhanced. It was observed that the equilibrium time for original GAC was almost 5 times longer than ground GAC. It is in accordance with the purpose of this study which was to carry out the experiments in rapid small-scale columns. The results were obtained much faster with rapid small-scale columns as shown in further sections.

5.3.3. Kinetic Experiments with the Mixture of Micropollutants

Two kinetic tests were carried out with a mixture of pharmaceuticals in order to determine the time for adsorption to reach equilibrium. In these tests ground GAC was used. The first experiment was carried out at relatively low GAC concentrations (50, 100, 150 and 200 mg/L) in a time period of 24 hours. For all pharmaceuticals the equilibrium concentration was reached in the first few hours. Only for ACT at the 50 mg/L GAC dose, equilibrium took place around 24 hours. The results are given in **Appendix B.**

In the second set 100, 200, 500, 750, 1000, 1500 and 2000 mg/L GAC was used and duration of the experiment was 49 hours. Results of this experiment showed that for all pharmaceuticals at lower GAC doses (100 and 200 mg/L GAC), the equilibrium times were between 24 and 30 hours. At higher GAC concentrations (from 500 mg/L to 2000 mg/L GAC) equilibrium took place earlier as expected. Increasing dosage gives the micropollutants more opportunities to attach to the surface of the activated carbon. Higher activated carbon dosage can increase the adsorbable area (Nam et al., 2014). Moreover, removal efficiencies by GAC adsorption were higher than 90% for all pharmaceuticals at

the end of this experiment. Figure 5.21, Figure 5.22, Figure 5.23 and Figure 5.24 show the change in ACT, CBZ, ERY and SMX concentrations in chambers during the experiment at higher GAC dosages, respectively. According to all results, the equilibrium time for pharmaceuticals was determined as 24 hours.

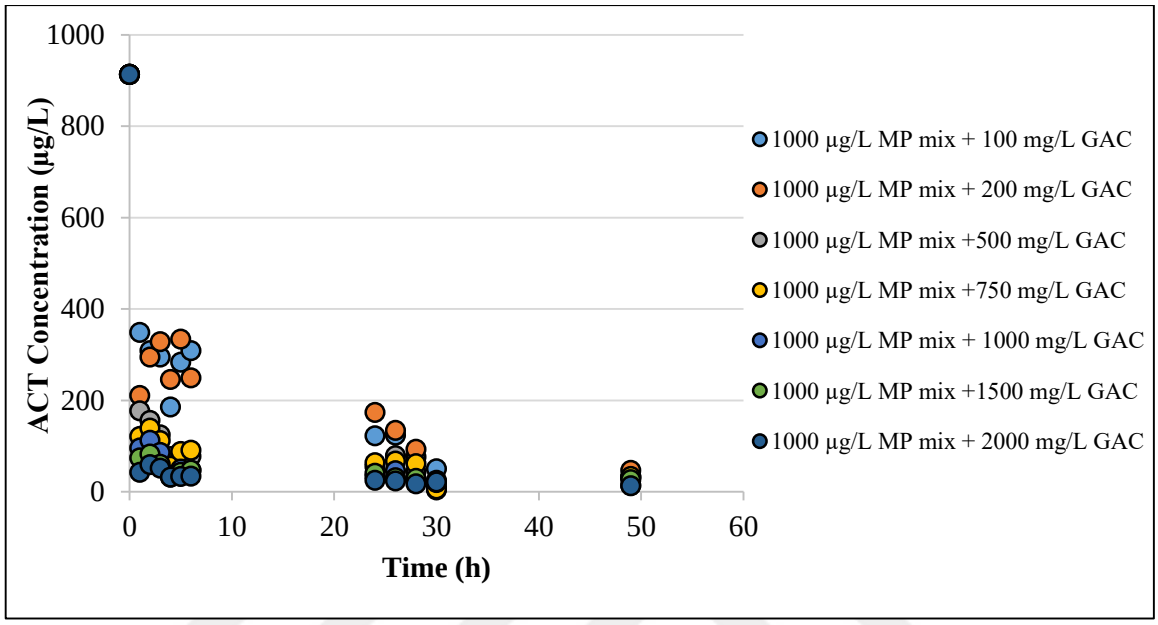

Figure 5.21. Change in the ACT concentrations with respect to time.

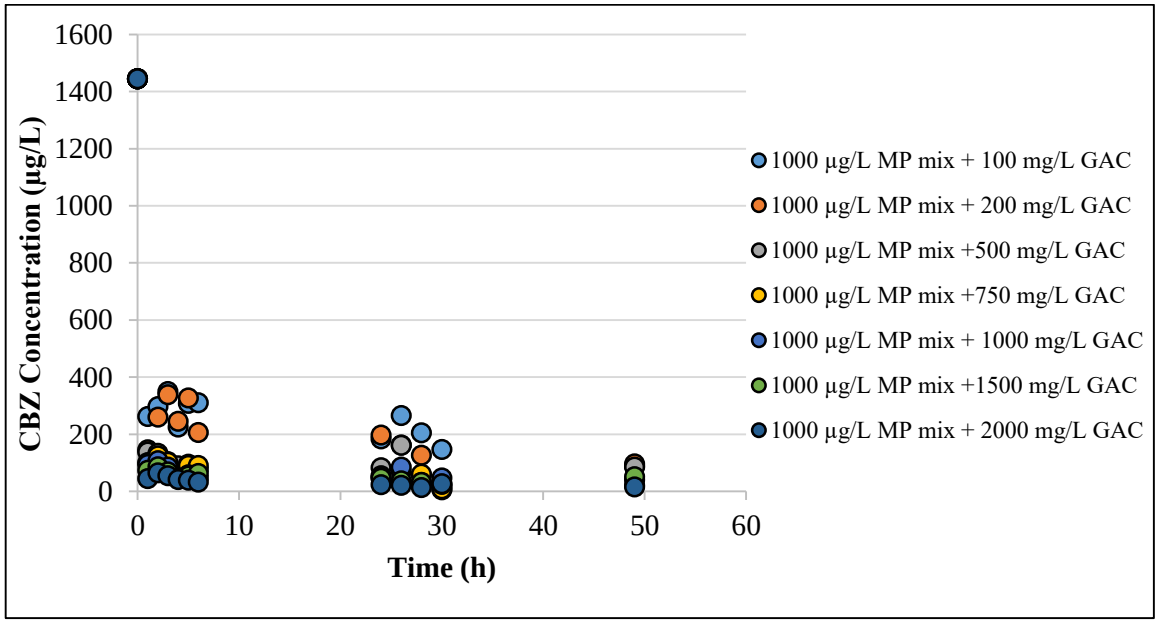

Figure 5.22. Change in the CBZ concentrations with respect to time.

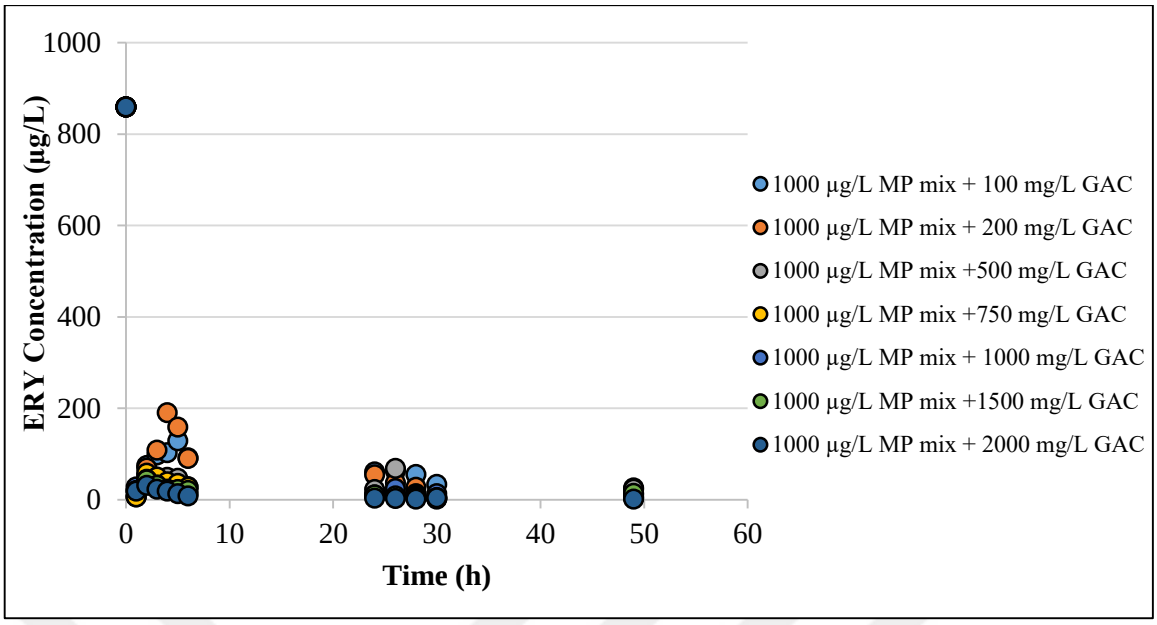

Figure 5.23. Change in the ERY concentrations with respect to time.

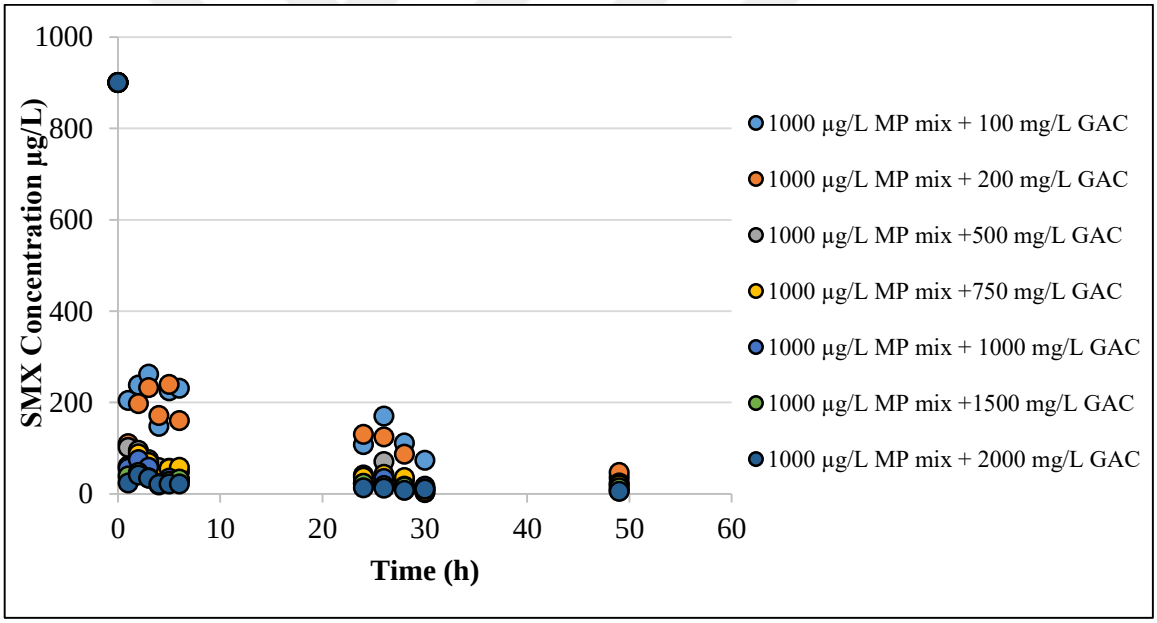

Figure 5.24. Change in the SMX concentrations with respect to time.

5.3.3.1 Adsorption kinetics. In addition, adsorption rates were also calculated for all pharmaceuticals by using the data of the kinetic experiments. There are two kinetic models that were used for describing the adsorption kinetics: pseudo first-order and pseudo second-order equations. Under the assumption that the adsorbate uptake follows a first-order rate law, the adsorption kinetics can be described by the Equation 5.3 and the linearized form is expressed in Equation 5.4, respectively:

$$\frac{dq_t}{d_t} = k_1 (q_e - q_t) \quad (5.3)$$

$$\ln(q_e - q_t) = \ln q_e - k_1 t \quad (5.4)$$

where k_1 is the rate constant, q_t is the amount of solute adsorbed on the adsorbent at time t, and q_e is the amount at equilibrium.

Another reaction kinetic approach is based on a pseudo second-order rate law. The equation and the linearized form are expressed in Equation 5.5 and Equation 5.6, respectively:

$$\frac{dq_t}{d_t} = k_2 (q_e - q_t)^2 \quad (5.5)$$

$$\frac{t}{q_t} = \frac{1}{k_2 {q_e}^2} + \frac{t}{q_e} \quad (5.6)$$

where k_2 is the rate constant (Worch, 2012). By using the Equation 5.4 ln (q_e – q_t) – time graphs were drawn for all pharmaceuticals as shown in Figure 5.25, Figure 5.26, Figure 5.27 and Figure 5.28.

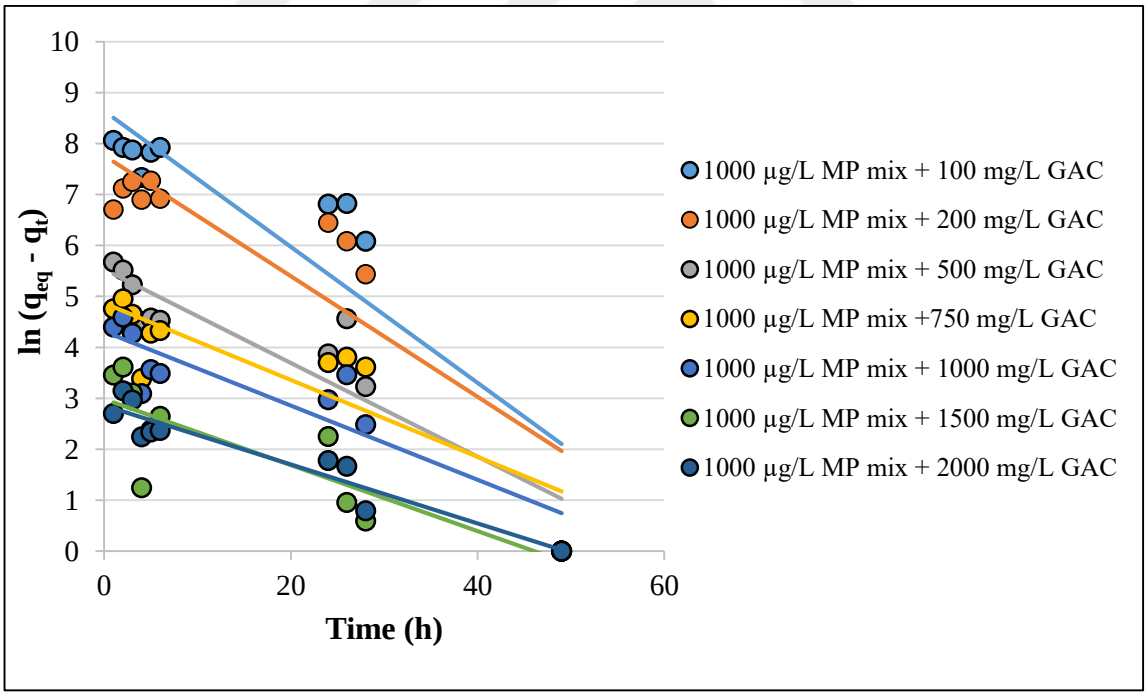

Figure 5.25. Experimental data of ACT and the fitted linear pseudo first-order rate equation.

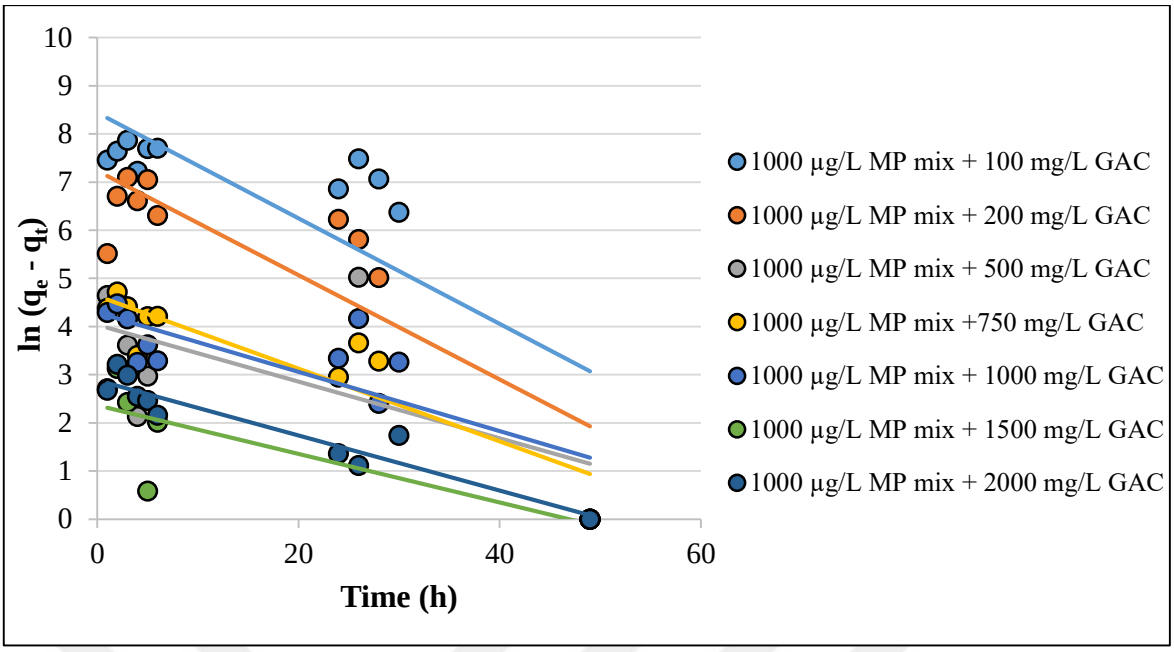

Figure 5.26. Experimental data of CBZ and the fitted linear pseudo first-order rate equation.

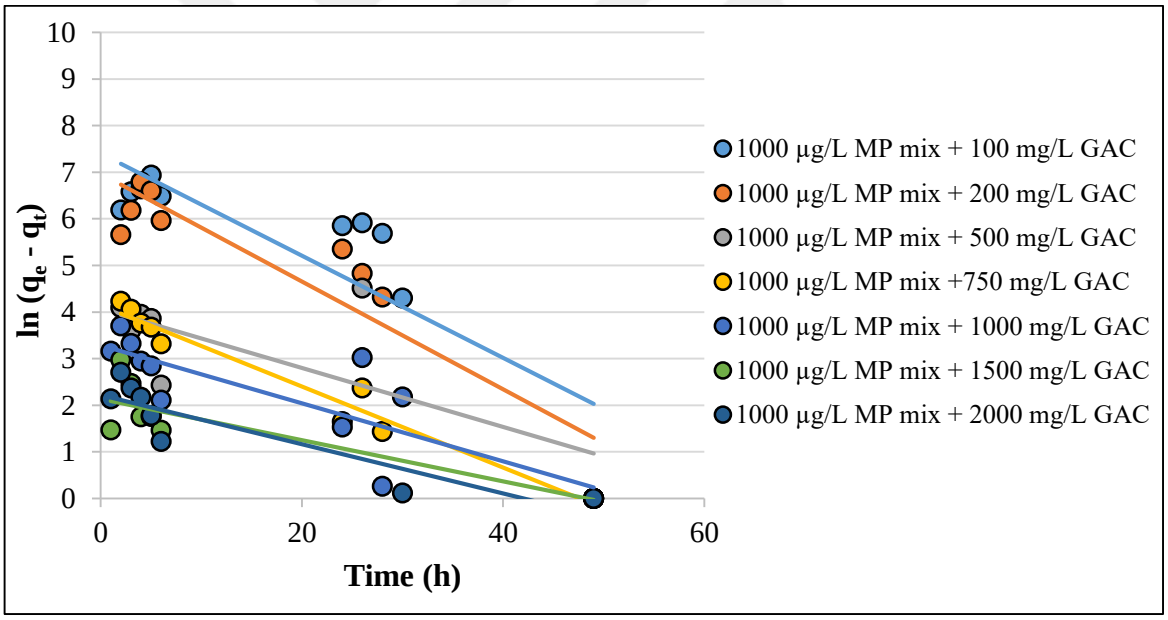

Figure 5.27. Experimental data of ERY and the fitted linear pseudo first-order rate equation.

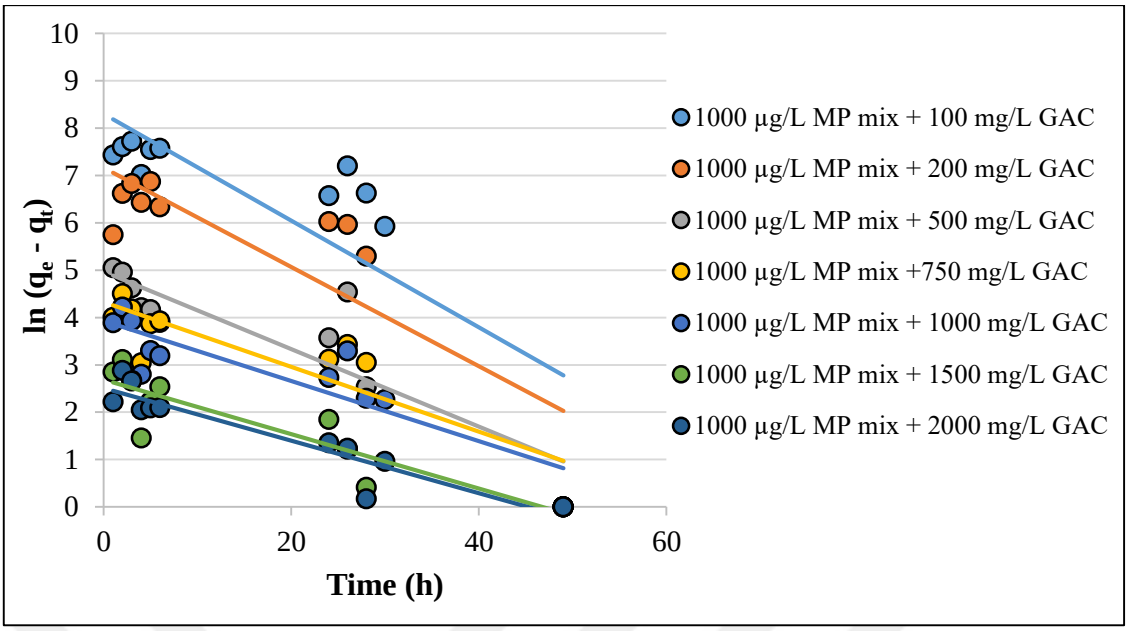

Figure 5.28. Experimental data of SMX and the fitted linear pseudo first-order rate equation.

In addition, by using the Equation 5.6 time/q_t – time graphs for all pharmaceuticals were drawn as shown in Figure 5.29, Figure 5.30, Figure 5.31 and Figure 5.32.

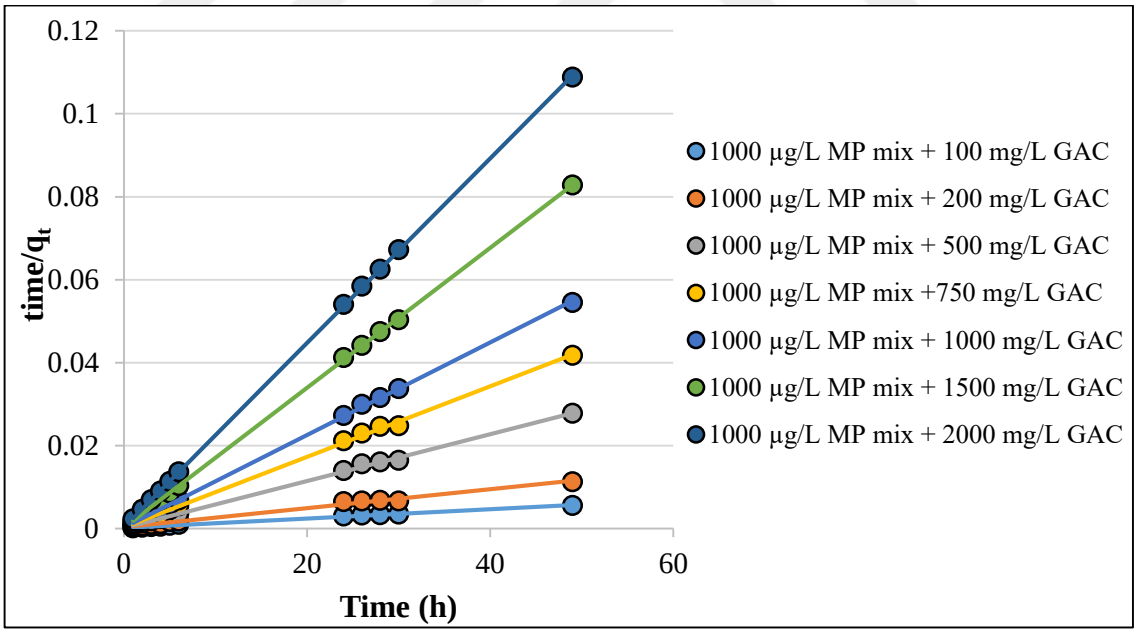

Figure 5.29. Experimental data of ACT and the fitted linear pseudo second-order rate equation.

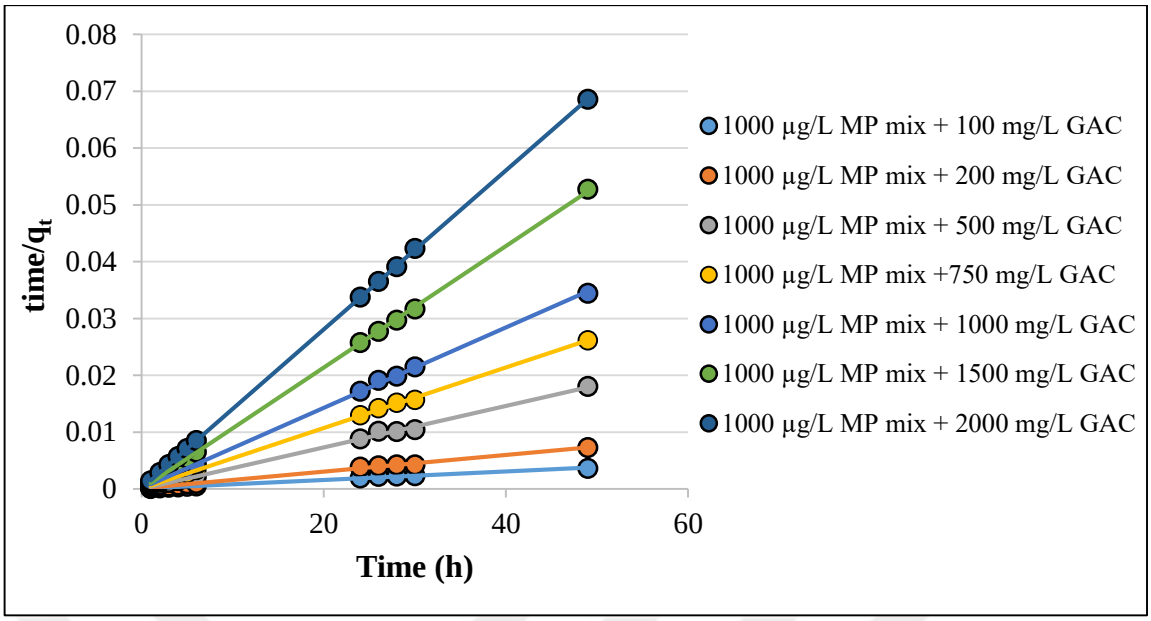

Figure 5.30. Experimental data of CBZ and the fitted linear pseudo second-order rate equation.

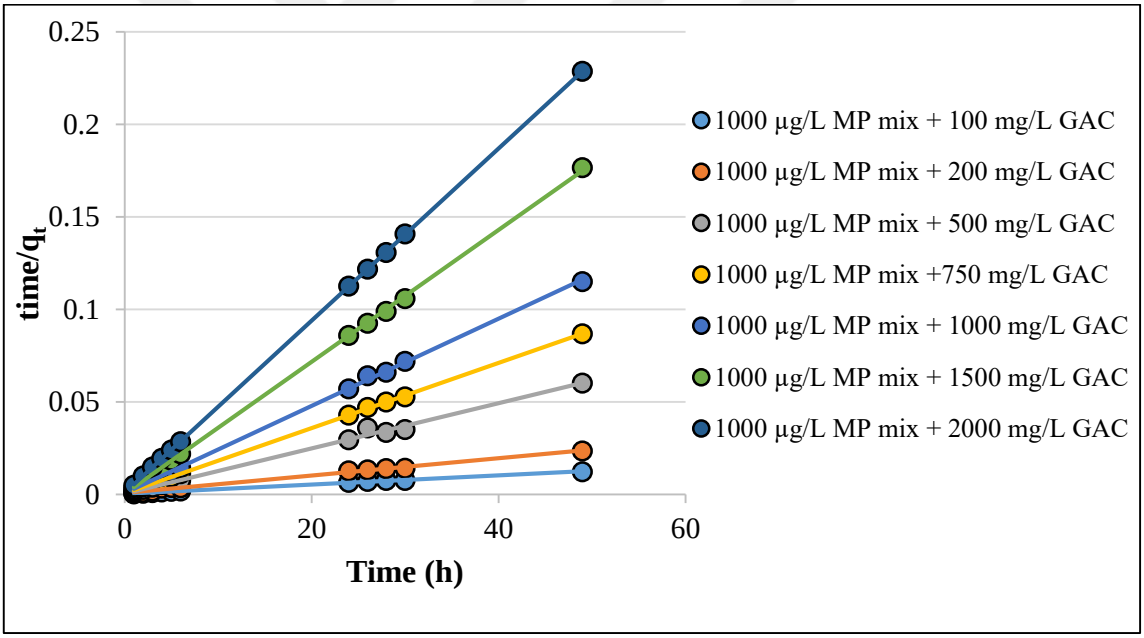

Figure 5.31. Experimental data of ERY and the fitted linear pseudo second-order rate equation.

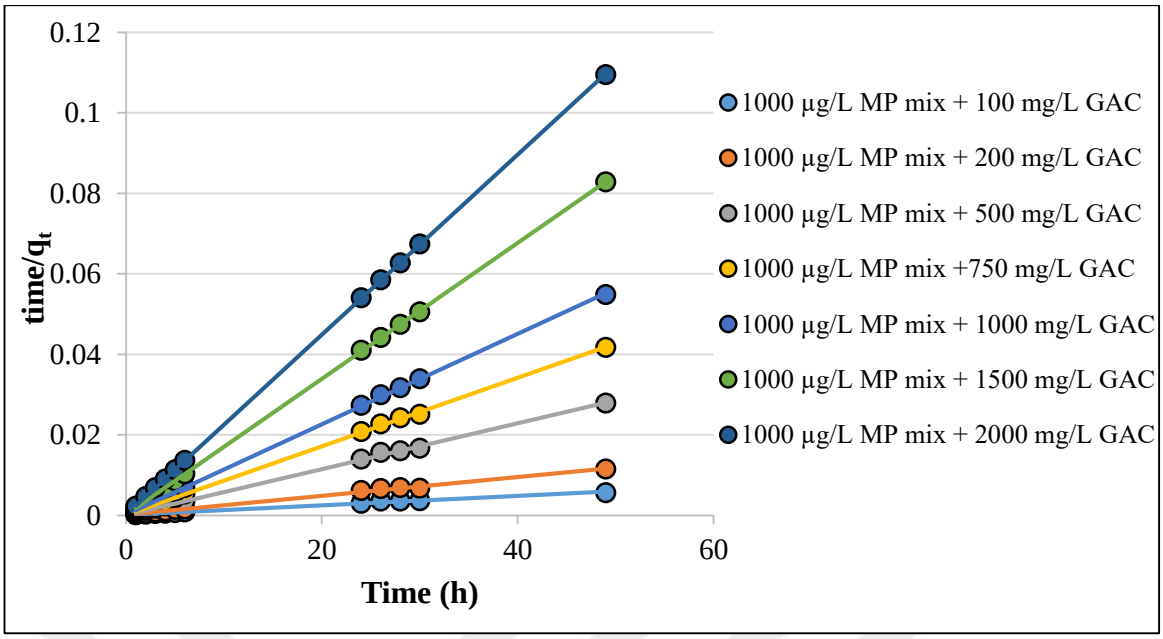

Figure 5.32. Experimental data of SMX and the fitted linear pseudo second-order rate equation.

The average rate constants (k_1 and k_2) and R^2 values are presented in Table 5.5. These values showed that the fit of the pseudo second-order model was better than the pseudo first-order model in the simulation of kinetics of all pharmaceuticals adsorption on GAC.

Table 5.5. Kinetic parameters obtained by using the linear kinetic models.

Pharmaceutical	**Pseudo first-order kinetic model**		**Pseudo second order kinetic model**	
	k_1 (1/h)	**R^2**	**k_2 (g/µg.h)**	**R^2**
ACT	0.080±0.02	0.78±0.06	0.0008±0.0005	0.99±0.003
CBZ	0.069±0.02	0.65±0.16	0.0006±0.0005	0.99±0.002
ERY	0.076±0.03	0.74±0.13	0.0021±0.0015	0.99±0.002
SMX	0.078±0.02	0.75±0.06	0.010±0.0007	0.99±0.003

The adsorption rates were also calculated using the k_2 values from the pseudo-second order model and presented in Table 5.6. For the calculations data belonging to the highest concentration of GAC (2000 mg/L) were used. According to the results, rate of the adsorption of SMX was the fastest among the others followed by CBZ, ACT and ERY.

Table 5.6. Adsorption rates of pharmaceuticals (2000 mg/L GAC).

Pharmaceutical	k_2 (g/µg.h)	q_e (µg/g)	Adsorption rate (µg/g.h)
ACT	0.0008	450	162
CBZ	0.0006	715	306.7
ERY	0.0021	214	96.2
SMX	0.010	447	1998

5.4. Isotherm Experiments

5.4.1. Isotherm Experiments with Ground/Original GAC and Synthetic Secondary Effluent

The purpose of these experiments was to investigate the adsorption of background organic matter onto GAC. Therefore, no pharmaceuticals were added. The equilibration time for each experimental set was determined from kinetic experiments as 120 and 24 hours for original and ground GAC, respectively. An experimental set-up similar to kinetic experiments was prepared for isotherm experiments by considering the equilibration time. Samples were taken at the beginning and end of experiments. Changes in background organic matter were characterized by DOC measurements and absorbance readings at 254, 280 and 436 nm wavelengths. According to the results, the Freundlich isotherm was fitted to data. As mentioned in Section 3.2.4.2, the linearized form of the Freundlich isotherm equation is expressed as follows:

$$\log q_e = \log K + n.\log C_e \qquad (5.7)$$

Adsorption isotherms were constructed using the initial and equilibrium concentrations of DOC, UV_{254}, UV_{280} and $Color_{436}$ for synthetic secondary effluent. q – C graphs were drawn and the K and n coefficients for each experimental set were calculated. 3 sets of isotherm experiments with ground GAC and 3 sets of isotherm experiments with original GAC were carried out with synthetic secondary effluent. All q – C graphs in terms of UV_{254}, UV_{280}, $Color_{436}$ and DOC parameters are given in **Appendix C.** The calculated K and n coefficients for each experimental set are presented in Table 5.7.

Table 5.7. Freundlich isotherm constants belonging to adsorption of background organic matter.

Experiment	# Set	Parameter	K (adsorption capacity)	n (adsorption intensity)	Equilibrium time
Synthetic secondary effluent + **Ground GAC**	1	UV_{254}	27 $(cm^{-1}/g\ GAC)(cm)^n$	1.05	24 h
		UV_{280}	25.7 $(cm^{-1}/g\ GAC)(cm)^n$	1.1	
		$Color_{436}$	2.4 $(cm^{-1}/g\ GAC)(cm)^n$	0.7	
		DOC	0.16 $(mg\ C/g\ GAC)(L/mg)^n$	3.4	
	2	UV_{254}	90.4 $(cm^{-1}/g\ GAC)(cm)^n$	1.3	
		UV_{280}	89.6 $(cm^{-1}/g\ GAC)(cm)^n$	1.3	
		$Color_{436}$	7.7 $(cm^{-1}/g\ GAC)(cm)^n$	0.9	
	3	UV_{254}	100.5 $(cm^{-1}/g\ GAC)(cm)^n$	1.5	
		UV_{280}	100.8 $(cm^{-1}/g\ GAC)(cm)^n$	1.5	
		$Color_{436}$	13 $(cm^{-1}/g\ GAC)(cm)^n$	1.02	
		DOC	0.01 $(mg\ C/g\ GAC)(L/mg)^n$	5.85	
Synthetic secondary effluent + **Original GAC**	1	UV_{254}	6.9 $(cm^{-1}/g\ GAC)(cm)^n$	0.9	120 h
		UV_{280}	5.6 $(cm^{-1}/g\ GAC)(cm)^n$	0.9	
		$Color_{436}$	2.2 $(cm^{-1}/g\ GAC)(cm)^n$	0.73	
		DOC	0.008 $(mg\ C/g\ GAC)(L/mg)^n$	4.7	
	2	UV_{254}	9.8 $(cm^{-1}/g\ GAC)(cm)^n$	0.75	
		UV_{280}	8.9 $(cm^{-1}/g\ GAC)(cm)^n$	0.72	
		$Color_{436}$	6.7 $(cm^{-1}/g\ GAC)(cm)^n$	0.81	
	3	UV_{254}	42.7 $(cm^{-1}/g\ GAC)(cm)^n$	1.3	
		UV_{280}	44 $(cm^{-1}/g\ GAC)(cm)^n$	1.3	
		$Color_{436}$	31 $(cm^{-1}/g\ GAC)(cm)^n$	1.08	
		DOC	0.13 $(mg\ C/g\ GAC)(L/mg)^n$	3.3	

When synthetic secondary effluent was used, isotherm constants in terms of UV_{254} and UV_{280} were close to each other. Since these parameters represent similar groups in background organic matter, this result was expected. Absorbance at 254 nm mainly corresponds to aromatic and unsaturated organic parts, whereas absorbance at 280 nm corresponds to lignin-derived parts (Çeçen and Aktaş, 2011).

The result of the experiments with original GAC showed that the K values representing adsorption capacity were lower than the experiments with ground GAC. It was concluded that affinity of the organic matter in synthetic secondary effluent to original GAC was low compared to ground GAC. It is recommended to grind larger adsorbent particles before the application because it shortens

the equilibration time and reduces the risk of experimental errors. However, it was indicated that the isotherms determined with ground material possibly do not exactly reflect the adsorption on the original particles (Worch, 2012). This could be explained by the smaller surface area of original GAC which has a bigger particle size. Consequently, adsorption capacity of ground GAC would be higher than original GAC.

In addition, it was observed that K values are too low and n values are too high in terms of DOC parameter for both original and ground GAC. These values indicate low adsorption of background organic matter present in the secondary effluent in terms of this parameter. There may be also a non-adsorbable fraction in synthetic secondary effluent solution. As seen in Figure C.4 and Figure C.8, approximately around 2 mg/L of DOC may be non-adsorbable, thus around 25-30% of the initial DOC. The low adsorption of background organic matter suggests a lower competition with pharmaceuticals.

As mentioned before, pH was not adjusted in the experiments. It was measured at the beginning and end. In experimental set 1 of ground GAC and experimental sets 1 and 2 of original GAC, the pH values were below 7. In these sets it was observed that adsorption capacities of GAC were lower compared to the other sets as indicated by K values. It can be said that low pH reduced the adsorption capacity.

5.4.2. Isotherm Experiments with Ground GAC and a Mixture of Pharmaceuticals

The purpose of these experiments was to investigate the adsorption of pharmaceuticals onto GAC in the absence and the presence of background organic matter. The equilibration time was determined as 24 hours for pharmaceuticals from kinetic experiments carried out with ground GAC as mentioned earlier. Experimental set-ups were prepared for isotherm experiments by considering the equilibration time. Samples were taken at the beginning and end of experiments. By using the Freundlich equation, the constants K and n were calculated for all pharmaceuticals as presented in Table 5.8. All q – C graphs belonging to pharmaceuticals are given in **Appendix D.**

5.4.2.1 Pharmaceuticals in a mixture. K values showed that when there was a mixture of pharmaceuticals, SMX had the highest adsorption capacity followed by ERY and ACT, while CBZ had the lowest capacity. In terms of adsorption capacity, ACT and SMX had similar values and it can be said that adsorption was favorable for these pharmaceuticals ($n<1$). On the other hand, CBZ had the highest n value (1.45) indicating unfavorable adsorption of this pharmaceutical. Overall, it can be

inferred that the selectivity of GAC for pharmaceuticals in experiments decreases in the following order: SMX, ERY, ACT and CBZ in the case of the mixture of pharmaceuticals.

5.4.2.2 Single pharmaceuticals. Additionally, 2 sets of experiments were carried out with single pharmaceuticals. According to the results, although n (adsorption intensity) values did not change much, K values were higher for all pharmaceuticals compared to the mixture. It was concluded that there was a competition between the four pharmaceuticals for adsorption sites on activated carbon.

Table 5.8. Freundlich isotherm constants belonging to adsorption of micropollutants onto ground GAC (Equilibrium time: 24 hours).

Experiment	**Pharmaceutical**	**K (adsorption capacity) ((µg/g GAC)(L/µg)^n)**		**n (adsorption intensity)**	
		Set 1	**Set 2**	**Set 1**	**Set 2**
1000 µg/L ACT only	ACT	259.3	295.2	0.86	1.36
1000 µg/L CBZ only	CBZ	216.5	202.3	1.06	1.30
1000 µg/L ERY only	ERY	306.6	77.2	1.12	2.35
1000 µg/L SMX only	SMX	187.5	236.3	1.70	1.25
Micropollutants mixture (1000 µg/L each)	ACT	43.5		0.89	
	CBZ	21.3		1.45	
	ERY	53.5		1.1	
	SMX	90.9		0.86	
		Set 1	**Set 2**	**Set 1**	**Set 2**
Micropollutants mixture (1000 µg/L each) + **Syn. Secondary WW**	ACT	46.5	38.7	1.04	0.94
	CBZ	$7.e^{-6}$	0.0002	4.81	3.70
	ERY	0.0022	22.5	3.87	1.05
	SMX	103.4	50.6	0.89	0.90
Micropollutants mixture (1000 µg/L each) + **Real WW** (Single experiment)	ACT	924.4		0.40	
	CBZ	751.8		0.44	
	ERY	718.9		0.47	
	SMX	696.2		0.41	

5.4.2.3 Pharmaceuticals in a mixture and in the presence of synthetic secondary effluent. Experiments were also carried out with a mixture of pharmaceuticals and synthetic secondary effluent in order to observe the competition between the pharmaceuticals and background organic matter. The adsorption capacity of CBZ, ERY an SMX decreased in the presence of background organic matter as seen from K values in Table 5.8. On the other hand, the adsorption capacities of ACT were close to each other in the absence and presence of background organic matter. In these experiments UV_{254}, UV_{280},

$Color_{436}$ and DOC were also measured and are presented in Table 5.9. In terms of color, n is the lowest, meaning that the adsorption intensity is high. Adsorption capacity in terms of DOC was too low and n value was too high which indicated low adsorption as in the case when there was only synthetic secondary effluent. In fact, adsorption of the background organic matter present in synthetic secondary effluent was much lower when there was a mixture of pharmaceuticals. Thus, the competition is probably low. Since background organic matter did not consist of a single compound (Table 4.4) in synthetic secondary effluent, the K and n values were not compared with the values of pharmaceuticals.

Table 5.9. Freundlich isotherm constants belonging to adsorption of background organic matter in the presence of micropollutants.

Experiment	# Set	Parameter	K (adsorption capacity)	n (adsorption intensity)
Synthetic secondary effluent + Micropollutants mixture (1000 μg/L each)	1	UV_{254}	187 $(cm^{-1}/g\ GAC)(cm)^n$	1.75
		UV_{280}	143.2 $(cm^{-1}/g\ GAC)(cm)^n$	1.62
		$Color_{436}$	3.7 $(cm^{-1}/g\ GAC)(cm)^n$	0.82
	2	UV_{254}	219 $(cm^{-1}/g\ GAC)(cm)^n$	1.78
		UV_{280}	230 $(cm^{-1}/g\ GAC)(cm)^n$	1.78
		$Color_{436}$	1.1 $(cm^{-1}/g\ GAC)(cm)^n$	0.59
		DOC	$6.e^{-5}$ (mg C/g GAC)(L/mg)^n	9.57
Real WW + Micropollutants mixture (1000 μg/L each)	1	UV_{254}	82.7 $(cm^{-1}/g\ GAC)(cm)^n$	0.68
		UV_{280}	146.9 $(cm^{-1}/g\ GAC)(cm)^n$	0.94
		$Color_{436}$	248.1 $(cm^{-1}/g\ GAC)(cm)^n$	1.23
		DOC	2.75 (mg C/g GAC)(L/mg)^n	2.04

5.4.2.4 Pharmaceuticals in a mixture and in the presence of a real secondary effluent. An experiment was also carried out with the real secondary effluent from the Paşaköy WWTP and the mixture of pharmaceuticals. The results showed that n values of all pharmaceuticals were low which indicate higher adsorption intensity compared to the synthetic secondary effluent. Also, K values in Table 5.8 showed that the affinity of all pharmaceuticals to GAC were much higher in the presence of the real WWTP effluent. The selectivity of GAC for pharmaceuticals decreases in the following order: ACT, CBZ, ERY and SMX. In this experiment, UV_{254}, UV_{280}, $Color_{436}$ and DOC were also measured and are presented in Table 5.9. It was observed that adsorption capacity in terms of UV_{254} was lower and UV_{280} is close to result of the 1st experiment, whereas adsorption capacities in terms of $Color_{436}$ and DOC were higher compared to the synthetic secondary effluent. Since only one experiment was

carried out with the real effluent sample and the sample qualities may change, different results might be obtained from different experiments in other cases.

5.5. Rapid Small Scale Column Tests (RSSCTs)

RSSCTs were carried out to investigate the removal of pharmaceuticals by GAC adsorption. Table 5.10 shows the details and the purposes of these experiments.

Table 5.10. Details of RSSCTs.

Section	Feed	GAC type	Purpose
5.5.1	Synthetic secondary effluent	Original	to investigate the adsorption of background organic matter onto original GAC
5.5.2	Synthetic secondary effluent	Ground	to investigate the adsorption of background organic matter onto ground GAC
5.5.3	A mixture of pharmaceuticals	Original	to investigate the adsorption of pharmaceuticals onto original GAC
5.5.4.1	A mixture of pharmaceuticals	Ground	to investigate the adsorption of pharmaceuticals onto ground GAC
5.5.4.2	A mixture of pharmaceuticals and Synthetic secondary effluent	Ground	to investigate the adsorption of pharmaceuticals onto ground GAC in the presence of background organic matter

5.5.1. RSSCTs with Original GAC and Synthetic Secondary Effluent

Two experiments were carried out with original (non-ground) GAC in order to make a comparison with the experiments carried out with ground GAC. In these experiments the rapid small-scale columns were filled with original GAC (particle size around 1 mm) and synthetic secondary effluent was fed to it for 14 and 30 days, respectively in order to observe the removal of background organic matter. There were no pharmaceuticals in the feed. Samples were taken for UV_{254}, UV_{280} and DOC measurements. Breakthrough curves, which reflect the concentration profile in the effluent of an adsorber column, were obtained with respect to time. Figure 5.33 shows the normalized concentration (C/C_0=effluent concentration/initial concentration) in terms of UV_{254} and UV_{280} parameters in both experiments. The UV_{254} and UV_{280} values of the influent synthetic secondary wastewater were 0.132 1/cm and 0.115 1/cm, respectively. For example, to reach 70% breakthrough in concentration (C/C_0=0.7), an operational period of approximately 10 days was needed. In the first experiment, it was observed that almost 90% of initial UV_{254} and UV_{280} were reached at the end of the experiment, while C/C_0 were around 0.8 at the end of the second experiment. It can be said that the complete breakthrough of background organic matter (C/C_0 = 1) would occur at the order of days.

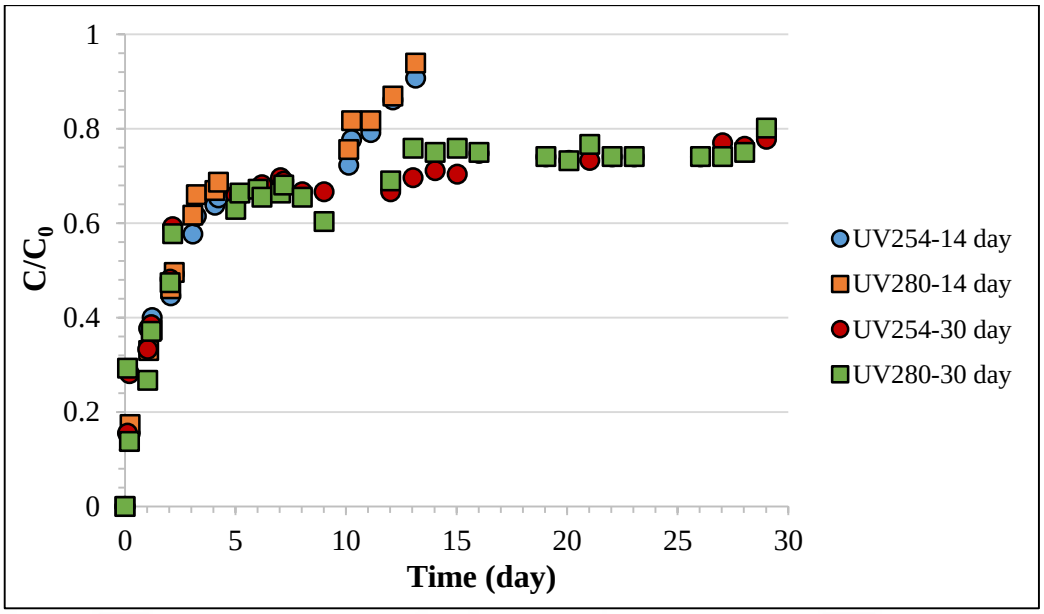

Figure 5.33. Breakthrough curves in terms of UV_{254} and UV_{280} in the RSSCT column filled with original GAC and fed with synthetic secondary effluent (14-day and 30-day experiments).

In the second experiment also DOC was regularly measured during 30 days. The DOC concentration in the influent was 3.6 mg/L. Figure 5.34 shows the breakthrough curve in terms of DOC. 80% breakthrough was reached after 10 days (C/C_0=0.8). In terms of this parameter, full breakthrough would also occur at the order of days.

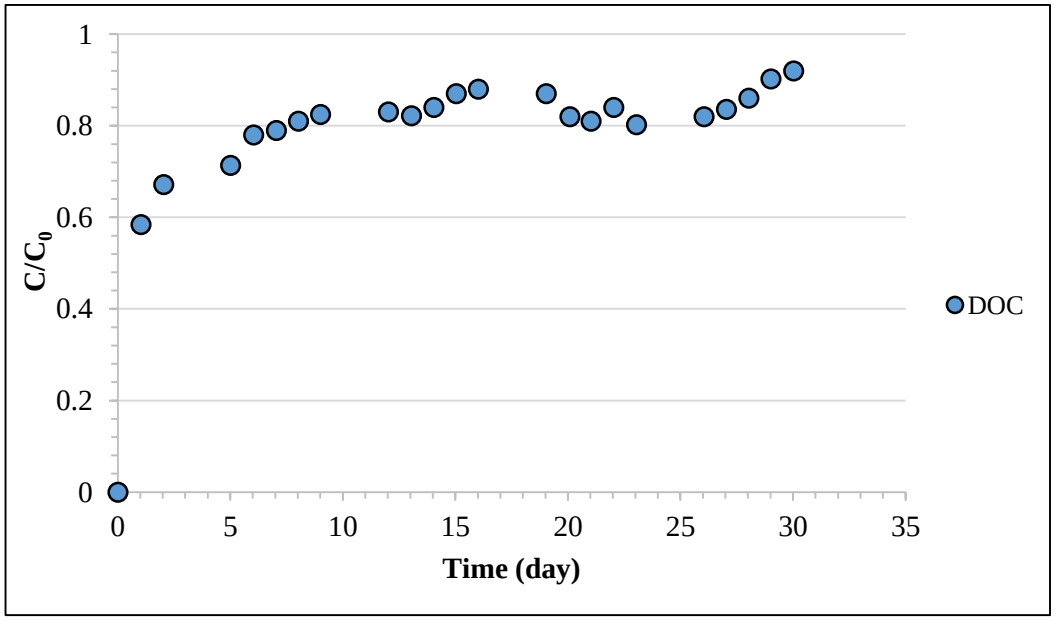

Figure 5.34. Breakthrough curve in terms of DOC in the RSSCT column filled with original GAC and fed with synthetic secondary effluent (30-day experiment).

5.5.2. RSSCTs with Ground GAC and Synthetic Secondary Effluent

Two experiments were carried out with ground GAC (particle size around 100 μm). In these experiments the column was filled with ground GAC and synthetic secondary effluent was fed to it for 24 and for 30 hours, respectively. There were no pharmaceuticals in the feed. During the experiments, samples were taken hourly for DOC, UV_{254} and UV_{280} analyses and breakthrough curves were obtained with respect to time.

Figure 5.35 and Figure 5.36 shows the C/C_0 in terms of UV parameters in both experiments and DOC in the first experiment, respectively. The breakthrough in terms of background organic matter was reached in any case much earlier, in hours with ground GAC compared to days with original GAC (shown in Figure 5.33). For example, in the first and second experiment with ground GAC, the normalized concentration (C/C_0) of UV parameters reached around 0.7 after around 8 hours.

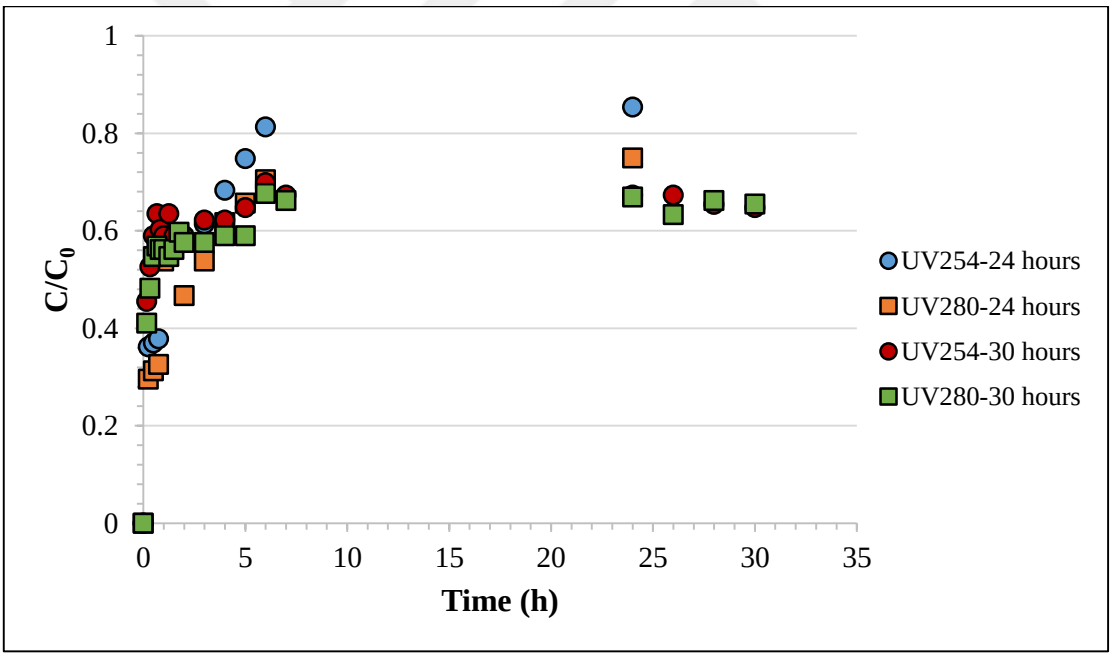

Figure 5.35. Breakthrough curves in terms of UV_{254} and UV_{280} during the experiments with ground GAC and fed with synthetic secondary effluent (24-hour and 30-hour experiments).

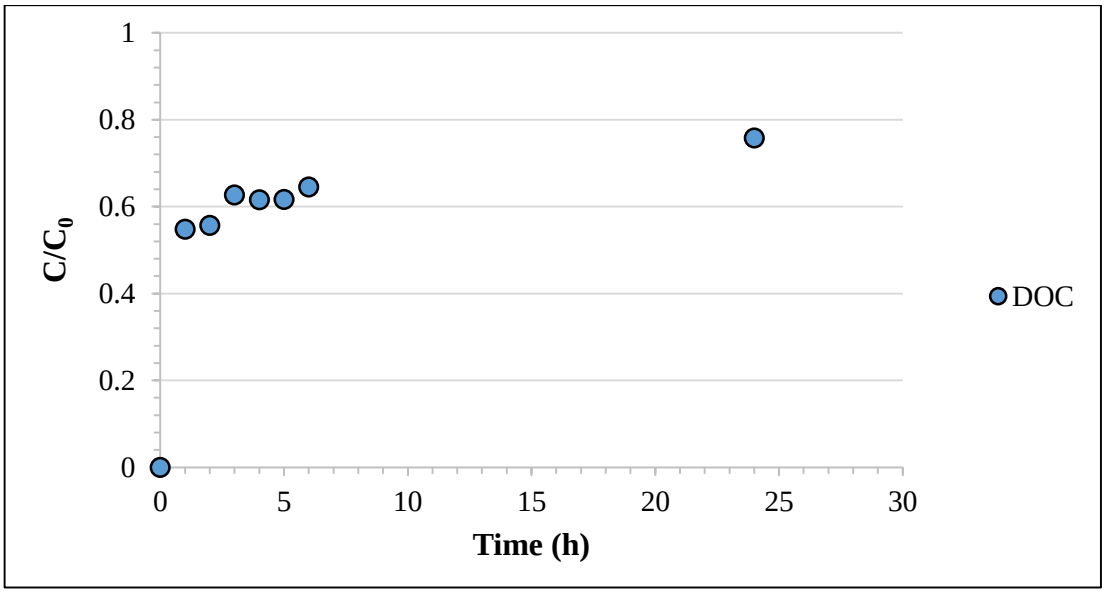

Figure 5.36. Breakthrough curves in terms of DOC in the RSSCT column filled with ground GAC and fed with synthetic secondary effluent (24-hour experiment).

As mentioned in previous sections, the most important point is to provide a similitude between pilot-scale and small-scale columns (Crittenden et al., 1991). If similarity is ideal, the breakthroughs obtained from the original and ground GAC should be equal to each other. Thus, it is possible to simulate pilot-scale performance by using different rapid small-scale columns. The shapes of the breakthrough curves were similar to each other and as seen from Figure 5.33 and Figure 5.35; Figure 5.34 and Figure 5.36. The time needed to reach breakthrough was longer in the case of original GAC as expected. For original GAC the breakthrough time was in the order of days, while for ground GAC it was in the order of hours.

5.5.3. RSSCTs with Original GAC and a Mixture of Micropollutants

An experiment was carried out with original (non- ground) GAC in order to make comparison with the experiments carried out with ground GAC. The rapid small-scale column was filled with original GAC (particle size around 1 mm) and a mixture of pharmaceuticals (initial concentrations of all pharmaceuticals were 200 µg/L) in deionized water was fed to it for 20 days. In the feed there was no background organic matter. Breakthrough curves were obtained with respect to time for all pharmaceuticals. Figure 5.37 shows the normalized concentrations (C/C_0=effluent concentration/initial concentration).

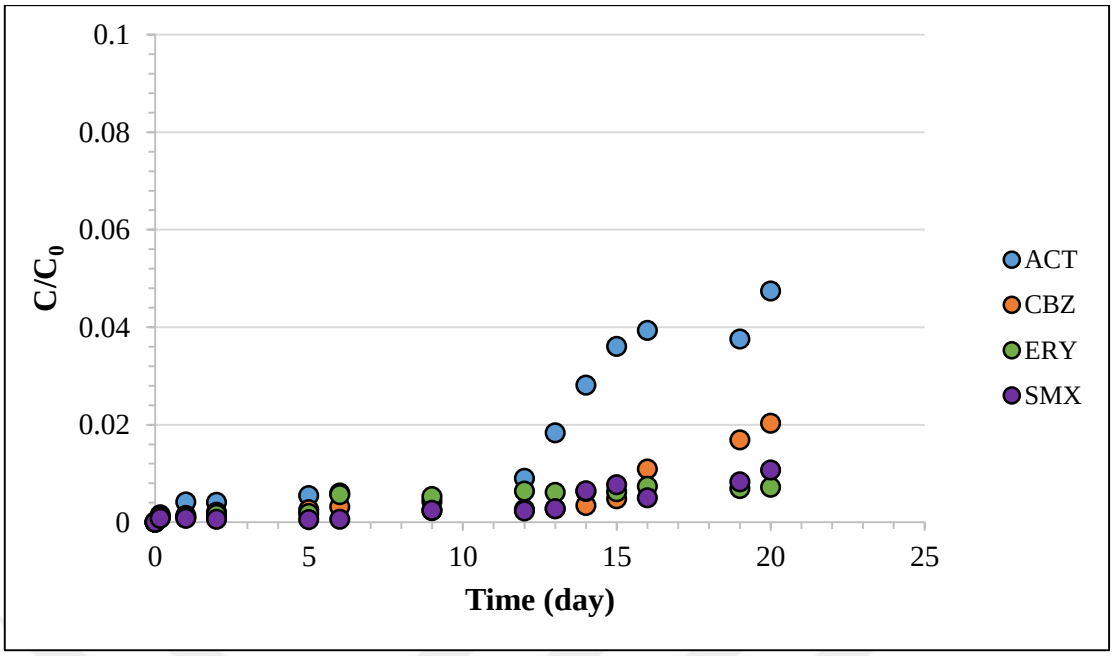

Figure 5.37. Normalized concentrations of pharmaceuticals in the RSSCT column filled with original GAC with respect to time.

It was observed that there was no full breakthrough ($C/C_0 = 1$) for any of the pharmaceuticals since they were at low concentrations in the influent. In the period monitored, the normalized concentrations (C/C_0) of ERY and SMX were very close to each other (around 0.01), while for CBZ this value was slightly higher ($C/C_0 = 0.02$) at the end of the experiment. In addition, C/C_0 of ACT reached to 0.05 after 20 days. This indicates that only 5% of initial concentration of ACT was reached to the effluent at the end of the experiment.

5.5.4. RSSCTs with Ground GAC and a Mixture of Micropollutants

5.5.4.1 Experiments with a mixture of micropollutants. Two experiments were carried out with ground GAC and a mixture of micropollutants. The same procedure was followed for both experiments as in the case of synthetic secondary effluent. The conditions were also the same. The column was filled with ground GAC and a mixture of micropollutants (initial concentrations of ACT, CBZ, ERY and SMX were 178 µg/L, 142 µg/L, 142 µg/L and 181 µg/L, respectively) was fed to it for 30 hours. There was no background organic matter. Samples were taken regularly during the experiments for monitoring the concentration of pharmaceuticals. Normalized concentrations (C/C_0) were calculated for all pharmaceuticals. The results of 1st and 2nd experiment are shown in Figure 5.38 and Figure 5.39, respectively.

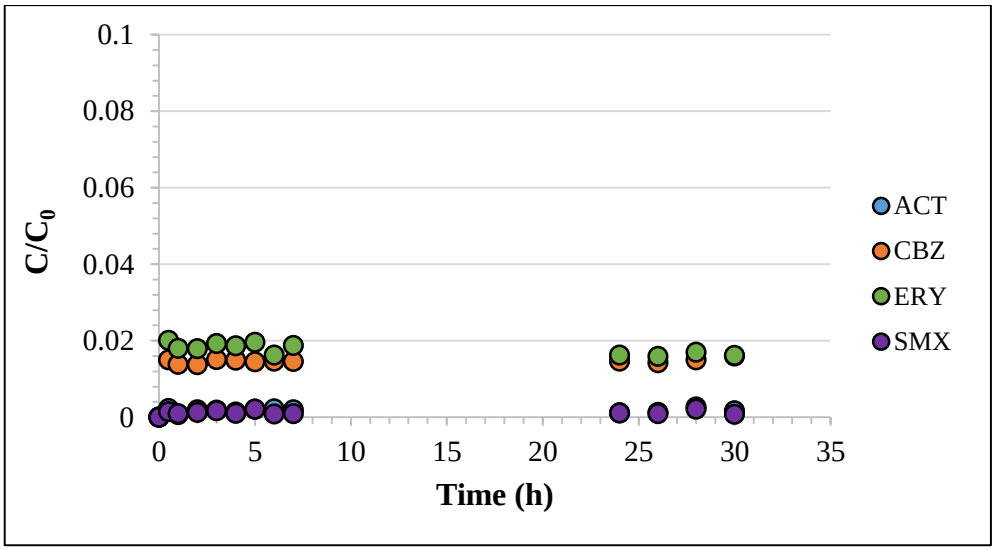

Figure 5.38. Normalized concentrations of pharmaceuticals in the RSSCT column filled ground GAC with respect to time (1st experiment).

It was observed in the first experiment that there was no full breakthrough ($C/C_0 = 1$) of either of the pharmaceuticals. In fact, the column is far away from saturation. The C/C_0 of ERY reached around 0.02 at the beginning of the experiment and remained constant for 30 hours, while for CBZ this value was 0.01 during the experiment and reached around 0.02 at the end. On the other hand, C/C_0 values were very close to each other (0.001) for ACT and SMX during the experiment.

The results of the second experiment were slightly different from the first experiment. As seen in Figure 5.39, for ERY the C/C_0 value reached around 0.02 at the beginning of the experiment and remained constant for 30 hours as in the first column test. Then, it reached to 0.03 at the end of the experiment. For CBZ the C/C_0 reached around 0.01 at the beginning and reached to 0.04 after 5 hours and remained constant. Also, the C/C_0 of ACT and SMX reached to 0.01 at the end of 30 hours. These higher ratios could be explained with slightly higher initial concentrations of all pharmaceuticals in the second experiment. Initial concentrations of ACT, CBZ, ERY and SMX were 285 µg/L, 328 µg/L, 272 µg/L and 270 µg/L, respectively in the influent. When these results were compared in terms of loading, which was expressed as QxC_0, in the first experiment loading of ACT, CBZ, ERY and SMX were 1.40 µg/min, 1.11 µg/min, 1.11 µg/min and 1.41 µg/min, respectively. For the second experiment loadings were 2.24 µg/min, 2.57 µg/min, 2.14 µg/min and 2.12 µg/min for ACT, CBZ, ERY and SMX, respectively. These slightly higher loadings may have led to higher effluent concentrations at the end of the experiment.

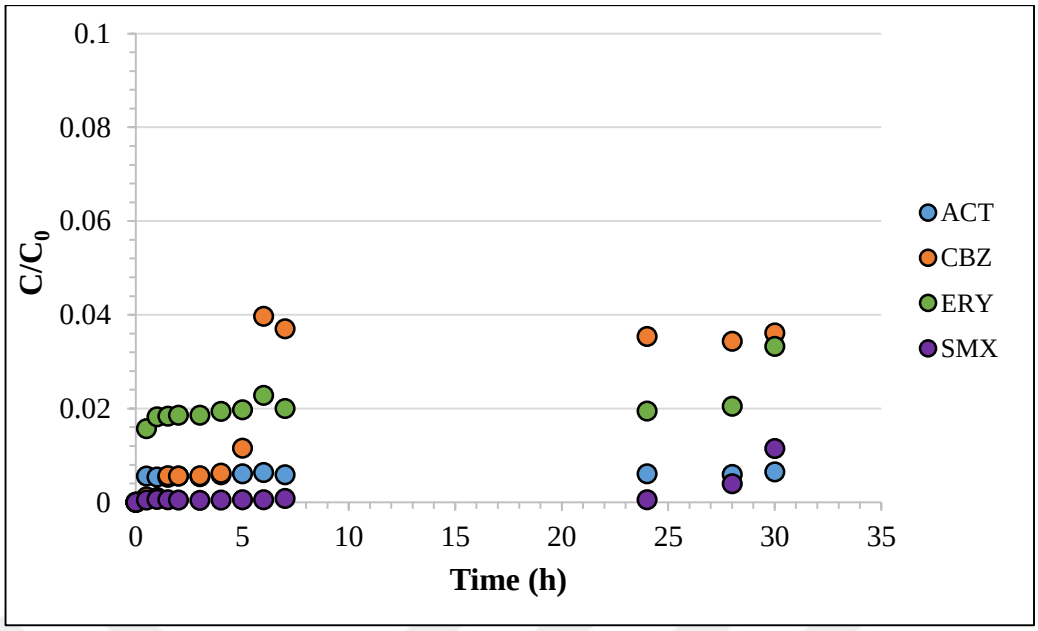

Figure 5.39. Normalized concentrations of pharmaceuticals in the RSSCT column filled ground GAC with respect to time (2nd experiment).

In addition, it was observed in the second experiment that CBZ and ERY reached higher C/C_0 ratios compared to ACT and SMX at the end of the experiment. However, isotherm experiments showed that the affinity of ERY to GAC was higher compared to ACT in the presence of a mixture of pharmaceuticals in the solution. This column test showed a different order of pharmaceutical adsorption. These kinds of disagreements between the batch experiments and RSSCTs were explained in a study that mass transfer processes in GAC filters are highly relevant, which need to be taken into account in adequate breakthrough curve determination. Furthermore, it was said that the potential for GAC pore fouling cannot be determined from batch experiments (Zietzschmann et al., 2014). Yet, since the duration of the experiment was very short, it is possible to observe a different pattern in breakthrough of pharmaceuticals in a long term.

The normalized effluent concentrations (C/C_0) of pharmaceuticals were observed to be very low during the short duration of experiments. So, these results were used as inputs in the AdDesign software to simulate the breakthrough curves for longer time periods. The detailed results are given and discussed in Section 5.8.

5.5.4.2 Experiments with a mixture of micropollutants and synthetic secondary effluent. Another experiment was carried out with ground GAC and a mixture of micropollutants and synthetic secondary effluent. In this experiment the column was filled with ground GAC and a mixture of micropollutants (initial concentrations of ACT, CBZ, ERY and SMX were 168 µg/L, 181 µg/L, 171

µg/L and 185 µg/L, respectively) and synthetic secondary effluent (initial DOC concentration was 6.2 mg/L) was fed to it for 24 hours. The purpose was to investigate the competition between the pharmaceuticals and the background organic matter in the synthetic secondary effluent. Results are shown in Figure 5.40.

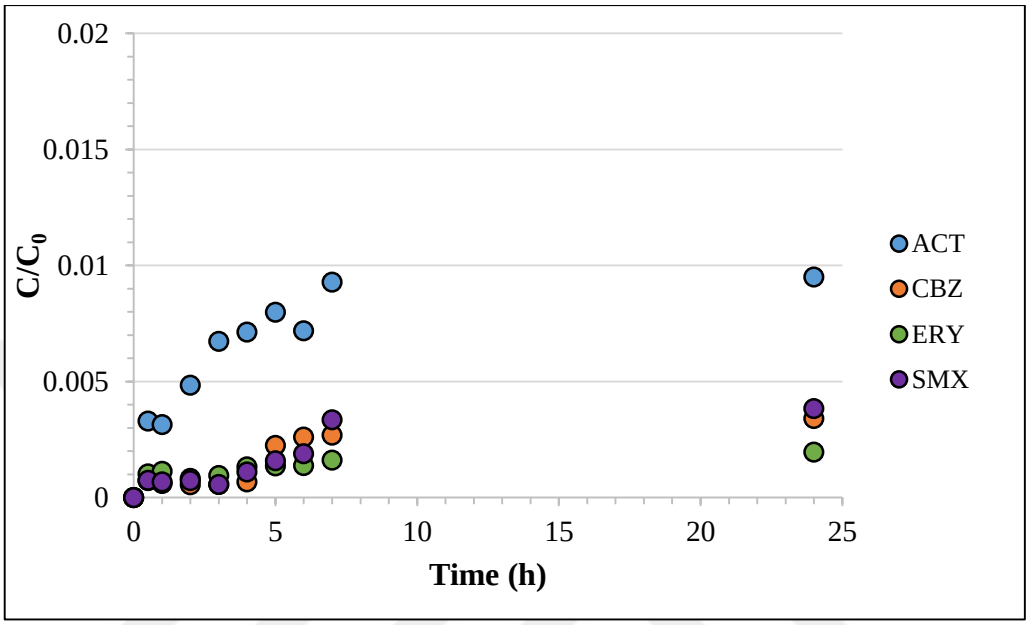

Figure 5.40. Normalized concentrations of pharmaceuticals in the presence of synthetic secondary effluent in the RSSCT column with respect to time.

It was observed that when there was background organic matter, C/C_0 value of ACT reached 0.01 after 3 hours and remained constant. On the other hand, the C/C_0 values of CBZ, ERY and SMX were close to each other at the end of the experiment. However, isotherm experiment with a mixture of pharmaceuticals and synthetic secondary effluent (Table 5.8) showed that CBZ had the lowest affinity to GAC compared to other pharmaceuticals. On the other hand, although isotherm test showed a high affinity of ACT to GAC compared to ERY and CBZ, in this RSSCT it reached to the highest C/C_0 ratio at the end of the experiment.

Besides, UV_{254}, UV_{280}, $Color_{436}$ and DOC parameters were also measured during the experiment in order to observe the adsorption of background organic matter. As seen in Figure 5.41 and Figure 5.42, C/C_0 reached 0.6 in the first hours of the experiment in terms of all parameters. Thus, the breakthrough of background organic matter occurred much earlier than pharmaceuticals. The affinity of background organic matter to GAC was too low according to Freundlich parameters as seen in isotherm experiments. When there was a mixture of pharmaceuticals, adsorption of background organic matter was much lower. In terms of DOC, almost 95% of influent concentration was observed

in the effluent of the column at the end of the experiment. This indicates almost complete breakthrough in the same period of time.

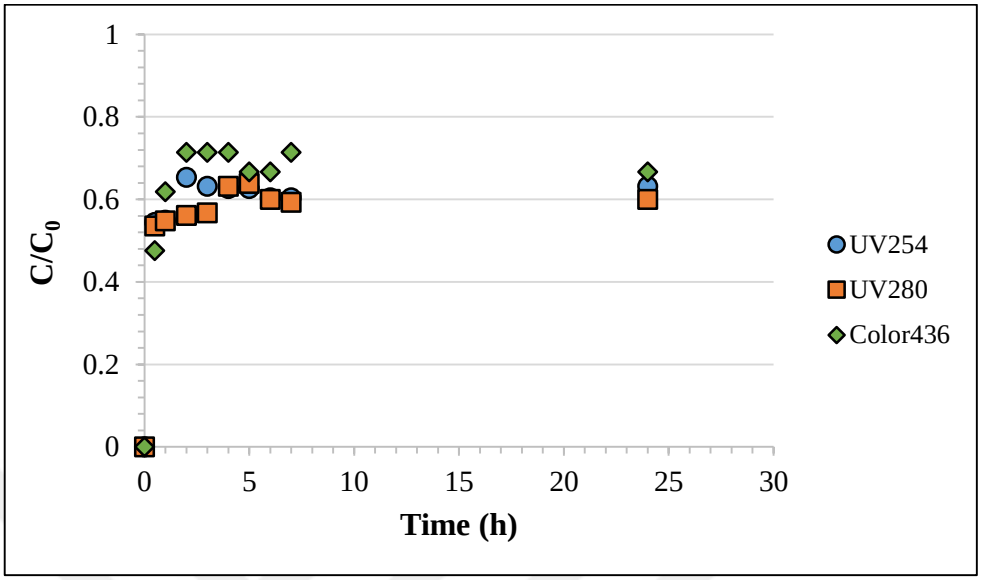

Figure 5.41. The normalized concentrations in terms of UV_{254}, UV_{280} and $Color_{436}$ of synthetic secondary effluent in GAC column with respect to time.

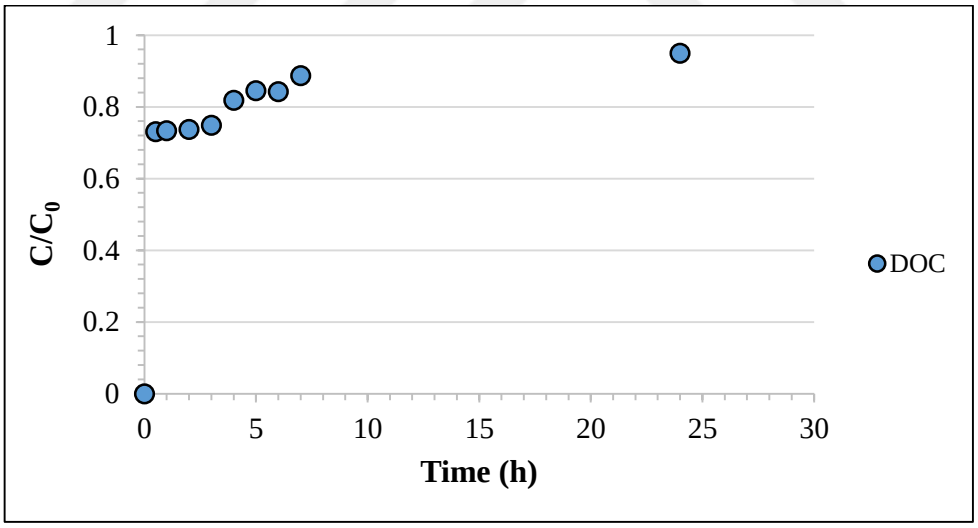

Figure 5.42. The normalized concentration in terms of DOC of synthetic secondary effluent in GAC column with respect to time.

5.5.5. Tracer Test

The dispersion coefficient and dispersivity values were determined from tracer test by matching the experiment results to the model concentrations of 1-D advection-dispersion solution. Figure 5.43 shows the tracer test and the best-fit of the model. The shape of the experimental data is very close to

the curve of model calculation. The best-fit dispersion coefficient and the other values are given in Table 5.11.

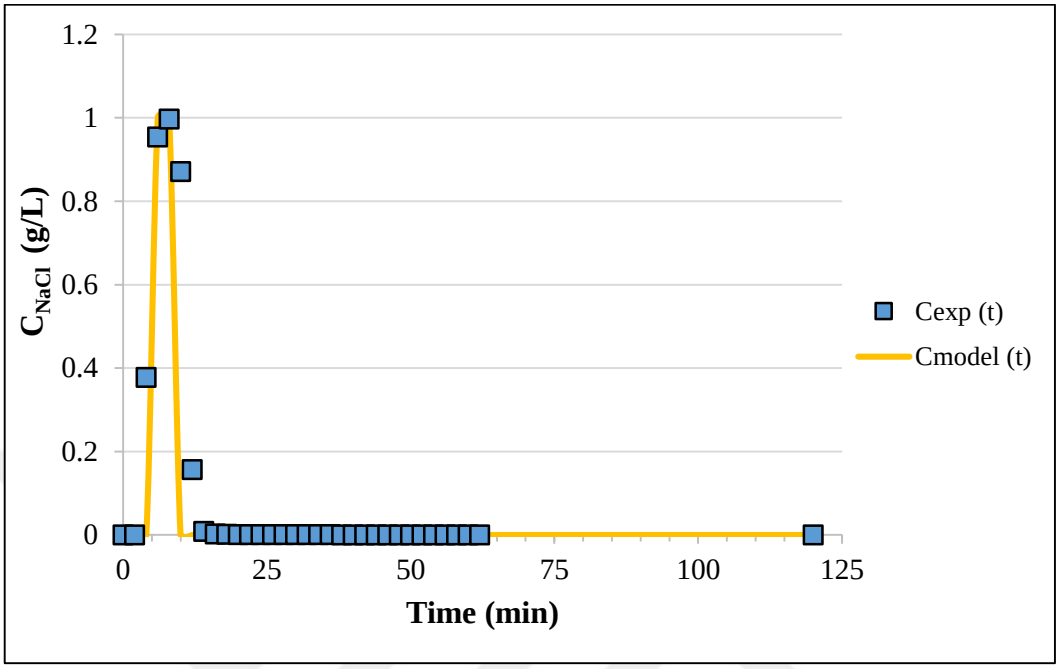

Figure 5.43. Experimental data of tracer test and model results.

Table 5.11. The parameters determined from tracer test.

Parameter	Value
Flow rate (mL/min)	7.85
Length (L) (cm)	2
Velocity (v) (cm/min)	20
Dispersion coefficient (D_x) (cm^2/min)	0.5
Longitudinal dispersivity (cm)	0.03
Peclet number ($Pe = vL/D_x$)	80

Peclet number defines the ratio of advection to dispersion along the column. High Peclet numbers show that advection controls the mass transport. As the Peclet number approaches to infinity, transport occurs only by advection and no axial dispersion occurs. On the other hand, if the Peclet number approaches to zero, only axial dispersion occurs and there is no transport by advection (Crittenden et al., 2012; Çeçen and Aktaş, 2011). High Peclet number in Table 5.11 showed that advection controls the mass transport in the column due to high flow rate and dispersion is low.

5.6. Ideal Breakthrough Time of RSSCTs

According to Worch (2012), in the case of infinitely fast mass transfer process and no dispersion, an ideal breakthrough occurs and the time to reach the breakthrough is termed the ideal breakthrough time. Each real breakthrough time can be approximately determined by the ideal breakthrough time for strongly adsorbable substances in GAC filters with the following equation:

$$t_b^{id} \approx t_{st} = \frac{q_0 m_A}{C_0 Q} \quad (5.8)$$

where q_0 is the adsorbed amount in equilibrium with the inlet concentration (calculated from isotherm experiments) (µg/g GAC), m_A is the GAC mass (g), Q is the flow rate (mL/min), and C_0 is the inlet concentration (µg/L). Figure 5.44 shows the ideal and real breakthrough time. In the case of a symmetrical S-shaped breakthrough curve, the ideal breakthrough time is the time where the relative concentration of the real breakthrough curve equals 0.5 (Worch, 2012).

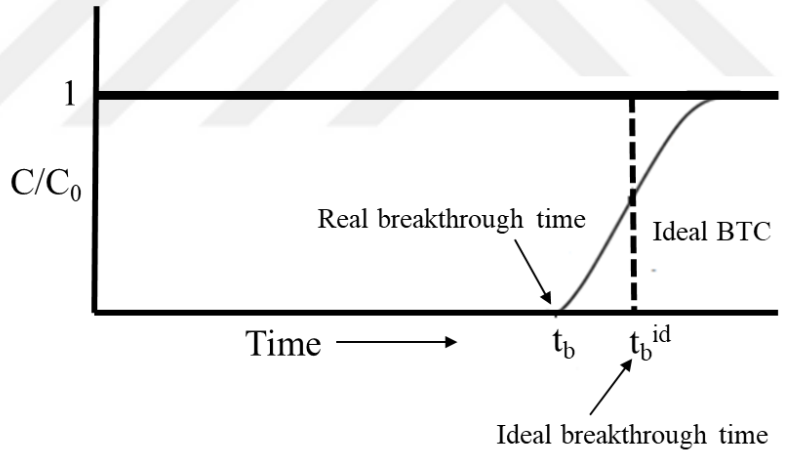

Figure 5.44. The ideal and real breakthrough time (Adapted from Worch, 2012).

According to Equation 5.8, ideal breakthrough times for ACT, CBZ, ERY and SMX were approximately calculated for each column test and presented in Table 5.12. For Freundlich parameters (K and n), data from the isotherm experiments were used to calculate the adsorbed amount in equilibrium ($q_0 = K.C_0^n$).

Table 5.12. Ideal breakthrough time for pharmaceuticals in column tests.

Exp.	Pharma.	K ((µg/g GAC)(L/µg)^n)	n	C_0 (µg/L)	m_A (g)	Q (mL/min)	t_b^{id} (d)
with original (non-ground) GAC **(Section 5.5.3)**	ACT	43.5	0.89	178	0.6593	0.078	144
	CBZ	21.3	1.45	142			1163
	ERY	53.5	1.1	142			515
	SMX	90.9	0.86	181			258
with ground GAC (Average of two experiments) **(Section 5.5.4.1)**	ACT	43.5	0.89	232	0.7110	7.85	1.5
	CBZ	21.3	1.45	235			15.6
	ERY	53.5	1.1	207			5.7
	SMX	90.9	0.86	226			2.7
with ground GAC in the presence of syn. secondary effluent **(Section 5.5.4.2)**	ACT	38.7	0.94	167	0.7839	7.85	2
	CBZ	0.0002	3.7	180			17
	ERY	22.5	1.05	171			2
	SMX	50.6	0.9	185			2

5.6.1. Column Test with Original GAC

As seen in the column test with original (non-ground) GAC, the normalized effluent concentrations (C/C_0) of pharmaceuticals were very low during the experiment. Ideal breakthrough times were approximately calculated for ACT, CBZ, ERY and SMX as 144, 1163, 515 and 258 days, respectively. When original GAC was used the breakthrough could be achieved in a long period of time, for example in weeks or months. Since there were internal and external mass transfer, dispersion and competition between compounds, this ideal case was not expected and shorter period of time would be necessary to reach the breakthrough. These results were also compared with a simulation model called AdDesign which provides evaluation and design systems that use GAC for the removal of contaminants. The detailed results were given and discussed in Section 5.8.

5.6.2. Column Test with Ground GAC

Two column tests were carried out with ground GAC and a mixture of pharmaceuticals. Ideal breakthrough times for ACT, CBZ, ERY and SMX were also calculated and presented in Table 5.12. For the calculations average values of two experiments were used. As mentioned before, these values give only a rough estimation on the breakthrough time if there is no mass transfer effect in the GAC column. According to the values, ideal breakthrough of CBZ is expected to be reached later than other pharmaceuticals.

In addition, the ideal breakthrough times for ACT, CBZ, ERY and SMX in the column experiment in the presence of synthetic secondary effluent were also calculated. These values showed that the ideal breakthrough times for ERY and SMX were shorter compared to the case when there was no background organic matter. The ideal breakthrough time for ACT and CBZ was longer compared to the absence of background organic matter, but close to each other in both cases. It was expected that in ideal case, the presence of background organic matter could affect the adsorption of pharmaceuticals.

5.7. Specific Throughput and Carbon Usage Rate of RSSCTs

Specific throughput and carbon usage rate (CUR) are also used to quantify the performance of a GAC adsorber. Specific throughput is the volume of water treated per mass of adsorbent used at a given treatment objective. CUR is the mass of adsorbent used per volume of water treated to a given treatment objective. These are defined as shown in Equation 5.9 and 5.10, respectively (Crittenden et al., 2012).

$$\text{Specific throughput} = \frac{V \cdot t_{bk}}{EBCT \cdot M_{GAC}} \tag{5.9}$$

where V is the volume occupied by adsorber media (mL), t_{bk} is the time to arbitrary breakthrough (h), EBCT is empty bed contact time (min) and M_{GAC} is mass of GAC (g).

$$\text{Carbon usage rate} = \frac{1}{\text{Specific throughput}} \tag{5.10}$$

By using these equations, specific throughput and CUR of all conducted RSSCTs were calculated and presented in Table 5.13. The breakthrough was chosen as $C/C_0 = 0.7$ for background organic matter in terms of DOC and $C/C_0 = 0.001$ for pharmaceuticals. Then, the breakthrough times were determined according to chosen breakthrough in order to compare the results of experiments. It was seen that when ground GAC was used, specific throughputs are higher and carbon usage rates (CUR) were lower due to the short period of time of the experiments. This indicates the use of RSSCTs is advantageous in terms of time and cost saving.

Table 5.13. Specific throughput and carbon usage rate of RSSCTs.

Experiment	V (mL)	t_{bk} (h)	EBCT (min)	M_{GAC} (g)	Specific throughput (m^3/kg GAC)	CUR (g/L)	Bed Volume (BV)
Original GAC with Syn. Secondary Eff. **(Section 5.5.1)**	1.57	120	20	0.6529	0.87	1.15	360
Ground GAC with Syn. Secondary Eff. **(Section 5.5.2)**	1.57	15	0.20	0.6782	10.42	0.10	4500
Original GAC with MPs **(Section 5.5.3)**	1.57	4	20	0.6593	0.03	33.3	12
Ground GAC with MPs **(Section 5.5.4.1)**	1.57	2	0.20	0.7114	1.32	0.76	600
Ground GAC with MPs and Syn. Secondary Eff. **(Section 5.5.4.2)**	1.57	1	0.20	0.7839	0.60	1.67	300

5.8. Comparison of RSSCTs Results with a Simulation Model

As mentioned in previous sections, the RSSCTs carried out within the scope of this study were simulated in the AdDesign Software and the results are presented in the following sections.

5.8.1. Simulation of an RSSCT with a Mixture of Pharmaceuticals and Ground GAC

The AdDesign model was used for simulating a 30-hour RSSCT and showing the breakthrough curve in a longer period of time. For this purpose, kinetic parameters of the pharmaceuticals from batch isotherm tests with ground GAC and the characteristics of the small column were entered as input parameters. There were two RSSCTs with a mixture of pharmaceuticals and ground GAC. So for showing the simulation, the averages of normalized concentrations were used. Table 5.14 shows the input parameters and Figure 5.45, Figure 5.46, Figure 5.47 and Figure 5.48 show the final breakthrough curves belonging to ACT, CBZ, ERY and SMX obtained from the model and the experiments, respectively.

Table 5.14. Input parameters in the AdDesign run for a mixture of pharmaceuticals and ground GAC.

Parameter	Value	
Flow rate (mL/min)	7.85	
EBCT (min)	0.20	
Particle size (mm)	0.1	
Initial concentration (µg/L)	ACT	232
	CBZ	235
	ERY	207
	SMX	226
Freundlich K ((µg/g)(L/µg)^n)	ACT	43.5
	CBZ	21.3
	ERY	53.5
	SMX	90.1
Freundlich n	ACT	0.89
	CBZ	1.45
	ERY	1.1
	SMX	0.86
Bed mass (g GAC)	0.7110	
Film diffusion coefficient (cm/s)	0.0212	
Surface diffusion coefficient (cm^2/s)	ACT	4.23xe^{-9}
	CBZ	4.30xe^{-10}
	ERY	1.11xe^{-9}
	SMX	2.38xe^{-9}
Pore diffusion coefficient (cm^2/s)	9.71xe^{-6}	

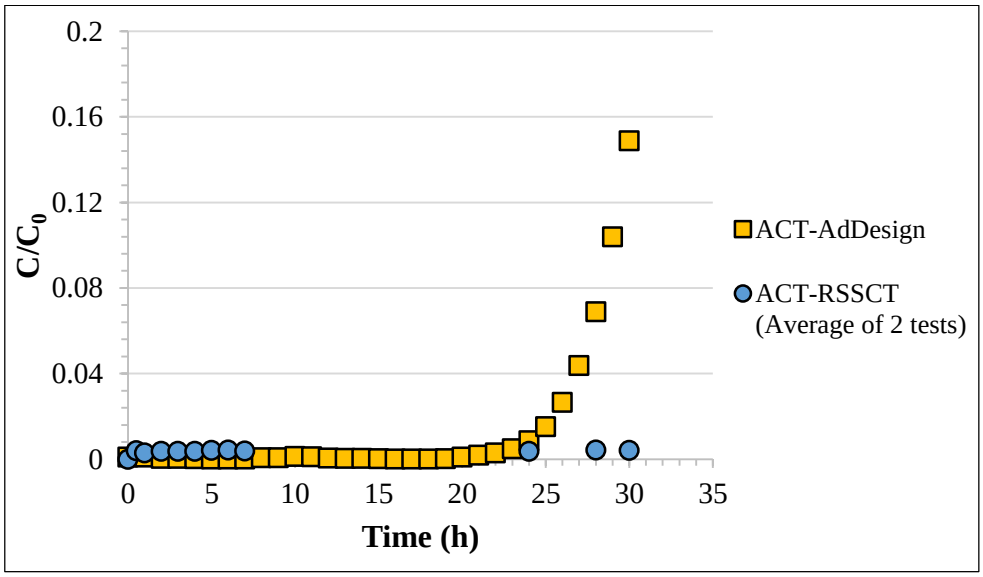

Figure 5.45. The breakthrough of ACT obtained from the experiments and the AdDesign model (Ground GAC).

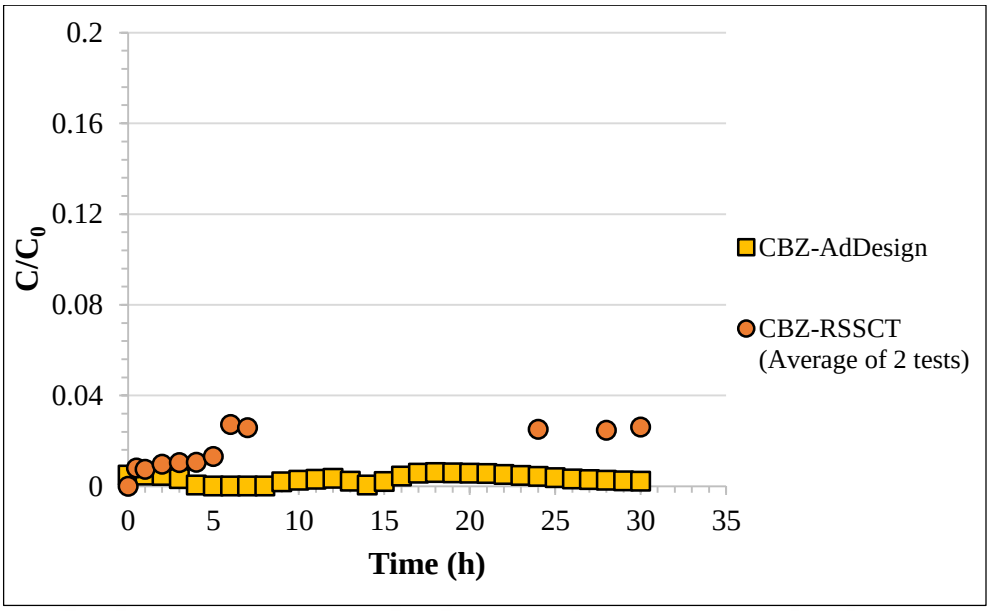

Figure 5.46. The breakthrough of CBZ obtained from the experiments and the AdDesign model (Ground GAC).

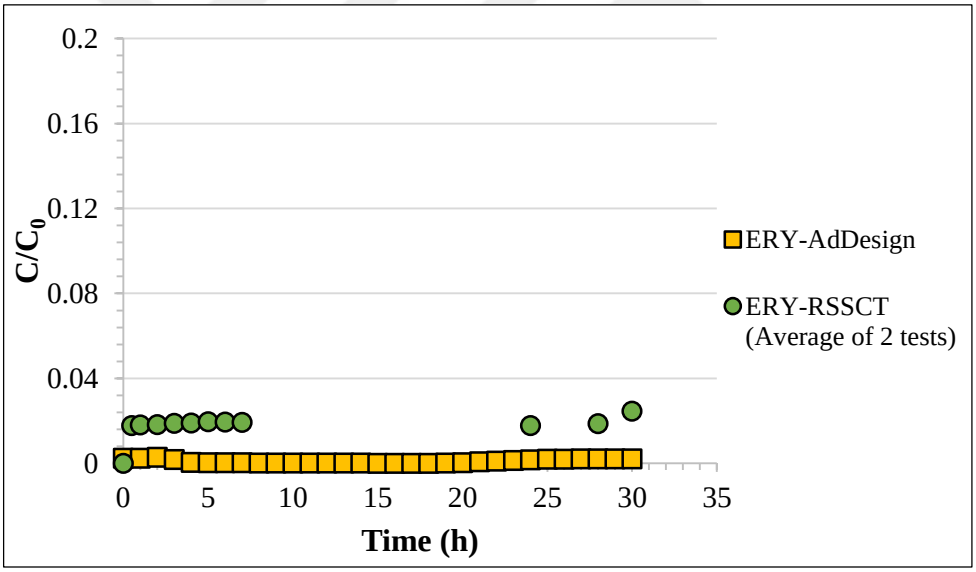

Figure 5.47. The breakthrough of ERY obtained from the experiments and the AdDesign model (Ground GAC).

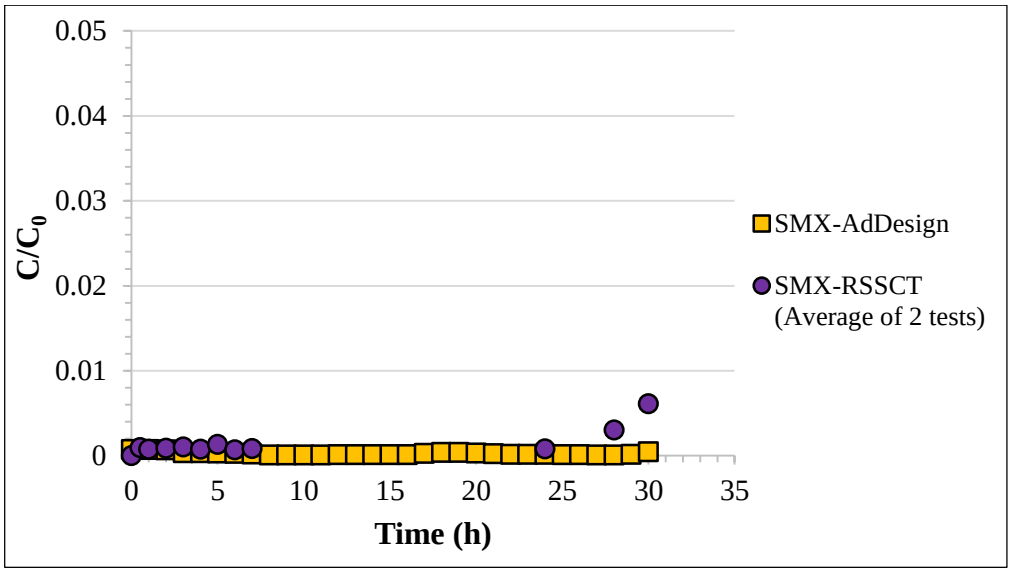

Figure 5.48. The breakthrough of SMX obtained from the experiments and the AdDesign model (Ground GAC).

The AdDesign model overestimated the normalized concentrations of ACT after 24th hour as seen in the breakthrough curve in Figure 5.45. On the other hand, the model slightly underestimated the normalized experimental concentrations of CBZ and ERY. Besides, the model data of SMX fitted the experimental data well. Since 30-hour was a very short duration and the experiments showed only the beginning of the adsorption, it was thought that the model results might not fully coincide with the experimental results. Additionally, isotherm parameters from the batch experiments were entered as input data, this could also be a reason for this dissimilarity between the RSSCT and AdDesign model results.

An additional 40-day RSSCT was run in the AdDesignS software by using the same data. A breakthrough graph was obtained as presented in Figure 5.49. The simulation was extended to a total run time of 40 days to simulate a full breakthrough (C/C_0=1) for all pharmaceuticals. Figure 5.49 also shows the calculated ideal breakthrough times (1.5 day for ACT, 15.6 day for CBZ, 5.7 for ERY and 2.7 for SMX). It was said that the ideal breakthrough time was the time where C/C_0 = 0.5 in the real breakthrough curve (Worch, 2012). When calculated ideal breakthrough times were compared with the results of the breakthrough curve acquired from the model, it was seen that the times for C/C_0 = 0.5 of all pharmaceuticals were very close to the ideal breakthrough times. Also, CBZ showed an S-shaped breakthrough curve as seen from Figure 5.49.

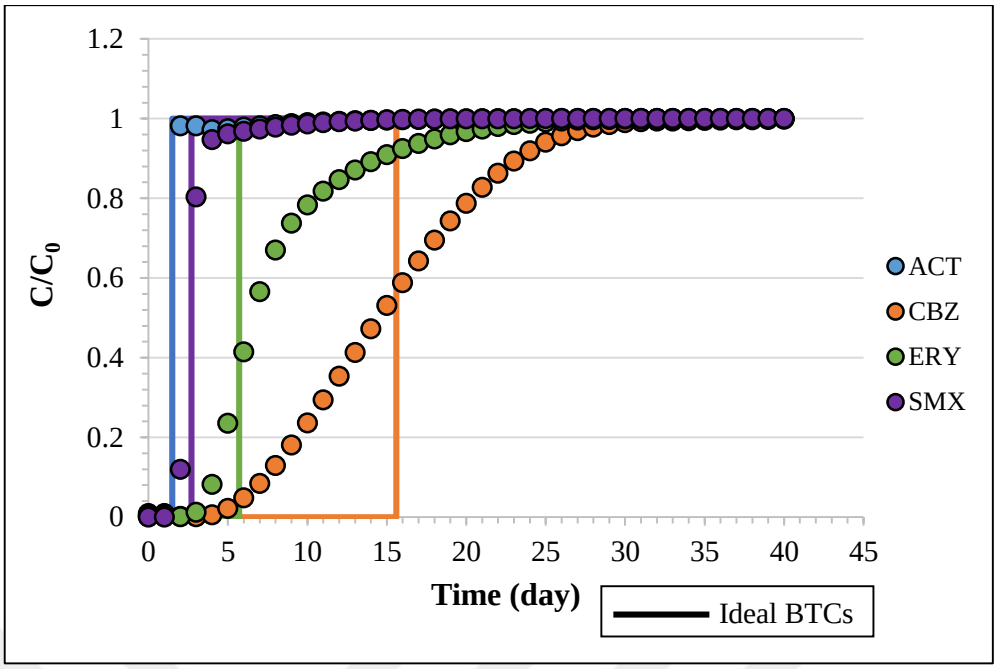

Figure 5.49. The output of the AdDesign software showing the breakthrough curves of pharmaceuticals in a 40-day run with ground GAC.

The full breakthrough was reached at around 13 days (around 93600 BV) for ACT and SMX, whereas CBZ and ERY reached the full breakthrough later, after around 30 days (around 216000 BV). Also, the specific throughput was calculated as 635.6 m^3/kg GAC and CUR was 0.002 g/L in the case of full breakthrough of all pharmaceuticals. If the breakthrough is chosen as 10% of initial concentrations (around 20 µg/L), the time of breakthrough was calculated as 1 day (7200 BV), 7.3 days (52560 BV), 4 days (28800 BV) and 1.8 days (12960 BV) for ACT, CBZ, ERY and SMX, respectively.

Besides, as mentioned before, some dimensionless parameters are given as outputs by the AdDesign model. These parameters for all pharmaceuticals obtained from this run are presented in Table 5.15. It was seen that all dimensionless parameters of pharmaceuticals were equal to each other. Higher surface diffusivities compared to pore diffusivities indicate that surface diffusion is faster and the controlling mechanism inside the particle. On the other hand, when Biot numbers are taken into consideration, Pore Biot numbers are higher than the Surface Biot numbers for all pharmaceuticals. All Biot number values of pharmaceuticals are between 0.5 and 50. This indicates that intraparticle diffusion and the film transfer were both significant for adsorption.

Table 5.15. Dimensionless parameters of pharmaceuticals obtained from the AdDesign run for a mixture of pharmaceuticals and ground GAC.

Pharma.	Stanton number (St)	Surface diffusivity modulus (Ed_s)	Surface Biot number (Bi_s)	Pore diffusivity modulus (Ed_p)	Pore Biot number (Bi_p)
ACT	24	5.5	4.36	1.10	21.8
CBZ	24	5.5	4.36	1.10	21.8
ERY	24	5.5	4.36	1.10	21.8
SMX	24	5.5	4.36	1.10	21.8

5.8.2. Simulation of a Column Test with a Mixture of Pharmaceuticals and Original GAC

Additionally, another column test was run in the AdDesign by using the same data in the RSSCT for pharmaceuticals. For this run, the flow rate, EBCT and the particle size of GAC were changed to 0.078 mL/min, 20 min and 1 mm, respectively according to the experiment carried out with original GAC.

In order to show the similarity, the breakthrough curve of the AdDesign model for 20 days was drawn together with the breakthrough curves of the RSSCT with original (non-ground) GAC carried out in this study. Results are presented in Figure 5.50, Figure 5.51, Figure 5.52 and Figure 5.53 for ACT, CBZ, ERY and SMX, respectively. Accordingly, it was seen that the AdDesign model underestimated the normalized concentrations of ACT and CBZ after 12th day and 15th day, respectively. On the other hand, for ERY and SMX the breakthrough curves fitted the experimental data well. It was thought that the fit could not be obtained because the experiments showed the very beginning of the adsorption onto original GAC.

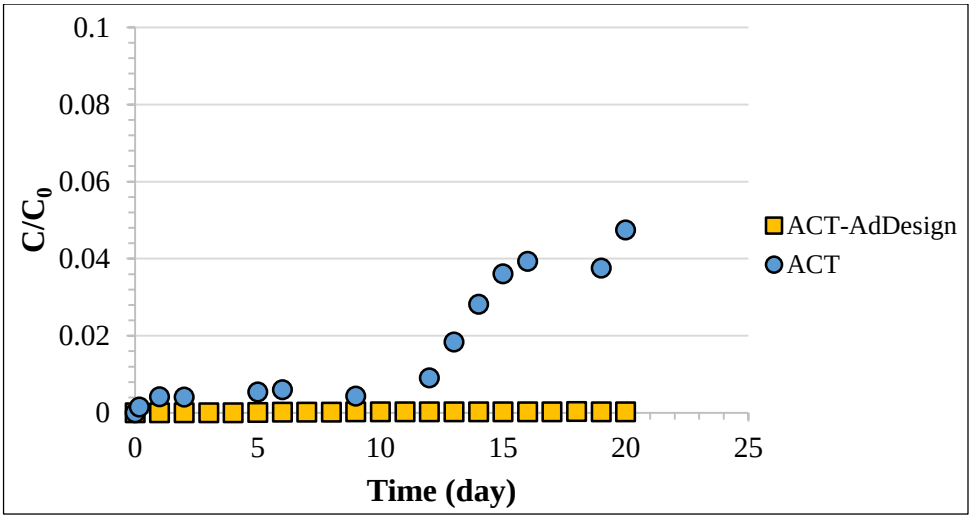

Figure 5.50. The breakthrough curves of ACT obtained from the RSSCT and AdDesign model (Original GAC).

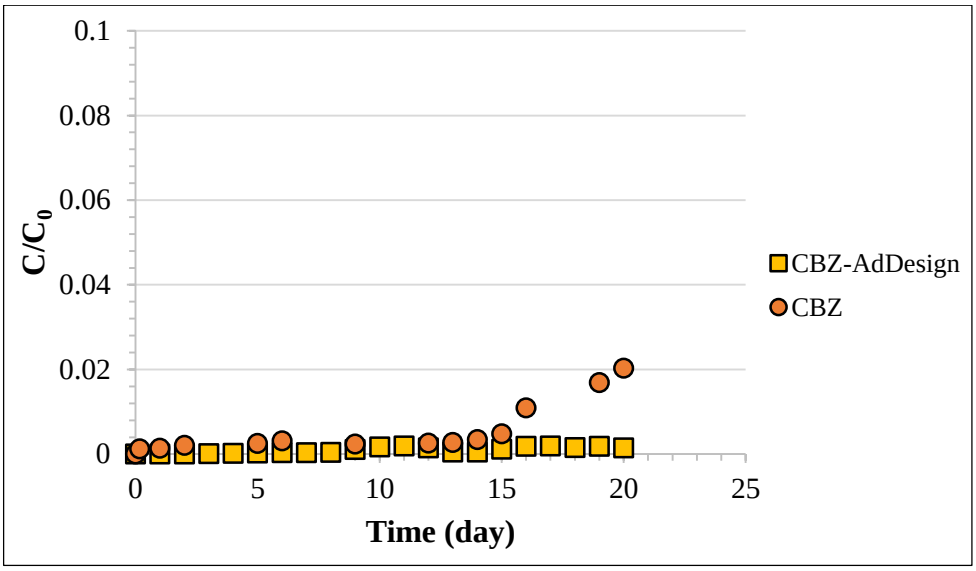

Figure 5.51. The breakthrough curves of CBZ obtained from the RSSCT and AdDesign model (Original GAC).

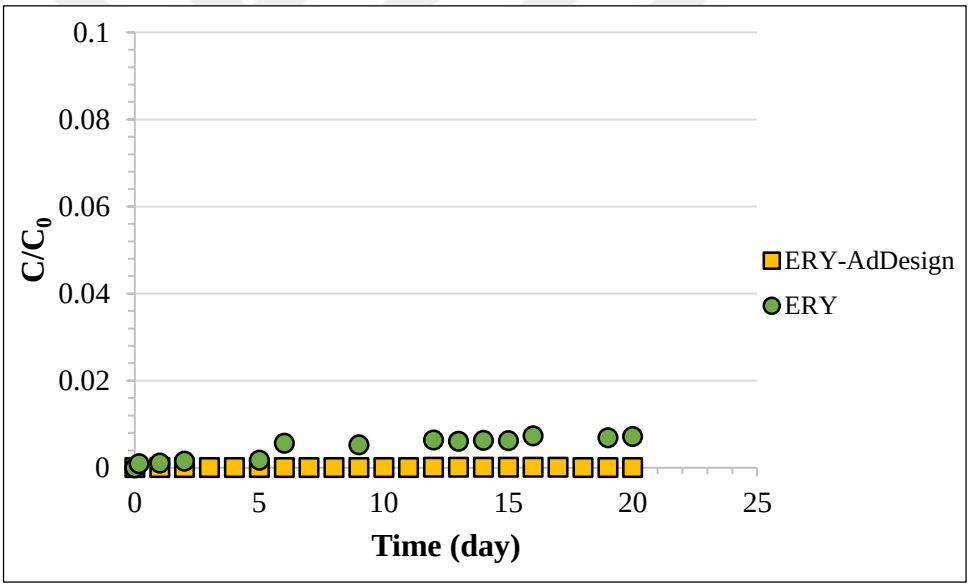

Figure 5.52. The breakthrough curves of ERY obtained from the RSSCT and AdDesign model (Original GAC).

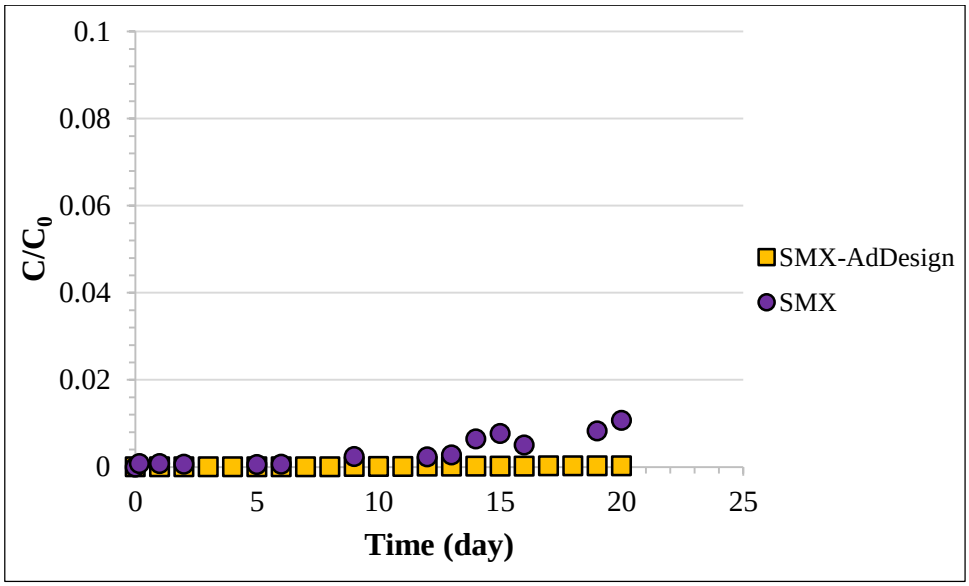

Figure 5.53. The breakthrough curves of SMX obtained from the RSSCT and AdDesign model (Original GAC).

The simulation was extended to a total run time of 4000 days to show full breakthrough (C/C_0=1) for all pharmaceuticals. A breakthrough graph was obtained as presented in Figure 5.54 with the calculated ideal breakthrough times (144 day for ACT, 1613 day for CBZ, 515 for ERY and 258 for SMX). It was seen that the times at C/C_0 = 0.5 of all pharmaceuticals were very close to the ideal breakthrough times. Also, CBZ showed an S-shaped breakthrough curve as in the case of ground GAC.

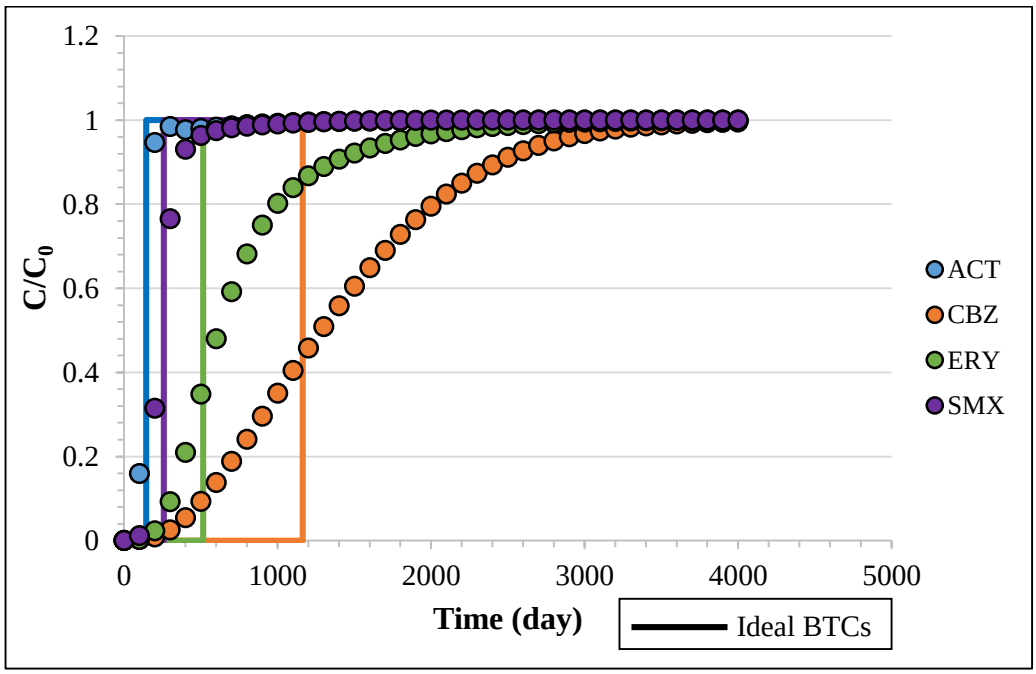

Figure 5.54. The output of the AdDesign software showing the breakthrough curves of pharmaceuticals in a 4000-day run with original GAC.

Full breakthrough was reached at around 2700 days (around 194400 BV) for ACT, ERY and SMX, while for CBZ this time was around 3800 days (around 273600 BV). It was observed that the CBZ breakthrough curve was the most dispersed. For the full breakthrough the specific throughput was calculated as 681.5 m^3/kg GAC and CUR was 0.002 g/L. If the breakthrough is chosen as 10% of initial concentrations as in the case of ground GAC, the time of breakthrough was calculated as 91 days (6552 BV), 516 days (37152 BV), 306 days (22032 BV) and 129 days (9288 BV) for ACT, CBZ, ERY and SMX, respectively. The breakthrough time of ACT was 91 times higher compared to RSSCT results with ground GAC, whereas for other pharmaceuticals this ratio was around 75. This result is in accordance with the relationship between scaling factor, EBCT and times to run the large and small column as shown in Table 3.3 indicating the advantage of using small columns in experiments to obtain results much faster.

5.8.3. Simulation of a Pilot-Scale Column with a Mixture of Pharmaceuticals and Original GAC

Additionally, another column test was run in the AdDesign software by using the same data of the RSSCT for pharmaceuticals. For the adsorber database, parameters representing the pilot-scale column were used. Flow rate was kept the same as the RSSCT with ground GAC. According to the correlations in Table 3.3, the EBCT was increased by a factor of 100, which is the square of the scaling factor of 10. Input parameters are presented in Table 5.16. The simulation was extended to a total run time of 4000 days to show full breakthrough ($C/C_0=1$) for all pharmaceuticals. A breakthrough graph was obtained as presented in Figure 5.55.

Table 5.16. Input parameters in the AdDesign run for a pilot-scale column test.

Parameter	Value
Bed length (cm)	50
Bed diameter (cm)	2
Flow rate (mL/min)	7.85
EBCT (min)	20
Particle size (mm)	1

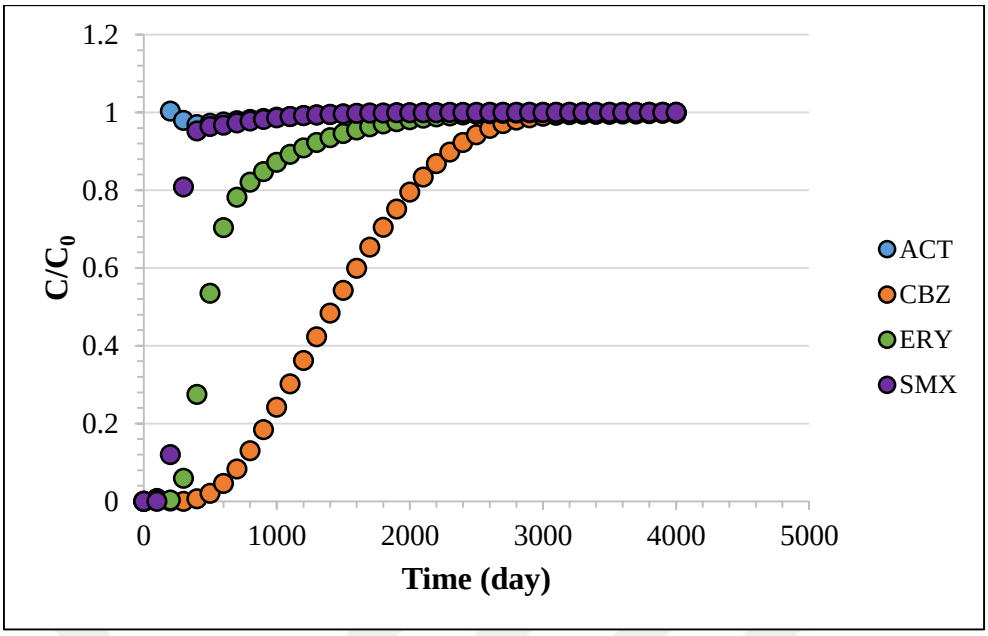

Figure 5.55. The output of AdDesign software showing the breakthrough curves of pharmaceuticals in a pilot-scale column with original GAC.

Full breakthrough was reached at around 2700 days (around 194400 BV) for ACT, ERY and SMX, while for CBZ this time was around 3800 days (around 273600 BV). It was observed that the CBZ breakthrough curve was the most dispersed. For the full breakthrough the specific throughput was calculated as 636 m^3/kg GAC and CUR was 0.002 g/L. These values are very close to the values from the experimental RSSCT with original GAC as expected. If the breakthrough is chosen as 10% of initial concentrations as in the case of ground GAC, the time of breakthrough was calculated as 110 days (7920 BV), 736 days (52992 BV), 319 days (22968 BV) and 183 days (13176 BV) for ACT, CBZ, ERY and SMX, respectively. The breakthrough times are around 100 times higher compared to RSSCT results with ground GAC. This result is in accordance with the relationship between scaling factor, EBCT and times to run the large and small column as shown in Table 3.3 indicating the advantage of using small columns to obtain results much faster. Also, the output of this run in the AdDesgin showed that the dimensionless parameters of pharmaceuticals remained the same which is important to assume that similar conditions and mass transfer processes are present at both small-scale and pilot-scale columns. It was said that perfect similarity can be obtained by setting the dimensionless groups which describe adsorbate transport in an RSSCT equal to those for pilot-scale column. In ideal case, if the similarity is perfect, breakthrough profiles of small-scale and pilot-scale column will be the same (Crittenden et al. 2012). Results of this run showed that RSSCTs can be used for designing the pilot-scale columns.

5.8.4. Simulation of an RSSCT with a Mixture of Pharmaceuticals at Real Concentrations and Ground GAC

The AdDesign model was also used for simulating an RSSCT with a mixture of pharmaceuticals at concentrations in real wastewater (Table 4.6) and ground GAC. For this purpose, the same data from the previous section was used. Initial concentrations of ACT, CBZ, ERY and SMX were 0.009 µg/L, 0.524 µg/L, 0.118 µg/L and 0.056 µg/L, respectively. The breakthrough curve graph is presented in Figure 5.56. Full breakthrough ($C/C_0 = 1$) was reached at around 6 days (around 43200 BV) for ACT, CBZ and ERY, whereas SMX reached the full breakthrough later, at around 17 days around 122400 BV). The difference in the initial concentrations affected the adsorption behaviour. For example, in the experiments, the initial concentrations of pharmaceuticals were around 200 µg/L and the full breakthrough time of CBZ was later than the others. But in this real wastewater case, its concentration was the highest and its full breakthrough time was earlier. For the full breakthrough, the specific throughput was calculated as 317.8 m^3/kg GAC and CUR was 0.003 g/L. If the breakthrough was chosen as 10% of initial concentrations, the time of breakthrough was calculated as 4.01 days (28872 BV), 0.16 days (approximately 4 hours) (1152 BV), 2.53 days (18216 BV) and 7.73 days (55656 BV) for ACT, CBZ, ERY and SMX, respectively.

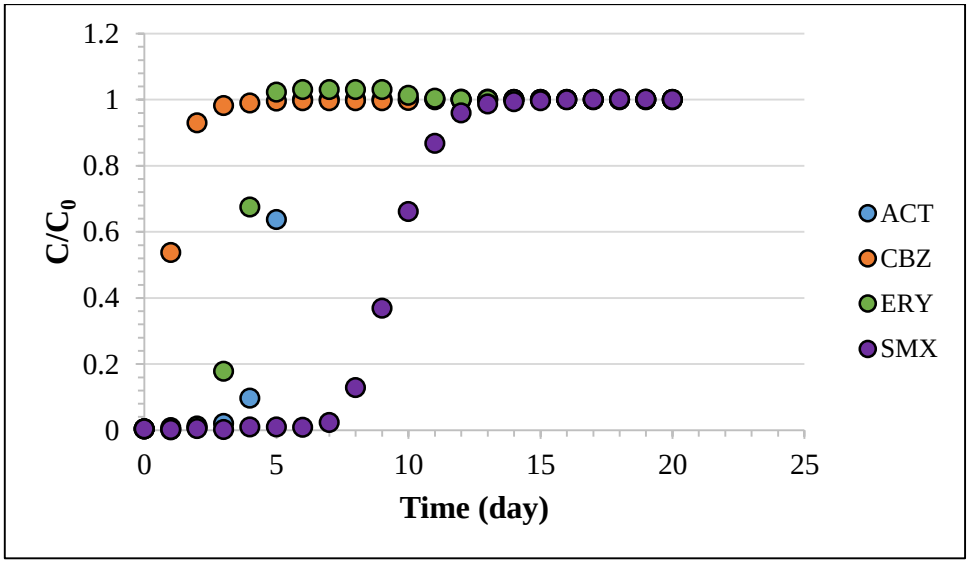

Figure 5.56. The output of AdDesign software showing the breakthrough curves of pharmaceuticals at real wastewater concentrations with ground GAC.

5.8.5. Calibration of AdDesign Model to Simulate RSSCTs

An alternative approach was also applied for calibrating the model and simulating RSSCTs. For this purpose, different scenarios were tested in the AdDesign model program. The purpose was to

provide a fit in breakthrough curves between the model and experimental results. The isotherm parameter n and the film diffusion coefficients were slightly modified. It was said that n values have an effect on the breakthrough curve (Çeçen and Aktaş, 2011) and the film diffusion affects only the beginning of the adsorption process. After a certain point, intraparticle diffusion becomes more important (Worch, 2012). The conducted experiments showed only the beginning of adsorption as presented in previous sections. So, different film diffusion coefficients ranging from 0.002 cm/s to 0.2 cm/s were tried in different runs. Also, n values were changed by 10%. The surface and pore diffusion coefficient values remained the same as calculated automatically by the AdDesign according to some correlations.

5.8.5.1 An RSSCT with a Mixture of Pharmaceuticals and Ground GAC. The input parameters entered into the AdDesign software are presented in Table 5.17. The final breakthrough curves belonging to ACT, CBZ, ERY and SMX obtained from the model and the experiments are shown in Figure 5.57, Figure 5.58, Figure 5.59 and Figure 5.60, respectively.

Table 5.17. Input parameters in the AdDesign run for a mixture of pharmaceuticals and ground GAC (with modified values).

Parameter	**Value**	
Initial concentration (µg/L)	ACT	232
	CBZ	235
	ERY	207
	SMX	226
Freundlich K ((µg/g)(L/µg)^n)	ACT	43.5
	CBZ	21.3
	ERY	53.5
	SMX	90.1
Freundlich n **(modified)**	ACT	1.12
	CBZ	1.3
	ERY	1.06
	SMX	1
Bed mass (g GAC)	0.7110	
Film diffusion coefficient (cm/s) **(modified)**	ACT	0.0208
	CBZ	0.0044
	ERY	0.0980
	SMX	0.0500
Surface diffusion coefficient (cm^2/s)	ACT	$1.21xe^{-9}$
	CBZ	$9.23xe^{-10}$
	ERY	$1.37xe^{-9}$
	SMX	$1.11xe^{-9}$
Pore diffusion coefficient (cm^2/s)	$9.71xe^{-6}$	

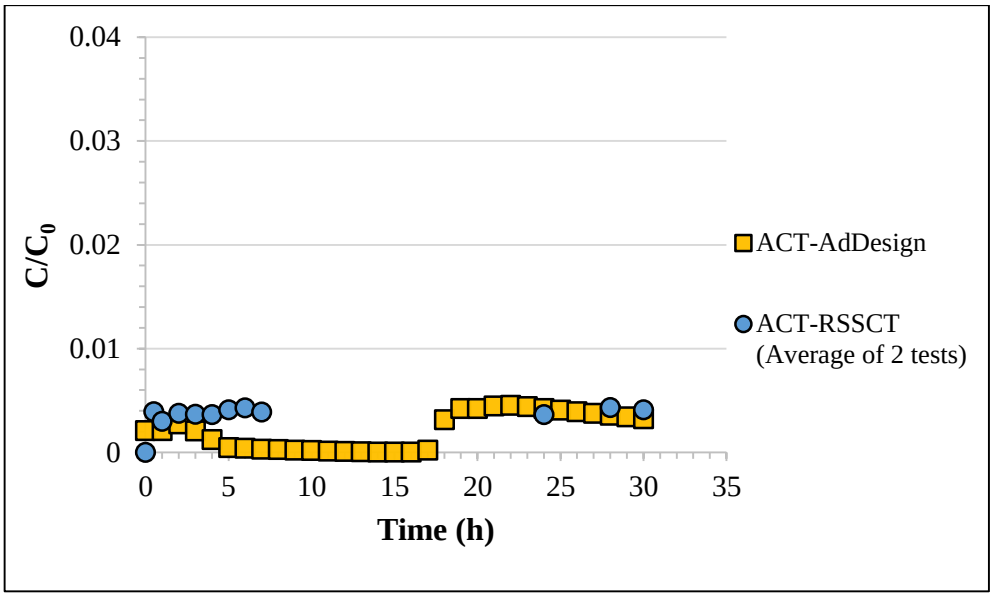

Figure 5.57. The breakthrough of ACT obtained from the RSSCTs and the AdDesign model with assumptions (Ground GAC).

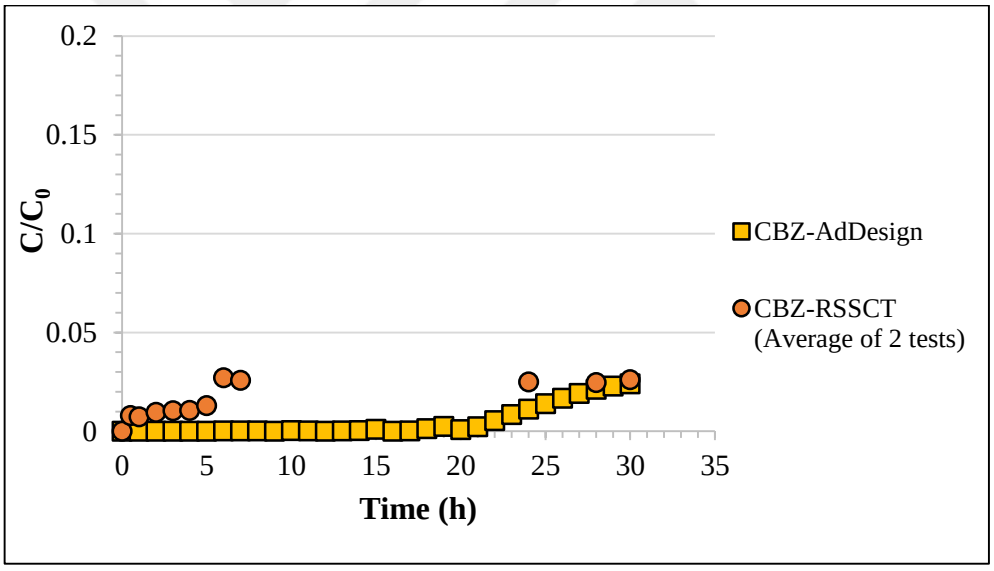

Figure 5.58. The breakthrough of CBZ obtained from the RSSCTs and the AdDesign model with assumptions (Ground GAC).

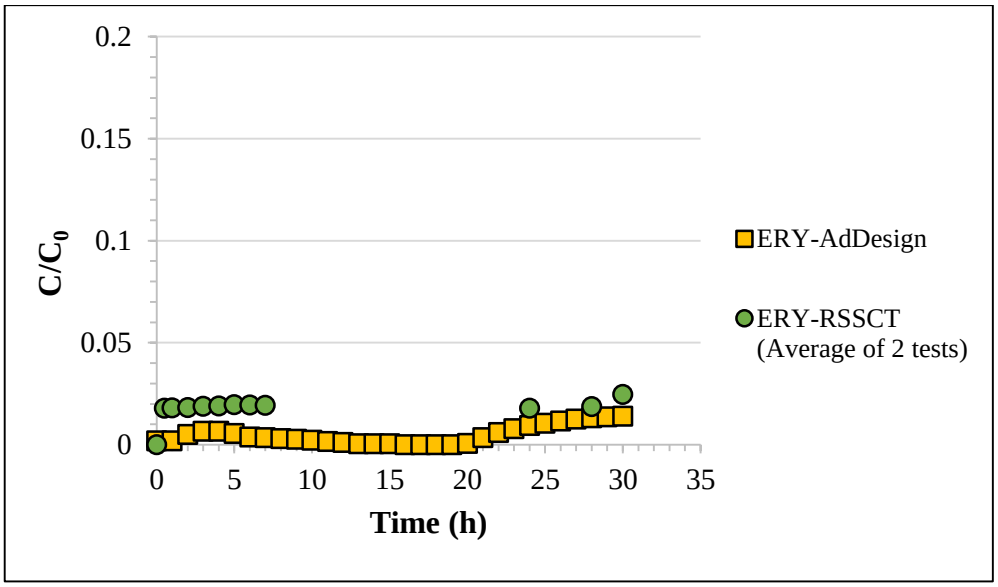

Figure 5.59. The breakthrough of ERY obtained from the RSSCTs and the AdDesign model with assumptions (Ground GAC).

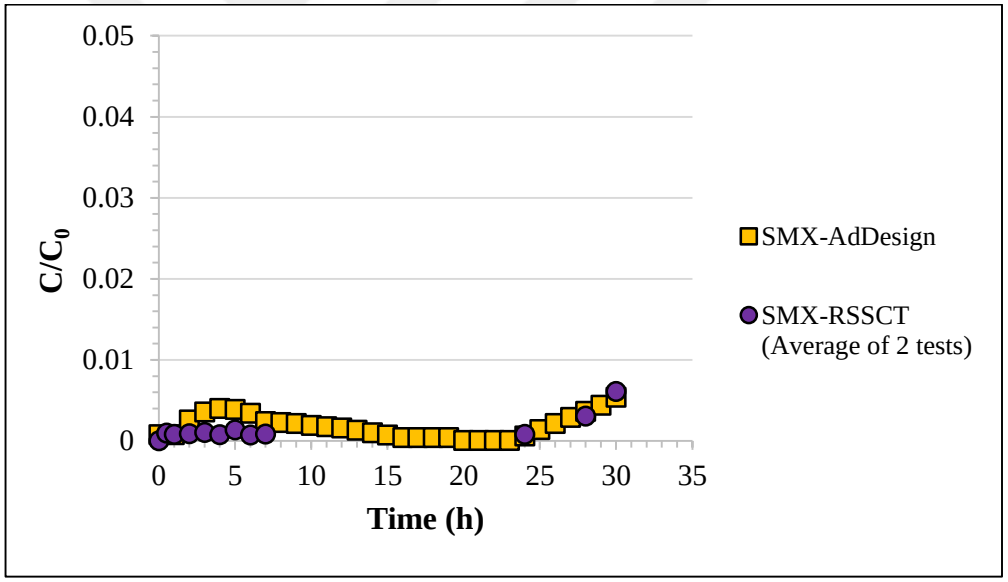

Figure 5.60. The breakthrough of SMX obtained from the RSSCTs and the AdDesign model with assumptions (Ground GAC).

The AdDesign model slightly underestimated the normalized concentrations of ACT, CBZ and ERY at the first hours of the experiments as seen from the breakthrough curves. Besides, it slightly overestimated the normalized concentrations of SMX in the same period. However, experimental results were similar at the end of 30 hours and breakthrough curves of all pharmaceuticals fitted experimental data well.

An additional 40-day RSSCT was run in the AdDesign software by using the same data. The simulation was extended to simulate a full breakthrough (C/C_0=1) for all pharmaceuticals. A breakthrough graph was obtained as presented in Figure 5.61.

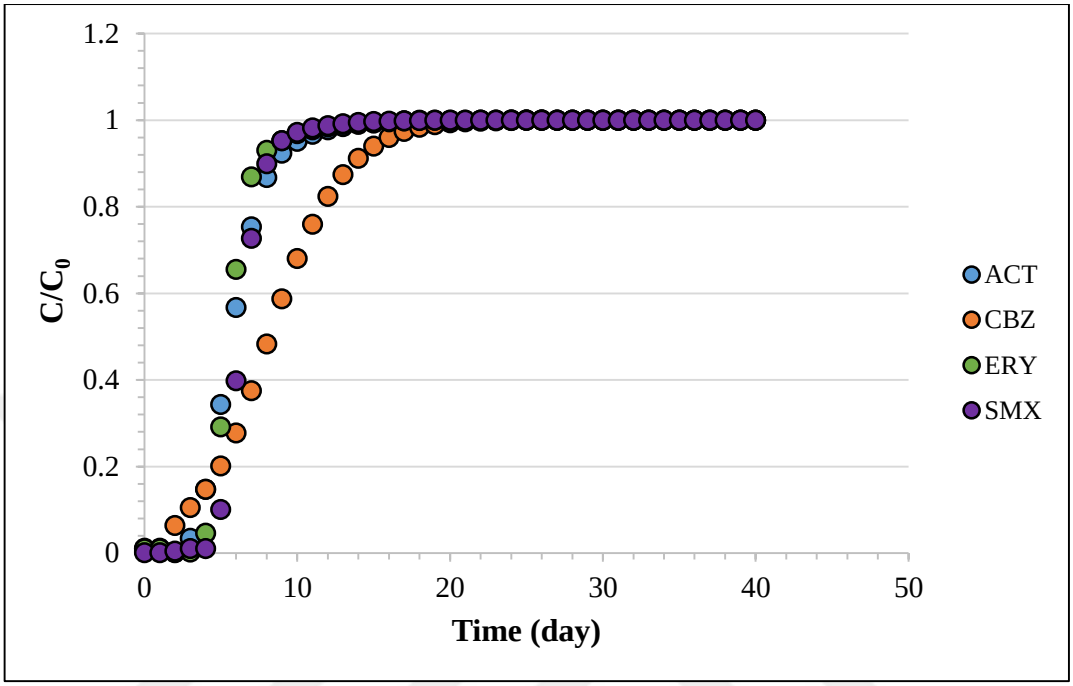

Figure 5.61. The output of the AdDesign software showing the breakthrough curves of pharmaceuticals in a 40-day run with ground GAC.

Results showed that full breakthrough was reached at around 17 days (around 122400 BV) for ACT, ERY and SMX, whereas CBZ reached the full breakthrough later, after around 25 days (around 180000 BV). Also, the specific throughput was calculated as 636.8 m^3/kg GAC and CUR was 0.002 g/L in the case of full breakthrough of all pharmaceuticals. If the breakthrough is chosen as 10% of initial concentrations (around 20 µg/L), the time of breakthrough was calculated as 3.58 days (25776 BV), 2.88 days (20736 BV), 4.22 days (30384 BV) and 4.99 days (35928 BV) for ACT, CBZ, ERY and SMX, respectively. When these results were compared with the results of previous section, it was seen that modifications on n values and film diffusion coefficients caused a slight change in the time to reach the full breakthrough of pharmaceuticals in long-term operation.

Since n values belonging to pharmaceuticals were slightly modified to obtain the best fit in the AdDesign model, the ideal breakthrough times of pharmaceuticals were recalculated for the conditions of this run and presented in Table 5.18.

Table 5.18. Ideal breakthrough time for pharmaceuticals in a RSSCT in AdDesign model.

Pharma.	K ((µg/g GAC)(L/µg)^n)	n	C_0 (µg/L)	GAC (g)	Q (mL/min)	t_b^{id} (d)
ACT	43.5	1.12	232	0.7110	7.85	5.3
CBZ	21.3	1.3	235			6.9
ERY	53.5	1.06	207			4.6
SMX	90.9	1	226			5.7

Then, these values were compared with the results of the breakthrough curve acquired from the model. According to the breakthrough curve, it was seen that the times for $C/C_0 = 0.5$ of ACT, CBZ, ERY and SMX were around 5 days, 8 days, 5 days and 6 days, respectively. These values are comparable with the calculated ideal breakthrough times.

Besides, as mentioned before, some dimensionless parameters are given as outputs by the AdDesign model. These parameters for all pharmaceuticals obtained from this run are presented in Table 5.19. Since some modifications were made on some parameters such as Freundlich n values and film diffusion coefficients, these dimensionless numbers also changed. For this run, it was seen that Ed_s and Ed_p of all pharmaceuticals were equal to each other. Higher surface diffusivities compared to pore diffusivities indicate that surface diffusion is faster and the controlling mechanism inside the particle. On the other hand, when Biot numbers are taken into consideration, Pore Biot numbers are higher than the Surface Biot numbers for all pharmaceuticals. All Biot number values of ACT and CBZ are lower than 50 that indicates intraparticle diffusion and the film transfer were significant for adsorption as in the previous case. However, Pore Biot number of ERY and SMX are higher than 50 that showed pore diffusion is the controlling mechanism for this run in the AdDesign model.

Table 5.19. Dimensionless parameters of pharmaceuticals obtained from AdDesign run for a mixture of pharmaceuticals and ground GAC.

Pharma.	Stanton number (St)	Surface diffusivity modulus (Ed_s)	Surface Biot number (Bi_s)	Pore diffusivity modulus (Ed_p)	Pore Biot number (Bi_p)
ACT	23.6	5.49	4.29	1.10	21.5
CBZ	4.97	5.49	0.906	1.10	4.53
ERY	111	5.49	20.2	1.10	101
SMX	56.5	5.49	10.3	1.10	51.5

5.8.5.2 An RSSCT with a Mixture of Pharmaceuticals and Original GAC. Additionally, another column test was run in the AdDesign by using the same data for pharmaceuticals from the previous section. For this run, the flow rate, EBCT and particle size of GAC were 0.078 mL/min, 20 min and

1 mm, respectively according to the experiment carried out with original GAC. The simulation was extended to a total run time of 3000 days to show full breakthrough (C/C_0=1) for all pharmaceuticals. A breakthrough graph was obtained as presented in Figure 5.62.

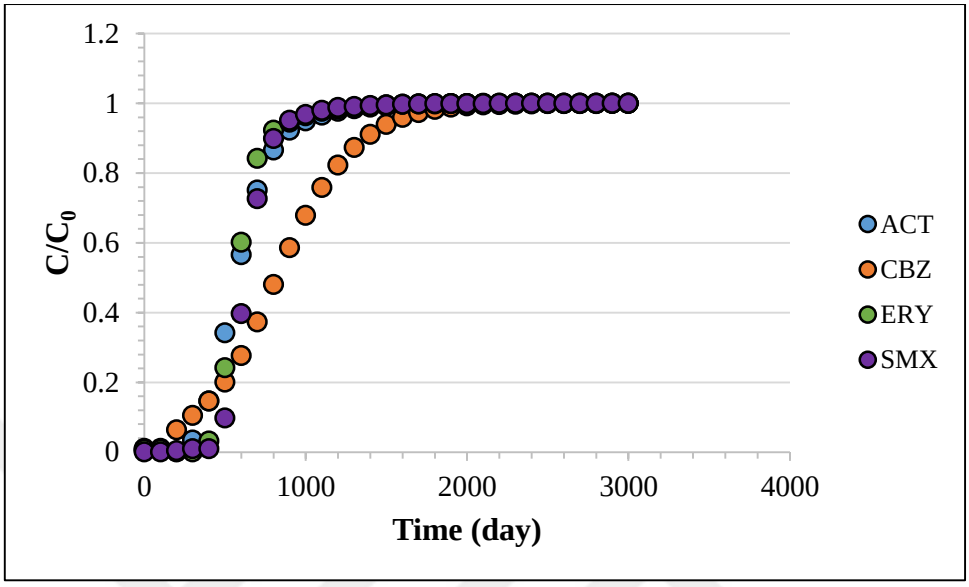

Figure 5.62. The output of AdDesign software showing the breakthrough curves of pharmaceuticals in a 3000-day run with original GAC.

Full breakthrough was reached at around 2000 days (around 144000 BV) for all pharmaceuticals. It was observed that CBZ was the most dispersed pharmaceutical. For the full breakthrough the specific throughput was calculated as 477 m^3/kg GAC and CUR was 0.002 g/L. If the breakthrough is chosen as 10% of initial concentrations as in the case of ground GAC, the time of breakthrough was calculated as 359 days (25848 BV), 288 days (20736 BV), 432 days (31104 BV) and 501 days (36072 BV) for ACT, CBZ, ERY and SMX, respectively. The breakthrough times are 100 times higher compared to RSSCT results with ground GAC. This result is in accordance with the relationship between scaling factor, EBCT and times to run the large and small column as shown in Table 3.3. The ideal breakthrough times of pharmaceuticals were also recalculated in the case of original GAC as presented in Table 5.20.

Table 5.20. Ideal breakthrough time for pharmaceuticals in an RSSCT in AdDesign model.

Pharma.	**K ((µg/g GAC)(L/µg)^n)**	**n**	**C_0 (µg/L)**	**GAC (g)**	**Q (mL/min)**	**t_b^{id} (d)**
ACT	43.5	1.12	232	0.7110	0.078	529
CBZ	21.3	1.3	235			694
ERY	53.5	1.06	207			466
SMX	90.9	1	226			575

These values were compared with the results of the breakthrough curve acquired from the model. According to the breakthrough curves, it was seen that the times for $C/C_0 = 0.5$ of ACT, CBZ, ERY and SMX were 571 days, 818 days, 572 days and 631 days, respectively. These values are comparable with the ideal breakthrough times.

5.9. RSSCTs with Ground GAC Covered by a Biofilm and a Mixture of Micropollutants

In this study, operation of biological activated carbon (BAC) columns was also investigated to observe whether it was possible to remove selected pharmaceuticals by both adsorption and biodegradation in RSSCTs. As mentioned before, a microbiological film may form on GAC filters and convert them into BAC as time passes. This process combines the carbon adsorption and biological activity. However, since empty-bed contact time (EBCT) is very small in RSSCTs (0.20 minutes) there was no time for conversion of GAC to BAC filter. So, a known amount of ground GAC was contacted with an activated sludge sample (200 mg/L VSS) taken from the R1 reactor in an Erlenmeyer flask for 15 days. Synthetic domestic wastewater was added as a feed. After that, the column was filled with this GAC sample. Then a mixture of micropollutants (initial concentrations were all 200 µg/L) and synthetic secondary effluent was fed to the column for 4 hours and 8 hours in two experimental sets.

Results of the 1st experiment (4-hour) showed that the normalized concentrations (C/C_0) of all pharmaceuticals started to increase in the first hours, but then the concentrations of all pharmaceuticals in the effluent of the column were decreasing as shown in Figure 5.63. It was thought that both adsorption and biodegradation processes took place at the same time and these pharmaceuticals could be removed by the biofilm formed on GAC in the batch reactor before the experiment started. Moreover, it was also possible that microorganisms were already saturated by background organic matter in the synthetic domestic wastewater or were still acclimating at the beginning of the experiment. The removal of pharmaceuticals started after the first hour due to possibly both biodegradation and adsorption.

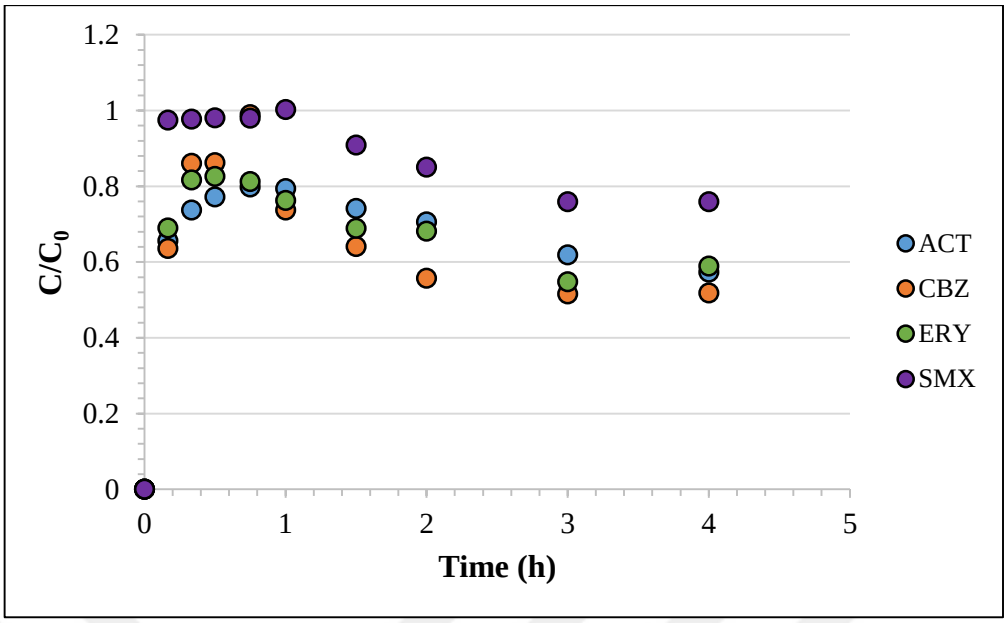

Figure 5.63. The normalized pharmaceutical concentrations in the effluent of the BAC column (4-hour experiment).

The 8-hour experiment showed different results compared to the 1st experiment in terms of pharmaceuticals. The C/C_0 of ACT and CBZ reached full breakthrough ($C/C_0 = 1$) after 4 hours and remained constant, whereas C/C_0 of ERY reached to 0.2 at the end of the experiment as seen in Figure 5.64. On the other hand, it was observed that the normalized concentration of SMX continued to increase. It was thought that ERY and SMX was adsorbed by GAC from the beginning of the experiment. It may also be possible that all pharmaceuticals would be removed by both adsorption and biodegradation if the experiment would last longer.

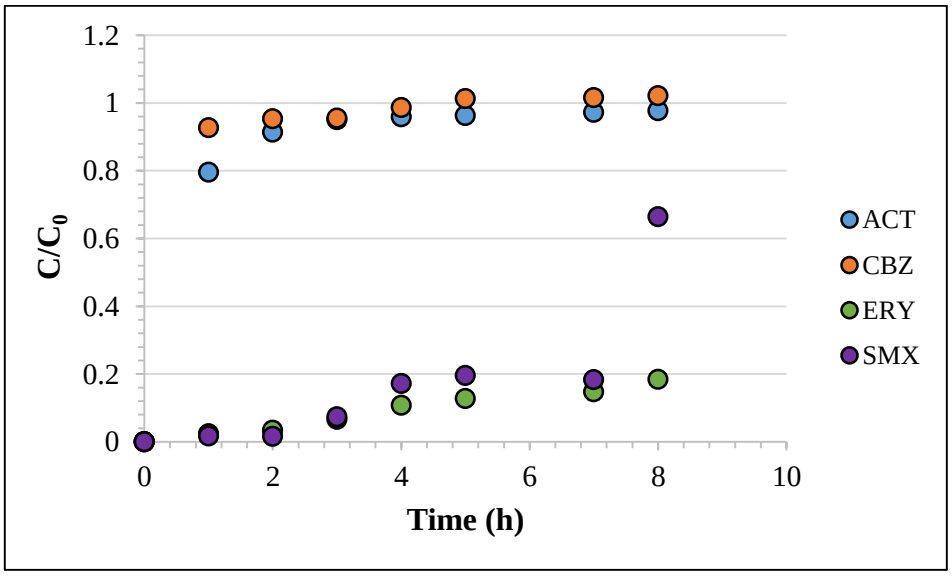

Figure 5.64. The normalized pharmaceutical concentrations in the effluent of the BAC column (8-hour experiment).

In addition, DOC, UV_{254}, UV_{280} and $Color_{436}$ parameters, reflecting the bulk organic matter, were also measured during these two experiments. As seen in Figure 5.65 and Figure 5.66, the breakthrough ($C/C_0 = 1$) was reached in the first hours in terms of all parameters. After 2-3 hours, the concentrations in the effluent started to decrease possibly due to biodegradation and adsorption in the column. The results of these two experiments showed similar trend in terms of DOC. It can be concluded that at the beginning GAC adsorption was more dominant and when the available sites were occupied, organic matters started to be biodegraded by microorganisms on the surface of GAC. In addition, although the full breakthrough ($C/C_0 = 1$) was reached in the 4-hour experiment in terms of UV and Color parameters, the normalized concentrations started to decrease after 3 hours in 8-hour experiment as presented in Figure 5.66. There is a possibility that the adsorbed background organic matter in the batch reactor might be desorbed at the beginning of the experiment.

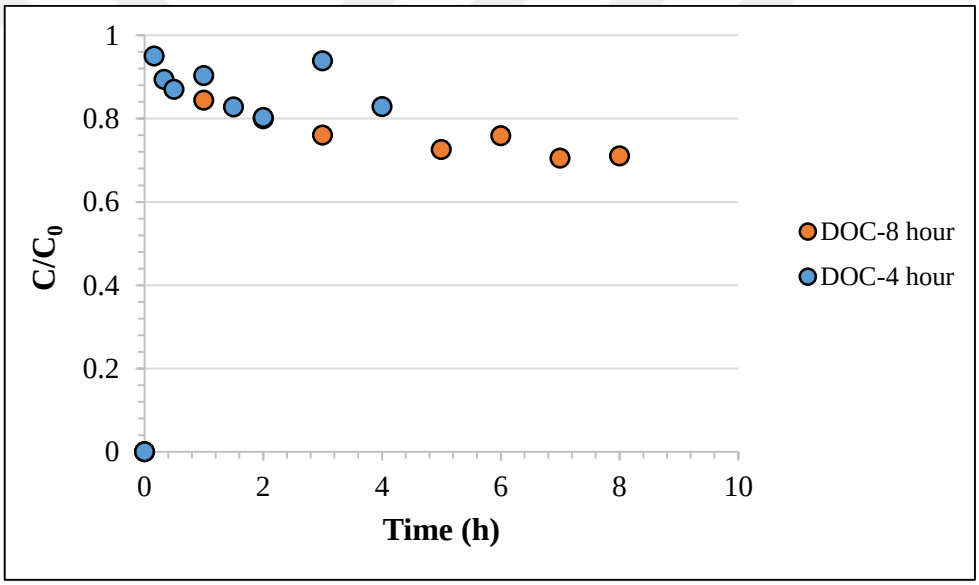

Figure 5.65. The normalized concentrations in terms of DOC of background organic matter in BAC columns with respect to time.

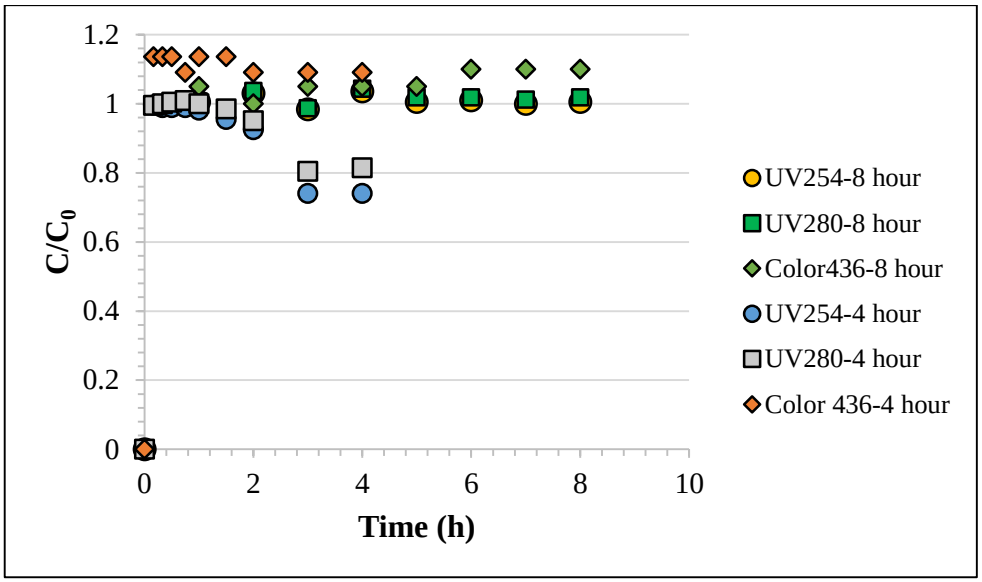

Figure 5.66. The normalized concentrations in terms of UV_{254}, UV_{280} and $Color_{436}$ of background organic matter in BAC columns with respect to time.

Since the results of two experiments were different from each other, it was not possible to make a comparison. It was thought that this difference might be observed because the biomass was contacted with GAC at different time periods for two tests. Because, it is possible that the level of the adsorption of microorganisms onto GAC particles might be at different levels. Also, the saturation of GAC by background organic matter could be at different level. Longer period of time may be needed to observe the real situation.

5.10. Adsorption and Biodegradation Experiments with Individual Pharmaceuticals

The results of two BAC column experiments were not clear to make a comparison and discussion. For this reason, two additional batch experiments were carried out to observe the effect of the presence of both GAC and activated sludge on the removal of pharmaceuticals. As mentioned in the **Materials and Methods** section, carbamazepine (CBZ) and sulfamethoxazole (SMX) were chosen.

5.10.1. Behavior of Carbamazepine in Batch Experiments

The results of the experiment with CBZ showed that it was not biodegraded by R1 sludge after four days as seen in Figure 5.67. It was the only compound in the solution, thus it was not removed as a primary substrate. This result is in accordance with the previous experiments shown in Section 5.2.2. The biodegradation potential of CBZ was low. The removal efficiency by activated sludge was

around 8% in the observed time and the k_{biol} value was calculated as 0.04 $L.g_{VSS}^{-1}.d^{-1}$. Moreover, it was observed that CBZ was adsorbed by granular activated carbon with around 75% removal efficiency. The isotherm experiments showed that the adsorption capacity of CBZ when present alone was higher compared to CBZ in a mixture. When both activated sludge and GAC were simultaneously present in the solution, the removal was enhanced. The removal efficiency was around 99% indicating that it could be completely eliminated within the same time.

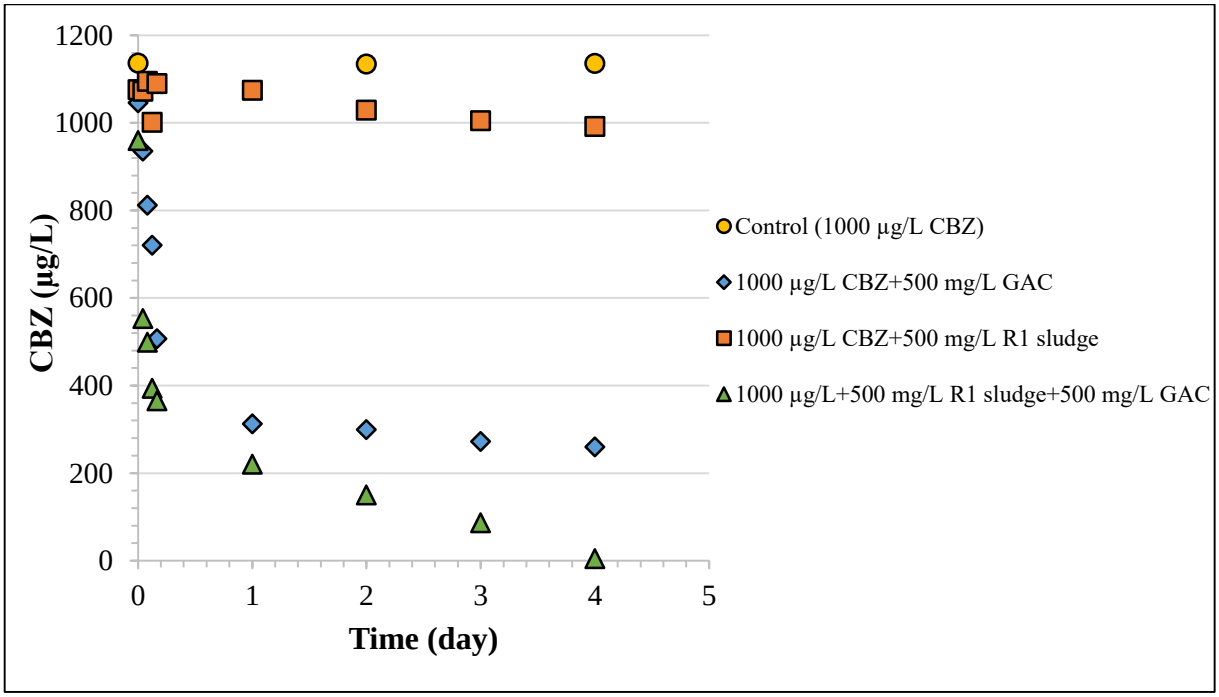

Figure 5.67. Results of the biodegradation and adsorption experiment with CBZ.

5.10.2. Behavior of Sulfamethoxazole in Batch Experiments

Another experiment was carried out with SMX under the same conditions. SMX was also not biodegraded by R1 sludge after four days as seen in Figure 5.68. It was the only compound in the solution, thus it was not removed as a primary substrate. According to biodegradation experiments in the previous sections, SMX was classified as a slowly biodegradable pharmaceutical (Section 5.2.2). The removal efficiency by activated sludge in this experiment was around 12% and the k_{biol} value was calculated as 0.06 $L.g_{VSS}^{-1}.d^{-1}$. SMX was adsorbed by granular activated carbon with around 99% removal efficiency. The isotherm experiments showed that the adsorption capacity of SMX to GAC was high. According to the results of combined adsorption and biodegradation, the presence of activated sludge in GAC solution did not increase the removal of SMX. It was not possible to distinguish between biodegradation and adsorption, since adsorption was already high. The removal

efficiency was also around 99% when there were both activated sludge and granular activated carbon. It can be said that the biodegradation had a negligible effect on the removal of SMX in this situation.

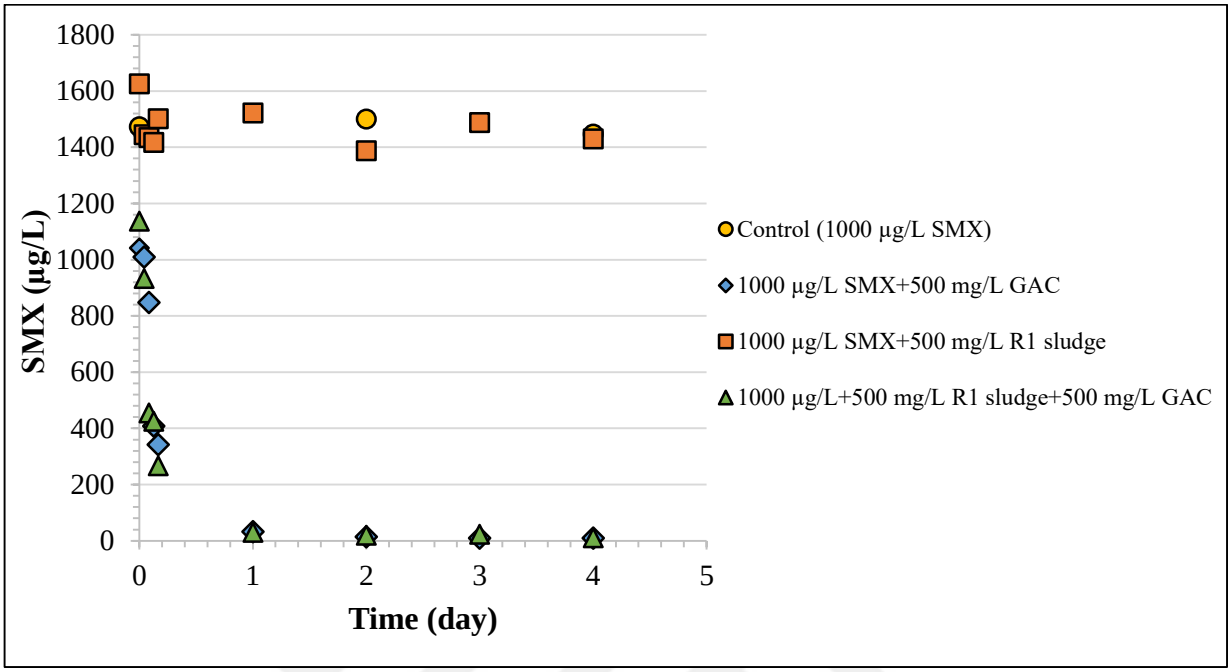

Figure 5.68. Results of the biodegradation and adsorption experiment with SMX.

5.10.3. RSSCTs with CBZ and SMX with Ground GAC

Additionally, in parallel to these experiments, two RSSCTs were carried out with CBZ and SMX in order to investigate the removal of these pharmaceuticals by GAC when they were alone in the influent of the column. Two columns were filled with ground GAC. CBZ or SMX solutions (initial concentrations of CBZ and SMX were 1050 µg/L and 1076 µg/L, respectively) in deionized water were fed to the columns for 76 hours. In these tests the loading was around 8 µg/min. This loading is actually higher than the loading in RSSCTs with a mixture of pharmaceuticals which was around 1.8 µg/min. Normalized concentrations (C/C_0) and the results of 1st and 2nd experiment are shown in Figure 5.69 and Figure 5.70 respectively.

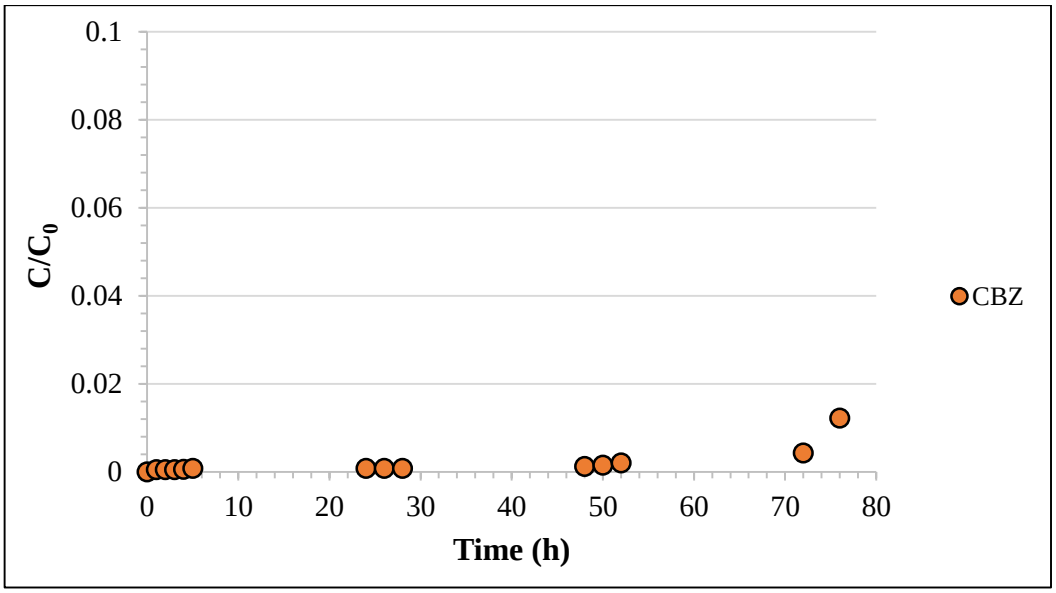

Figure 5.69. Normalized concentration of single CBZ in GAC column with respect to time.

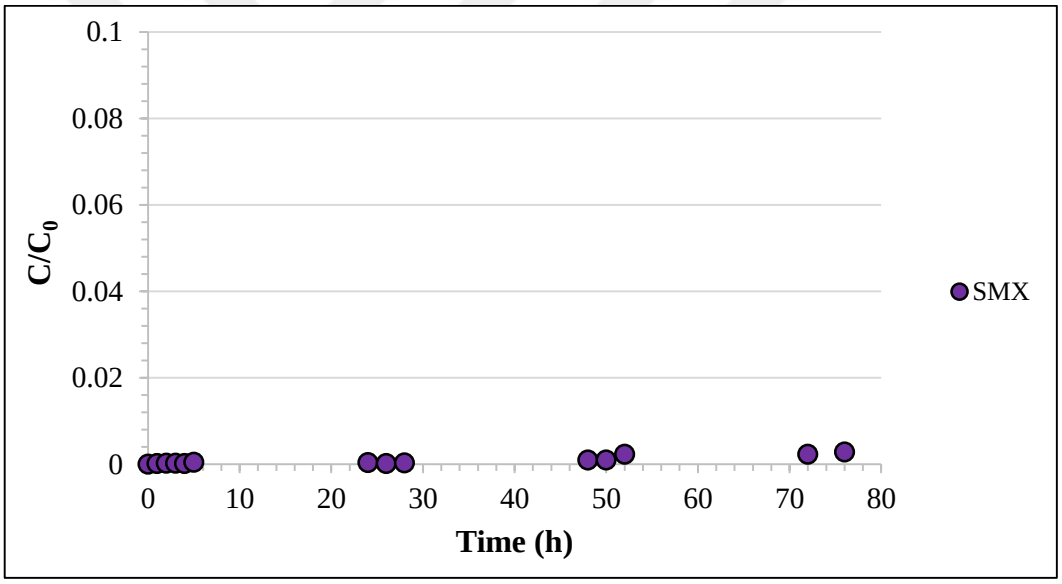

Figure 5.70. Normalized concentration of single SMX in GAC column with respect to time.

There was no full breakthrough ($C/C_0 = 1$) of either of the pharmaceuticals. The C/C_0 of CBZ and SMX did not change much during the experiments and reached only 0.012 and 0.003 after 76 hours, respectively. This means that 1.2% of CBZ and 0.3% of SMX was only seen in the effluent. For example, C/C_0 for CBZ reached 0.001 at 3rd hour, while for SMX this ratio reached the same value after 48 hours. According to isotherms, the affinities of CBZ and SMX to GAC were high and close to each other when they were the single pharmaceuticals as seen in Table 5.8. As a result, full breakthrough was not observed as expected. Moreover, there was not a significant effect of influent concentration on the removal of these pharmaceuticals. Even if the initial concentration was increased to around 1000 µg/L and the loading to around 8 µg/min, low effluent concentrations were observed

at the end of the experiments indicating high adsorption potential of CBZ and SMX by ground GAC. The breakthrough curves in longer time periods were also obtained from the AdDesign model and presented in following section.

5.10.4. Simulation of RSSCTs with Single Pharmaceuticals and Ground GAC

The AdDesign model was also used for simulating the two column tests with single CBZ and single SMX and also showing the breakthrough curves in a longer period of time. For this purpose, kinetic parameters of these pharmaceuticals from isotherm tests were used.

5.10.4.1 Simulation of an RSSCT with single CBZ. Table 5.21 shows the parameters used as inputs and Figure 5.71 shows the breakthrough curves obtained from the model and the result of the experiment. The film diffusion, surface diffusion and pore diffusion coefficients remained the same as calculated automatically by the AdDesign with correlations. Results showed a good fit between the output of the model and the experiment.

Table 5.21. Input parameters of AdDesign run for single CBZ.

Parameter	Value
Initial concentration (µg/L)	1050
Freundlich K ((µg/g)(L/µg)^n)	202
Freundlich n	1.3
Bed mass, GAC (g)	0.6870
Film diffusion coefficient (cm/s)	0.017
Surface diffusion coefficient (cm^2/s)	7.66xe^{-11}
Pore diffusion coefficient (cm^2/s)	9.71xe^{-6}

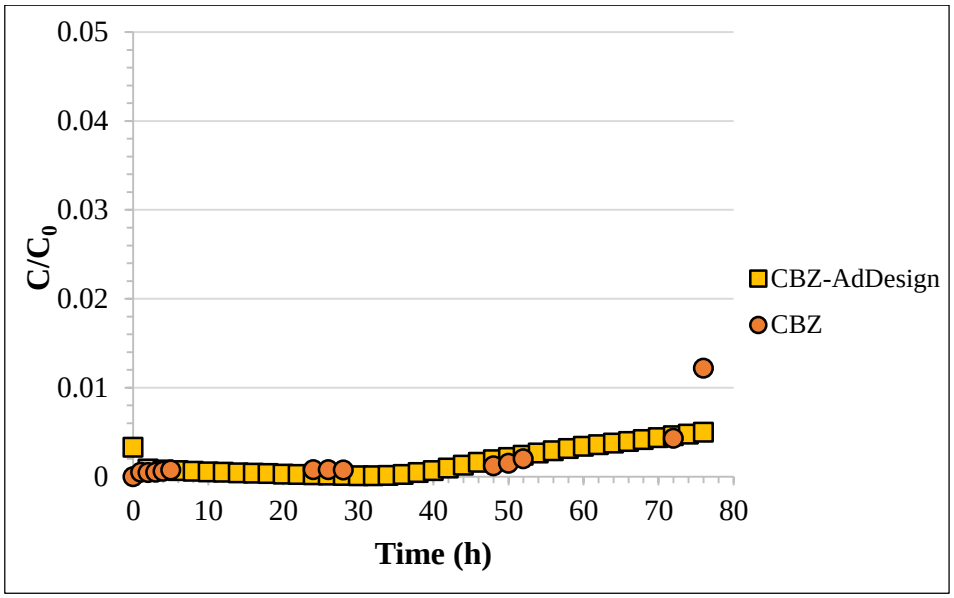

Figure 5.71. The breakthrough curves of single CBZ obtained from the RSSCT and AdDesign model.

Then, the simulation was extended to a total run time of 200 days to show full breakthrough (C/C_0=1) for single CBZ as presented in Figure 5.72.

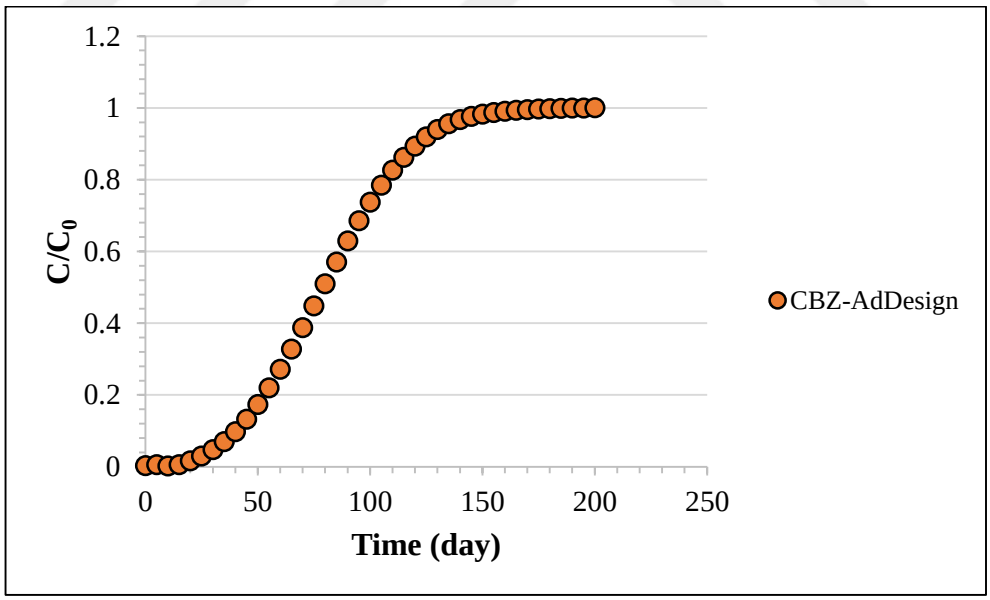

Figure 5.72. The output of AdDesign software showing the breakthrough curve of CBZ in a 200-day run with ground GAC.

Results showed that full breakthrough was reached at around 180 days (around 1296000 BV) when CBZ was the single pharmaceutical. Additionally, the specific throughput was calculated as 3291 m^3/kg GAC and CUR was 0.0003g/L. If the breakthrough was chosen as 10% of initial concentration, the time of breakthrough was calculated as around 40 days (288000 BV) When CBZ

was in the mixture this time was 7.3 days (52560 BV). This indicated that there was a competition between the pharmaceuticals. CBZ reached the breakthrough later when it was the single pharmaceutical indicating better adsorption.

5.10.4.2 Simulation of an RSSCT with single SMX. Table 5.22 shows the parameters used as inputs and Figure 5.73 shows the breakthrough curves obtained from the model and the result of the experiment. The film diffusion, surface diffusion and pore diffusion coefficients remained the same as calculated automatically by the AdDesign with correlations. Results showed a very good fit between the output of the model and the experiment.

Table 5.22. Input parameters of AdDesign run for single SMX.

Parameter	Value
Initial concentration (µg/L)	1076
Freundlich K ((µg/g)(L/µg)^n)	236
Freundlich n	1.25
Bed mass, GAC (g)	0.6917
Film diffusion coefficient (cm/s)	0.0176
Surface diffusion coefficient (cm^2/s)	7.49xe^{-11}
Pore diffusion coefficient (cm^2/s)	9.71xe^{-6}

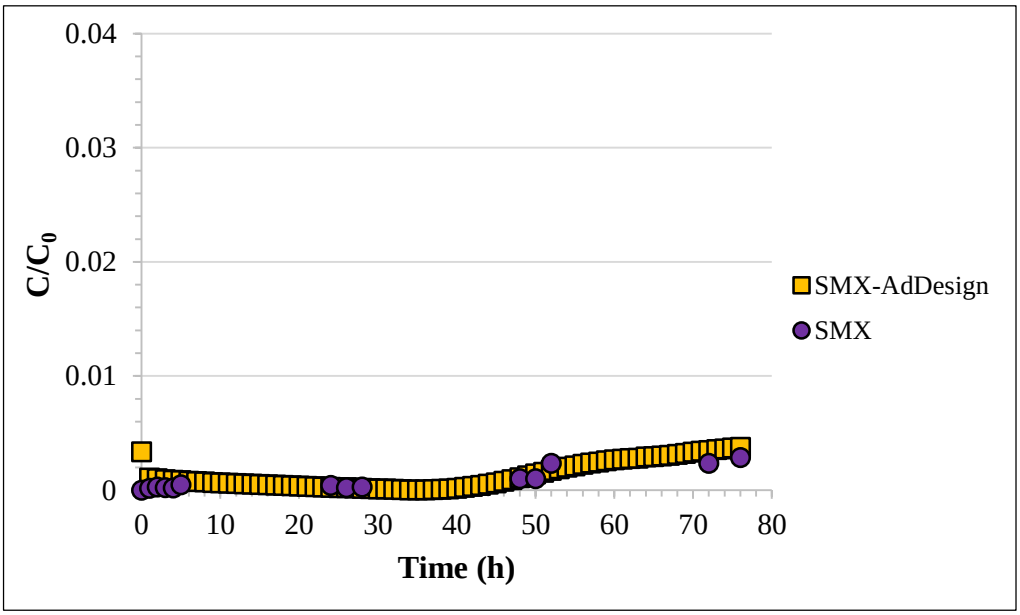

Figure 5.73. The breakthrough curves of single SMX obtained from the RSSCT and AdDesign model.

Then, the simulation was extended to a total run time of 200 (around 1440000 BV) days to show full breakthrough (C/C_0=1) for single SMX as presented in Figure 5.74. Results showed that full

breakthrough was reached at around 200 days when SMX was the single pharmaceutical. Additionally, the specific throughput was calculated as 3268 m³/kg GAC and CUR was 0.0003 g/L. If the breakthrough was chosen as 10% of initial concentration, the time of breakthrough was calculated as around 43 days (309600 BV). When SMX was in the mixture this time was 1.8 days (12960 BV). SMX reached the breakthrough later when it was the single pharmaceutical as in the case of CBZ. This indicates that the adsorption of SMX onto GAC was better when it was the only pharmaceutical.

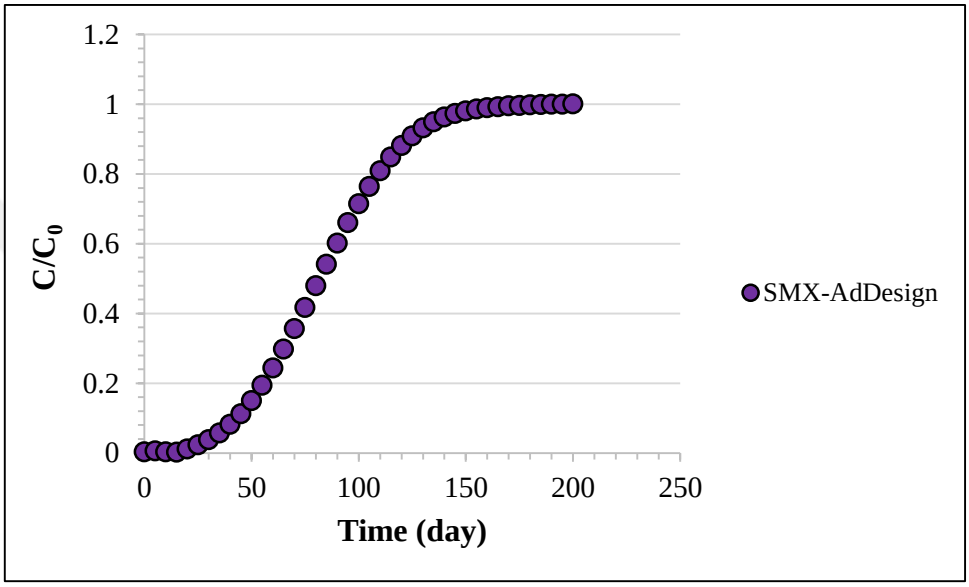

Figure 5.74. The output of AdDesign software showing the breakthrough curve of SMX in a 200-day run with ground GAC.

The ideal breakthrough times of CBZ and SMX were also calculated as presented in Table 5.23. These values were compared with the results of the breakthrough curve acquired from the model. According to the breakthrough curves, it was seen that the times for $C/C_0 = 0.5$ of CBZ and SMX were 80 days and 82 days, respectively as seen from Figure 5.72 and Figure 5.74. It was seen that these times were very close to the calculated ideal breakthrough times.

Table 5.23. Ideal breakthrough time for single CBZ and single SMX in RSSCTs in AdDesign model.

Pharma.	**K ((µg/g GAC)(L/µg)^n)**	**n**	**C_0 (µg/L)**	**GAC (g)**	**Q (mL/min)**	**t_b^{id} (d)**
Single CBZ	202.3	1.3	1050	0.6870	7.85	80
Single SMX	236.3	1.25	1076	0.6917	7.85	83

Besides, dimensionless parameters obtained from the AdDesign model are presented in Table 5.24.

Table 5.24. Dimensionless parameters of CBZ and SMX obtained from two AdDesign runs.

Pharma.	**Stanton number (St)**	**Surface diffusivity modulus (Ed_s)**	**Surface Biot number (Bi_s)**	**Pore diffusivity modulus (Ed_p)**	**Pore Biot number (Bi_p)**
CBZ	18.6	5.31	3.50	1.06	17.5
SMX	19.4	5.35	3.63	1.07	18.1

It was seen that all parameters of these two pharmaceuticals were very close to each other. Higher surface diffusivities compared to pore diffusivities indicate that surface diffusion is faster and the controlling mechanism inside the particle. On the other hand, when Biot numbers are taken into consideration, Pore Biot numbers are around 5 times higher than the Surface Biot numbers. All Biot number values are lower than 50 which indicates both intraparticle diffusion and the film transfer were significant for adsorption. The results are also in accordance with the results of the run in AdDesign model with a mixture of pharmaceuticals.

6. CONCLUSIONS AND RECOMMENDATIONS

The major objective of this study was to investigate the removal of 4 hazardous pharmaceuticals: acetaminophen (ACT), carbamazepine (CBZ), erythromycin (ERY) and sulfamethoxazole (SMX) by biodegradation and adsorption using GAC. In the first part, biodegradation potential of selected pharmaceuticals was studied. For this purpose, BIOWIN estimation models were used. These models gave general information about biodegradability or the time required for biodegradation. Results showed that ACT was the most readily biodegradable pharmaceutical. BIOWIN estimations for CBZ and SMX were very close to each other and indicated slow biodegradation, whereas ERY was classified as refractory according to BIOWIN 3 value.

In order to compare the results with BIOWIN estimations and investigate the removal mechanisms (primary, secondary and cometabolic substrate, etc.), short-term and long-term biodegradation experiments were carried out with selected pharmaceuticals. Short-term experiments were carried out with R1 sludge which contained both heterotrophic and nitrification activity. Results showed that the biodegradation rate constants (k_{biol} values) of all pharmaceuticals were higher than 1 $L.g_{VSS}^{-1}.d^{-1}$ in short-term experiments without background organic matter. This indicated high biodegradation potential of these pharmaceuticals by R1 sludge in the absence of background organic matter. Short-term experiment in the presence of background organic matter showed that ACT was highly biodegradable, whereas partial removal could be expected for CBZ and ERY. On the other hand, SMX was the least biodegraded pharmaceutical with around 16% removal efficiency when there was background organic matter.

In long term experiments, in addition to the R1 sludge, also the R2 sludge was used which was enriched in nitrifiers. According to the results:

- ACT was biodegraded by both heterotrophic and nitrification activity with high degradation efficiencies (around 99% removal efficiency).
- CBZ was the least biodegraded pharmaceutical by both activated sludge types. Its biodegradation rate constant varied in the range of 0.01 and 0.04 $L.g_{VSS}^{-1}.d^{-1}$ and indicated slow biodegradation.
- Although ERY was classified as refractory by BIOWIN models, experimental studies showed that it could be biodegraded by activated sludge to some extent, possibly as a secondary substrate in the presence of background organic matter. It was also biodegraded in the presence of nitrification activity as a cometabolite when no organic

matter was present. On the other hand, when it was the single pharmaceutical, its biodegradation rate constant decreased from around 0.5 $L.g_{VSS}^{-1}.d^{-1}$ to around 0.2 $L.g_{VSS}^{-1}.d^{-1}$ which led to the conclusion that the presence of other pharmaceuticals also enhanced its biodegradation.

- BIOWIN models showed that SMX was a slowly degradable pharmaceutical. However, experimental results indicated that it was biodegraded by both sludges. Additionally, it was observed that SMX was biodegraded at a higher rate (k_{biol} = 0.24 $L.g_{VSS}^{-1}.d^{-1}$) by an activated sludge enriched in terms of nitrifiers when it was the single pharmaceutical.

Adsorption experiments were carried out in batch reactors to obtain the isotherm constants belonging to the adsorption of organic matter stemming from the synthetic secondary effluent and pharmaceuticals. Results showed low adsorption of the bulk organics present in the synthetic secondary effluent on GAC when the DOC parameter was taken a criterion. The affinity of pharmaceuticals to adsorb onto GAC was in the following order when they were in a mixture: CBZ, ACT, ERY and SMX. On the other hand, when the pharmaceuticals were alone, the affinities to GAC increased indicating that there was a competition between these pharmaceuticals. Besides, in the presence of background organic matter, the adsorption capacity of pharmaceuticals slightly decreased and adsorption of background organic matter was much lower when there was a mixture of pharmaceuticals. Also, the affinity of pharmaceuticals to GAC in this experiment was in the following order: CBZ, ERY, ACT and SMX.

In addition, the removal of pharmaceuticals was examined in rapid small-scale continuous-flow GAC columns, by tests called RSSCTs. 30-hour experiments showed that there was no full breakthrough (C/C_0 = 1) of either of the pharmaceuticals. In fact, the column was far away from saturation. Only 1% to 4% of initial concentrations could be observed in the effluent of the column at the end of experiments.

In the presence of background organic matter, higher concentrations of pharmaceuticals were observed in the effluent which indicates a competition between the pharmaceuticals and the background organic matter in the synthetic secondary effluent.

The experimental results from RSSCTs were also compared to a simulation model called AdDesign. Different scenarios were tried to obtain the best fit of the breakthrough curves between the simulation model and the experiments. After the best fit was obtained, the operation time was increased to observe the full breakthrough. It was seen that the time to reach the breakthrough for all

pharmaceuticals was much longer in the case of using original GAC. This indicates that the use of ground GAC in a small-scale column is advantageous to investigate the removal of pharmaceuticals under different conditions in a short period of time.

Additionally, two biological activated carbon (BAC) columns were prepared to observe both the adsorption and biodegradation of selected pharmaceuticals. However, according to the results it was concluded that further research is needed for this part of the study. Batch experiments in the presence of both GAC and activated sludge gave promising results for pharmaceuticals removal. So, for future studies, it is recommended that BAC columns should be studied in detail. Especially preparation of the column should be taken into consideration. BAC experiments may be carried out in a longer period of time in order to understand the effect of simultaneous biodegradation and adsorption processes for removal of pharmaceuticals. These studies may provide insights for understanding the effect of these mechanisms.

In future work, RSSCTs can be used to investigate the removal of pharmaceuticals under different conditions with low cost and high water savings. Also, it may be recommended to use different types of activated carbon to evaluate the adsorption behavior of pharmaceuticals and to investigate the effective removal. After the kinetic parameters are obtained from batch experiments, RSSCTs can be used for observing the adsorption of pharmaceuticals in continuous-flow systems. Also, competition between pharmaceuticals and background organic matter in the secondary effluent should be taken into consideration during the operation of RSSCTs. In addition, the use of simulation models such as the AdDesign may also help for obtaining the best results. This approach may provide time and cost savings.

REFERENCES

Ahmed, M.B., Zhou, J.L., Ngo, H.H., Guo, W., Thomaidis, N.S., & Xu, J. (2017). Progress in the biological and chemical treatment technologies for emerging contaminant removal from wastewater: A critical review. *Journal of Hazardous Materials*, *323*, 274–298.

Akkurt, Ş. & Oğuz, M. (2019). Atıksu arıtma tesislerinde mikro kirleticilerin arıtılabiliriliği. *KSÜ Mühendislik Bilimleri Dergisi*, *22*(2), 58–77.

Al-Kaf, A.G., Naji, K.M., Abdullah, Q.Y.M., & Edrees, W.H.A. (2017). Occurrence of paracetamol in aquatic environments and transformation by microorganisms: a review. *Chronicles of Pharmaceutical Science*, *1*(6), 341-355.

Altmann, J., Ruhl, A.S., Zietzschmann, F., & Jekel, M. (2014). Direct comparison of ozonation and adsorption onto powdered activated carbon for micropollutant removal in advanced wastewater treatment. *Water Research*, *55*, 185-193.

Ashani, H.S. (2017). Use of granular activated carbon and carbon block filters at municipal and point of use drinking water treatment for removal of organics. MSc. Thesis, Arizona State University.

Balakrishnan, A., Kanchinadham, S.B.K., & Kalyanaraman, C. (2020). Assessment on biodegradability prediction of tannery wastewater using EPI Suite BIOWIN model. *Environmental Monitoring and Assessment*, 192:732.

Baresel, C., Cousins, A.P., Hörsing, M., Ek, M., Ejhed, H., Allard, A.S., Magnér, J., Westling, K., Wahlberg, C., Fortkamp, U., & Söhr, S. (2015). Pharmaceuticals residues and other emerging substances in the effluent of sewage treatment plants – Review on concentrations, quantification, behavior, and removal options. Swedish Environmental Research Institute, Report Number B 2226.

Bausk, A. (2015). Methodology for selecting the column configuration with lowest media replacement cost for small adsorption. MSc. Thesis, The Faculty of the Graduate College at the University of Nebraska.

Bofill, J. (2023). Microplastics and micropollutants in water: contaminants of emerging concern. European Investment Bank, 2023 Project-EIB sector paper-ENR/Water Management.

Cardenas, M.A.R., Ali, I., Lai, F.Y., Dawes, L., Thier, R., & Rajapakse, J. (2016). Removal of micropollutants through a biological wastewater treatment plant in a subtropical climate, Queensland-Australia. *Journal of Environmental Health Science and Engineering*, 14:14. DOI 10.1186/s40201-016-0257-8

Clara, M., Strenn, B., Gans, O., Martinez, E., Kreuzinger, N., & Kroiss, H. (2005). Removal of selected pharmaceuticals, fragrances and endocrine disrupting compounds in a membrane bioreactor and conventional wastewater treatment plants. *Water Research, 39*, 4797–4807.

Crittenden, J.C., Berrigan, J.K., & Hand, D.W. (1986). Design of rapid small-scale adsorption tests for a constant diffusivity. *Journal of Water Pollution Control Federation, 58*(4), 312-319.

Crittenden, J.C., Reddy, P.S., Arora, H., Trynoski, J., Hand, D.W., Perram, D.L., & Summers, R.S. (1991). Predicting GAC performance with rapid small-scale column tests. *Journal-American Water Works Association, 83*(1), 77-87.

Crittenden, J.C., Trussell, R.R., Hand, D.W., Howe, K.J., Tchobanoglous, G. (2012). *MWH's water treatment: principles and design, Third Edition*. Hoboken, New Jersey: John Wiley & Sons, Inc.

Çeçen, F. (2017). Removal and behaviour of hazardous pollutants in biological treatment systems. In Çeçen, F., & Tezel, U. (Eds.), *Hazardous Pollutants in Biological Treatment Systems: Fundamentals and a Guide to Experimental Research*. London, UK: IWA Publishing.

Çeçen, F. (2024). Activated Carbon. In John Wiley & Sons Inc (Ed.), *Kirk-Othmer Encyclopedia of Chemical Technology*. John Wiley & Sons, Inc. DOI: 10.1002/0471238961.0103200902011105.a01.pub4.

Çeçen, F., & Aktaş, Ö. (2011). *Activated carbon for water and wastewater treatment: integration of adsorption and biological treatment*. NY, USA: John Wiley and Sons.

Çeçen, F., & Gül, G. (2021). Biodegradation of five pharmaceuticals: estimation by predictive models and comparison with activated sludge data. *International Journal of Environmental Science and Technology*, *18*, 327–340. https://doi.org/10.1007/s13762-020-02820-y

De Castro, C.L., & Mitchell, B.S. (2002). Nanoparticles from Mechanical Attrition. In Baraton, M.I. (Ed.), *Synthesis, Functionalization and Surface Treatment of Nanoparticles*. France: American Scientific Publishers.

DiGiano, F.A., Anveiler, S., Hartmann, C., & Riddick, J.A. (1999). Compliance with EPA's information collection rule for North Carolina surface water supplies: bench-scale testing of the efficacy of carbon adsorption and membrane separation. Department of Environmental Sciences and Engineering, University of North Carolina, WRRI Project No. 70145 Report.

Dimitrov, S., Pavlov, T., Nedelcheva, D., Reuschenbach, P., Silvani, M., Bias, R., Comber, M., Low, L., Lee, C., Parkerton, T., & Mekenyan, O. (2007). A kinetic model for predicting biodegradation. *SAR and QSAR in Environmental Research*, *18*(5-6):443-457.

Doğruel, S., Gürel, M. & Pehlivanoglu-Mantaş, E. (2022). Mikrokirleticiler: tanım, mevzuat ve ülkemizde atıksularda ve yerüstü sularında mevcudiyetleri. *Çevre, İklim ve Sürdürülebilirlik*, *23*(2), 133–144.

Fernandez-Fontaina, E., Omil, F., Lema, J.M., & Carballa, M. (2012). Influence of nitrifying conditions on the biodegradation and sorption of emerging micropollutants. *Water Research*, *46*, 5434–5444.

Fernandez-Fontaina, E., Gomes, I.B., Aga, D.S., Omil, F., Lema, J.M., & Carballa, M. (2016). Biotransformation of pharmaceuticals under nitrification, nitratation and heterotrophic conditions. *Science of the Total Environment*, *541*, 1439–1447. https ://doi.org/10.1016/j.scito tenv.2015.10.010

Gauthier, H., Yargeau, V., & Cooper, D.G. (2010). Biodegradation of pharmaceuticals by *Rhodococcus rhodochrous* and *Aspergillus niger* by co-metabolism. S*cience of the Total Environment, 408*, 1701–1706.

Gerrity, D., Gamage, S., Holady, J.C., Mawhinney, D.B., Quiñones, O., Trenholm, R.A., & Snyder, S.A. (2011). Pilot-scale evaluation of ozone and biological activated carbon for trace organic contaminant mitigation and disinfection. *Water Research*, *45*, 2155-2165.

Göktaş, R.K., & Macleod, M. (2017). Hazardous pollutants in the water environment. In Çeçen, F., & Tezel, U. (Eds.), *Hazardous Pollutants in Biological Treatment Systems: Fundamentals and a Guide to Experimental Research*. London, UK: IWA Publishing.

Grover, D.P., Zhou, J.L., Frickers, P.E., & Readman, J.W. (2011). Improved removal of estrogenic and pharmaceutical compounds in sewage effluent by full scale granular activated carbon: Impact on receiving river water. *Journal of Hazardous Materials, 185*, 1005–1011.

Hand, D.W., Crittenden, J.C., Hokanson, D.R., & Bulloch, J.L. (1997). Predicting the performance of fixed-bed granular activated carbon adsorbers. *Water Science and Technology*, *35*(7), 235-241.

Hollender, J., Zimmermann, S., Koepke, S., Krauss, M., Mcardell, C.S., Ort, C., Singer, H., Gunten, U.V., & Siegrist, H. (2009). Elimination of organic micropollutants in a municipal wastewater treatment plant upgraded with a full-scale post-ozonation followed by sand filtration. *Environmental Science & Technology*, *43*(20), 7862–7869.

Hristovski, K.D., Westerhoff, P.K., Crittenden, J.C., & Olson, L.W. (2008). Arsenate removal by nanostructured ZrO_2 spheres, *Environmental Science & Technology*, *42*(10), 3786–3790.

Hung, Y.T., Lo, H.H., Wang, L.K., Taricska, J.R., & Li, K.H. (2005). Granular activated carbon adsorption. In Wang, L.K., Hung, Y.T., & Shammas, N.K. (Eds), *Handbook of Environmental Engineering, Volume 3: Physiochemical Treatment Processes.* Totowa, NJ: The Humana Press Inc.

Junpirom, S. (2006). Activated carbon from longan seed: its activation model and adsorption of water vapor and benzene. PhD. Thesis, Suranaree University of Technology.

Karelid, V., Larsson, G., & Björlenius, B. (2017). Pilot-scale removal of pharmaceuticals in municipal wastewater: Comparison of granular and powdered activated carbon treatment at three wastewater treatment plants. *Journal of Environmental Management*, *193*, 491-502.

Kassotaki, E., Buttiglieri, G., Ferrando-Climent, L., Rodriguez-Roda, I., & Pijuan, M. (2016). Enhanced sulfamethoxazole degradation through ammonia oxidizing bacteria co-metabolism and fate of transformation products. *Water Research, 94,* 111–119.

Kılıç, B., & Çeçen, F. (2023). Review of experimental biodegradation data on pharmaceuticals and comparison with predictive BIOWIN models. *Journal of Environmental Management, 344*:118310. DOI: 10.1016/j.jenvman.2023.118310

Kim, M.K., & Zoh, K.D. (2016). Occurrence and removals of micropollutants in water environment. *Environmental Engineering Research, 21*(4), 319-332.

Latawiec, A., & Schreiber, A. (2014). Analysis of personal care products (PPCP) in water samples by way of large volume sample injections. AB SCIEX, Publication number: 10160814-01.

Luo, Y., Guo, W., Ngo, H.H., Nghiem, L.D., Hai, F.I., Zhang, J., Liang, S., & Wang, X.C. (2014). A review on the occurrence of micropollutants in the aquatic environment and their fate and removal during wastewater treatment. *Science of the Total Environment, 473–474,* 619–641. http://dx.doi.org/10.1016/j.scitotenv.2013.12.065.

Magnuson, M.L., & Speth, T.F. (2005). Quantitative structure-property relationships for enhancing predictions of synthetic organic chemical removal from drinking water by granular activated carbon. *Environmental Science & Technology, 39*(19), 7706– 7711.

Mastropole, A.J. (2011). Evaluation of available scale-up approaches for the design of GAC contactors. MSc. Thesis, Graduate Faculty of North Carolina State University.

Matamoros, V., Gutiérrez, R., Ferrer, I., García, J., & Bayona, J.M. (2015). Capability of microalgae-based wastewater treatment systems to remove emerging organic contaminants: A pilot-scale study. *Journal of Hazardous Materials, 288,* 34–42.

Mertz, K.A., Gobin, F., Hand, D.W., Hokanson, D.R., & Crittenden, J.C. (1999). Manual Adsorption Design Software for Windows (AdDesignS^{TM}), Michigan Technological University.

Müller E., Schüssler, W., Horn, H., & Lemmer, H. (2013). Aerobic biodegradation of the sulfonamide antibiotic sulfamethoxazole by activated sludge applied as co-substrate and sole carbon and nitrogen source. *Chemosphere, 92*, 969–978.

Nam, S.W., Choi, D.J., Kim, S.K., Her, N., & Zoh, K.D. (2014). Adsorption characteristics of selected hydrophilic and hydrophobic micropollutants in water using activated carbon. *Journal of Hazardous Materials, 270*, 144–152.

Nas, B., Dolu, T., Ateş, H., Argun, M.E., & Yel, E. (2017). Treatment alternatives for micropollutant removal in wastewater. S*elcuk University Journal of Engineering Science and Technology (SUJEST), 5*(2), 133-143. doi: 10.15317/Scitech.2017.77.

Nugroho, W.A., Reungoat, J., & Keller, J. (2010). The performance of biological activated carbon in removing pharmaceuticals in drinking water treatment. *Journal of Applied Sciences in Environmental Sanitation, 5*(2), 131-141.

Ortuzar, M., Esterhuizen, M., Olicon-Hernandez, D.R., Gonzalez-Lopez, J., & Aranda, E. (2022). Pharmaceutical pollution in aquatic environments: a concise review of environmental impacts and bioremediation systems. *Frontiers in Microbiology, 13*, 1–25. doi: 10.3389/fmicb.2022.869332.

Patterson, C., Burkhardt, J., Schupp, D., Krishnan, E.R., Dyment, S., Merritt, S., Zintek, L., & Kleinmaier, D. (2019). Effectiveness of point-of-use/point-of-entry systems to remove per- and polyfluoroalkyl substances from drinking water. *AWWA Water Science, 1*(2), 1-12.

Patni, A.G., Ludlow, D.K., & Adams, C.D. (2008). Characteristics of ground granular activated carbon for rapid small-scale column tests. *Journal of Environmental Engineering, 134*(3), 216–221.

Paxéus, N. (2004). Removal of selected NSAIDs, gemfibrozil, carbamazepine, ß-blockers, trimethoprim and triclosan in conventional wastewater treatment plants in five EU countries and their discharge to the aquatic environment. *Water Science and Technology, 50*(5), 253-260.

Petrie, B., Barden, R., & Kasprzyk-Hordern, B. (2015). A review on emerging contaminants in wastewaters and the environment: Current knowledge, understudied areas and recommendations for future monitoring. *Water Research, 72*, 3-27.

Petrovic, M., Gonzalez, S., & Barcelo, D. (2003). Analysis and removal of emerging contaminants in wastewater and drinking water. *Trends in Analytical Chemistry*, *22*(10), 685-696.

Plosz, B.G., Langford, K.H., & Thomas, K.V. (2012). An activated sludge modeling framework for xenobiotic trace chemicals (ASM-X): assessment of diclofenac and carbamazepine. Biotechnology and Bioengineering, *109*:2757–2769. https ://doi.org/10.1002/bit.24553

Poddar, M., Brijesh Nair, A.N., & Mahindrakar, A.B. (2013). A review on the use of rapid small scale column test (RSSCT) on predicting adsorption of various contaminants. *IOSR Journal of Environmental Science, Toxicology and Food Technology*, *3*(1), 77-85.

Putz, A.R.H. (2004). Biological activated carbon: the relative role of metabolism and cometabolism in extending service life and improving process performance. PhD. Thesis, The Faculty of the Graduate School of the University of Texas.

Rattier, M., Reungoat, J., Gernjak, W., Joss, A., & Keller, J. (2012a). Investigating the role of adsorption and biodegradation in the removal of organic micropollutants during biological activated carbon filtration of treated wastewater. *Journal of Water Reuse and Desalination*, *2*(3), 127-139.

Rattier, M., Reungoat, J., Gernjak, W., & Keller J. (2012b). Organic micropollutant removal by biological activated carbon filtration: a review. Urban Water Security Research Alliance Technical Report No: 53.

Reinert, A.M. (2013). Granular activated carbon adsorption of micropollutants from surface water: field-scale adsorber performance and scale-up of bench-scale data. MSc. Thesis, Graduate Faculty of North Carolina State University.

Rogers, H.R. (1996). Sources, behaviour and fate of organic contaminants during sewage treatment and in sewage sludges. *The Science of the Total Environment*, *185*, 3-26.

Rücker, C., & Kümmerer, K. (2012). Modeling and predicting aquatic aerobic biodegradation – a review from a user's perspective. *Green Chemistry*, *14*, 875–887.

Sampaio, E.F.S., Guimarães, V., Soares, O.S.G.P., Pereira, M.F.R., Rodrigues, C.S.D., & Madeira, L.M. (2022). Degradation of toluene from gas streams by heterogeneous Fenton oxidation in a slurry

bubble reactor with activated carbon-based catalysts. *Nanomaterials*, *12*, 3274. https://doi.org/10.3390/nano12193274

Schafhauser, B.H., Kristofco, L.A., de Oliveira, C.M.R., & Brooks, B.W. (2018). Global review and analysis of erythromycin in the environment: Occurrence, bioaccumulation and antibiotic resistance hazards. *Environmental Pollution, 238*, 440-451.

Schreiber, A. (2012). Comprehensive quantitation and identification of pesticides in food samples using the new Eksigent ekspert™ ultraLC 100 and the new AB SCIEX QTRAP® 4500 system. AB SCIEX, Publication number: 5090212-01.

Shkal, F., Lopez, S.G., Slocombe, D., & Porch, A. (2018). Microwave characterization of activated carbons. *Journal of Computer and Communications*, *6*, 112–123.

Snyder, S.A., Adham, S., Redding, A.M., Cannon, F.S., DeCarolis, J., Oppenheimer, J., Wert, E.C., & Yoon, Y. (2007). Role of membranes and activated carbon in the removal of endocrine disruptors and pharmaceuticals. *Desalination, 202*, 156–181.

Stewart, B.A. (2011). A framework for evaluating sorbent usage rate of various sorption column configurations with and without bypass blending. MSc. Thesis, The Faculty of the Graduate College at the University of Nebraska.

Suarez, S., Reif, R., Lema, J.M., & Omil, F. (2012). Mass balance of pharmaceutical and personal care products in a pilot-scale single-sludge system: influence of T, SRT and recirculation ratio. *Chemosphere*, *89*(2), 164–171.

Sui, Q., Huang, J., Deng, S., Yu, G., & Fan, Q. (2010). Occurrence and removal of pharmaceuticals, caffeine and DEET in wastewater treatment plants of Beijing, China. *Water Research*, *44*, 417-426.

Ternes, T.A., Herrmann, N., Bonerz, M., Knacker, T., Siegrist, H., Joss, A. (2004). A rapid method to measure the solid–water distribution coefficient (K_d) for pharmaceuticals and musk fragrances in sewage sludge. *Water Research, 38*, 4075–4084.

Ternes, T.A., Joss, A. (2006). *Human Pharmaceuticals, Hormones and Fragrances – the Challenge of Micropollutants in Urban Water Management*. IWA Publishing: London.

Thanh, T.P. (2018). Occurrence of pharmaceutical residues in water and treatment solutions. B.S. Thesis, Environmental Engineering Degree Programme, Metropolia University of Applied Sciences.

Tran, N.H., Urase, T., & Kusakabe, O. (2009). The characteristics of enriched nitrifier culture in the degradation of selected pharmaceutically active compounds. *Journal of Hazardous Materials*, *171*, 1051–1057.

Tüzün, S.C. (2017). Occurrence and fate of micropollutants and their metabolites in WWTPs. MSc. Thesis, Graduate School of Science Engineering and Technology, Department of Environmental Engineering, Environmental Sciences, Engineering, and Management Programme, Istanbul Technical University.

US EPA (2012). Estimation Programs Interface Suite™ for Microsoft® Windows, v 4.11. United States Environmental Protection Agency, Washington, DC, USA.

Verlicchi, P., Aukidy, M.A., & Zambello, E. (2012). Occurrence of pharmaceutical compounds in urban wastewater: Removal, mass load and environmental risk after a secondary treatment—A review. *Science of the Total Environment*, *429*, 123–155.

Worch, E. (2012). *Adsorption Technology in Water Treatment Fundamentals, Processes, and Modeling*. Germany: Walter de Gruyter GmbH & Co.

Xu, W., & Duran, M. (2017). Removal of hazardous pollutants in full-scale wastewater treatment plant. In Çeçen, F., & Tezel, U. (Eds.), *Hazardous Pollutants in Biological Treatment Systems: Fundamentals and a Guide to Experimental Research*. London, UK: IWA Publishing.

Zietzschmann, F., Müller, J., Sperlich, A., Ruhl, A.S., Meinel, F., Altmann, J., & Jekel, M. (2014). Rapid small-scale column testing of granular activated carbon for organic micro-pollutant removal in treated domestic wastewater. *Water Science & Technology*, *70*(7), 1271-1278.

APPENDIX A: MONITORING OF ACTIVATED SLUDGE REACTORS

Table A.1. Operational results of R1 – December 2022.

Run	**1**		**2**		**3**	
Date	**12/12/2022**	**15/12/2022**	**19/12/2022**	**22/12/2022**	**26/12/2022**	**30/12/2022**
pH	7	7.02	6.75	6.68	7	7.23
Temperature (^{o}C)	22.9	27.9	22.1	25.4	20.1	19.7
COD (mg/L)	1734	30	1284	24	1839	23
COD removal (%)	98		98		99	
Daily COD (mg/L)	536		435		460	
NH_4-N (mg/L)	123	0.25	92	0.25	115.0	0.2
NH_4-N removal (mg/L)	99.8		99.7		99.8	
Daily NH_4-N (mg/L)	38		31		29	
SS (mg/L)	3695		4640		5215	
VSS (mg/L)	2820		3465		3775	
Run period (day)	3.23		2.95		4.00	
F:M Ratio (mg COD/mg MLVSS*day)	0.19		0.13		0.12	
Initial Substrate/Initial Biomass (S_0/X_0) (mg COD/mg MLVSS)	0.61		0.37		0.49	

Table A.2. Operational results of R1 – January 2023.

Run	**1**		**2**		**3**		**4**	
Date	**02/01/2023**	**05/01/2023**	**09/01/2023**	**12/01/2023**	**16/01/2023**	**20/01/2023**	**24/01/2023**	**27/01/2023**
pH	7.37	6.47	6.85	6.32	7.27	6.63	7	6.96
Temperature (^{o}C)	18.1	22.9	17.9	23.3	17.1	21.4	21.3	22.2
COD (mg/L)	1286	40	1230	26	1758	9	1307	45
COD removal (%)	97		98		99.5		97	
Daily COD (mg/L)	396		480.9		439.5		438.3	
NH_4-N (mg/L)	82	0.55	82	0.05	108	0.1	91	0.1
NH_4-N removal (mg/L)	99.3		99.9		99.9		99.9	
Daily NH_4-N (mg/L)	25		32		27		30	
SS (mg/L)	4435		3435		3850		4050	
VSS (mg/L)	3425		2725		3125		3310	
Run period (day)	3.25		2.56		4.00		2.98	
F:M Ratio (mg COD/mg MLVSS*day)	0.12		0.18		0.14		0.13	
Initial Substrate/Initial Biomass (S_0/X_0) (mg COD/mg MLVSS)	0.38		0.45		0.56		0.39	

Table A.3. Operational results of R1 – February 2023.

Run	**1**		**2**		**3**		**4**	
Date	**30/01/2023**	**02/02/2023**	**07/02/2023**	**10/02/2023**	**13/02/2023**	**16/02/2023**	**20/02/2023**	**24/02/2023**
pH	6.98	6.98	6.28	6.25	7.7	7.04	6.87	6.79
Temperature (^{o}C)	17.3	19.1	15.4	24	17	24.4	18.5	24.2
COD (mg/L)	1246	18	1494	14	1326	10	1732	34
COD removal (%)	99		99		99		98	
Daily COD (mg/L)	420		501		443		423	
NH_4-N (mg/L)	74	0.05	97	0.3	80	0.05	115	0.15
NH_4-N removal (mg/L)	99.9		99.7		99.9		99.9	
Daily NH_4-N (mg/L)	25		32		26		28	
SS (mg/L)	3445		3370		4045		3660	
VSS (mg/L)	2825		2790		3255		3030	
Run period (day)	2.97		2.98		3.00		4.09	
F:M Ratio (mg COD/mg MLVSS*day)	0.15		0.18		0.14		0.14	
Initial Substrate/Initial Biomass (S_0/X_0) (mg COD/mg MLVSS)	0.44		0.54		0.41		0.57	

Table A.4. Operational results of R1 – March 2023.

Run	**1**		**2**		**3**		**4**		**5**	
Date	**27/02/2023**	**03/03/2023**	**06/03/2023**	**10/03/2023**	**13/03/2023**	**17/03/2023**	**20/03/2023**	**23/03/2023**	**27/03/2023**	**30/03/2023**
pH	6.23	7.19	7.18	6.38	6.6	7.77	6.50	7.25	7.77	8.55
Temperature (^{o}C)	24.2	23.8	18.4	25.6	20.4	28	16.4	24.2	19.1	18.8
COD (mg/L)	1658	10	1795	25	1732	15	1694	41	1342	40
COD removal (%)	99		99		99		98		97	
Daily COD (mg/L)	416		447		430		571		446	
SS (mg/L)	3850		3710		3000		3395		3385	
VSS (mg/L)	3150		3075		2415		2750		2600	
Run period (day)	3.99		4.02		4.03		2.97		3.01	
F:M Ratio (mg COD/mg MLVSS*day)	0.13		0.15		0.18		0.21		0.17	
Initial Substrate/Initial Biomass (S_0/X_0) (mg COD/mg MLVSS)	0.53		0.58		0.72		0.62		0.52	

Table A.5. Operational results of R1 – April 2023.

Run	**1**		**2**		**3**		**4**	
Date	**03/04/2023**	**06/04/2023**	**10/04/2023**	**13/04/2023**	**17/04/2023**	**19/04/2023**	**24/04/2023**	**28/04/2023**
pH	6.98	7.71	7.03	8	6.51	7.69	7.06	7.51
Temperature (^{o}C)	20.6	20.9	19.1	21.3	21.3	21.5	19.4	21.2
COD (mg/L)	1191	47	1360	9	789	12	1616	127
COD removal (%)	96		99		98		92	
Daily COD (mg/L)	392		458		393		403	
SS (mg/L)	4445		4175		3540		4055	
VSS (mg/L)	3620		3460		3045		3325	
Run period (day)	3.04		2.97		2.01		4.01	
F:M Ratio (mg COD/mg MLVSS*day)	0.11		0.13		0.13		0.12	
Initial Substrate/Initial Biomass (S_0/X_0) (mg COD/mg MLVSS)	0.33		0.39		0.26		0.49	

Table A.6. Operational results of R1 – May 2023.

Run	**1**		**2**		**3**		**4**		**5**	
Date	**02/05/2023**	**05/05/2023**	**08/05/2023**	**12/05/2023**	**16/05/2023**	**18/05/2023**	**22/05/2023**	**25/05/2023**	**29/05/2023**	**02/06/2023**
pH	6.49	7.96	6.14	7.72	7.32	7.87	6.85	7.91	6.35	7.13
Temperature (^{o}C)	19.9	21.8	19.4	22.4	21.2	21.8	20.5	21.8	20.2	22.9
COD (mg/L)	1357	28	1513	23	781	14	1229	16	1629	26
COD removal (%)	98		98		98		99		98	
Daily COD (mg/L)	446		373		380		410		416	
SS (mg/L)	4125		3655		4970		4400		4915	
VSS (mg/L)	3420		3195		4140		3680		4190	
Run period (day)	3.04		4.06		2.06		2.99		3.92	
F:M Ratio (mg COD/mg MLVSS*day)	0.13		0.12		0.09		0.11		0.10	
Initial Substrate/Initial Biomass (S_0/X_0) (mg COD/mg MLVSS)	0.40		0.47		0.19		0.33		0.39	

Table A.7. Operational results of R1 – June 2023.

Run	**1**		**2**		**3**	
Date	**05/06/2023**	**08/06/2023**	**12/06/2023**	**15/06/2023**	**19/06/2023**	**23/06/2023**
pH	7.29	7.15	6.54	7.81	6.02	7.05
Temperature (°C)	21.3	22	21.9	23.2	22.5	25.7
COD (mg/L)	1167	23	1090	41	1312	24
COD removal (%)	98		96		98	
Daily COD (mg/L)	379		372		335	
SS (mg/L)	4755		3715		3660	
VSS (mg/L)	4140		3345		3310	
Run period (day)	3.08		2.93		3.92	
F:M Ratio (mg COD/mg MLVSS*day)	0.09		0.11		0.10	
Initial Substrate/Initial Biomass (S_0/X_0) (mg COD/mg MLVSS)	0.28		0.33		0.40	

Table A.8. Operational results of R1 – July 2023.

Run	**1**		**2**		**3**	
Date	**10/07/2023**	**13/07/2023**	**17/07/2023**	**20/07/2023**	**24/07/2023**	**28/07/2023**
pH	5.52	6.99	5.61	6	6.61	5.17
Temperature (°C)	24.4	28.1	26.8	28.1	26.8	27.5
COD (mg/L)	1295	12	1287	35	1560	20
COD removal (%)	99		97		99	
Daily COD (mg/L)	429		443		389	
SS (mg/L)	1740		2485		3520	
VSS (mg/L)	1705		2245		2860	
Run period (day)	3.02		2.90		4.01	
F:M Ratio (mg COD/mg MLVSS*day)	0.25		0.20		0.14	
Initial Substrate/Initial Biomass (S_0/X_0) (mg COD/mg MLVSS)	0.76		0.57		0.55	

Table A.9. Operational results of R1 – August 2023.

Run	**1**		**2**		**3**		**4**	
Date	**31/07/2023**	**03/08/2023**	**07/08/2023**	**10/08/2023**	**14/08/2023**	**17/08/2023**	**21/08/2023**	**25/08/2023**
pH	5.8	6.01	5.86	6.63	6.61	7.24	6.69	7.95
Temperature (^{o}C)	25	27.4	27.6	27.1	25.5	27.1	25.5	28.2
COD (mg/L)	1126	32	1181	16	1190	25	1631	16
COD removal (%)	97		99		98		99	
Daily COD (mg/L)	376		389		395		406	
SS (mg/L)	4210		4115		5210		5710	
VSS (mg/L)	3625		3690		4485		4805	
Run period (day)	3.00		3.03		3.01		4.02	
F:M Ratio (mg COD/mg MLVSS*day)	0.10		0.11		0.09		0.08	
Initial Substrate/Initial Biomass (S_0/X_0) (mg COD/mg MLVSS)	0.31		0.32		0.27		0.34	

Table A.10. Operational results of R1 – September 2023.

Run	**1**		**2**		**3**		**4**	
Date	**04/09/2023**	**07/09/2023**	**11/09/2023**	**13/09/2023**	**18/09/2023**	**21/09/2023**	**25/09/2023**	**29/09/2023**
pH	6.52	6.39	7.51	6.61	6.59	6.16	6.12	6.05
Temperature (^{o}C)	25.3	26.4	24.5	25.2	22.8	23.9	22.6	24.7
COD (mg/L)	1540	14	763	21	1146	24	1576	13
COD removal (%)	99		97		98		99	
Daily COD (mg/L)	507		388		384		388	
SS (mg/L)	5455		4555		4610		4250	
VSS (mg/L)	4725		4310		4545		4015	
Run period (day)	3.04		1.97		2.98		4.06	
F:M Ratio (mg COD/mg MLVSS*day)	0.11		0.09		0.08		0.10	
Initial Substrate/Initial Biomass (S_0/X_0) (mg COD/mg MLVSS)	0.33		0.18		0.25		0.39	

Table A.11. Operational results of R1 – October 2023.

Run	**1**		**2**		**3**		**4**		**5**	
Date	**02/10/2023**	**06/10/2023**	**09/10/2023**	**12/10/2023**	**16/10/2023**	**19/10/2023**	**23/10/2023**	**26/10/2023**	**30/10/2023**	**02/11/2023**
pH	6.16	6.02	7.33	7.37	7.11	7.92	6.83	8.25	7.39	7.96
Temperature (^{o}C)	21.7	22.8	20.9	21	20.7	20.7	21.8	23.3	22.5	22.6
COD (mg/L)	1276	13	1090	10	1278	16	1087	6	1295	17
COD removal (%)	99		99		99		99		99	
Daily COD (mg/L)	317		373		438		363		433	
SS (mg/L)	4100		4265		4105		4535		5160	
VSS (mg/L)	3980		4070		3760		4075		4550	
Run period (day)	4.03		2.92		2.92		2.99		2.99	
F:M Ratio (mg COD/mg MLVSS*day)	0.08		0.09		0.12		0.09		0.10	
Initial Substrate/Initial Biomass (S_0/X_0) (mg COD/mg MLVSS)	0.32		0.27		0.34		0.27		0.28	

Table A.12. Operational results of R1 – November 2023.

Run	**1**		**2**		**3**		**4**	
Date	**06/11/2023**	**10/11/2023**	**13/11/2023**	**17/11/2023**	**20/11/2023**	**23/11/2023**	**27/11/2023**	**30/11/2023**
pH	6.63	7.8	6.4	7.64	6.44	7.53	6.5	7.4
Temperature (^{o}C)	20.9	20.2	19.3	22.2	18.5	21.6	19.2	22
COD (mg/L)	1738	15	1597	10	1170	16	1330	22
COD removal (%)	99		99		99		98	
Daily COD (mg/L)	434		400		390		442	
SS (mg/L)	5460		5540		4955		4875	
VSS (mg/L)	4665		4680		4410		4045	
Run period (day)	4.00		3.99		3.00		3.01	
F:M Ratio (mg COD/mg MLVSS*day)	0.09		0.09		0.09		0.11	
Initial Substrate/Initial Biomass (S_0/X_0) (mg COD/mg MLVSS)	0.37		0.34		0.27		0.33	

Table A.13. Operational results of R1 – December 2023.

Run	**1**		**2**		**3**		**4**	
Date	**04/12/2023**	**07/12/2023**	**11/12/2023**	**14/12/2023**	**18/12/2023**	**21/12/2023**	**25/12/2023**	**29/12/2023**
pH	6.24	7.37	6.33	7.56	6.83	7.5	6.11	7.77
Temperature (^{o}C)	21.4	22.1	19.6	21.8	19.3	21.1	20	22.1
COD (mg/L)	1168	11	1158	12	1211	22	1636	14
COD removal (%)	99		99		98		99	
Daily COD (mg/L)	390		385		405		413	
SS (mg/L)	4775		4180		3790		4975	
VSS (mg/L)	3965		3540		3200		4240	
Run period (day)	2.99		3.01		2.99		3.96	
F:M Ratio (mg COD/mg MLVSS*day)	0.10		0.11		0.13		0.10	
Initial Substrate/Initial Biomass (S_0/X_0) (mg COD/mg MLVSS)	0.29		0.33		0.38		0.39	

Table A.14. Operational results of R1 – January 2024.

Run	**1**		**2**		**3**		**4**		**5**	
Date	**02/01/2024**	**05/01/2024**	**08/01/2024**	**11/01/2024**	**15/01/2024**	**19/01/2024**	**22/01/2024**	**26/01/2024**	**29/01/2024**	**01/02/2024**
pH	6.67	7.95	6.57	8	6.84	8.34	6.37	8.03	6.67	8
Temperature (^{o}C)	20.7	22.2	20.7	20	17.9	21.8	17.9	21.6	18.3	21.3
COD (mg/L)	1136	18	1380	19	1604	21	1440	43	1358	40
COD removal (%)	98		99		99		97		97	
Daily COD (mg/L)	390		467		397		361		454	
SS (mg/L)	5495		4830		5245		5640		5700	
VSS (mg/L)	4565		3960		4395		4480		4630	
Run period (day)	2.99		2.95		4.04		3.99		2.99	
F:M Ratio (mg COD/mg MLVSS*day)	0.08		0.12		0.09		0.08		0.10	
Initial Substrate/Initial Biomass (S_0/X_0) (mg COD/mg MLVSS)	0.25		0.35		0.36		0.32		0.29	

Table A.15. Operational results of R1 – February 2024.

Run	**1**		**2**		**3**		**4**	
Date	**05/02/2024**	**09/02/2024**	**12/02/2024**	**15/02/2024**	**19/02/2024**	**22/02/2024**	**26/02/2024**	**01/03/2024**
pH	6.79	7.71	6.32	7.55	5.63	6.92	5.93	6.78
Temperature (^{o}C)	18.4	21.8	20.8	20.7	20.9	23.3	21.4	24.6
COD (mg/L)	1611	65	1207	11	1339	51	1734	54
COD removal (%)	96		99		96		97	
Daily COD (mg/L)	405		400		448		434	
NH_4-N (mg/L)	75	2.5	75	2.5	58	2.5	118	5
NH_4-N removal (mg/L)	97		97		96		96	
Daily NH_4-N (mg/L)	19		25		19		29	
SS (mg/L)	5385		5410		5305		4805	
VSS (mg/L)	4365		4375		4380		3695	
Run period (day)	3.98		3.02		2.99		4.00	
F:M Ratio (mg COD/mg MLVSS*day)	0.09		0.09		0.10		0.12	
Initial Substrate/Initial Biomass (S_0/X_0) (mg COD/mg MLVSS)	0.37		0.28		0.31		0.47	

Table A.16. Operational results of R1 – March 2024.

Run	**1**		**2**		**3**		**4**	
Date	**04/03/2024**	**08/03/2024**	**11/03/2024**	**14/03/2024**	**18/03/2024**	**22/03/2024**	**25/03/2024**	**29/03/2024**
pH	6.19	7.24	6.28	7.99	6.38	7.94	6.9	7.71
Temperature (^{o}C)	18.8	25.2	21	22.7	19.8	23.6	20	24.6
COD (mg/L)	1911	77	1467	97	1866	77	1986	91
COD removal (%)	96		93		96		95	
Daily COD (mg/L)	473		491		460.6		504.0	
SS (mg/L)	3650		4920		3705		4155	
VSS (mg/L)	3045		3755		3025		3360	
Run period (day)	4.04		2.99		4.05		3.94	
F:M Ratio (mg COD/mg MLVSS*day)	0.16		0.13		0.15		0.15	
Initial Substrate/Initial Biomass (S_0/X_0) (mg COD/mg MLVSS)	0.63		0.39		0.62		0.59	

Table A.17. Operational results of R1 – April 2024.

Run	**1**		**2**		**3**		**4**	
Date	**01/04/2024**	**05/04/2024**	**15/04/2024**	**18/04/2024**	**22/04/2024**	**25/04/2024**	**29/04/2024**	**03/05/2024**
pH	6.28	6.93	6.14	6.59	6.55	5.88	5.95	7.32
Temperature (°C)	21.7	22.7	20.3	23.5	19.1	22	18.6	21
COD (mg/L)	1866	65	1401	138	1606	54	1892	104
COD removal (%)	967		90		97		94	
Daily COD (mg/L)	467		467		524		480	
SS (mg/L)	4465		5690		4305		4825	
VSS (mg/L)	3505		3550		3610		4025	
Run period (day)	4.00		3.00		3.06		3.94	
F:M Ratio (mg COD/mg MLVSS*day)	0.13		0.13		0.15		0.12	
Initial Substrate/Initial Biomass (S_0/X_0) (mg COD/mg MLVSS)	0.53		0.39		0.44		0.47	

Table A.18. Operational results of R1 – May 2024.

Run	**1**		**2**		**3**		**4**	
Date	**06/05/2024**	**10/05/2024**	**13/05/2024**	**16/05/2024**	**20/05/2024**	**24/05/2024**	**27/05/2024**	**30/05/2024**
pH	5.7	7.02	6	6.8	6.01	5.61	5.72	5.85
Temperature (°C)	19.1	21.8	20.1	21.9	19.3	20.9	20	23
COD (mg/L)	1918	88	1302	89	1960	121	1690	149
COD removal (%)	95		93		94		91	
Daily COD (mg/L)	479		435		492		554	
SS (mg/L)	3960		4275		5015		4260	
VSS (mg/L)	3265		3575		4295		3690	
Run period (day)	4.00		2.99		3.98		3.05	
F:M Ratio (mg COD/mg MLVSS*day)	0.15		0.12		0.11		0.15	
Initial Substrate/Initial Biomass (S_0/X_0) (mg COD/mg MLVSS)	0.59		0.36		0.46		0.46	

Table A.19. Operational results of R1 – June 2024.

Run	**1**		**2**	
Date	**03/06/2024**	**05/06/2024**	**24/06/2024**	**28/06/2024**
pH	6.17	6.29	5.63	6.77
Temperature (^{o}C)	24.6	26.7	22.2	25.4
COD (mg/L)	967	140	2040	158
COD removal (%)	85		92	
Daily COD (mg/L)	471.4		506.9	
SS (mg/L)	4785		3815	
VSS (mg/L)	3825		3320	
Run period (day)	2.05		4.02	
F:M Ratio (mg COD/mg MLVSS*day)	0.12		0.15	
Initial Substrate/Initial Biomass (S_0/X_0) (mg COD/mg MLVSS)	0.25		0.61	

Table A.20. Operational results of R1 – July 2024.

Run	**1**		**2**		**3**	
Date	**01/07/2024**	**05/07/2024**	**08/07/2024**	**12/07/2024**	**16/07/2024**	**19/07/2024**
pH	6.2	6.9	6.38	7.52	6.02	7.18
Temperature (^{o}C)	24.3	26.5	26.1	28.5	26.9	29.2
COD (mg/L)	1905	202	1768	114	1783	142
COD removal (%)	89		94		92.0	
Daily COD (mg/L)	472		443		594	
SS (mg/L)	4145		4505		5180	
VSS (mg/L)	3545		3815		4315	
Run period (day)	4.04		3.99		3.00	
F:M Ratio (mg COD/mg MLVSS*day)	0.13		0.12		0.14	
Initial Substrate/Initial Biomass (S_0/X_0) (mg COD/mg MLVSS)	0.54		0.46		0.41	

Table A.21. Operational results of R1 – August & September 2024.

Run	**1**		**2**		**3**	
Date	**05/08/2024**	**08/08/2024**	**09/09/2024**	**12/09/2024**	**30/09/2024**	**03/10/2024**
pH	5.84	7.25	6.72	7.86	6.16	7.70
Temperature (^{o}C)	24.7	27.2	24.2	25.9	22.7	21.6
COD (mg/L)	1745	144	1771	175	1679	129
COD removal (%)	92		90		92	
Daily COD (mg/L)	575		594		552	
SS (mg/L)	5575		6120		6415	
VSS (mg/L)	4800		5000		5360	
Run period (day)	3.03		2.98		3.05	
F:M Ratio (mg COD/mg MLVSS*day)	0.12		0.12		0.10	
Initial Substrate/Initial Biomass (S_0/X_0) (mg COD/mg MLVSS)	0.36		0.35		0.31	

Table A.22. Operational results of R1 – October, November, December 2024.

Run	**1**		**2**		**3**	
Date	**14/10/2024**	**17/10/2024**	**04/11/2024**	**07/11/2024**	**16/12/2024**	**19/12/2024**
pH	6.45	7.68	6.14	8.14	6.78	7.98
Temperature (^{o}C)	20.9	20.1	17.4	17.3	18.2	23.7
COD (mg/L)	1426	127	1705	124	1685	126
COD removal (%)	91		93		92.5	
Daily COD (mg/L)	465		570		555	
SS (mg/L)	7150		5815		6000	
VSS (mg/L)	5990		4790		4665	
Run period (day)	3.07		2.99		3.04	
F:M Ratio (mg COD/mg MLVSS*day)	0.08		0.12		0.12	
Initial Substrate/Initial Biomass (S_0/X_0) (mg COD/mg MLVSS)	0.24		0.36		0.36	

Table A.23. Operational results of R2 – April 2023.

Run	**1**		**2**		**3**		**4**	
Date	**03/04/2023**	**06/04/2023**	**10/04/2023**	**13/04/2023**	**17/04/2023**	**19/04/2023**	**24/04/2023**	**28/04/2023**
pH	9.57	9.92	8.76	9.82	7.2	7.55	9.54	7.76
Temperature (ºC)	19.5	19.3	28.1	20.2	19	21.3	19.7	20.4
NH_4-N (mg/L)	965	625	960	935	560	370	350	305.0
NH_4-N removal (%)	35		2.6		34		13	
Daily NH_4-N (mg/L)	316		323		279		87	
SS (mg/L)	4560		4810		4825		3795	
VSS (mg/L)	1365		1330		1545		1125	
Run period (day)	3.05		2.97		2.01		4.01	
F:M Ratio (mg NH_4-N/mg MLVSS*day)	0.23		0.24		_		0.08	
Initial Substrate/Initial Biomass (S_0/X_0) (mg NH_4-N/mg MLVSS)	0.71		0.72		_		0.31	

Table A.24. Operational results of R2 – May 2023.

Run	**1**		**2**		**3**		**4**		**5**	
Date	**02/05/2023**	**05/05/2023**	**08/05/2023**	**12/05/2023**	**16/05/2023**	**18/05/2023**	**22/05/2023**	**25/05/2023**	**29/05/2023**	**02/06/2023**
pH	7.97	9.29	7.87	9.67	7.05	8.13	7.45	6.92	7.64	6.68
Temperature (ºC)	19.4	20.8	19	19.4	21.4	22.1	20.8	21.8	20.7	22.7
NH_4-N (mg/L)	220	190	260	170	310	270	160	115	270	90
NH_4-N removal (%)	14		35		13		28		67	
Daily NH_4-N (mg/L)	72		64		151		54		69	
SS (mg/L)	3235		3205		3075		2815		3450	
VSS (mg/L)	1050		1050		1010		990		1215	
Run period (day)	3.04		4.06		2.06		2.99		3.92	
F:M Ratio (mg NH_4-N/mg MLVSS*day)	0.07		0.06		0.15		0.05		0.06	
Initial Substrate/Initial Biomass (S_0/X_0) (mg NH_4-N/mg MLVSS)	0.21		0.25		0.31		0.16		0.22	

Table A.25. Operational results of R2 – June 2023.

Run	**1**		**2**		**3**	
Date	**05/06/2023**	**08/06/2023**	**12/06/2023**	**15/06/2023**	**19/06/2023**	**23/06/2023**
pH	7.75	6.98	7.64	7.12	7.65	7.21
Temperature (°C)	21.7	22.2	22.7	23.3	23.5	25.4
NH_4-N (mg/L)	230	60	250	65	382	70
NH_4-N removal (%)	74		74		82	
Daily NH_4-N (mg/L)	75		85		98	
SS (mg/L)	4005		3775		6150	
VSS (mg/L)	1270		1220		2240	
Run period (day)	3.08		2.93		3.92	
F:M Ratio (mg NH_4-N/mg MLVSS*day)	0.06		0.07		0.04	
Initial Substrate/Initial Biomass (S_0/X_0) (mg NH_4-N/mg MLVSS)	0.18		0.20		0.17	

Table A.26. Operational results of R2 – July 2023.

Run	**1**		**2**		**3**	
Date	**10/07/2023**	**13/07/2023**	**17/07/2023**	**20/07/2023**	**24/07/2023**	**28/07/2023**
pH	8.29	9.56	7.22	9.15	7.39	8.45
Temperature (°C)	25.1	27.9	27.7	27.1	28.3	27
NH_4-N (mg/L)	542	318	338	185	358	82
NH_4-N removal (%)	42		45		77	
Daily NH_4-N (mg/L)	180		116		89	
SS (mg/L)	4910		6360		4175	
VSS (mg/L)	1410		1715		1130	
Run period (day)	3.02		2.90		4.01	
F:M Ratio (mg NH_4-N/mg MLVSS*day)	0.13		0.07		0.08	
Initial Substrate/Initial Biomass (S_0/X_0) (mg NH_4-N/mg MLVSS)	0.38		0.20		0.32	

Table A.27. Operational results of R2 – August 2023.

Run	**1**		**2**		**3**		**4**	
Date	**31/07/2023**	**03/08/2023**	**07/08/2023**	**10/08/2023**	**14/08/2023**	**17/08/2023**	**21/08/2023**	**25/08/2023**
pH	8.98	9.77	7.26	9.36	7.49	9.65	8.72	10.08
Temperature (ºC)	25.8	27.9	28.6	26.7	26.1	27.1	27.1	28
NH_4-N (mg/L)	520	368	42	208	375	298	362	180
NH_4-N removal (%)	29		51		21		50	
Daily NH_4-N (mg/L)	174		139		125		90	
SS (mg/L)	5790		6550		7385		6555	
VSS (mg/L)	1410		1880		1665		1650	
Run period (day)	3.00		3.03		3.01		4.02	
F:M Ratio (mg NH_4-N/mg MLVSS*day)	0.12		0.07		0.07		0.05	
Initial Substrate/Initial Biomass (S_0/X_0) (mg NH_4-N/mg MLVSS)	0.37		0.22		0.23		0.22	

Table A.28. Operational results of R2 – September 2023.

Run	**1**		**2**		**3**		**4**	
Date	**04/09/2023**	**07/09/2023**	**11/09/2023**	**13/09/2023**	**18/09/2023**	**21/09/2023**	**25/09/2023**	**29/09/2023**
pH	8.91	8	8.89	8.29	8.42	10.07	8.08	7.22
Temperature (ºC)	26.3	26.2	24.7	24.8	23.1	24.3	24.5	24.3
NH_4-N (mg/L)	158	12	112	0	468	325	170	98
NH_4-N removal (%)	92		100		30		43	
Daily NH_4-N (mg/L)	52		57		157		42	
SS (mg/L)	4915		3925		3840		3815	
VSS (mg/L)	1335		1305		1495		1420	
Run period (day)	3.04		1.97		2.98		4.06	
F:M Ratio (mg NH_4-N/mg MLVSS*day)	0.04		0.04		0.10		0.03	
Initial Substrate/Initial Biomass (S_0/X_0) (mg NH_4-N/mg MLVSS)	0.12		0.09		0.31		0.12	

Table A.29. Operational results of R2 – October 2023.

Run	**1**		**2**		**3**		**4**		**5**	
Date	**02/10/2023**	**06/10/2023**	**09/10/2023**	**12/10/2023**	**16/10/2023**	**19/10/2023**	**23/10/2023**	**26/10/2023**	**30/10/2023**	**02/11/2023**
pH	7.94	7.38	8.31	7.75	8.88	8.35	8.8	8.2	8.2	7.78
Temperature (ºC)	22.8	22.8	21.5	21	21.1	20.6	22.5	23	23	22.5
NH_4-N (mg/L)	188	52	158	22	190	15	185	5	262	12
NH_4-N removal (%)	72		86		92		97		95	
Daily NH_4-N (mg/L)	47		54		65		62		88	
SS (mg/L)	4040		4380		3570		4170		4335	
VSS (mg/L)	1770		1215		1035		1180		1250	
Run period (day)	4.03		2.92		2.92		2.99		2.99	
F:M Ratio (mg NH_4-N/mg MLVSS*day)	0.03		0.04		0.06		0.05		0.07	
Initial Substrate/Initial Biomass (S_0/X_0) (mg NH_4-N/mg MLVSS)	0.11		0.13		0.18		0.16		0.21	

Table A.30. Operational results of R2 – November 2023.

Run	**1**		**2**		**3**		**4**	
Date	**06/11/2023**	**10/11/2023**	**13/11/2023**	**17/11/2023**	**20/11/2023**	**23/11/2023**	**27/11/2023**	**30/11/2023**
pH	8.58	9.2	8.96	9.66	9.16	9.41	9.12	9.44
Temperature (ºC)	21.7	19.3	198	21	18.1	21.6	19.3	22
NH_4-N (mg/L)	402	38	470	262	145	70	245	210
NH_4-N removal (%)	91		44		52		14	
Daily NH_4-N (mg/L)	101		118		48		82	
SS (mg/L)	6060		4675		3670		4510	
VSS (mg/L)	2155		1160		1020		820	
Run period (day)	4.00		3.99		3.00		3.01	
F:M Ratio (mg NH_4-N/mg MLVSS*day)	0.05		0.10		0.05		0.10	
Initial Substrate/Initial Biomass (S_0/X_0) (mg NH_4-N/mg MLVSS)	0.19		0.41		0.14		0.30	

Table A.31. Operational results of R2 – December 2023.

Run	**1**		**2**		**3**		**4**	
Date	**04/12/2023**	**07/12/2023**	**11/12/2023**	**14/12/2023**	**18/12/2023**	**21/12/2023**	**25/12/2023**	**29/12/2023**
pH	7.16	6.97	7.3	6.81	7.19	6.83	7.51	7.94
Temperature (ºC)	22.7	22.4	19.2	21.6	18	21	20.6	22.2
NH_4-N (mg/L)	212	118	210	78	215	70	235	100
NH_4-N removal (%)	45		6		67		57	
Daily NH_4-N (mg/L)	71		70		72		59	
SS (mg/L)	2760		4155		3520		2990	
VSS (mg/L)	620		975		790		900	
Run period (day)	2.99		3.01		3.01		3.96	
F:M Ratio (mg NH_4-N/mg MLVSS*day)	0.11		0.07		0.09		0.07	
Initial Substrate/Initial Biomass (S_0/X_0) (mg NH_4-N/mg MLVSS)	0.34		0.22		0.27		0.26	

Table A.32. Operational results of R2 – January 2024.

Run	**1**		**2**		**3**		**4**		**5**	
Date	**02/01/2024**	**05/01/2024**	**08/01/2024**	**11/01/2024**	**15/01/2024**	**19/01/2024**	**22/01/2024**	**26/01/2024**	**29/01/2024**	**01/02/2024**
pH	7.68	6.83	7.3	7.42	8.16	7.39	7.42	6.97	8.3	8.45
Temperature (ºC)	21.3	22.2	21	18.1	16.6	21.9	17.1	20.1	17	18.1
NH_4-N (mg/L)	205	85	225	82	242	92	250	60	258	130
NH_4-N removal (%)	58		63		62		76		50	
Daily NH_4-N (mg/L)	69		76		60		63		86	
SS (mg/L)	3720		6585		6740		4560		4640	
VSS (mg/L)	880		1375		1630		1195		1045	
Run period (day)	2.99		2.95		4.04		3.99		2.99	
F:M Ratio (mg NH_4-N/mg MLVSS*day)	0.08		0.06		0.04		0.05		0.08	
Initial Substrate/Initial Biomass (S_0/X_0) (mg NH_4-N/mg MLVSS)	0.23		0.16		0.15		0.21		0.25	

Table A.33. Operational results of R2 – February 2024.

Run	**1**		**2**		**3**		**4**	
Date	**05/02/2024**	**09/02/2024**	**12/02/2024**	**15/02/2024**	**19/02/2024**	**22/02/2024**	**26/02/2024**	**01/03/2024**
pH	8.2	7.19	7.51	7.18	7.5	7.51	7.61	7.35
Temperature (ºC)	17.7	22	20.9	20	17.6	19.9	20.6	19.4
NH_4-N (mg/L)	290	68	215	50	138	50	225	48
NH_4-N removal (%)	77		77		64		79	
Daily NH_4-N (mg/L)	73		71		46		56	
SS (mg/L)	4500		4460		4760		3590	
VSS (mg/L)	1190		1325		1140		875	
Run period (day)	3.98		3.02		2.99		4.00	
F:M Ratio (mg NH_4-N/mg MLVSS*day)	0.06		0.05		0.04		0.06	
Initial Substrate/Initial Biomass (S_0/X_0) (mg NH_4-N/mg MLVSS)	0.24		0.16		0.12		0.26	

Table A.34. Operational results of R2 – March 2024.

Run	**1**		**2**		**3**		**4**	
Date	**04/03/2024**	**08/03/2024**	**11/03/2024**	**14/03/2024**	**18/03/2024**	**22/03/2024**	**25/03/2024**	**29/03/2024**
pH	7.62	7.36	7.77	7.3	7.48	7.31	7.69	7.14
Temperature (ºC)	17.9	19.3	18.6	21.5	18.6	20	19.6	24
NH_4-N (mg/L)	243	50	195	53	175	60	198	45
NH_4-N removal (%)	79		73		66		77	
Daily NH_4-N (mg/L)	60		65		43		50	
SS (mg/L)	5425		4010		5210		5210	
VSS (mg/L)	1245		1065		1340		1220	
Run period (day)	4.04		2.99		4.05		3.94	
F:M Ratio (mg NH_4-N/mg MLVSS*day)	0.05		0.06		0.03		0.04	
Initial Substrate/Initial Biomass (S_0/X_0) (mg NH_4-N/mg MLVSS)	0.19		0.18		0.13		0.16	

Table A.35. Operational results of R2 – April 2024.

Run	**1**		**2**		**3**		**4**	
Date	**01/04/2024**	**05/04/2024**	**15/04/2024**	**18/04/2024**	**22/04/2024**	**25/04/2024**	**29/04/2024**	**03/05/2024**
pH	7.54	7.13	7.5	7.32	7.52	7.44	7.4	7.17
Temperature (ºC)	22.9	22.5	20.8	23.4	20	22.2	19.6	21
NH_4-N (mg/L)	190	77	275	80	222	62	168	48
NH_4-N removal (%)	59		71		72		72	
Daily NH_4-N (mg/L)	48		92		73		42	
SS (mg/L)	5030		5010		5950		4880	
VSS (mg/L)	1220		1220		1630		1210	
Run period (day)	4.00		3.00		3.06		3.94	
F:M Ratio (mg NH_4-N/mg MLVSS*day)	0.04		0.08		0.04		0.04	
Initial Substrate/Initial Biomass (S_0/X_0) (mg NH_4-N/mg MLVSS)	0.16		0.23		0.14		0.14	

Table A.36. Operational results of R2 – May 2024.

Run	**1**		**2**		**3**		**4**	
Date	**06/05/2024**	**10/05/2024**	**13/05/2024**	**16/05/2024**	**20/05/2024**	**24/05/2024**	**27/05/2024**	**30/05/2024**
pH	7.52	7.11	7.44	7.1	7.39	7.05	7.62	7.32
Temperature (ºC)	20.2	21.9	21.2	21.8	21.4	22	21.3	22.9
NH_4-N (mg/L)	178	40	170	38	170	32	158	52
NH_4-N removal (%)	78		78		81		67	
Daily NH_4-N (mg/L)	44		57		43		52	
SS (mg/L)	6540		5725		4500		7160	
VSS (mg/L)	1595		1300		1145		1590	
Run period (day)	4.00		2.99		3.98		3.05	
F:M Ratio (mg NH_4-N/mg MLVSS*day)	0.03		0.04		0.04		0.03	
Initial Substrate/Initial Biomass (S_0/X_0) (mg NH_4-N/mg MLVSS)	0.11		0.13		0.15		0.10	

Table A.37. Operational results of R2 – June 2024.

Run	**1**		**2**	
Date	**03/06/2024**	**05/06/2024**	**24/06/2024**	**28/06/2024**
pH	7.25	7.04	7.12	7.1
Temperature (ºC)	25.4	27.3	25	25.6
NH_4-N (mg/L)	190	40	202	48
NH_4-N removal (%)	79		76	
Daily NH_4-N (mg/L)	93		50	
SS (mg/L)	5170		6680	
VSS (mg/L)	1220		2690	
Run period (day)	2.05		4.02	
F:M Ratio (mg NH_4-N/mg MLVSS*day)	0.08		0.02	
Initial Substrate/Initial Biomass (S_0/X_0) (mg NH_4-N/mg MLVSS)	0.16		0.08	

Table A.38. Operational results of R2 – July 2024.

Run	**1**		**2**		**3**	
Date	**01/07/2024**	**05/07/2024**	**08/07/2024**	**12/07/2024**	**16/07/2024**	**19/07/2024**
pH	7.44	7.12	7.18	7.12	7.2	6.9
Temperature (ºC)	26.1	27	27.3	28.2	27.8	28.6
NH_4-N (mg/L)	233	70	183	48	210	7.5
NH_4-N removal (%)	70		74		96	
Daily NH_4-N (mg/L)	58		46		70	
SS (mg/L)	5090		4230		6445	
VSS (mg/L)	1370		1830		1395	
Run period (day)	4.04		3.99		3.00	
F:M Ratio (mg NH_4-N/mg MLVSS*day)	0.04		0.02		0.05	
Initial Substrate/Initial Biomass (S_0/X_0) (mg NH_4-N/mg MLVSS)	0.17		0.10		0.15	

Table A.39. Operational results of R2 – August & September 2024.

Run	**1**		**2**		**3**	
Date	**05/08/2024**	**08/08/2024**	**09/09/2024**	**12/09/2024**	**30/09/2024**	**03/10/2024**
pH	7.22	7.13	8.96	9.17	9.08	9.31
Temperature (ºC)	27	26.8	25.2	26.3	23.3	21.4
NH_4-N (mg/L)	270	60	298	75.0	188	75
NH_4-N removal (%)	78		75		60	
Daily NH_4-N (mg/L)	89		100		62	
SS (mg/L)	5230		7310		5410	
VSS (mg/L)	1550		1625		1210	
Run period (day)	3.03		2.98		3.05	
F:M Ratio (mg NH_4-N/mg MLVSS*day)	0.06		0.06		0.05	
Initial Substrate/Initial Biomass (S_0/X_0) (mg NH_4-N/mg MLVSS)	0.17		0.18		0.15	

Table A.40. Operational results of R2 – October, November, December 2024.

Run	**1**		**2**		**3**	
Date	**14/10/2024**	**17/10/2024**	**04/11/2024**	**07/11/2024**	**16/12/2024**	**19/12/2024**
pH	9.24	9.32	9.23	9.34	7.44	9.38
Temperature (ºC)	21.3	19.6	17.6	17.3	15.8	16
NH_4-N (mg/L)	225	85	210	160	158	55
NH_4-N removal (%)	62		24		65	
Daily NH_4-N (mg/L)	73		70		52	
SS (mg/L)	4735		4330		5760	
VSS (mg/L)	1150		845		710	
Run period (day)	3.07		2.99		3.04	
F:M Ratio (mg NH_4-N/mg MLVSS*day)	0.06		0.08		0.07	
Initial Substrate/Initial Biomass (S_0/X_0) (mg NH_4-N/mg MLVSS)	0.20		0.25		0.22	

APPENDIX B: RESULTS OF KINETIC EXPERIMENTS WITH GAC AND A MIXTURE OF PHARMACEUTICALS

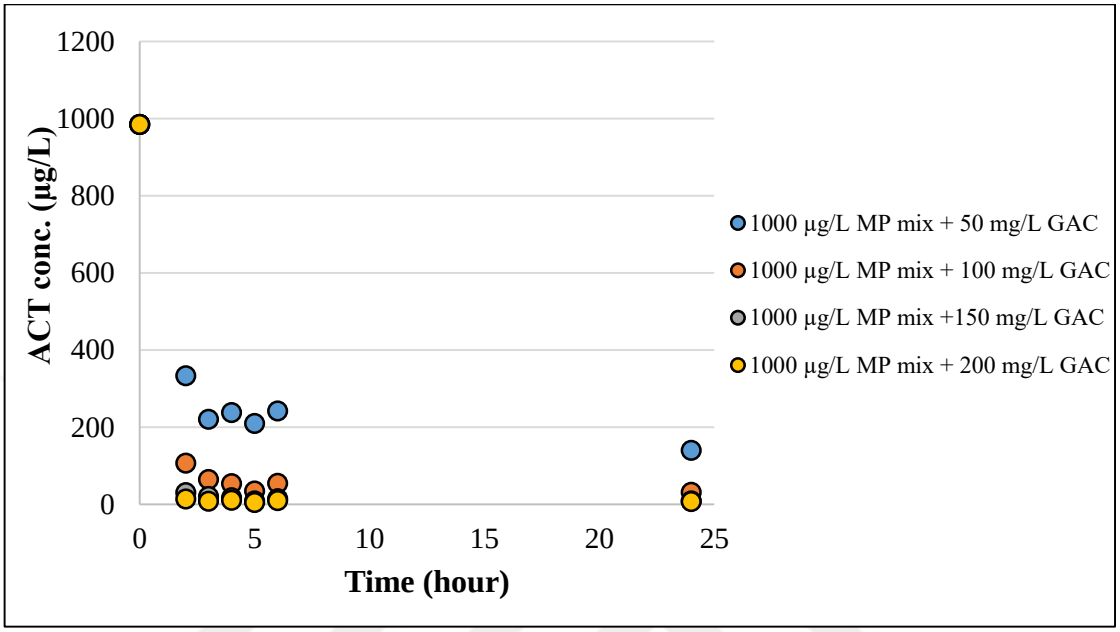

Figure B.1. Change in ACT concentrations with respect to time.

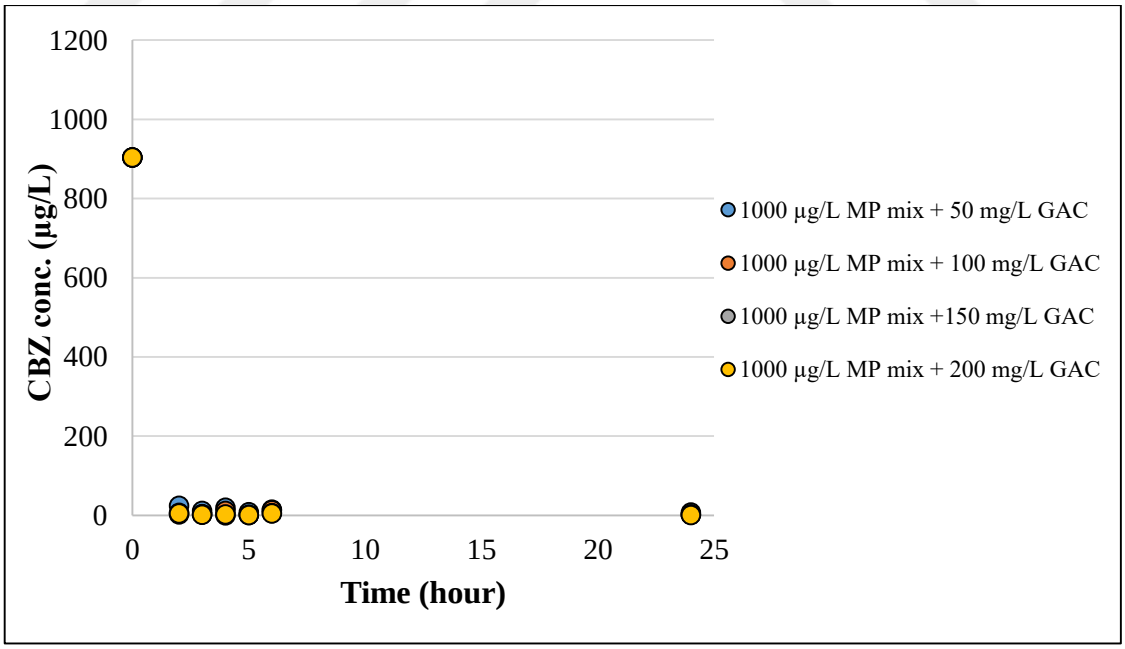

Figure B.2. Change in CBZ concentrations with respect to time.

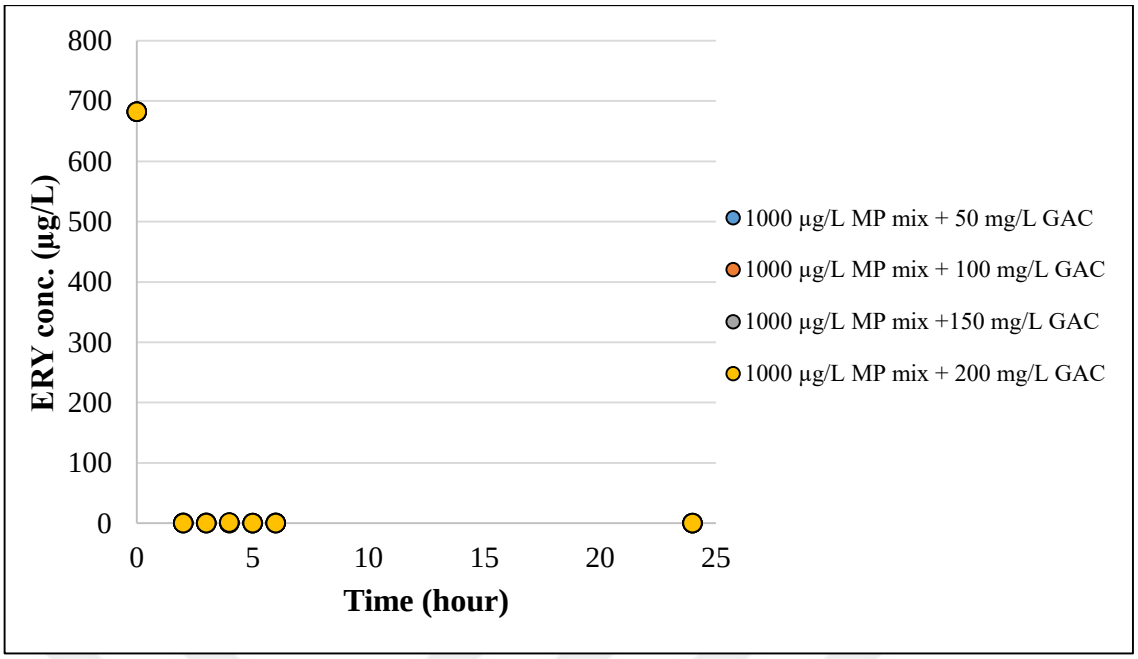

Figure B.3. Change in ERY concentrations with respect to time.

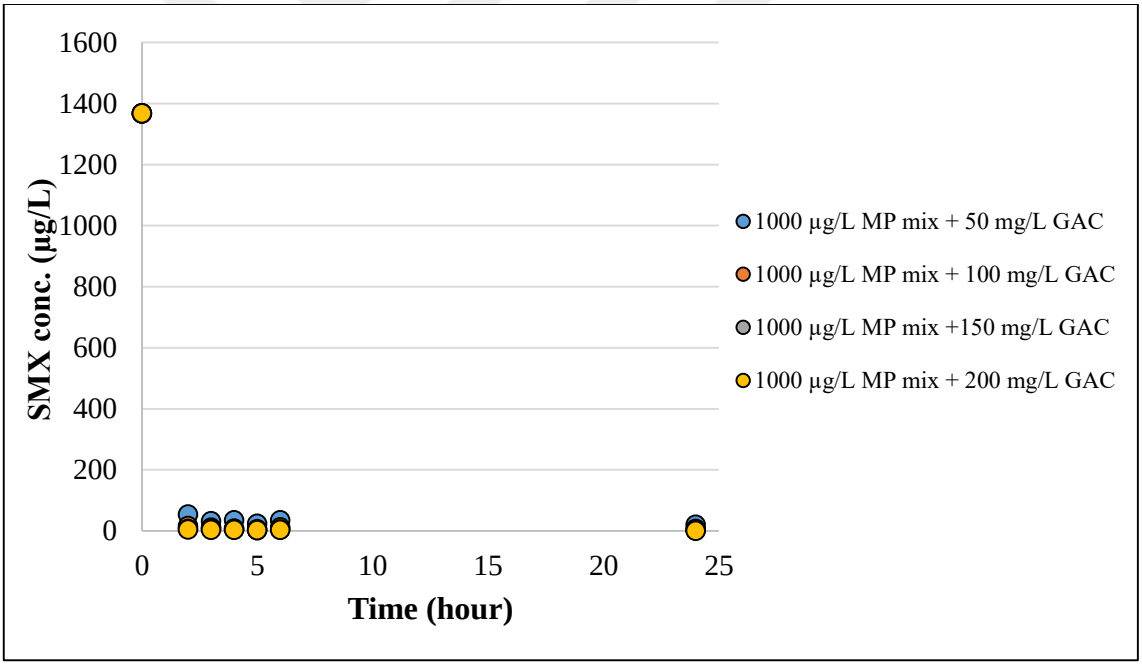

Figure B.4. Change in SMX concentrations with respect to time.

APPENDIX C: RESULTS OF ISOTHERM EXPERIMENTS WITH GROUND/ORIGINAL GAC AND SYNTHETIC SECONDARY EFFLUENT

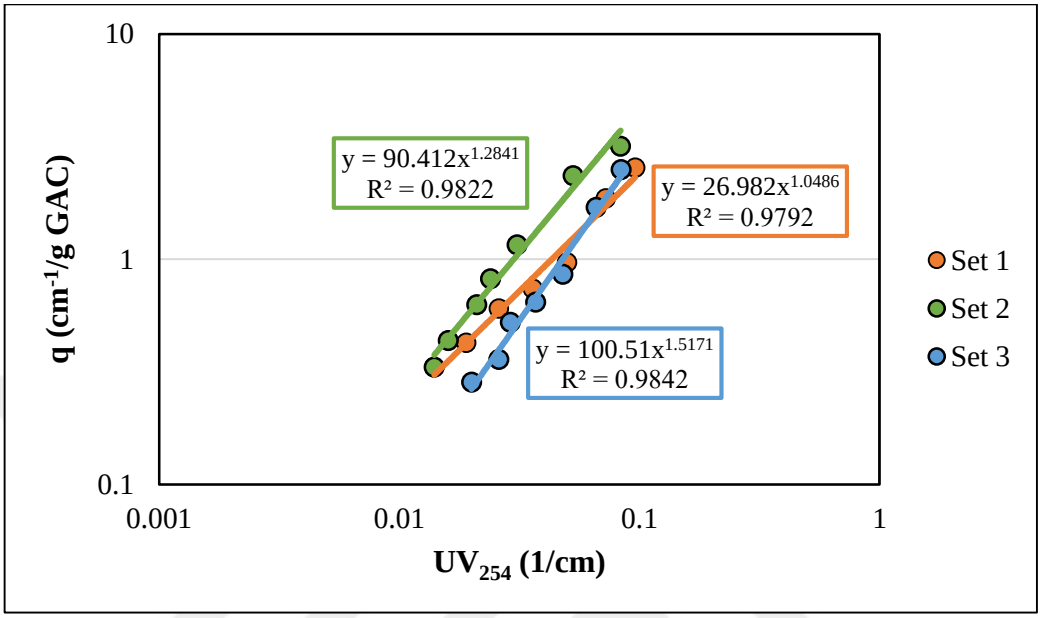

Figure C.1. Adsorption isotherm in terms of UV_{254} (Ground GAC).

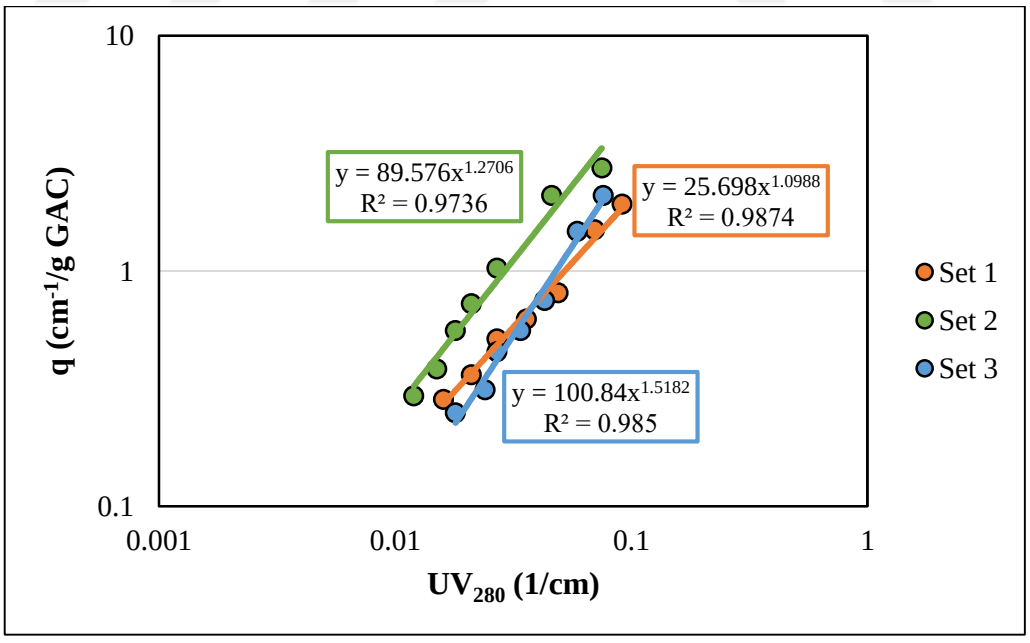

Figure C.2. Adsorption isotherm in terms of UV_{280} (Ground GAC).

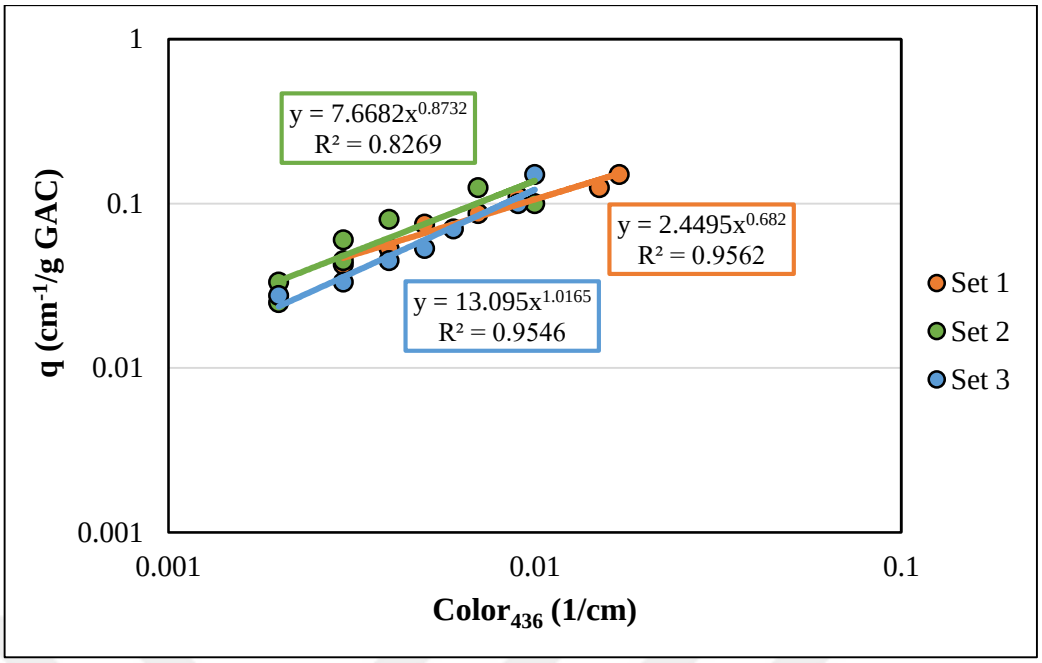

Figure C.3. Adsorption isotherm in terms of $Color_{436}$ (Ground GAC).

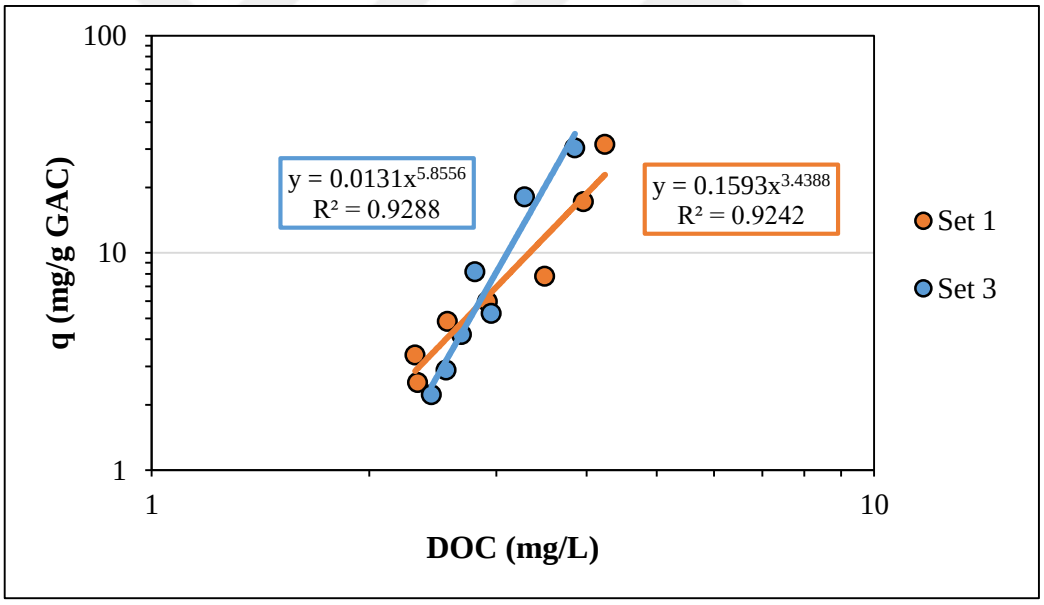

Figure C.4. Adsorption isotherm in terms of DOC (Ground GAC).

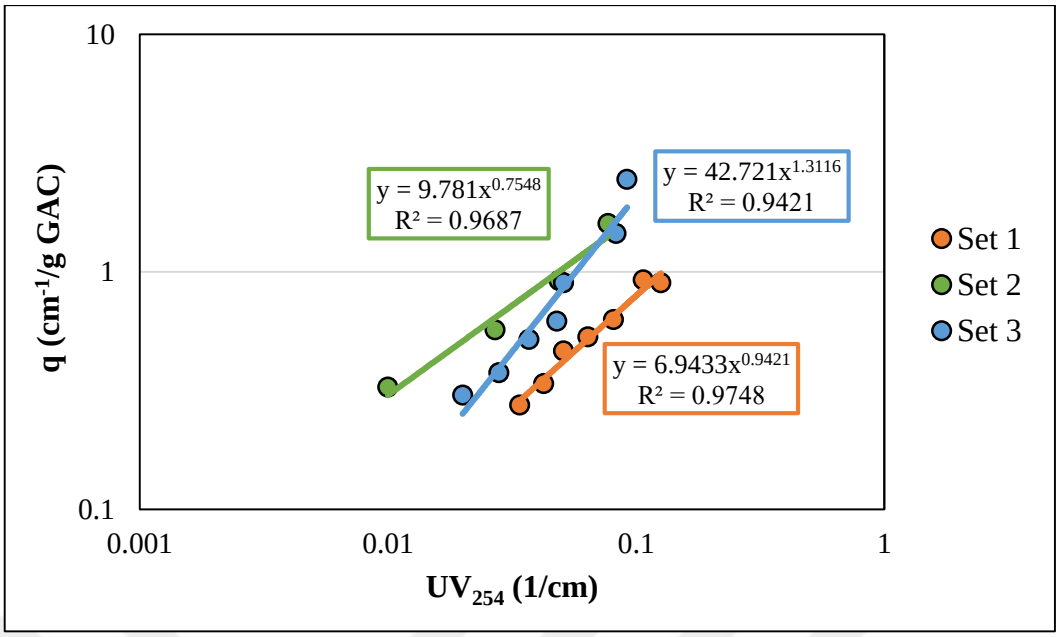

Figure C.5. Adsorption isotherm in terms of UV_{254} (Original GAC).

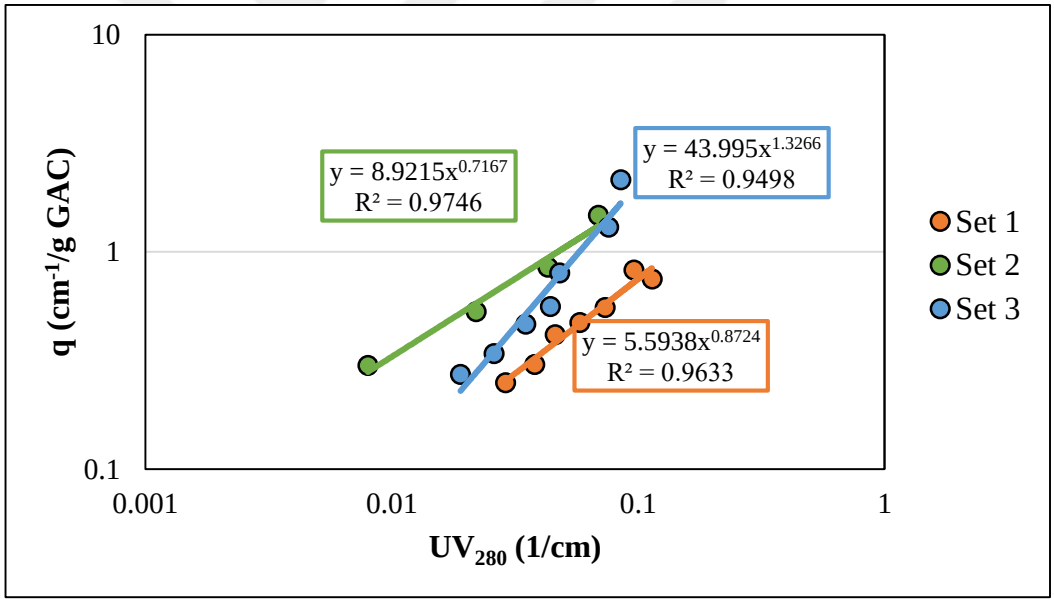

Figure C.6. Adsorption isotherm in terms of UV_{280} (Original GAC).

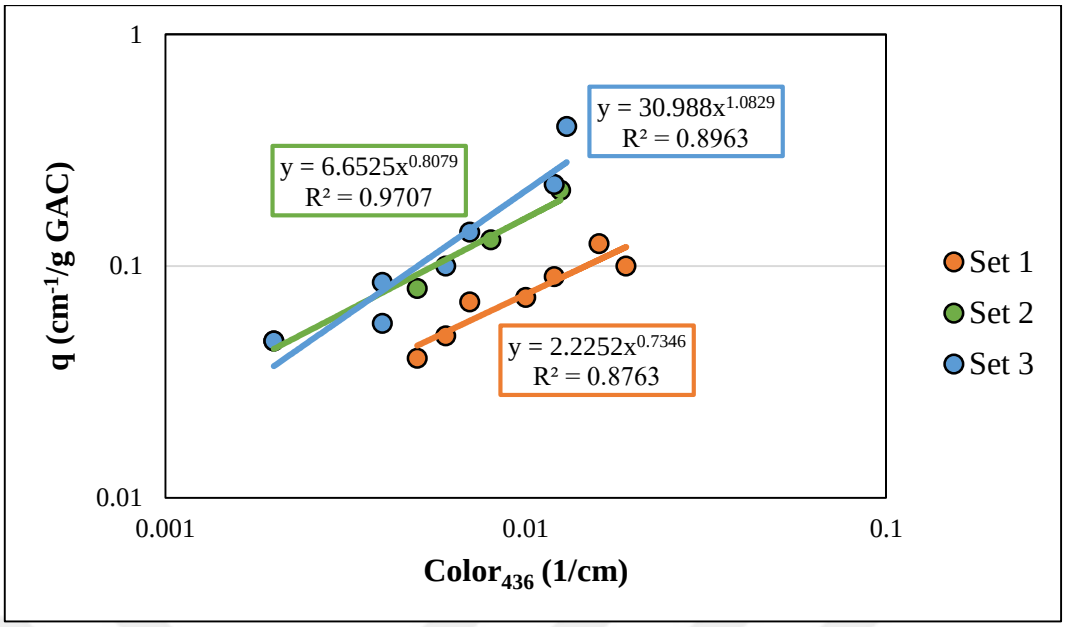

Figure C.7. Adsorption isotherm in terms of $Color_{436}$ (Original GAC).

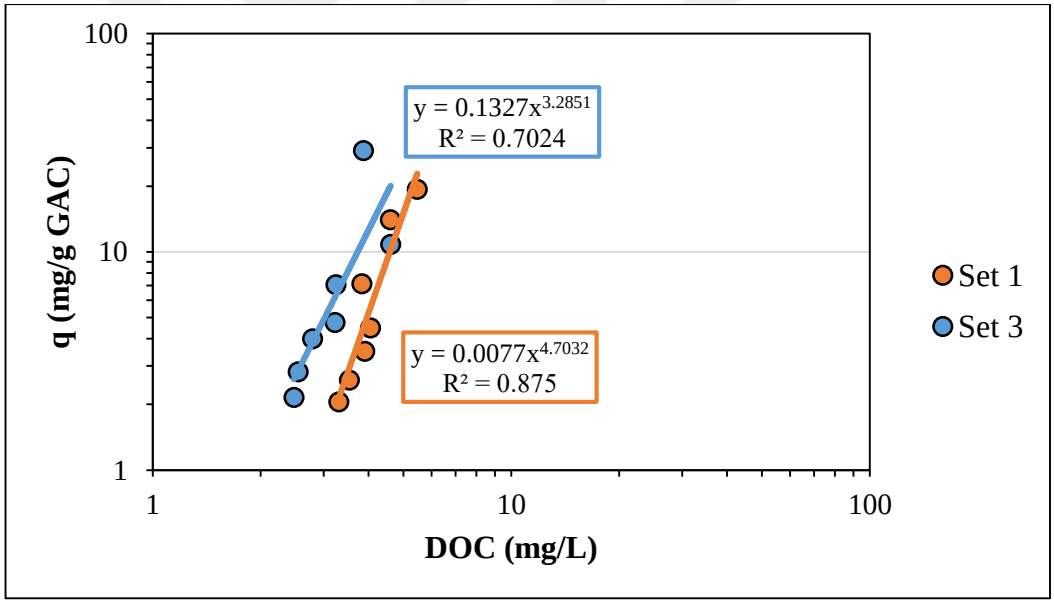

Figure C.8. Adsorption isotherm in terms of DOC (Original GAC).

APPENDIX D: RESULTS OF ISOTHERM EXPERIMENTS WITH GROUND GAC AND PHARMACEUTICALS

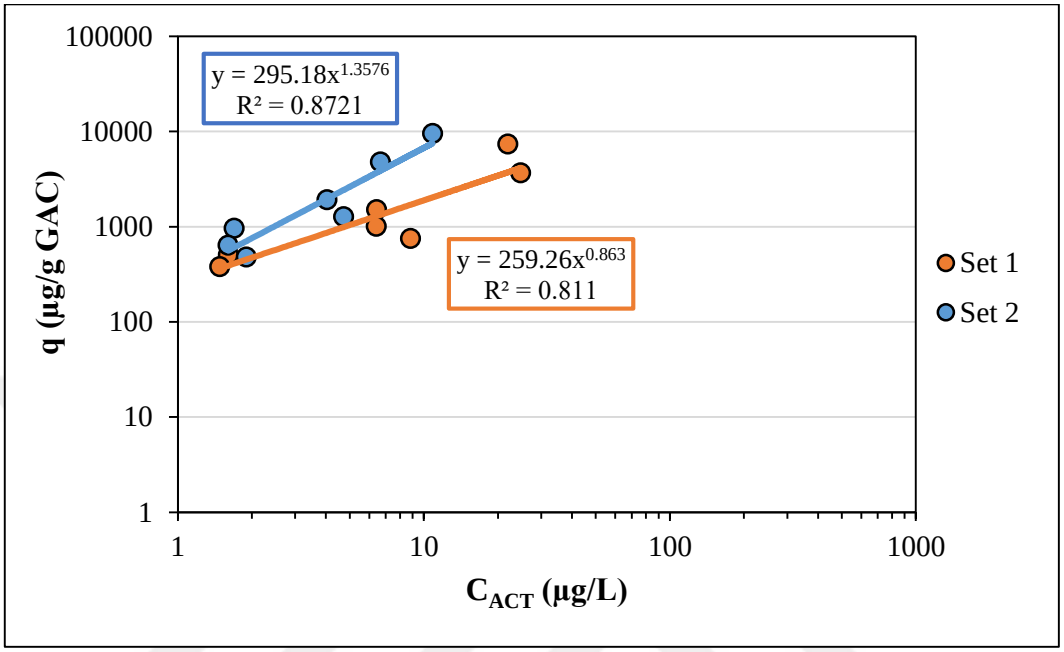

Figure D.1. Adsorption isotherm of ACT only (Ground GAC).

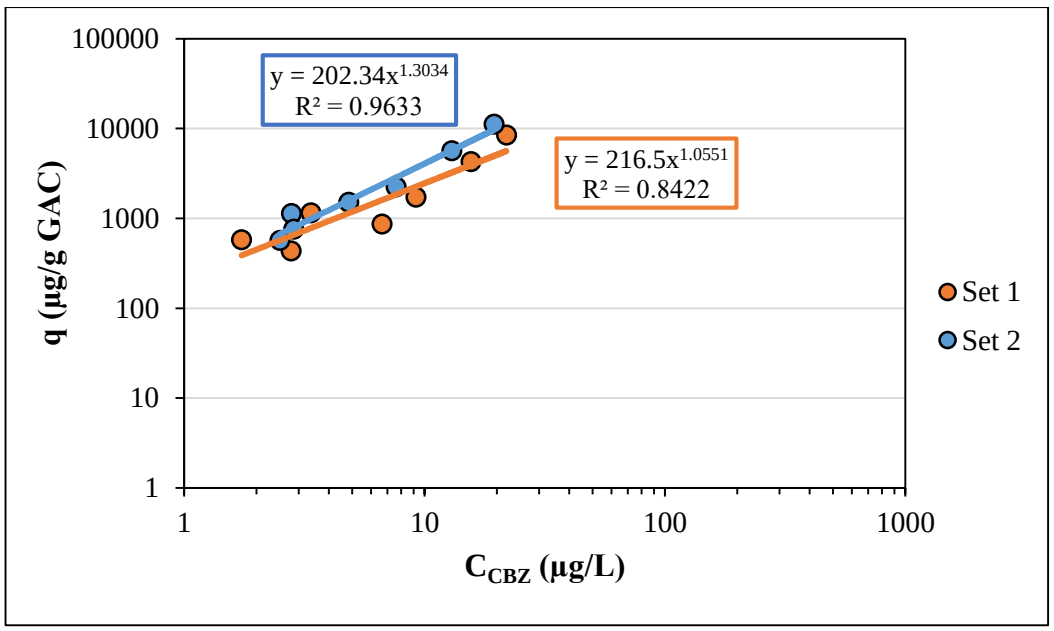

Figure D.2. Adsorption isotherm of CBZ only (Ground GAC).

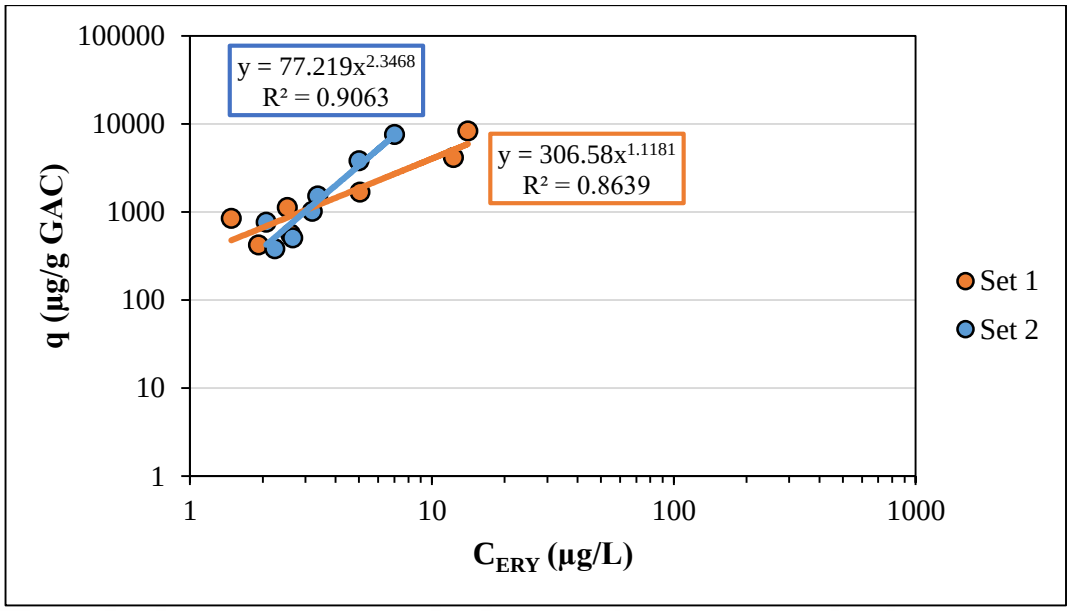

Figure D.3. Adsorption isotherm of ERY only (Ground GAC).

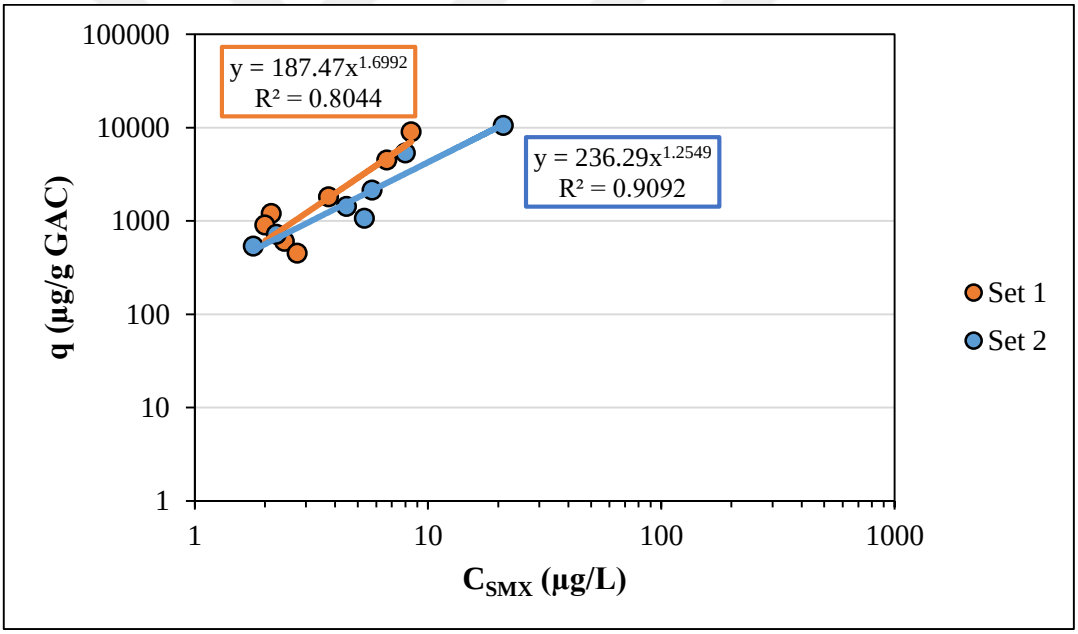

Figure D.4. Adsorption isotherm of SMX only (Ground GAC).

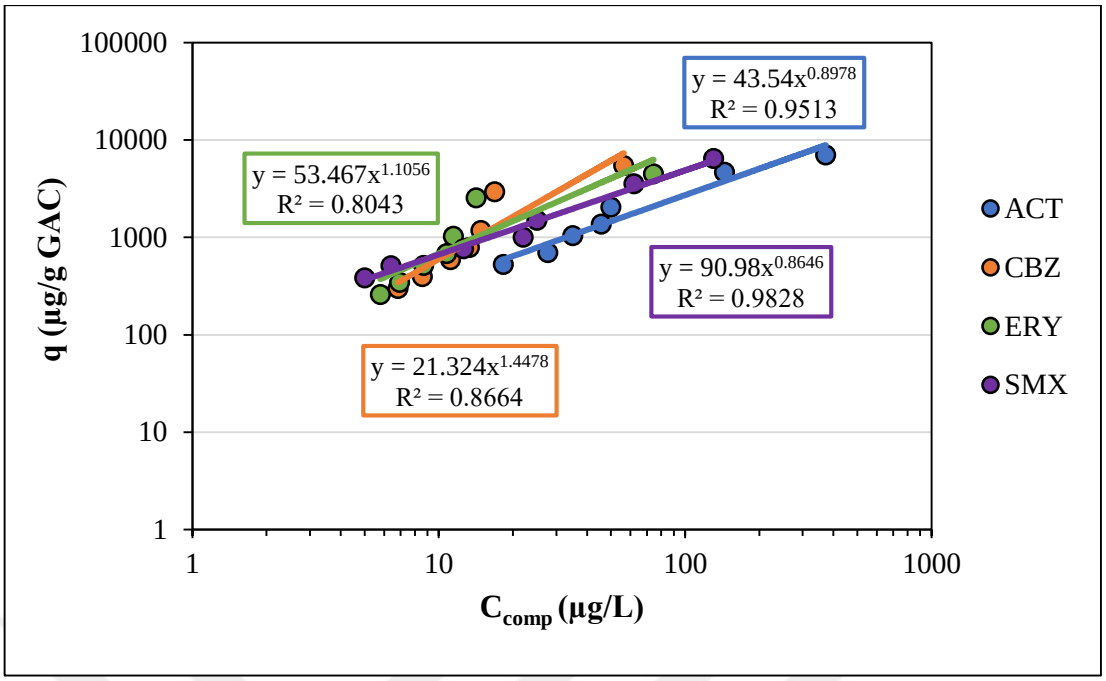

Figure D.5. Adsorption isotherm of pharmaceuticals in a mixture (Ground GAC).

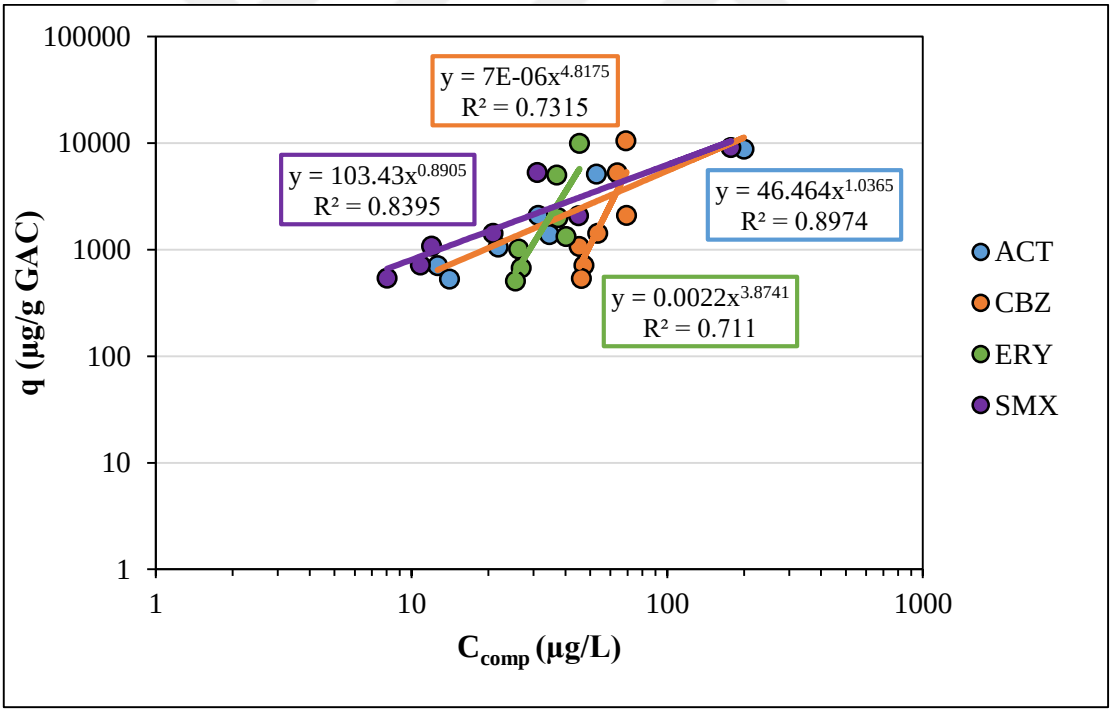

Figure D.6. Adsorption isotherm of pharmaceuticals in a mixture in the presence of background organic matter (Ground GAC) – Set 1.

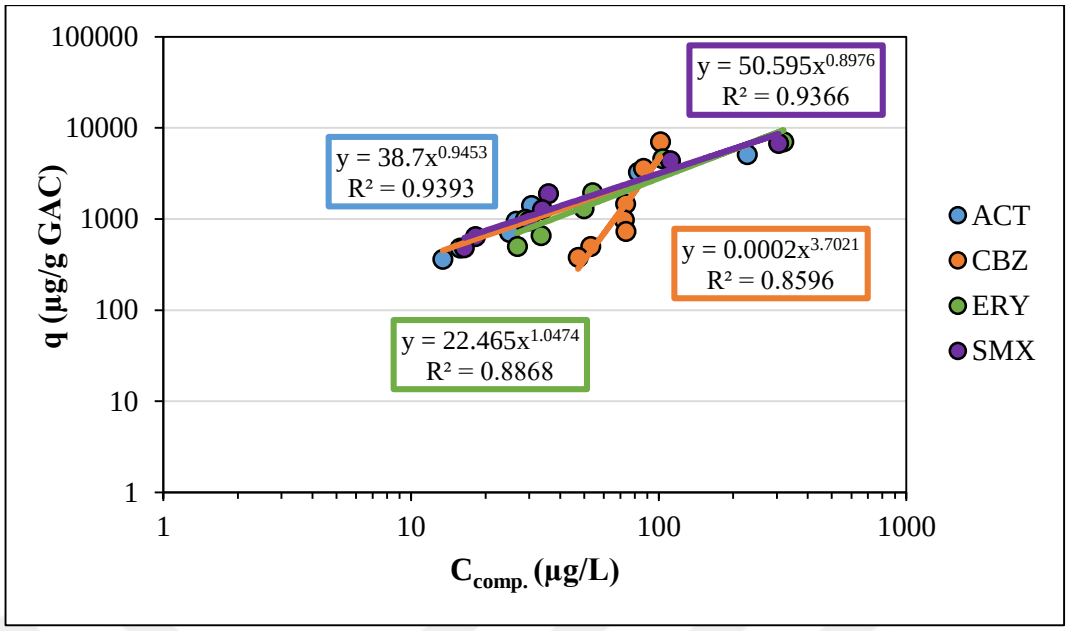

Figure D.7. Adsorption isotherm of pharmaceuticals in a mixture in the presence of background organic matter (Ground GAC) – Set 2.